Proteome analysis of *Schizosaccharomyces pombe*

using two-dimensional gel electrophoresis and mass spectrometry

Examination of 11-deoxycorticosterone (DOC)

induced differential protein patterns

Dissertation

zur Erlangung des Grades

des Doktors der Naturwissenschaften

der Naturwissenschaftlich-Technischen Fakultät III

Chemie, Pharmazie, Bio- und Werkstoffwissenschaften

der Universität des Saarlandes

von

Kyung Hoon Hwang

Saarbrücken

2007

ACKNOWLEDGMENT

Abbreviations:

11β-HSD2	11β-hydroxysteroid dehydrogenase-2
11β-OHD	11β-hydroxylase deficiency
17α-OHD	17α-hydroxylase deficiency
2-D	two-dimensional
2-DE	two-dimensional gel electrophoresis
2-D reference map	two-dimensional gel electrophoresis reference map
3βHSD	3β-hydroxysteroid dehydrogenase
ACE	angiotensin converting enzyme
ACN	acetonitrile
ACTH	adrenocorticotrophic hormone
AGT	angiotensinogen
AME	apparent mineralocorticoid excess
AMES	apparent mineralocorticoid excess syndrome
Ang I	angiotensin I
Ang II	angiotensin II
APS	ammonium persulfate
AR	androgen receptor
AT_1	angiotensin II type-1
ATP	adenosine triphosphate
BSA	bovine serum albumin
BSE	bovine spongiform encephalopathy
CAH	congenital adrenal hyperplasia
cAMP	cyclic adenosine monophosphate
CBB	coomassie brilliant blue
CJD	Creutzfeldt-Jakob disease
CSF	cerebrospinal fluid
cGMP	cyclic guanosine monophosphate
CHAPS	3-[(3-cholamidopropyl)dimethylamonio]-1-propane-sulfonate
CHCA	α-cyano-4-hydroxycinnamic acid
CTL	control
CYP11A1	side chain cleavage enzyme, cytochrome P450scc
CYP11B1	11β-hydroxylase, cytochrome P450c11

CYP11B2	aldosterone synthase, cytochrome P450c11Aldo
Da	dalton
DHB	dihydrobenzoic acid
DNA	deoxyribonucleic acid
DOC	11-deoxycorticosterone
DTT	dithiothreitol
EC	enzyme commission
e.g.	for example
EMM	edinburgh minimal medium
ER	estrogen receptor
ES	electrospray
ESI	electrospray ionization
FTICR	fourier transform ion cyclotron resonance
G protein	guanine nucleotide binding protein
GAPDH	glyceraldehyde-3-phosphate dehydrogenase
GO	Gene Ontology
GR	glucocorticoid receptor
GSH	glucocorticoid-suppressible hyperaldosteronism
HDL	high-density lipoprotein
i.d.	internal diameter
i.e.	that is
IEF	isoelectric focusing
IPG	immobilized pH gradient
IU	image units
kb	kilobase
kDa	kilodalton
LC	liquid chromatography
LC-MS/MS	liquid chromatography-tandem mass spectrometry
m/z	mass to charge
MALDI	matrix assisted laser desorption/ionization
MALDI-TOF	matrix assisted laser desorption/ionization-time of flight
MAPK	mitogen-activated protein kinase
MCH	mineralocorticoid hypertension
MR	mineralocorticoid receptor

Mr	relative molecular mass
MS	mass spectrometry
MS/MS	tandem mass spectrometry
NAD-ME	NAD-dependent malic enzyme
nanoES	nanoelectrospray
nanoLC-MS/MS	nanoscale capillary liquid chromatography-tandem mass spectrometry
OD	optical density
ORFs	open reading frames
PAGE	polyacrylamide gel electrophoresis
PDC	pyruvate decarboxylase
PHA1	pseudohypoaldosteronism type 1
p*I*	isoelectric focusing point
PI3	phosphatidyl-inositol-3
PKA	protein kinase A
PKC	protein kinase C
PMF	peptide mass fingerprinting
PMM	peptide-mass mapping
PMSF	phenylmethylsulfonyl fluoride
PPAR	peroxisome proliferator-activated receptor
PR	progestin receptor;
pS	phosphorylated serine
pT	phosphorylated threonine
pS/T	phosphorylated serine/threonine
RAS	renin-angiotensin system
RNA	ribonucleic acid
S. cerevisiae	*Saccharomyces cerevisiae*
S. pombe	*Schizosaccharomyces pombe*
SDS	sodium dodecyl sulfate
TEMED	*N,N,N',N'*-tetramethylethylenediamine
TOF	time of flight
YEA	yeast extract agar

Units:

Length	Meter	m
	Centimeter	cm
Mass	Gram	g
Molecular weight	Dalton	Da
Current strength	Ampere	A
Tension	Volt	V
Electricity	Watt	W
Temperature	Celsius	C
Volume	Liter	L
	Milliliter	mL
	Microliter	μL
Wave length	Nanometer	nm
Time	Second(s)	sec
	Minute(s)	min
	Hour(s)	hr

Multiple and fraction:

10^6	Mega	M
10^3	Kilo	k
10^{-3}	Milli	m
10^{-6}	Mikro	μ
10^{-9}	Nano	n

Standard abbreviations for amino acids:

A	Ala	Alanine	L	Leu	Leucine
R	Arg	Arginine	K	Lys	Lysine
N	Asn	Asparagine	M	Met	Methionine
D	Asp	Aspartic acid	F	Phe	Phenylalanine
C	Cys	Cysteine	P	Pro	Proline
Q	Gln	Glutamine	S	Ser	Serine
E	Glu	Glutamic acid	T	Thr	Threonine
G	Gly	Glycine	V	Val	Valine
H	His	Histidine	W	Trp	Tryptophan
I	Ile	Isoleucine	Y	Tyr	Tyrosine

Summary

A) Zusammenfassung *(German version)*

Die Spalthefe *Schizosachromyces pombe* (*S. pombe*) ist ein einzelliger Eukaryont, der über nur ca. 5000 verschiedene Gene verfügt. Da die meisten Signalübertragungskaskaden und zellulären Prozesse zwischen Hefen und Mammalierzellen sehr konserviert sind, stellt dieses relativ simple eukaryotische System ein exzellentes Modell für die Identifikation von bisher unbekannten zellulären Mechanismen dar. Die Spalthefe besitzt darüber hinaus viele Gene und Regulationsmechanismen, die mit denen von Säugetieren nahe verwandt sind. Daher ist die Spalthefe ein geeignetes Modell zur Untersuchung von verschiedensten biologischen Prozessen, wie z. B. der Analyse der Zell-Zykluskontrolle, der Mitose und Meiose sowie von DNA Reparatur- und Rekombinationsmechanismen. Die Sequenzierung des *S. pombe* Genoms wurde 2002 abgeschlossen. Dies vereinfacht die Analyse des Proteoms dieses Organismus. Die Untersuchung des Proteoms der Spalthefe wird von großer Bedeutung für den Einsatz dieser interessanten Hefe in der Grundlagenforschung sowie für biotechnologische Abwendungen sein.

Der Nutzen von zwei-dimensionalen Geleelektrophorese Referenz-Karten (2-D Referenz-Karten) liegt darin, dass diese Karten Informationen über die Expression, Funktion und Regulation von Proteinen sowie eine Übersicht über Proteine, die an verschiedenen physiologischen Prozessen beteiligt sind, liefert. Das Ziel des ersten Teils dieser Arbeit bestand in der Herstellung einer 2-D Referenz-Karte für das Proteom der Spalthefe h^{-s} L972. Eine Referenz-Karte wurde unter Verwendung der 2-DE Technik in Kombination mit einer Protein Identifikation mittels Massenspektrometrie (MS) generiert. Es wurde eine Proteomanalyse unter Einsatz von unterschiedlichen pH Bereichen reproduzierbar mit einer hohen Auflösung durchgeführt. In dem pH Bereich von 3-10 konnten mehr als 1500 Protein-Spots auf silbergefärbten zwei-dimensionalen (2-D) Gelen und mehr als 800 Protein Spots auf coomassiegefärbten 2-D Gelen visualisiert werden. In dem pH Bereich von 4-7 wurden über 1000 Protein-Spots auf Silbergefärbten 2-D Gelen und mehr als 500 Protein Spots auf coomassiegefärbten 2-D Gelen visualisiert. Anschließend wurden 298 von insgesamt 800 coomassiegefärbten Spots im pH Bereich zwischen 3-10 sowie 101 von insgesamt 500 coomassiegefärbten Spots im pH Bereich zwischen 4-7 ausgeschnitten, entfärbt und danach über MALDI-TOF-MS sowie über nanoLC-MS/MS in der Arbeitsgruppe von Herrn Prof.

Alain Van Dorsselear, Strasbourg, Frankreich untersucht. Bis jetzt konnten 364 Proteine unter Nutzung beider MS Verfahren identifiziert werden. Es ist im Allgemeinen schwierig, Membranproteine mit der Technik der 2-DE zu darzustellen, da sie unter den gegebenen Proteingewinnungsmethoden schwer in Lösung zu bringen sind. In dieser Arbeit ist es gelungen, zwei Membranproteine zu identifizieren: eine mitochondriale Rezeptor Untereinheit tom 40 (O13656), und ein äußeres mitochondriales Membranprotein Porin (Q9P544). Durch die Verwendung der Software PDQuest, wurden die Molekülmassen sowie die korrespondierenden p*I* Werte der jeweiligen Protein Spots analysiert. Darüber hinaus ist es, basierend auf Swiss-Prot und TrEMBL, GeneDB und KEGG Datenbank Untersuchungen, gelungen, 157 verschiedene Proteine (364 Proteine mit Redundanzen, z. B. Isoformen) funktionell aufgrund ihrer Beteiligung an biologischen Prozessen einzuteilen. Von diesen identifizierten Proteinen sind 41,4 % an metabolischen Prozessen beteiligt. 14,6 %, der identifizierten Proteine besitzen bis jetzt unbekannte Funktionen. Zurzeit stellt die 2-DE die am häufigsten verwendete Methode für die Untersuchung von komplexen Proteingemischen wie z.B. Proben aus Zellen, Geweben oder anderen biologischen Materialien dar. Diese Technik wird auch eingesetzt, um quantitative Proteinmuster von Proteomen, die unter verschiedenen Bedingungen inkubiert worden sind, zu analysieren. Unter Berücksichtigung des letztgenannten stellt die im ersten Teil dieser Arbeit generierte 2-D Referenz-Karten von *S. pombe* ein nützliches Hilfsmittel für die Identifikation von Proteinen im zweiten Teil dieser Arbeit dar.

Steroidhormone wirken als chemische Signalüberträger in einer Vielzahl von Spezies und Zielgeweben. Dabei produzieren sie sowohl genomische als auch nichtgenomische Effekte. Die genomischen Effekte werden über verschiedene Kernrezeptoren vermittelt. Im Gegensatz hierzu verläuft die nichtgenomische Steroidwirkung über ein großes Feld von Second-Messenger-Kaskaden. Sie wirken dabei laut Definition nicht initiell und direkt über die DNA, sondern vermitteln sehr schnelle Effekte über die Aktivierung von Signalkaskaden, wie z.B. die Mitogen-aktivierte Proteinkinase, die Phosphatidyl-Inositol-3-Kinase und die Protein-Kinase C (PKC). Steroidhormone spielen eine essentielle Rolle in der Regulation von wichtigen zellulären und physiologischen Antworten im menschlichen Körper. Mineralocorticoide im Speziellen regulieren die Natrium-, Kalium- und Wasserhomöostase. Damit tragen sie zur Kontrolle des Blutdrucks bei und spielen bei einigen physiologischen Erkrankungen eine Rolle. Die wichtigsten Mineralocorticoide sind Aldosteron und 11-Desoxycorticosteron (DOC). DOC wird in der *Zona glumerulosa* der Nebennierenrinde

synthetisiert und kann abschießend zu Aldosteron umgewandelt werden. Ein Überschuss an Mineralocorticoiden, wie er z. B. durch verstärkte Aldosteron-Sekretion oder übermäßige Produktion von DOC entsteht, verursacht Bluthochdruck und charakteristische Imbalancen der Elektrolyte. Das Ziel des zweiten Teils der Arbeit war die Identifikation von Proteinen, die durch MR-unabhängige Wirkung von DOC in *S. pombe* verändert sind. Die Spalthefe *S. pombe* wurde gewählt, da sie natürlicherweise keine Kernrezeptoren für Steroide besitzt. Zur Identifikation der Proteine wurde eine Kombination aus 2-DE, Gelanalyse mit PDQuest und MS verwendet. Durch Nutzung spezifischer Analysesets in PDQuest konnten 42 Spots in silbergefärbten Gelen (davon 33 Spots aus 2-D Gelen mit einem pH-Gradienten von 4-7 und 9 Spots (pH > 7) von Gelen im pH Bereich 3-10) gefunden werden, die signifikante Intensitätsunterschiede zwischen mit 8 µM DOC-behandelten Proben und Nullkontrollen aufwiesen. Bei der anschließenden MS-Analyse konnten 19 verschiedene Proteine (24 Proteine mit Redundanzen, z. B. Isoformen) in 23 Spots identifiziert werden (davon 18 aus Gelen mit dem pH Bereich 4-7 und 5 (pH > 7) von 2-D Gelen im Bereich 3-10). Unter diesen identifizierten Proteinen konnten 4 Proteine gefunden werden, die eine Verbindung zur PKC-Signalkaskade aufweisen: das „Cofilin (P78929)", das „DNA damage checkpoint protein rad 24 (P42656)", das „guanine nucleotide-binding protein beta subunit-like protein (Q10281)" und das „Protein vip1 (P87216)". Diese Proteine könnten mit einer spezifischen nichtgenomischen Wirkung von Mineralocorticoiden assoziiert sein. Neun weitere identifizierte Proteine sind in den Metabolismus involviert. Die Glycerinaldehyd-3-Phosphat Dehydrogenase 1 (P78958) könnte auch eine relevante Rolle im Aufbau des Cytoskeletts spielen. Die Enolase 1-1 (P40370), die Enolase 1-2 (Q8NKC2) und das NAD-abhängige Malat-Enzym (P40375) können mit Osmoregulation in Verbindung gebracht werden. Fünf differentiell regulierte Proteine weisen eine mögliche Verbindung zu oxidativem Stress auf : Mangansuperoxid-Dismutase (Q9UQX0), Glutathion-Peroxidase (O59858), SPCC576.03 Protein (O74887, Thioredoxin Peroxidase), ein äußeres mitochondriales Membranprotein Porin (Q9P544) und das Hitzeschockprotein sks2 (Q10284). Die identifizierten Proteine (Spots) konnten anhand eines Vergleichs mit der im ersten Teil dieser Arbeit hergestellten Referenzkarten bestätigt werden.

Die identifizierten Proteine könnten neue Targets für die Entwicklung von Medikamenten gegen Bluthochdruck und Mineralocorticoid-induzierte Herzerkrankungen darstellen.

B) Version in English

The fission yeast *Schizosaccharomyces pombe* (*S. pombe*) is a unicellular eukaryote possessing only about 5,000 different genes. The fission yeast contains many genes and regulatory mechanisms that are close to those of mammals. Since the major signaling pathways and cellular processes are conserved between yeasts and mammalian cells, these simple eukaryotic systems are also excellent models for the identification of unknown molecular as well as cellular mechanisms. Therefore, *S. pombe* is an excellent model organism for the study of numerous biological processes such as cell cycle control, mitosis and meiosis, and DNA repair and recombination. The sequencing of the *S. pombe* genome was completed in 2002 and thus made it possible to study the intracellular proteome of this yeast. Therefore, analyzing its proteome will be of great help for the use of this interesting yeast in model studies and biotechnological applications.

The benefit of two-dimensional gel electrophoresis reference map (2-D reference map) is that they can provide much information such as the expression, function and regulation of proteins and a survey of proteins affected during different physiological processes. The aim of the first part of this work was to establish a 2-D reference map for proteins of *S. pombe* wild type strain h^{-S} L 972. Investigation of this subject was performed using a combination of 2-DE and mass spectrometry (MS). A global proteome analysis of the fission yeast has been performed. For this purpose, two-dimensional (2-D) gels of two different pH ranges with a high resolution and high reproducibility were successfully produced. In the 3-10 pH range, more than 1500 protein spots on silver stained 2-D gels and more than 800 protein spots on colloidal blue stained 2-D gels were visualized. In the 4–7 pH range, more than 1000 protein spots on silver stained 2-D gels and more than 500 protein spots on colloidal blue stained 2-D gels were also visualized. Thereafter, 298 spots out of 800 colloidal blue stained spots in the 3-10 pH range and 101 spots out of 500 colloidal blue stained spots in the 4-7 pH range were excised, destained, and analyzed independently by matrix assisted laser desorption/ionization-time of flight (MALDI-TOF) MS as well as nanoscale capillary liquid chromatography-tandem mass spectrometry (nanoLC-MS/MS) in the lab of Prof. Alain Van Dorsselaer, ECPM, Strasbourg, France. So far, 364 proteins have been identified by both MS approaches. Generally, membrane proteins are difficult to resolve by ordinary sample preparation methods and therefore rarely detected by 2-DE. In this work, two membrane proteins have been identified: a mitochondrial import receptor subunit tom40 (O13656) and an outer

mitochondrial membrane protein porin (Q9P544). By using PDQuest software, the gel-estimated relative molecular mass (Mr) and isoelectric focussing point (p*I*) values of all identified proteins were determind. Moreover, based on annotations from Swiss-Prot and TrEMBL, GeneDB as well as the KEGG database, 157 distinct proteins (364 identified proteins with redundancies, *e.g.* isoforms) were functionally classified according to their biological process. Of these identified proteins, 41.4% are involved in metabolism. 14.6% of the identified proteins display unknown functions. Currently, 2-DE is the most often used technique for the analysis of complex protein mixtures extracted from cells, tissues, or other biological samples as well as for obtaining a quantitative picture of protein expression levels of a proteome under various conditions. Thus, the present 2-D reference maps provide a very useful information for the second part of this work using *S. pombe* as a model organism.

Steroid hormones act as chemical messengers in many species and target tissues to produce both genomic actions, and non-genomic actions. The genomic actions of steroid hormones are mediated via several different nuclear receptors. In contrast to the genomic action, the non-genomic actions are mediated by a wide array of cellular second-messenger systems. It defines any action that does not directly and initially influence gene expression, but rather drives more rapid effects such as the activation of signalling cascades: *e.g.* mitogen-activated protein kinase, phosphatidyl-inositol-3-kinase and protein kinase C (PKC). Steroid hormones play an essential role in the regulation of important cellular and physiological responses in the human body. In particular, mineralocorticoids exert crucial roles in regulating sodium, potassium and water homeostasis. They contribute to the control of blood pressure and in some physiological disorders. The most important mineralocorticoids are aldosterone and 11-deoxycorticosterone (DOC). DOC is produced in the zona glomerulosa in the adrenal cortex and can be finally converted to aldosterone. Mineralocorticoid excess, which will arise due to increased aldosterone secretion or grossly excessive production of DOC, causes hypertension and characteristic disturbances of the electrolyte balance. The aim of this part was to identify proteins, which are altered due to the MR-independent action of DOC in *S. pombe*. The fission yeast *S. pombe* was chosen since it does not contain nuclear steroid receptors. Investigation of this subject was performed by combining 2-DE, PDQuest software and MS. By using specific Analysis Sets in PDQuest, a total number of 42 spots from silver stained gels (33 spots from 2-D gels with a pH 4-7 range and 9 spots (pH > 7) from 2-D gels with a pH range 3-10) displayed significant intensity differences between the samples treated with 8 µM DOC and control samples. After MS analysis, 19 distinct proteins (24 identified

proteins with redundancies, *e.g.* isoforms) out of 23 spots have been identified (18 spots were obtained from 2-D gel with a pH 4-7 range and 5 spots (pH > 7) from 2-D gel with a pH range 3-10). Of these identified proteins, four proteins may be connected with the PKC signalling cascade: cofilin (P78929), DNA damage checkpoint protein rad24 (P42656), guanine nucleotide-binding protein beta subunit-like protein (Q10281) and protein vip1 (P87216). These proteins seem to be specifically associated with general non-genomic actions of DOC and aldosterone, or only DOC. Nine other proteins are involved in metabolism. Glyceraldehyde-3-phosphate dehydrogenase 1 (P78958) may also play a relevant role in cytoskeleton assembly. Enolase 1-1 (P40370), enolase 1-2 (Q8NKC2) and NAD-dependent malic enzyme (P40375) may be also associated with the osmotic regulation. Five differentially regulated proteins are connected to oxidative stress, including manganese superoxide dismutase (Q9UQX0), glutathione peroxidase (O59858), SPCC576.03c protein (O74887, thioredoxin peroxidase), outer mitochondrial membrane protein porin (Q9P544) and heat shock protein sks2 (Q10284). These identified proteins could be confirmed according to the comparison with the 2-D reference maps produced in the first part of this work. The identified proteins might be new targets for the development of drugs against hypertension and mineralocorticoid-caused heart disease.

Abstract

The overall aim of this work was the investigation of the proteom of the fission yeast *Schizosaccharomyces pombe* (*S. pombe*) by two-dimensional gel electrophoresis (2-DE) and mass spectrometry (MS). The first goal of this study was to establish a two-dimensional gel electrophoresis reference maps (2-D reference map) for proteins of *S. pombe* wild type strain h^-S L 972. The benefit of 2-D reference map is that they can provide much information on the expression, function and regulation of proteins and a survey of proteins affected during different physiological processes. In this study 364 proteins have been identified by MS approaches, amongst others two membrane proteins. After subsequent database searches, 157 out of these 364 distinct proteins could be functionally classified.

The aim of the second part was to identify proteins, which are altered in *S. pombe* due to the mineralocorticoid receptor (MR) -independent action of the steroid hormone 11-deoxycorticosterone (DOC). The fission yeast *S. pombe* was chosen since it does not contain nuclear steroid receptors. Investigation of this subject was performed by combining two dimensional electrophoresis, PDQuest software and MS. By using specific Analysis Sets in PDQuest, a total number of 42 spots from silver stained gels displaying significant intensity differences between the samples treated with DOC and control samples were visualized. After MS analysis, 19 distinct proteins have been identified.

Kurze Zusammenfassung

Ziel dieser Arbeit war die Untersuchung des Proteoms der Spalthefe *Schizosaccharomyces pombe* (*S. pombe*) mittels zwei-dimensionaler Geleelektrophorese (2-DE) und anschließender Massenspektrometrie (MS) -Analyse. Im ersten Teil wurde eine zwei-dimensionalen Geleelektrophorese Referenz-Karten (2-D Referenz-Karten) für das Proteom der Spalthefe h^-s L972 hergestellt. Der Nutzen von 2-D Referenz-Karte liegt darin, dass diese Karten Informationen über die Expression, Funktion und Regulation von Proteinen sowie eine Übersicht über Proteine, die an verschiedenen physiologischen Prozessen beteiligt sind, liefert. In dieser Arbeit konnten 364 Proteine mittels MS identifiziert werden, u.a. zwei Membranproteine und durch Datenbank Untersuchungen, konnten 157 dieser Proteine funktionell klassifiziert werden.

Das Ziel des zweiten Teils der Arbeit war die Identifikation von Proteinen, die durch Mineralocorticoid Rezeptor (MR) -unabhängige Wirkung des Steroidhormons, 11-Deoxycorticosterone (DOC) in *S. pombe* verändert sind. Die Spalthefe *S. pombe* wurde gewählt, da sie natürlicherweise keine Kernrezeptoren für Steroide besitzt. Zur Identifikation der Proteine wurde eine Kombination aus 2-DE, Gelanalyse mit PDQuest und MS verwendet. Durch Nutzung spezifischer Analysesets in PDQuest konnten 42 Spots in silbergefärbten Gelen gefunden werden, die signifikante Intensitätsunterschiede zwischen DOC-behandelten Proben und Nullkontrollen aufwiesen. Bei der anschließenden MS-Analyse konnten 19 verschiedene Proteine identifiziert werden.

1. Introduction

1.1 The Mineralocorticoids 11-deoxycorticosterone and aldosterone

Steroid hormones play an essential role in the regulation of important cellular and physiological responses in the human body. Steroid hormones in the adrenal cortex are classified into three groups based on their biological actions: mineralocorticoids, glucocorticoids and adrenal androgens. Mineralocorticoids and other adrenal steroids are synthesised through a series of enzymatic steps from cholesterol (see Figure 1.1). In particular, mineralocorticoids exert crucial roles in regulating sodium, potassium and water homeostasis. They contribute to the control of blood pressure and play a role in some physiological disorders (Connell *et al.,* 2001). In addition, mineralocorticoids have been related to severe heart failure (Pitt *et al.,* 1999; Ramires *et al.,* 2000; Nussberger, 2003).
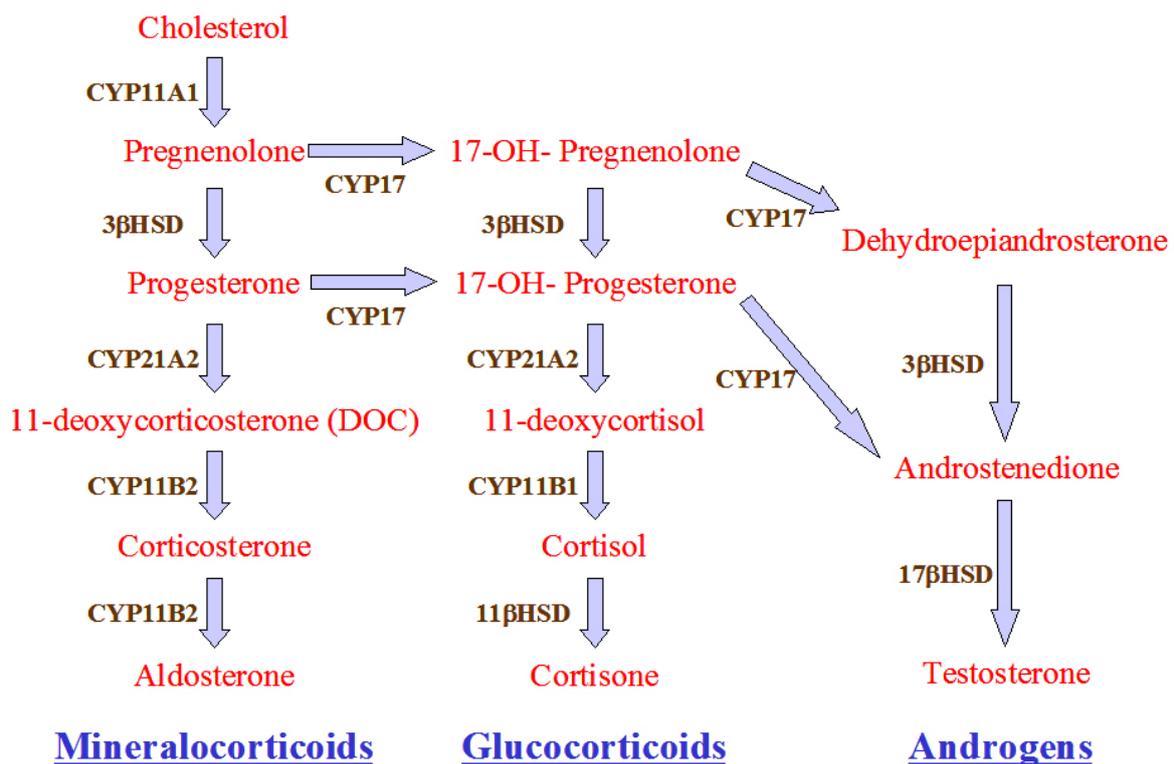
Figure 1.1 Principal pathways of human adrenal steroidogenesis (Ghulam *et al.,* 2003).

The most important mineralocorticoids are aldosterone, which is synthesized in zona glomerulosa and 11-deoxycorticosterone (DOC) being produced in the zona glomerulosa and fasciculata. The early steps in steroidogenesis of mineralocorticoids are common to all

cortical zones and consist of the sequential conversion of cholesterol to pregnenolone by the side chain cleavage enzyme, cytochrome P450scc (*CYP11A1*), and of pregnenolone to progesterone by 3β-hydroxysteroid dehydrogenase (3βHSD). Progesterone in the zona glomerulosa is hydroxylated at carbon 21 by the adrenal 21-hydroxylase, CYP21A2, to yield DOC. The conversion of DOC to aldosterone involves three consecutive reactions: 11β-hydroxylation of DOC to form corticosterone, 18-hydroxylation to yield 18-hydroxycorticosterone and finally 18-oxidation to aldosterone. In human, the single mitochondrial enzyme, aldosterone synthase, cytochrome P450c11Aldo (*CYP11B2*), carries out all of these steps (see Figure 1.2). This enzyme is regulated by angiotensin II and potassium via protein kinase C (PKC). DOC posseses an at least 10 fold weaker mineralocorticoid activity compared with aldosterone in humans.
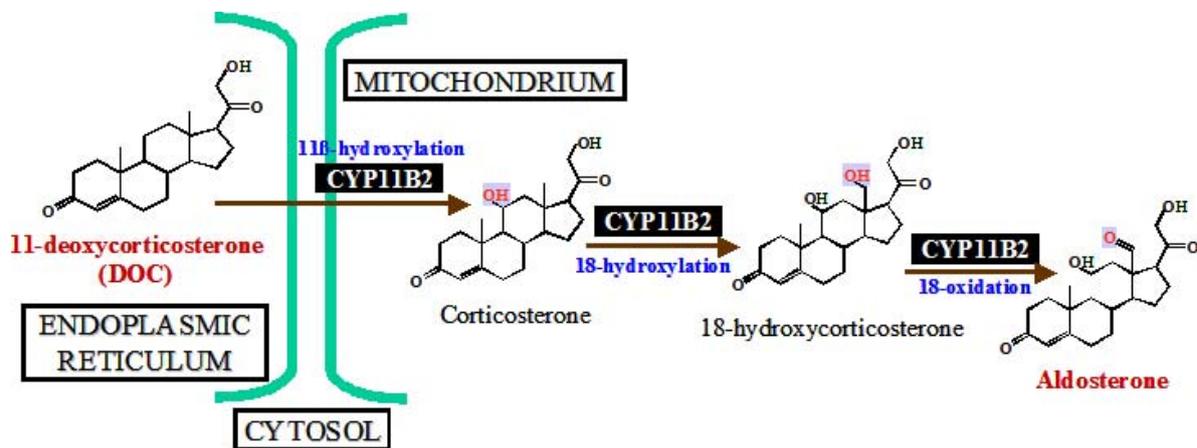
Figure 1.2 *CYP11B2* converts DOC via corticosterone and 18-hydroxycorticosterone to aldosterone.

Moreover, produced DOC in the zona fasciculata may be converted to corticosterone by 11β-hydroxylase, cytochrome P450c11 (*CYP11B1*), which is synthesized under the control of the adrenocorticotrophic hormone (ACTH) via cyclic adenosine monophosphate (cAMP) and protein kinase A (PKA) (Connell *et al.,* 2001). These two enzymes (*CYP11B2* or *CYP11B1*) have been implicated in the genesis of arterial hypertension through an increase in the aldosterone synthesis, as occurs in the glucocorticoid-remediable aldosteronism (Lifton *et al.,* 1992; Pascoe *et al.,* 1992). Moreover, *in vitro* studies have demonstrated that specific mutations in *CYP11B2* or *CYP11B1* should also explain some forms of hyperaldosteronism (Fardella *et al.,* 1995; Fardella *et al.,* 1996; Curnow *et al.,* 1997).

Abnormalities of mineralocorticoid synthesis as well as metabolism profoundly affect the regulation of electrolyte and water balance and of blood pressure. Mineralocorticoid excess causes hypertension and characteristic disturbances of the electrolyte balance. Several mechanisms may lead to mineralocorticoid excess, including increased production of aldosterone or DOC, reduced inactivation of cortisol by 11β-hydroxysteroid dehydrogenase type 2 (11β-HSD2), and constitutive activation of the distal renal tubule sodium channel. Especially, elevated levels of DOC cause several diseases, including hypertension (Stewart, 1999; Nussberger, 2003), congenital adrenal hyperplasia (CAH) (Biglieri and Kater, 1991; Peters *et al.,* 1998; Collett-Solberg, 2001), Cushing's syndrome (Yasuda *et al.,* 1993) and adrenal tumors (adenomas or carcinomas) (Egoshi *et al.,* 1998; Pitt *et al.,* 1999). Furthermore, DOC produces a mineralocorticoid excess state and the mechanism of hypertension is similar to that seen with aldosterone in primary aldosteronism. Moreover, elevated DOC may also be an indicator for aldosterone synthase defects type I and II, and hypokalemia, whereas low levels of DOC may be the cause for the apparent mineralocorticoid excess syndrome (AMES), hypotension and hyperkalemia (Ghulam *et al.,* 2003).

1.2 Mineralocorticoid Hypertension (MCH)

Heart failure is a leading cause of both morbidity and mortality. In particular, elevated blood pressure is a frequent component of the metabolic syndrome. This disorder is a major risk factor for many common causes of both morbidity and mortality including the cardiovascular diseases - like heart attack, stroke, myocardial infarction, congestive heart failure, end-stage renal disease, kidney failure and more (Mosterd *et al.,* 1999; Kannel, 2000). In all those cases, hypertension was found as the preceding condition.

Hypertension is a substantial public health problem, affecting about 20-25% of the adult populations (Burt *et al.,* 1995): *e.g.* in Germany, with a population of 80 millions, the daily turnover of hypertension pills is estimated to be 50 - 75 million EUR (about US$ 75 - 94 millions: see http://www.dr-schnitzer.de/hypertension.html). Furthermore, hypertension is more frequent in subjects with either insulin resistance or obesity (Reaven, 1988; Must *et al.,* 1999).

Historically, hypertension has been subdivided into "essential" and "secondary" forms. In most cases, no clear reason for the patient's raised blood pressure is apparent and they are diagnosed as having essential hypertension. It is assumed that essential hypertension is caused by multiple factors and that no single cause exists. Essential hypertension has traditionally been viewed as a consequence of interaction between environmental factors (*e.g.*, sodium intake) and genetic background. Although, in few cases, a convincing link between blood pressure and the candidate gene has been found (Williams and Fisher, 1997), it is obvious that the identification of genes predisposing hypertension still require continuous intensive research. In addition, essential clues for the understanding of the mode of action of their genes and their encoded proteins remain incompletely understood (Freel and Connell, 2004). In contrast to essential hypertension, a specific causal abnormality for hypertension can be found in only 10-15% of hypertensive patients (Moneva and Gomez-Sanchez, 2002) and they are diagnosed as having secondary hypertension.

Hypertension with hypokalaemia and suppression of the plasma renin activity is known as mineralocorticoid hypertension (MCH). The MCH appears now as the most common of these secondary forms of hypertension. It is a potentially reversible cause of high blood pressure, because mineralocorticoids can modulate blood pressure centrally (Gomez-Sanchez and Gomez-Sanchez, 1992). Namely, MCH may be caused by elevated aldosterone and DOC or corticosterone levels, or by a combination of both. In addition, within the past ten years, the genetic basis for several forms of MCH has been elucidated (see Table 1.1) and this research has renewed interest in the role of mineralocorticoids in the control of blood pressure.

The incidence of MCH is difficult to assess but it is probably near to 1% of all hypertensive patients (Drury, 1985). The most common cause of MCH is probably primary aldosteronism (Conn's syndrome) due to an adrenal adenoma or bilateral hyperplasia of the adrenal glands (Fardella *et al.,* 2000). Primary aldosteronism was first described by Conn in 1955 (Conn, 1955) and can be defined as overproduction of aldosterone independent of its normal chronic regulator, angiotensin II (Ang II) (Gordon *et al.,* 1994). Classically, Conn's syndrome is characterized by hypersecretion of aldosterone and by severe hypokalaemia, hypernatraemia, alkalosis and an increased renal tubular reabsorption of sodium and water. Furthermore, excessive DOC is found in patients with adrenal tumours (adenomas or carcinomas) (Nussberger, 2003). DOC-secreting tumors cause primary aldosteronism-like symptoms, show low plasma aldosterone but very high DOC levels (Egoshi *et al.,* 1998). In rare cases,

carcinoma also cause primary aldosteronism in less than 1% of patients with MCH. Moreover, the mechanisms by which the variants develop are poorly understood.

Table 1.1 Differential diagnosis of mineralocorticoid hypertension (Stewart, 1999).

Cause	Mineralocorticoid
Primary aldosteronism	
Aldosterone-producing adenoma	
Bilateral idiopathic hyperplasia	Aldosterone
Glucocorticoid-suppressible hyperaldosteronism (GSH)	
Adrenal carcinoma	
Congenital adrenal hyperplasia (CAH)	
11β-hydroxylase deficiency	DOC
17α-hydroxylase deficiency	
Glucocorticoid-receptor resistance	
Glucocorticoid receptor mutations	DOC
Metyrapone, mifepristone (RU486) ingestion	
DOC-secreting adrenal tumour	DOC
Liddle's syndrome	Not known
11β-hydroxysteroid dehydrogenase deficiency	
Apparent mineralocorticoid excess (AME)	
Liquorice and carbenoxolone ingestion	Cortisol
Ectopic corticotropin syndrome	

Another case of MCH is congenital adrenal hyperplasia (CAH). CAH is one of the most frequent inborn errors of metabolism, inherited in an autosomal recessive trait and is a group of disorders with deficiencies of specific cytochrome P450 hydroxylating enzymes. The mineralocorticoid in hypertensive forms of CAH is DOC. In the three major forms of CAH, 11β-hydroxylase deficiency (11β-OHD), 17α-hydroxylase deficiency (17α-OHD) and 21-hydroxylase deficiency, DOC production is changed, but hypertension only occurs in the 11β-OHD and 17α-OHD (Biglieri and Kater, 1991). In particular, the high DOC levels due to the 11β-OHD cause transient volume dependent hypertension, renal potassium wasting and suppression of aldosterone. In the 17α-OHD, DOC is produced in quantities sufficient to suppress the renin-aldosterone system and cause hypokalemia. Blood pressure can be severely

elevated in these disorders. A similar process is thought to explain hypertension in patients with glucocorticoid resistance due to mutations in the glucocorticoid-receptor gene (see Table 1.1).

Moreover, three monogenic forms of MCH have been described: glucocorticoid-suppressible hyperaldosteronism (GSH), Liddle's syndrome and apparent mineralocorticoid excess (AME), which have provided new insights into mineralocorticoid hormone action. In particular, GSH, also known as dexamethasone-supressible hyperaldosteronism, familial hyperaldosteronism type I, or glucocorticoid-remediable aldosteronism, is an autosomal, dominant form of MCH in which the excessive aldosterone production and clinical syndrome are corrected by the administration of glucocorticoids (Ghulam *et al.,* 2003). GSH is a cause of aldosterone excess due to the production of a hybrid gene *CYP11B1*/*CYP11B2* within the adrenal cortex. A hybrid gene is formed at meiosis from unequal crossover of the *CYP11B1* and *CYP11B2* genes, and this hybrid contains proximal components of *CYP11B1* and distal components of *CYP11B2* (Lifton *et al.,* 1992; Pascoe *et al.,* 1992). *In vitro* studies have demonstrated that specific mutations in *CYP11B2* or *CYP11B1* should also explain some forms of hyperaldosteronism (Fardella *et al.,* 1995; Fardella *et al.,* 1996; Curnow *et al.,* 1997). Many patients with monogenic forms of MCH are now known to have normal serum potassium concentrations.

Although several factors clearly contribute to the pathogenesis and maintenance of blood pressure elevation, the basis for these forms of hypertension requires an understanding of the renin-angiotensin system (RAS).

1.3 Renin-Angiotensin System (RAS)

The RAS and cyclic guanosine monophosphate (cGMP) signaling pathways (*e.g.* atrial natriuretic polypeptide/guanylyl cyclases-A) create a critical balance in blood pressure regulation (Nakao *et al.,* 1996; Kishimoto and Garbers, 1997). The RAS pathway is a principal mediator of vasoconstriction, sodium retention, and cellular proliferation. Furthermore, important alterations in the RAS have been described in heart failure, allowing the use of mechanism-specific treatments such as angiotensin converting enzyme (ACE) inhibition. Angiotensin is an oligopeptide in the blood that causes vasoconstriction and sodium retention (Lavoie and Sigmund, 2003), increased blood pressure, and release of aldosterone from the adrenal cortex. It is derived from the precursor molecule

angiotensinogen (AGT), which is a member of the serine protease inhibitor gene superfamily. Angiotensins play an important role in the RAS (see Figure 1.3).
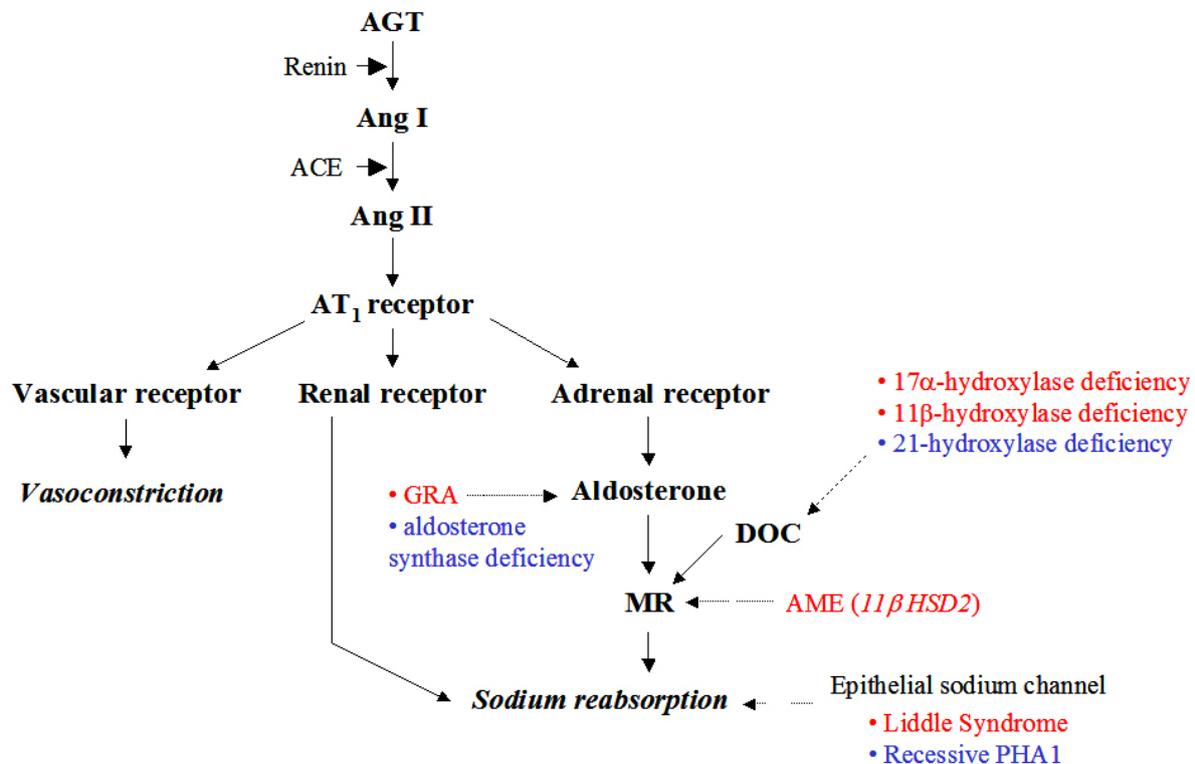
Figure 1.3 Schematic presentation of the known and possible genetic defects that can affect blood pressure by altering the activity of the renin-angiotensin-aldosterone axis or renal sodium reabsorption. Inherited diseases affecting these pathways are indicated (hypertensive disorders: **red color** and hypotensive disorders: **blue color**) (Lifton *et al.,* 2001). *GRA, glucocorticoid-remediable aldosteronism; AME, apparent mineralcorticoid excess; 11β-HSD2, 11β-hydroxysteroid dehydrogenase-2; PHA1, pseudohypoaldosteronism type 1*

Angiotensin I (Ang I) is formed by the action of renin on angiotensinogen and appears to have no biological activity and exists solely as a precursor to Ang II. Ang I is converted to Ang II through removal of two terminal residues by the enzyme ACE. Ang II is the most potent stimulus to aldosterone synthesis, which, in turn, controls sodium and water excretion on the tubules in the kidneys (Fardella and Miller, 1996). Potassium is secreted into the tubule in exchange for the sodium, which is reabsorbed. The cleavage of AGT by renin is the rate-limiting step in the RAS system. Short-term regulation (seconds to minutes) of RAS appears to be mediated through renin release by juxtaglomerular cells in the kidney, but longer-term (hours to days) through regulation of AGT synthesis by the liver and perhaps other tissues. The RAS is a hormone system and a key mechanism that helps regulate long-term blood pressure and blood volume in the body. Local regulation of RAS is independent from

circulating RAS and is important in mediating the effects of Ang II in vascular smooth muscle, the heart, and the brain (Dostal *et al.,* 1997; Sernia *et al.,* 1997).

The angiotensin receptors are a class of guanine nucleotide binding protein (G protein) - coupled receptors with angiotensins as ligands. They are important in the RAS since they are responsible for the signal transduction of the main effector hormone. Especially, the angiotensin II type-1 (AT_1) receptor is the best-elucidated angiotensin receptor. It is coupled to phospholipase C and Ang II increases the cytosolic Ca^{2+} level. It also inhibits adenylate cyclase and activates various tyrosine kinases. Effects mediated by the AT_1 receptor include vasoconstriction, aldosterone synthesis and secretion, renal tubular sodium reuptake, central osmocontrol and extracellular matrix formation. In particular, the mineralocorticoid receptor (MR) serves as the final effector molecule of the RAS in the kidney, upregulating distal nephron sodium reuptake in response to aldosterone. The MR is also expressed in extrarenal tissues such as the heart and the vascular endothelium. Although the role of the MR in regulating distal renal sodium reabsorption is established, its role in a variety of extrarenal tissues remains unclear (Mantero and Lucarelli, 2000).

1.4 Genomic and Non-Genomic Steroid Action

Steroid hormones are major determinants of both physiological and pathological processes. Alterations of steroid hormone biosynthesis and metabolism seem to be involved in the pathogenesis of several diseases (Auchus and Miller, 2001). Traditionally, steroid hormones act as chemical messengers in many species and target tissues to produce both genomic actions and non-genomic actions (Norman *et al.,* 2004).

The genomic effects of steroid hormones are mediated via several different nuclear receptors, *e.g.* the estrogen, androgen, glucocorticoid receptor (GR) or MR. According to the classic genomic mode of action, steroid hormones bind to these specific receptors, which act as ligand-inducible transcription factors (Pearce *et al.,* 2003; Sheppard, 2003). These genomic receptor-mediated effects are well investigated. In case of mineralocorticoids, they bind to the cytosolic MR. This type of receptor is activated upon ligand binding. After a hormone binds to the corresponding receptor, the newly formed receptor-ligand complex translocates itself into the cell nucleus, where it binds to many hormone response elements in the promoter region of the target genes (see Figure 1.4). As shown above, the mineralocorticoid DOC is

derived metabolically from progesterone and is converted to corticosterone and eventually aldosterone. DOC itself is a potent agonist of the MR (Sakai *et al.,* 2000) and a mild antagonist of the GR (Marks *et al.,* 1982). Corticosterone is an agonist of MR and GR, and aldosterone is an agonist of MR. Recently, it was found that the MR is also expressed in nonepithelial cells, such as cardiac and aortic myocytes, brain tissue or possibly in certain fibroblasts (Sheppard and Autelitano, 2002; Young and Funder, 2002; Sheppard, 2003; Frey *et al.,* 2004).

In contrast to the genomic action, the non-genomic actions are mediated by a wide array of cellular second-messenger systems. A non-genomic action defines any action that does not directly and initially influence gene expression, but rather drives more rapid effects such as the activation of signalling cascades: *e.g.* mitogen-activated protein kinase (MAPK), phosphatidyl-inositol-3 (PI3) kinase, PKC, cAMP, Ca^{2+} and adenylyl cyclase (see Figure 1.4). In case of mineralocorticoids, non-genomic actions of aldosterone in vitro on intracellular ion concentrations such as sodium, potassium and calcium have been demonstrated in a variety of cell types, including human mononuclear leukocytes and vascular smooth muscle cells (Wehling, 1997). Furthermore, these effects are insensitive to transcription (*e.g.* actinomycin D) inhibitors, which exclude genomic action on gene expression level. In a similar way, insensitivity to cycloheximide, a protein synthesis inhibitor, provides evidence for a non-genomic mechanism. Moreover, non-genomic action can be shown in systems lacking these classical nuclear receptors like for example by examining the effects of aldosterone in MR-knockout mice (Haseroth *et al.,* 1999), or as described in the present study.

Recently, Böhmer *et al.* (Böhmer *et al.,* 2006) used a proteomic approach to identify MR-independent effects of aldosterone as well as corticosterone in *S. pombe,* a nuclear receptor-free system. 11 proteins have been identified. Among these proteins, NAD-dependent malic enzyme and glycerol-3-phosphate-dehydrogenase are associated with a connection to osmotic regulation. Protein vip1 and glyceraldehyde-3-phosphate dehydrogenase (GAPDH) are involved in the overall organization of the cytoskeleton. In particular, GAPDH was also found to be specifically affected by aldosterone in human HCT116 cells. They suggested that these proteins may represent newly identified players and pathways of aldosterone-induced non-genomic action.

The mechanism of the non-genomic action of DOC is still unknown. In the present study, the possible connection of a related non-genomic action of DOC on protein levels will be discussed for the first time.
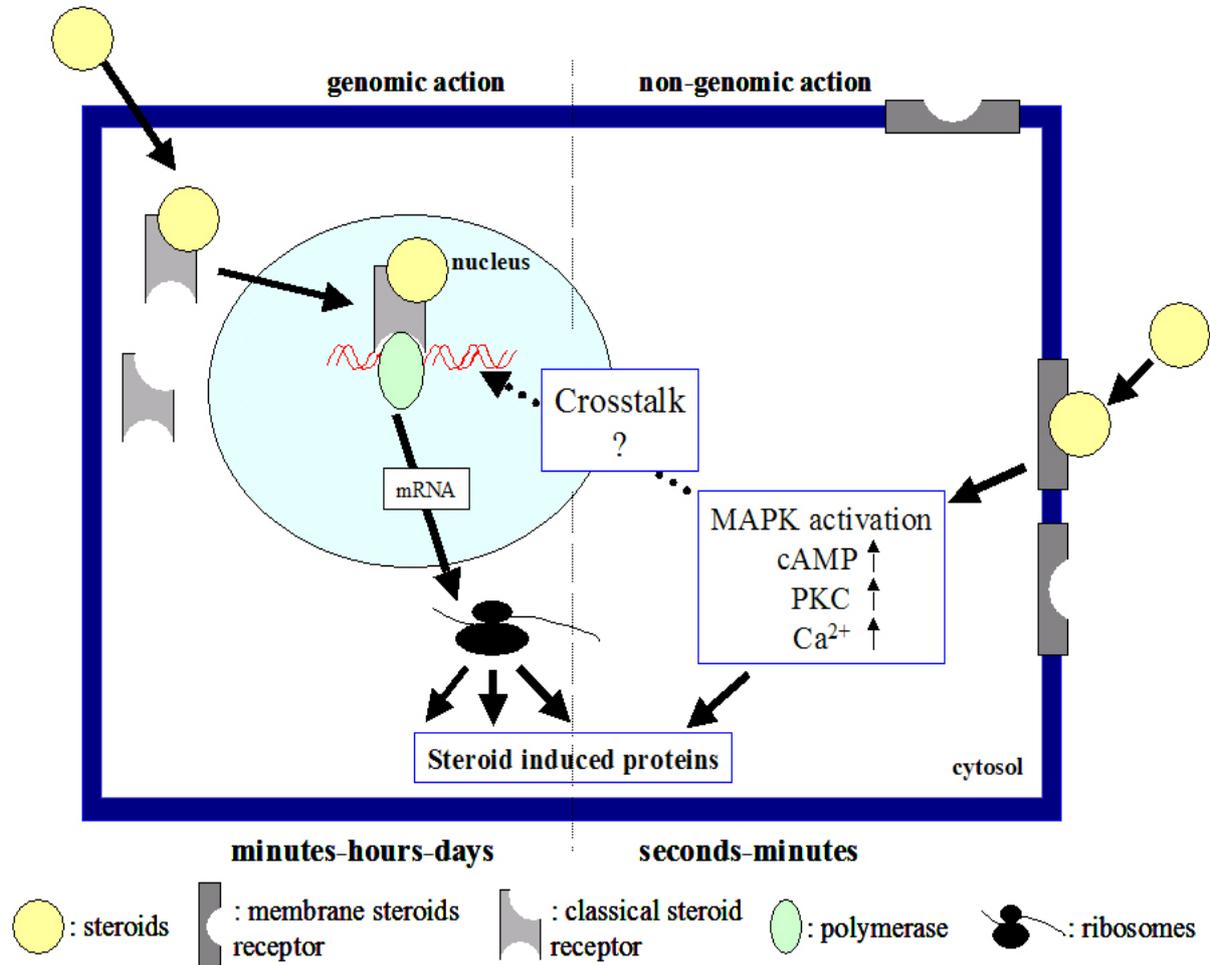
Figure 1.4 Pathways for generating biological responses by steroid hormones. Reproduced from Losel and Wehling (Losel and Wehling, 2003).

Since non-genomic action mostly involves second messengers and modulates signal-transduction pathways such as protein kinase pathways, these rapid signaling pathways can finally result in genomic effects ("crosstalk" between non-genomic and genomic action) (see Figure 1.4). Many rapid signaling messengers can indirectly modulate gene expression by action on transcription factors. The velocity can vary from seconds (*e.g.* the opening of ion channels) to an hour or so (*e.g.* the inhibition of apoptosis) (see Table 1.2) (Norman *et al.,* 2004). Although rapid responses of steroid hormones have been described on all biological levels from intracellular signaling to human physiology (see Table 1.2), it is obvious that

many aspects of rapid non-genomic action still require continuous intensive research, because essential clues for their understanding are still lacking.

Table 1.2 Examples of rapid responses for steroid hormones and related compounds (Norman *et al.,* 2004).

Steroid system	Rapid response(s)	Tissue
Oestradiol	Increase intracellular Ca^{2+}; opening of maxi-K channels	Endometrial Endothelial
	Activation of PI3 kinase linked to cardiovascular protective effects	Endothelial
	Plasma-membrane receptors signal to block apoptosis	Breast cancer cells
Androgens	Cellular Ca^{2+} influx	Splenic T cells osteoblasts
	Inhibition of apoptosis	Osteoblasts, HeLa cells
	Triggers S-phase entry via activation of SRC and PI3 kinase	NIH3T3 cells
	Testosterone or oestradiol activate the AR or ER to interact with SRC and activate MAPK to promote cell proliferation	LNCaP prostate cells
	Stimulation of intracellular Ca^{2+} release and MAPK	Skeletal muscle myotubes
Progesterone	Cellular maturation	*Xenopus* oocytes
	Activation of PI3 kinase by nuclear progesterone receptor	*Xenopus* oocytes
	Liganded PR forms a heterodimer with the ER which in turn forms a ternary complex with c-SRC to activate the MAPK pathway.	T47D breast cancer cells
	Ca2+ influx linked to the acrosome reaction	Spermatozoa
1α, 25(OH)2-vitamin D3	Opening of voltage-gated Ca^{2+} and Cl^- channels	Osteoblasts
	Activation of PKC and PI3 kinase	Cartilage Endothelial
	Stimulation of insulin secretion	Pancreas
	Activation of MAPK linked to cell differentiation	Leukemia cells
Glucocorticoids	Inhibition of nicotine-induced Ca^{2+} influx through a G protein–PKC pathway	PC-12 cells
	Stimulation of mating response in male newts	Newt salamanders
Mineralocorticoids	Rapid effects of aldosterone	Working rat heart; positive inotropic action
Thyroid hormones	Activation of MAPK by a G protein-coupled receptor	HeLa cells
	Shortening of action potentials	Rat ventricular myocytes
	Stimulates oxygen consumption	Rat ventricular myocytes
	Activation of PKA and PKC are linked to interferon-γ-induced antiviral activity	HeLa cells
PPAR	None yet clearly identified	
Retinoids	None yet clearly identified	
Brassinosteroids	Stimulation of H_2O_2 production in 30 min	*Arabidopsis*

AR, androgen receptor; ER, estrogen receptor; PR, progestin receptor; PPAR, peroxisome proliferator-activated receptor.

1.5 Proteomic Research (Proteomics)

Although the human genome project is providing a wealth of information about the sequences of individual genes, yet much information, such as the expression, function and regulation of proteins encoded by an organism, cannot be obtained from the study of genes alone. Furthermore, it is impossible to elucidate mechanisms of disease, aging and effects of the environment solely by studying the genome (Graves and Haystead, 2002). Only through the study of proteins, it is possible to understand how they are altered in disease states, and how they differ in various cell types. Thus, the focus of research is now moving to the immense task of identifying the structure, function, and interactions of the proteins produced by individual genes and their roles in specific disease processes.

In 1995, the global analysis of cellular proteins has been termed proteomics and is a key area of developing research in the post-genome era. Proteomics was defined as the study of the proteome, *i.e.* the entire protein complement of a cell line, tissue, or organism (Wasinger *et al.,* 1995; Anderson and Anderson, 1996; Wilkins *et al.,* 1996). Today, two definitions of proteomics are encountered. The first is the more classical definition, restricting the large-scale analysis of gene products to studies involving only proteins. The second and more inclusive definition combines protein studies with analyses that have a genetic readout such as mRNA analysis, genomics, and the yeast two-hybrid analysis (Pandey and Mann, 2000). Using the more inclusive definition of proteomics, many different areas of study are now grouped under the rubric of proteomics (see Figure 1.5). These include protein expression, protein modifications, protein-protein interaction, protein localization, and protein function studies.
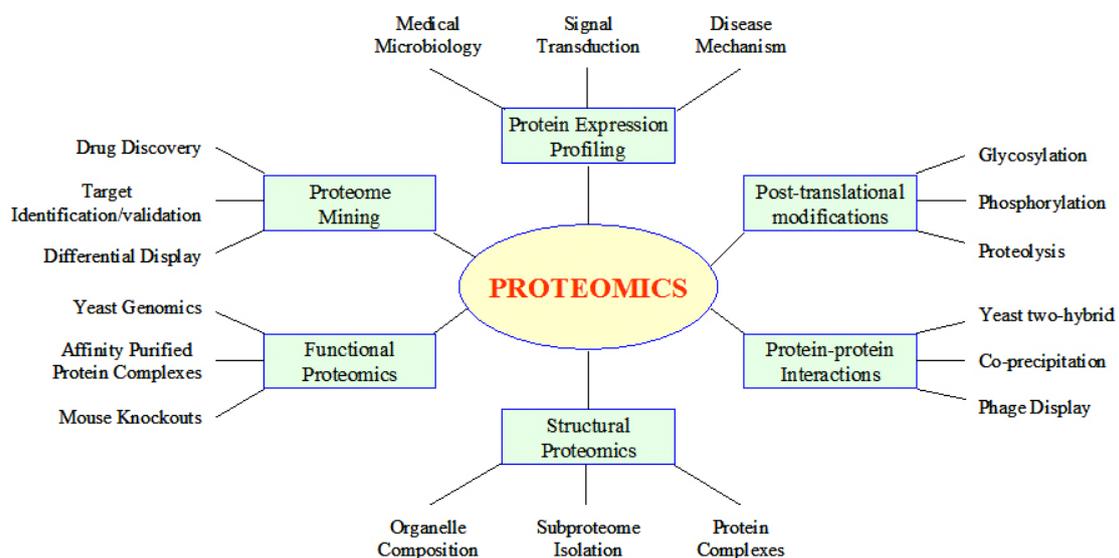
Figure 1.5 Proteomics and their applications to biology (Graves and Haystead, 2002).

Proteomics uses a combination of sophisticated techniques including two-dimensional gel electrophoresis (2-DE) to resolve, image analysis to quantify, mass spectrometry (MS) and bioinformatics to characterize proteins.

1.5.1 Two-dimensional gel electrophoresis (2-DE)

More than thirty years ago, when 2-DE was first introduced by O'Farrell (O'Farrell, 1975) and Klose (Klose, 1975), very few proteomic tools existed. This technique sorts proteins according to two independent properties in two discrete steps. The first dimension step is a seperation of the proteins in one direction by isoelectric focussing (IEF) usually in a gel strip: the charged polypeptide subunits migrate along a polyacrylamide gel strip that contains a pH gradient of an appropriate range, until they reach the pH where their net charge is zero (isoelectric focussing point or p*I*; see Figure 1.6).
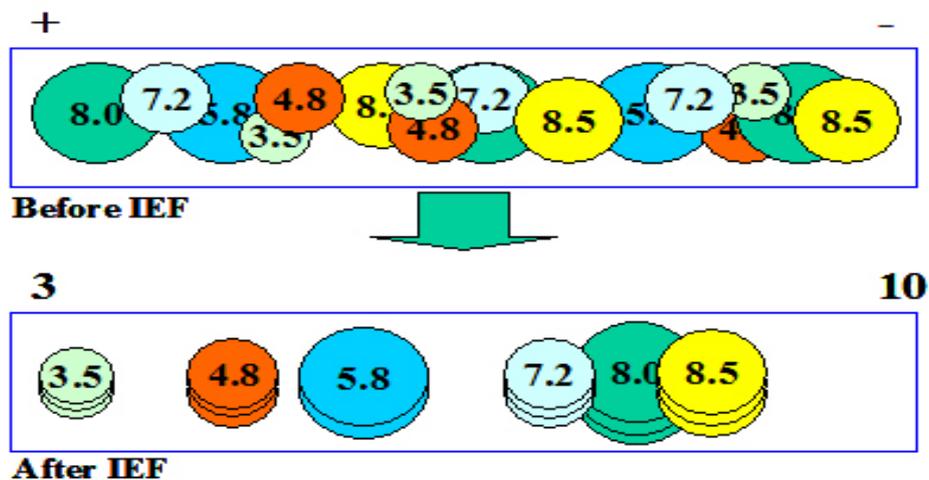
Figure 1.6 Schematic diagram showing 1st separation of proteins by IEF.

Thereafter, this process is combined with a second-dimension separation on sodium dodecyl sulfate (SDS) polyacrylamide gels. The gel strip is applied to the edge of a two-dimensional (2-D) SDS gel and the focussed polypeptides migrate in an electric field into the second gel, proteins now separating on the basis of their relative molecular mass (Mr; see Figure 1.7). Resulting protein spot patterns are conventionally presented with acidic pH to the left of the gel and low molecular weight proteins at the bottom of the gel. Using this approach, several thousands of protein species can be resolved in a single slab gel.
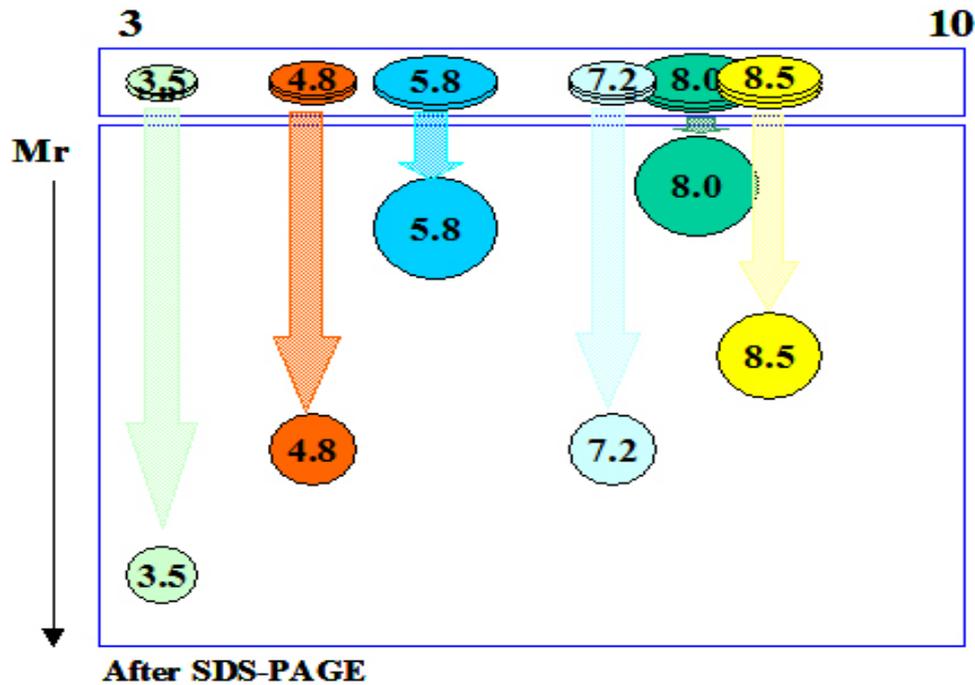
Figure 1.7 Schematic diagram showing 2nd separation of proteins by SDS-PAGE.

2-DE is currently the core technology for studying the differences in protein expression levels and their post-translational modifications between various biological samples. The power of 2-DE technique lies in its capacity to separate simultaneously thousands of proteins for subsequent protein identification and quantitative comparison studies. On the other hand, the summarized protein information itself is useful for several types of investigations and applications. These include the investigations of the interaction between components of signal transduction pathways (Fountoulakis *et al.,* 1999), the study of the primary and secondary metabolism (Hesketh *et al.,* 2002), the comparison of intracellular protein expression in different types of cells (Hayashi *et al.,* 2005), the identification of novel targets for therapeutic drugs in different types of cancers (Hanash *et al.,* 2002), and the expression of the identified proteins under various growth conditions (Hanash *et al.,* 2002).

1.5.2 Protein visualisation and Image analysis

Visualisation of separated proteins fixed in a gel is usually achieved by staining the whole gel, using coomassie blue, silver, fluorescence staining or autoradiography. The staining methods should provide high sensitivity. Therefore, the staining methods ideally possess a high

dynamic range. In addition, it is advantageous if the staining method used is compatible with subsequent protein identification by MS.

Traditionally, protein staining following gel electrophoresis is performed using coomassie brilliant blue (CBB), however this has very limited sensitivity. CBB stained spots are excised from the electrophoresis gel or the blotting membrane with a scalpel. These spots can be subjected directly or after cleavage to identify the contained proteins (*e.g.* Edman degradation using a gas phase amino acid sequence analyzer, amino acid composition analysis, or MS).

While increased sensitivity can be achieved using CBB in a colloidal form, a preferred alternative is silver staining of polyacrylamide gels. This was first introduced in 1979 by Switzer (Switzer *et al.,* 1979) and quickly became very popular due to its high sensitivity (approximately 10-100 times more sensitive than various coomassie blue staining techniques). Consequently, this is the method of choice when very low amounts of protein have to be detected on electrophoresis gels. A huge number of silver staining protocols have been published, based on the silver nitrate staining technique of the Merril method (Merril *et al.,* 1981) and modifications of the Blum method (Blum, 1987). Coomassie or silver staining, which are all compatible with MS analysis, can visualize proteins. Although glutaraldehyde in the sensitization step of silver staining could be required for high sensitivity, it can interfere with subsequent identification by MS. Therefore, to achieve optimal MS analysis of silver stained proteins, glutaraldehyde must be eliminated from the sensitization step.

Recently, much effort has been put in investigating the compatibility of fluorescence stains (Sypro Ruby) with MS: Sypro Ruby demonstrates a broad linear dynamic range and enhanced recovery of peptides from in-gel digests for matrix assisted laser desorption/ionization-time of flight (MALDI-TOF) MS.

The major advantage of the 2-DE technique is that it allows the study of differences in protein expression levels and their post-translational modifications between various biological samples. The 2-DE coupled with various MS technologies enables the simultaneous separation, visualization and identification of more than thousand proteins at different modification states (Yates, 1998; Stoll *et al.,* 2002; Templin *et al.,* 2002). No other method is able to achieve this with a similar resolution at the present time.

In order to reveal differential protein expression across multiple experiments, the quantitative analysis of numerous sets of gels after staining is sequenced. The evaluation and comparison of the complex 2-D patterns with the eye is impossible. Therefore, the gel images have to be converted into digital data with a scanner or camera. It is important to acquire the image as a

gray-scale TIFF file with adequate resolution. Thereafter, the gel images can be analysed with a computer. Several software packages have been developed to facilitate rapid, accurate and objective analysis of 2-D gels. Most of the original computer systems have matured into commercial packages, *e.g.* PDQuest (Bio-Rad) and ImageMaster (Amersham Biosciences).

A standard computer-assisted analysis of 2-D gels includes at least the following three basic steps: protein spot detection, spot quantitation and gel-to-gel matching of spot patterns. The most important step is the protein spot detection, where different parameters have to be optimised: *e.g.* size of pixel matrix used for detection, sensitivity to include small spots, and background factor. The next step is spot quantitation which can be tested by analyzing artificial gels containing spots with known volumes. The last step, spot matching can be tested by aligning distorted gels with undistorted original ones. In practice, there are many sources of systematic and random variations inherent in 2-DE experiments, which affect the efficiency of the algorithms to cope with the analysis task.

1.5.3 Mass Spectrometry (MS)

Although 2-DE can effectively separate all the component proteins of a proteome, providing quantitative data, protein identification and function remain unknown. MS is a venerable technique whose beginnings date back to the early days of the last century. MS is an analytical technique that measures an intrinsic property of a molecule based upon the motion of a charged particle in an electric or magnetic field. Therefore it is used in a wide range of applications. MS enables protein structural information, such as peptide masses or amino acid sequences, to be obtained. The sample molecules are converted into ions in the gas phase and separated according to their mass to charge (m/z) ratio. Positively and negatively charged ions can be formed. The basic components of all mass spectrometers are the same; they all must possess an ionization source, a mass analyzer and a detector (see Figure 1.8). The ionization source creates ions from the sample to be analyzed. Mass analyzers measure the m/z ratio of gas-phase ions generated from the ionization source. The detector determines the mass of the ions.

Biomolecules being large and polar are not easily transferred into the gas phase and ionized. Beginning in the 1980s and on a larger scale in the 1990s, MS has played an increasingly significant role in the biological sciences. MALDI (Karas and Hillenkamp, 1988) and

electrospray ionization (ESI) (Fenn *et al.,* 1989) are the two most common types of ionization techniques. Thus, MS has become an important technology for proteomics and the technology of choice for the identification of the proteins and mapping of post-translational modifications.
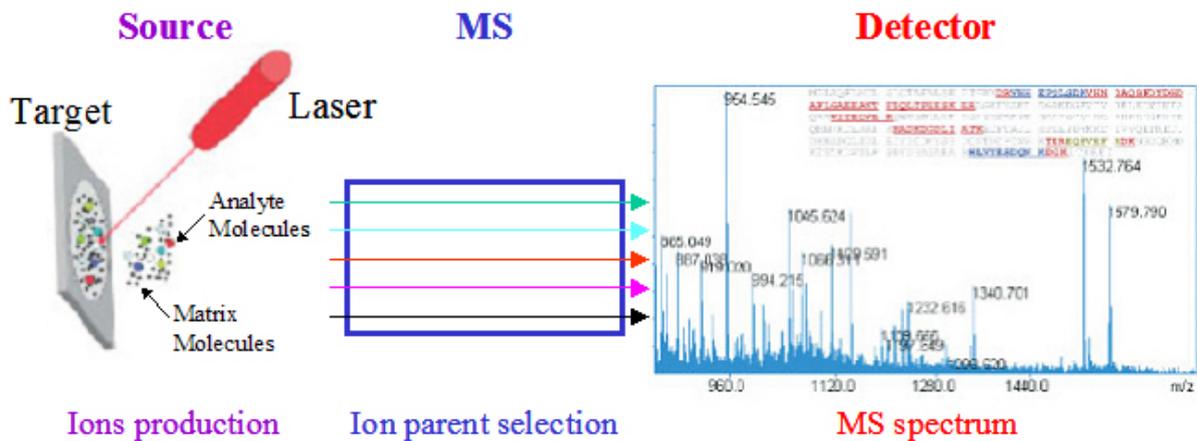
Figure 1.8 Schematic diagram showing the basic components of all MS.

MALDI, developed by Karas & Hillenkamp in the late 1980s (Karas and Hillenkamp, 1988), is one of the two ionization methods, which produces quasimolecular ions of large organic molecules of up to several 100 kDa molecular mass. TOF mass spectrometers are possibly the simplest mass analyzers by principle, and are ideally suited for MALDI ion sources. The ability of the MALDI technique in analyzing different classes of biomolecules has been thoroughly demonstrated (Kaufmann, 1995; Mann and Talbo, 1996). Work with biomolecules almost exclusively uses matrices of α-cyano-4-hydroxy-cinnamic acid (CHCA) or dihydrobenzoic acid (DHB). MALDI creates ions by using a small nitrogen laser (at 337 nm) to excite a crystalline mixture of analyte molecules and energy absorbing matrix into the gas phase.

ESI has been developed for use in biological MS by Fenn *et al*. (Fenn *et al.,* 1989). It can analyse a wide range of compounds, including proteins, oligonucleotides, sugars, and polar lipids. Electrospray (ES) is typically performed in either the infusion mode, the nanoelectrospray (nanoES) format, or in combination with high-performance liquid chromatography (LC). NanoES (Wilm and Mann, 1996; Wilm *et al.,* 1996) is a miniaturized version of ES that operates without pumps and at very low flow rates in the range of a few

nanoliters per minute. Samples have to be substantially free of salt and detergent, but can conveniently be cleaned up in a reversed-phase packing loop in the injector valve. Namely, ESI allows for constant ionization and monitoring but is more sensitive to contaminating salts, buffers, and detergents than MALDI. ESI utilizes a potential difference between a capillary and the inlet of the MS to cause charged droplets to be released from the tip of the capillary.

Several types of mass analyzers are utilized for proteomic analysis: including quadrupoles, ion traps, time of flight (TOF) and fourier transform ion cyclotron resonance type analyzers. The type of single stage MS that has found the widest application in proteomics is the TOF mass analyzer, which measures the *m/z* ratio of an ion by the time it takes to progress through a field-free region to the detector (see Figure 1.8). Both MALDI and ESI are used to create ions for analysis by TOF.

The tandem mass spectrometry (MS/MS), which is particularly useful in proteomics, is able to select a particular ion, fragment it within a collision cell, and then detect the resulting fragment ions (see Figure 1.9). Thus, additional structural information is obtained about the selected precursor ion; in the case of peptide length fragments, actual amino acid sequence data can be deduced. The primary advantage of a MS/MS is the ability to select a particular precursor ion from a mixture of ions. In addition, hybrid instruments incorporating one type of analyzer with another (*e.g.* quadrupole-TOF) have also been utilized with great success.
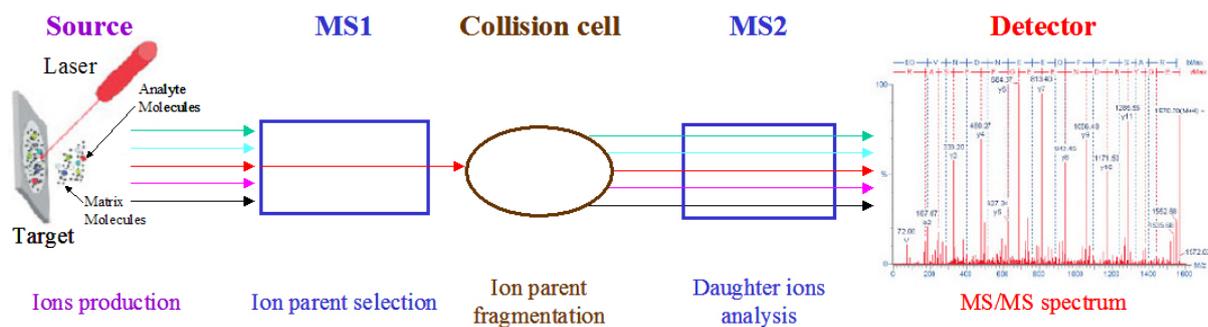
Figure 1.9 Schematic diagram showing the MS/MS.

1.6 The fission yeast Schizosaccharomyces pombe *as a model system*

First described in 1893 by P. Lindner, *Schizosaccharomyces pombe* (*S. pombe*) was named after 'pombe', the Swahili word for beer, since it was originally isolated in millet beer from

eastern Africa. The fission yeast S. pombe is a unicellular eukaryote belonging to the Ascomycetes (Sipiczki, 2000). It was called fission yeast because it only reproduces by means of fission, besides spores. The whole genome of *S. pombe* is only slightly bigger in size than that of *S. cerevisiae*. The 13.8 Mb genome of *S. pombe* is distributed between chromosomes I (5.7 Mb), II (4.6 Mb) and III (3.5 Mb) (Smith *et al.,* 1987), together with a 20 kilobase (kb) mitochondrial genome (Lang *et al.,* 1987).

S. pombe cells are cylindrical, oval or round, with a diameter of 3-4 µm and a length of up to 7-15 µm (see Figure 1.10), but upon starvation the cells shorten and could easily be mistaken for *Saccharomyces* cells.
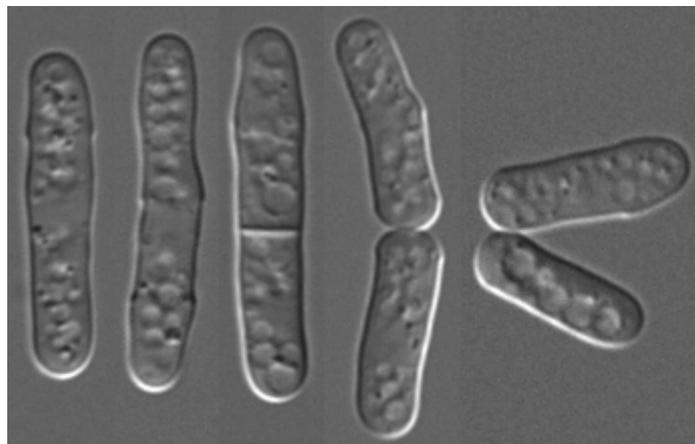
Figure 1.10 Picture of the fission yeast *Schizosaccharomyces pombe* from Steve's place (see http://www.steve.gb.com/science/model_organisms.html).

It has been more than 10 years since *Saccharomyces cerevisiae* (*S. cerevisiae*) has been completely sequenced as the first eukaryotic genome (Goffeau *et al.,* 1996). Till now, 48 eukaryotic genomes have been completely sequenced (http://www.genomesonline.org/ gold.cgi?want=Published+Complete+Genomes). In particular, the fission yeast has only 4824 different genes (Wood *et al.,* 2002), which is significantly less than the number of genes in the human genome (about 23,000) (Pennisi, 2003). It is also substantially lower than the 6200 different genes found in *S. cerevisiae*.

The main benefit of a single cell eukaryote is its amenability to genetic analysis. This is particularly applicable to *S. pombe* because of its ease of growth, haploid lifestyle and the fact that it is amenable to molecular analysis. It is well-known that some features such as cell cycle, chromosome structure, and ribonucleic acid (RNA)-splicing are more similar between

mammalian cells and *S. pombe* than between mammalian cells and *S. cerevisiae* (Moreno *et al.,* 1991). Moreover, for several aspects described in (Remacle *et al.,* 1997), such as cell cycle control and heat shock response, the fission yeast seems to be more closely related to mammalian cells than the budding yeast. For example, work done in *S. pombe* has greatly improved our understanding of the eukaryotic cell cycle (Nurse, 2000) and its regulation (Moser and Russell, 2000), and contributed to our knowledge of many related areas, such as microtubule formation (Hagan and Petersen, 2000), cellular morphogenesis (Brunner and Nurse, 2000), stress response mechanisms (Toone and Jones, 1998), and the response to deoxyribonucleic acid (DNA) damage (Zhou and Elledge, 2000).

Another advantage of studying this yeast is that its cellular signaling pathways are similar to those of humans (Wood *et al.,* 2002), e.g. MAPK and DNA checkpoint-signaling pathways. MAPK are expressed in all eukaryotic cells and regulate a variety of cellular functions, including gene expression, cellular homeostasis, and differentiation in response to different extracellular stimuli (Herskowitz, 1995; Schaeffer and Weber, 1999; Widmann *et al.,* 1999; Nguyen *et al.,* 2002; Rodriguez-Gabriel and Russell, 2005). In addition, the DNA checkpoint-signaling pathway induces a cell cycle arrest in response to DNA damage. Many of the proteins involved in this pathway in all eukaryotes from yeast to mammalian cells have been identified genetically and are well conserved throughout evolution. The study of checkpoint signaling in model systems including the yeasts *S. cerevisiae* and *S. pombe* has been useful in elucidating these pathways in mammalian cells (Latif *et al.,* 2001).

Moreover, Wood *et al.* (Wood *et al.,* 2002) reported that 50 genes associated with human diseases like cystic fibrosis, diabetes or cancer have been identified in *S. pombe*. In addition, *S. pombe* is an interesting host for recombinant protein expression (Bureik *et al.,* 2002).

Therefore, this yeast is an excellent model organism for the study of numerous biological processes such as cell cycle control, mitosis and meiosis (Fantes, 2000), DNA repair and recombination (Davis and Smith, 2001), and the analysis of checkpoint controls important for genome stability (Humphrey, 2000). Since the major signaling pathways and cellular processes are conserved between yeasts and mammalian cells, these simple eukaryotic systems could also be excellent models for the identification of molecular as well as cellular mechanisms (Perego *et al.,* 2000). The availability of the genomic sequence of this yeast as well as of new technologies (microarrays, proteomics) is expected to allow the identification of potential drug targets, since the drug discovery process is moving toward a genomic orientation.

1.7 Aim of the Work

The goals of this work consisted in the construction of a two-dimensional gel electrophoresis reference map (2-D reference map) of the proteome of the fission yeast *S. pombe* wild type h^{-S} L 972 and in the investigation of DOC induced changes on the protein pattern of the fission yeast. The fission yeast is increasingly attractive as an experimental system for investigating various gene and protein functions, especially regarding cell growth and division. *S. pombe* is a harmless and rapidly growing eukaryote. The sequencing of the fission yeast genome (only about 5,000 different genes) was completed in 2002. Another advantage studying this yeast is that its cellular signal-pathways are similar to those of humans. Considering all these reasons, *S. pombe* is a highly interesting organism for various purposes and can be used as an excellent model system since it resembles higher eukaryotes in various aspects.

The aim of the first part of this work is to establish a 2-D reference map for proteins of *S. pombe* wild type h^{-S} L 972. Investigation of this subject will be performed using a combination of 2-DE and MS. Currently, 2-DE is a powerful and the commonly used technique for the analysis of complex protein mixtures extracted from cells, tissues, or other biological samples and for obtaining a global picture of the expression levels of a proteome under various conditions. The major advantage of this technique is that it enables the simultaneous separation, visualization and identification of more than thousand proteins at different modification states (Yates, 1998; Stoll *et al.,* 2002; Templin *et al.,* 2002). The technology has successfully been applied to gain more information on the protein profile of several organisms such as *Saccharomyces cerevisiae* (Garrels *et al.,* 1994), *Escherichia coli* (VanBogelen *et al.,* 1997), *Drosophila melanogaster* (Vierstraete *et al.,* 2003) and *Candida albicans* (Hernandez *et al.,* 2004). The benefit of 2-D reference maps is that they can provide much information on the expression, function and regulation of proteins as well as a survey of proteins affected during different physiological processes such as apoptosis (Thiede and Rudel, 2004).

Steroid hormones act as chemical messengers in many species and target tissues to produce both genomic actions and non-genomic actions. The genomic actions of steroid hormones are mediated via several different nuclear receptors like the mineralocorticoid receptor (MR) in case of Aldosterone and DOC. In contrast to the genomic action, the non-genomic actions are mediated by a wide array of cellular second-messenger systems. Non-genomic actions do not

directly and initially influence gene expression, but rather drive more rapid effects such as the activation of signalling cascades: *e.g.* MAPK, PI3 kinase and PKC. Steroid hormones play an essential role in the regulation of important cellular and physiological responses in the human body. In particular, mineralocorticoids exert crucial roles in regulating sodium, potassium and water homeostasis. They contribute to the control of blood pressure and in some physiological disorders. Mineralocorticoid excess, which will arise due to increased aldosterone secretion or excessive production of DOC, causes hypertension and characteristic disturbance of the electrolyte balance as well as heart disease. In addition, DOC is known to play a role in several diseases such as congenital adrenal hyperplasia (CAH), Cushing's syndrome and adrenal tumors. In a preliminary study, a MR-independent effect on the protein pattern has been shown (Böhmer *et al.,* 2006). The aim of the second part of this work is to identify proteins that are altered due to the MR-independent action of DOC in *S. pombe*. The fission yeast *S. pombe* is choosen since it does not contain nuclear steroid receptors. In addition, the 2-D reference maps of first part can be used to facilitate the identification of proteins that have been influenced by the action of DOC. Investigation of this subject will be performed using a combination of 2-DE and MS. The different intensities of the protein spots on the 2-D gels were compared with PDQuest software.

2. Materials and Methods

2.1 Materials

2.1.1 Fission Yeast

The fission yeast *Schizosaccharomyces pombe* (*S. pombe*) wild type h^{-S} L 972 was kindly provided by the group of Prof. Kaeufer, Technical University of Braunschweig, Germany. The cells were cultured on rich medium yeast extract agar (YEA) for 3 days at 30°C (Gutz, 1974).

2.1.2 Culture Medium

The medium components (see Table 2.1) were sterilized by autoclaving for 20 min at 121 °C.

Table 2.1 Composition of media used for cell culture

YEA (Yeast Extract Agar)		EMM (Edinburgh Minimal Medium)	
Amount	Contents	Amount	Contents
2.0 g	Yeast Extract	4.0 g	Potassium Hydrogen Phthallate
12.0 g	Glucose	2.2 g	$Na_2 HPO_4$
8.0 g	Agar Agar	5.0 g	NH_4Cl
add 400.0 mL	H_2O dest.	20.0 g	D- Glucose
		add 1.0 L	H_2O dest.
		After autoclave, to add:	
		20.0 mL	Salt Stock (x50) *
		1.0 mL	Vitamin Stock (x1000) *
		0.1 mL	Mineral Stock (x10,000) *
		* see supplement	

2.1.3 Chemicals

All chemicals used were of the highest quality available. DOC was obtained from Sigma (Taufkirchen, Germany) and diluted in pure HPLC-grade ethanol. Urea was purchased from Amersham Biosciences (Freiburg, Germany) and phenylmethylsulfonyl fluoride (PMSF) from Serva (Heidelberg, Germany). 3-[(3-cholamidopropyl)dimethylamonio]-1-propane-sulfonate (CHAPS) was provided by Fluka (Buchs, Switzerland) and dithiothreitol (DTT) by dcl (Charlottetown, Canada). Iodoacetamide was obtained from Merck (Darmstadt, Germany).

2.2 Cell Culture

A single grown colony of *S. pombe* on YEA media was moved to 50 mL reaction-tube containing 10 mL volumes of EMM and was incubated for 24 hours (hr) with shaking (at 185 rpm) at 30°C. For the main culture, 10 mL of the precultured cells were moved to 250 mL Erlenmeyer flask containing 55 mL volumes of fresh EMM and were cultivated for 18 hr with shaking (at 185 rpm) at 32°C (Moreno *et al.,* 1991). All cultures were stopped at the mid-exponential growth between 2×10^6 and 3×10^6 cells/mL. The concentration of the cells was measured at OD_{600}. The optical density (OD) of a culture can be used to measure the concentration of cells, $OD_{600} = 0.1$ corresponds to approximately 2×10^6 cells/mL (this wavelength measures light scattering).

For differential analysis, the main culture was then divided into 6 aliquots of 10 mL in 50 mL reaction-tubes (Moreno *et al.,* 1991). Each experiment contained each two samples with different concentrations (2, or 8 µM) of DOC solved in ethanol as well as two control samples (just ethanol of same volume). Cells were incubated for 3.5 hr at 32°C and 185 rpm.

2.3 Preparation of whole-cell protein extract

10 mL of culture medium was centrifuged for 5 min at $5000 \times g$ (Sigma 2K15, Rotor Nr. 19776; St. Louis, MO, USA) at 4°C and the pellet was washed with ice-cold water followed by centrifugation at $5000 \times g$ for 5 min. In order to solubilize proteins, the pellet was then resuspended in 700 µL of lysis buffer (see Table 2.2). Glass beads (2 mL) as well as PMSF

(final concentration : 1 mM) were added. The tubes were than vortexed 6 times for 30 sec and chilled on ice in between. After centrifugation for 5 min at 3500 × g at 4°C, the supernatant was transferred in 1.5 mL reaction tubes, centrifuged for 5 min at 13000 rpm (Sigma 2K15, Rotor Nr. 12153; St. Louis, MO, USA) at 4°C and splitted to appropriate volumes before storage at -80°C.

Table 2.2 Components of buffer used for protein lysis

Contents	Final concentration	Amount
Urea	9.0 M	5.4 g
CHAPS	4.0%	400 mg
DTT	1.0%	100 mg
IPG Buffer 3-10 or 4-7	2.0%	200 µL
Millipore-H_2O		add 10 mL

2.4 Determination of the protein concentration

2-DE samples represent a particularly difficult quantification challenge due to the possible presence of interfering carrier ampholyte and thiourea in addition to the detergents and reductants typically used in sample preparation for electrophoresis. In this study, Ettan 2-D Quant Kit (Amersham Biosciences) was used to measure the protein concentration in samples. The assay is based on the specific binding of copper ions to protein. Precipitated proteins are resuspended in a copper-containing solution and unbound copper is measured with a colorimetric agent. The absorbance of each sample and bovine serum albumin (BSA) standard solution were determined at 480 nm using millipore-water as a reference.

2.5 Two-dimensional gel electrophoresis (2-DE)

Isoelectric focusing (IEF) (first dimension) was conducted using the Ettan IPGphor-System (Amersham Biosciences) with the Ettan IPGphor Strip Holder (Amersham Biosciences) or the Ettan IPGphor Manifold (Amersham Biosciences). The second dimension was performed on the Ettan DALT*twelfe* (Amersham Biosciences).

2.5.1 Rehydration

The immobilized pH gradient (IPG) gel strips with a linear separation range of pH 3-10 (18 cm, 17-1234-01, Amersham Biosciences) or pH 4-7 (18 cm, 17-1233-01, Amersham Biosciences) were rehydrated overnight at room temperature in the Immobiline DryStrip Reswelling Tray (Amersham Biosciences). 340 µL of the rehydration solution (see, Table 2.3) without the sample is applied to the reservoir slots of the Reswelling Tray, and then the IPG strips are soaked individually. Strips were prevented from dehydration and oxidation by covering with mineral oil (PlusOne Immobiline DryStrip Cover Fluid, Amersham Biosciences).

Table 2.3 Components of the rehydration solution with IPG Buffer

Contents	Final concentration	Amount
Urea	8.0 M	9.6 g
CHAPS	1.0%	200 mg
DTT	0.4%	80 mg
IPG Buffer 3-10 or 4-7	0.5%	100 µL
Bromophenol blue	0.002%	50 µL 1% solution
Millipore-H_2O		add 20 mL

2.5.2 Isoelectric focussing (IEF)

The rehydrated IPG strips were placed in the Ettan IPGphor Strip Holder for analytical gels or in the Ettan IPGphor Manifold (Amersham Biosciences) for preparative gels. Thereafter, the samples were cup-loaded at the anode and the proteins were separated on the basis of their p*I*. The IEF was carried out at 20 °C with the IPGphor-System, covered with mineral oil, for 29,650 Vhr (volt × hours) (between 20 and 80 µg protein per strip; see Table 2.4) or for 45,015 Vhr (between 180 and 240 µg protein per strip; see Table 2.5).

During the IEF, the filter papers were exchanged four time (see Table 2.4 and 2.5). After IEF, the Strips were frozen at -20°C until needed.

Table 2.4 The IEF protocol for the analytical gels

IEF Parameters	20°C	50 μA/strip		
Type	Hours (hr)	Volt (V)	Vh	filter papers change
1	Step	1 hr	150 V	150	Yes
2	Step	2 hr	300 V	600	Yes
3	Step	1 hr	600 V	600	Yes
4	Gradient	1 hr	600 – 8,000 V	4,300	Yes
5	Step	3 hr	8,000 V	24,000	No
	Total	8 hr		29,650	

Table 2.5 The IEF protocol for the preparative gels

IEF Parameters	20°C	50 μA/strip		
Type	Hours (hr)	Volt (V)	Vhr	filter papers change
1	Step	6 hr	30 V	180	No
2	Step	6 hr	60 V	360	No
3	Step	1.5 hr	150 V	225	Yes
4	Step	3 hr	300 V	900	Yes
5	Step	1.5 hr	600 V	900	Yes
6	Gradient	1.5 hr	600 – 8,000 V	6,450	Yes
7	Step	4.5 hr	8,000 V	36,000	No
	Total	24 hr		45,015	

2.5.3 Preparation of polyacrylamide gels

Prior to preparation of the polyacrylamide gel solutions, the Ettan DALT Gelcaster (Amersham Biosciences) was prepared. For the separation on the second dimension, the 12.5% polyacrylamide gel solutions (see Table 2.6) were prepared.

Table 2.6 12.5% polyacrylamide gel solutions

Contents	Amount
40% w/v Protogel (Biozym)	271 mL
Millipore-H_2O	259 mL
1.5 M Tris/HCl, pH 8.8	162.5 mL
10% w/v SDS	6.5 mL
10% w/v APS	6.5 mL
TEMED	216.5 µL

Finishing, ammonium persulfate (APS) and *N,N,N',N'*-tetramethylethylenediamine (TEMED) were added to the solution. Thereafter, the solution was casted quickly through a tube into the gel caster. In addition, displacing solution (see Table 2.7) was casted quickly through a tube into the gel caster. Each gel was overlaid with 4 ml of a butanol - millipore water mix solution (10:1) to obtain a uniform gel surface. After 3 hr at room temperature, the gels were polymerised and the overlaid deionized water was removed. Thereafter, the gels were stored in soaked papers with storage-solution (see Table 2.8) at 4°C until the use.

Table 2.7 Components of the displacing solution

Contents	Amount
1.5 M Tris-HCl, pH 8.8	25 mL
99% glycerol	50 mL
Millipore-H_2O	25 mL
Bromophenol blue	trace

Table 2.8 Components of the storage-solution

Contents	Amount
1.5 M Tris-HCl, pH 8.8	250 mL
10% SDS	10 mL
Millipore-H_2O	740 mL

Table 2.9 Components of the equilibration solution

Contents	Final concentration	Amount
1.5 M Tris-HCl, pH 8.8	0.05 M	6.7 mL
urea	6 M	72 g
99% glycerol	30%	61 mL
SDS	2%	4 g
Millipore-H_2O		add 200 mL

2.5.4 Equilibration

Prior to separation in the second dimension, the IEF gels (IPGs) were equilibrated twice under mild shaking for 15 min in 10 ml equilibration solution (see Table 2.9), first with an addition of 65 mM DTT (reduction step), and finally with 135 mM iodoacetamide (alkylation step). Excess of equilibration solution was removed by briefly dipping the IEF gels into deionized water.

2.5.5 SDS-Polyacrylamide gel electrophoresis (PAGE)

The Ettan DALT*twelfe* (Amersham Biosciences) was filled with $1 \times$ electrophoresis buffer (prepared from $10 \times$ electrophoresis buffer: see Table 2.10). The casting cassettes (containing the polymerized gels) were shortly washed with deionized water to remove gel pieces and put into the separation chamber of the Ettan DALT*twelfe* (Amersham Biosciences). Thereafter, the IPG strips were placed directly onto the acrylamide gel surface and remaining air bubbles between both gels were removed. 20 µL protein marker (prestained, broad range, NEB) dropped on a piece of filter paper (markerpad) and a dried markerpad were also placed onto the acrylamide gel surface by the Strips. Strips and markerpad were covered air bubble free with heated agarose-sealing solution (at 60 °C, see Table 2.11). Finally, the 2-D gels were overlaid with $2 \times$ electrophoresis buffer (prepared from $10 \times$ electrophoresis buffer: see Table 2.10) and the proteins were separated 45 min at 25 °C with 5 W per gel (Ettan DALT II system, Amersham Biosciences) and afterwards with 15 W per gel until the bromophenol blue front reached the bottom of the gel.

Table 2.10 Components of electrophoresis buffer (10 ×)

Contents	Amount
Tris	60.4 g
Glycine	288.4 g
SDS	20 g
Millipore-H$_2$O	add 2 L

Table 2.11 Components of agarose-sealing solution

Contents	Amount
Agarose	125 mg
Electrophoresis buffer (1 ×)	25 mL
Bromophenol blue	trace

2.6 Protein staining

2.6.1 Analytical gels

After electrophoresis was completed, the gels were silver stained according to Blum (Blum, 1987) with slight modifications. The gels were fixed in solution 1 (see Table 2.12) for at least 1.5 hr under mild shaking on a IKA$^®$ KS 260 basic (IKA$^®$-WERKE, Germany) and were shortly rinsed with Millipore-H$_2$O to remove the fixation components. After that, gels were shaked for 20 min in solution 2a (see Table 2.12) followed by 20 min incubation using solution 2b (see Table 2.12). After this step, the gels were washed 3 times for 20 min in Millipore-H$_2$O. The gels were incubated in solution 3 (see Table 2.12) for 2 min, and were washed 3 times for 30 sec in Millipore-H$_2$O. Thereafter, the gels were incubated in solution 4 (see Table 2.12) for 20 min and then washed 3 times for 30 sec in Millipore-H$_2$O. Subsequently, the gels were developed in solution 5 (see Table 2.12) for a maximum of 10 min and then washed 3 times for 30 sec in Millipore-H$_2$O. The staining reaction was stopped by incubating the gels in Solution 6 (see Table 2.12) for 10 min. Finally, the gels were fixed in solution 7 (see Table 2.12) for 30 min and were placed in solution 8 (see Table 2.12) for 30 min. The silver stained gels were then slowly dried on a gel dryer (Model 583 gel dryer, Bio-

Rad) and afterwards scanned (Image Scanner UMAX, Amersham Biosciences). The scanned images of the analytical gels were analysed for spot detection and Mr/p*I* calibration with PDQuest version 7.2 (Bio-Rad).

Table 2.12 Scheme for the fixation and silver staining

	Amount	**Contents**	**Comments**
Solution 1	1000 mL	Methanol	
	240 mL	Acetic acid	
	1250 µL	HCOH	
	add 2 L	Millipore-H_2O	
Solution 2a	750 mL	Ethanol	50% Ethanol
	add 1.5 L	Millipore-H_2O	
Solution 2b	375 ml	Ethanol	25% Ethanol
	add 1.5 L	Millipore-H_2O	
Solution 3	300 mg	$Na_2S_2O_3$	Freshly prepare ! keep 30 ml for solution 5
	1.5 L	Millipore-H_2O	
Solution 4	3 g	$AgNO_3$	Freshly prepare !
	1140 µL	HCOH	
	1.5 L	Millipore-H_2O	
Solution 5	90 g	Na_2CO_3	Freshly prepare !
	30 mL	Solution 3	
	750 µL	HCOH	
	ad 1.5 L	Millipore-H_2O	
Solution 6	750 mL	Methanol	
	90 mL	Acetic acid	
	660 mL	Millipore-H_2O	
Solution 7	450 mL	Methanol	30% Methanol
	add 1.5 L	Millipore-H_2O	
Solution 8	200 ml	3% Glycerol	Prepare out of stock solution (30%)

2.6.2 Preparative gels

The preparative gels were stained with colloidal blue G-250 (Sigma) (Tryoen-Toth *et al.*, 2003). The gels were fixed three times for 30 min with solution A (see Table 2.13). Gels were

rinsed 3 times for 20 min with solution B (see Table 2.13) and then equilibrated with a solution C (see Table 2.13) for 30 min. Colloidal Blue G (Sigma) was added to the solution C at a final concentration of 0.02%. Gels were stained for 24 - 36 h, washed with water to decrease background, and scanned. Finally, the protein spots were carefully excised in order to avoid keratin contaminations and stored at -20°C until mass spectrometry analysis. After scanning, a part of the preparative gels were additionally silver stained according to Blum with slight modifications (Blum, 1987). This additional step was performed in order to compare the protein pattern on both gel type *i.e.* analytical and preparative gels.

Table 2.13 Scheme for the fixation and colloidal blue G staining

	Contents	**Final concentration**	**Amount**
	Ethanol	30%	450 mL
Solution A	Phosphoric acid	2%	37.5 mL
	Millipore-H$_2$O		add 1.5 L
Solution B	Phosphoric acid	2%	375 ml
	Millipore-H$_2$O		aad 1.5 L
	Ethanol	18%	270 mL
Solution C	Phosphoric acid	2%	37.5 mL
	Ammonium sulfate	15%	225 g
	Millipore-H$_2$O		aad 1.5 L

2.7 Image detection and analysis

Silver or colloidal blue-stained 2-D gels were scanned (300 dpi resolution) with an Image Scanner UMAX (Amersham Biosciences) and Photoshop (Version 5.0 LE, Adobe Systems) software. The gel images were saved (∗.TIFF files) and analyzed with the Discovery Series PDQuest™ (Version 7.2.0) 2-D gel analysis software (Bio-Rad).

PDQuest software displays the digital data on a personal computer monitor screen in the form of a gray scale. This data-object (spot) is composed of individual screen pixels. The total intensity of a spot is the sum of the intensities of all of the pixels that comprise that spot. The mean intensity of a spot is the total intensity divided by the number of pixels in the object. If

the mean intensity is larger by a given ratio (determined by the sensitivity parameter) than the background, this object is marked as a spot.

The size and orientation of each gel image was adjusted with the cropping and rotating tools in the image menu. Spots were detected by following the PDQuest software instructions. The spots on one gel were detected with the spot-detection wizard, and afterwards four gels belonging to the same replicate group were processed. The spot-detection wizard automates the process of selecting the proper spot-detection parameters for each gel. These parameters were adjusted until most (generally 95%) of the spots of interest were identified in the gel. After spot detection, three separate images are created: the original unaltered scan (2-D scan), the filtered and processed scan (filtered-image), and the synthetic image that contains the Gaussian spots (Gaussian-scan image) with a defined volume and quality. All of the spot matching and analysis was performed on the Gaussian spots. Within a matchset, the protein spots from the different gels were matched to each other, and were included in a synthetic image called the matchset standard.

By entering Mr and pI values for a few known spots, the software offers the possibility to calculate the Mr and pI values of all spots on the 2-D gels.

2.8 Spot Quantification

For quantitative analysis, gels were silver-stained. All spot values were normalized according to total density in the gel image, which allows the precise comparison of gels even with different (high and low) backgrounds. Five gels (control and 8 µM DOC), which were run in parallel, were analyzed. After automated detection and matching, manual editing was carried out. Five gels of each sample were used to create "replicate groups". Qualitative, Quantitative and Statistical "Analysis Sets" were created between control group and treated group. In the Quantitative Analysis Sets, the upper limit and the lower limit were set to 2 and 0.5, respectively. In the Statistical Analysis Sets, the Student's t-test with significance level of 95% were chosen. Only spots displaying reproducible change patterns was considered to be differentially expressed proteins. Spot volumes were compared with "master gel" for each matched spot, and data were analyzed in Excel.

2.9 Spot Excision und Digestion

Finally, the protein spots shown to be different in 8 µM DOC samples compared to the control were cut out of the preparative gels by using pipette tips or a dissection needle with caution to avoid keratin contamination and stored at - 20 °C until mass spectrometry analysis.

In-gel digestion[**] was performed with an automated protein digestion system, MassPREP station (Waters, Milford, MA). The gel plugs were washed twice with 50 µL of 25 mM NH_4HCO_3 and 50 µL of acetonitrile (ACN). The cysteine residues were reduced by 50 µL of 10 mM DTT at 57°C and alkylated by 50 µL of 55 mM iodoacetamide at room temperature. After dehydration with ACN, the proteins were digested in gel with 8 µL of 12.5 ng/µL of modified porcine trypsin (Promega, Madison, WI) in 25 mM NH_4HCO_3 (freshly diluted), at room temperature overnight. The generated peptides were extracted with 60% ACN in 5% formic acid. The peptide extracts were used for MALDI-TOF-MS as well as nanoLC-MS/MS analysis.

2.10 Mass Spectrometry analysis

2.10.1 Matrix Assisted Laser Desorption/Ionization-Time of Flight-Mass Spectrometry (MALDI-TOF-MS) [*]

Matrix assisted laser desorption/ionization-time of flight-mass spectrometry (MALDI-TOF-MS) measurements were carried out on an Ultraflex[TM] TOF/TOF (Bruker Daltonics, Bremen, Germany). This instrument operated in the positive ion reflectron mode at 20 kV accelerating voltage. 0.5 µL of the peptide extracts were manually spotted on a MTP 384 polished steel target plate and co-cristallized in 0.5 µL α-cyano-4-hydroxycinnamic acid (CHCA) matrix for the MALDI-TOF-MS analysis. An internal calibration using two trypsin

---

[**] These experiments have been performed in the lab of Prof. Van Dorsselaer, ECPM, Strasbourg, France by Christine Carapito.

[*] These experiments have been performed in the lab of Prof. Van Dorsselaer, ECPM, Strasbourg, France by Christine Carapito and me.

autolysis peaks at m/z 842.510 and m/z 2211.105 was performed. Monoisotopic peptide masses were assigned and used for peptide mass fingerprinting (PMF) database searches.

The PMF data generated by the MALDI-TOF-MS experiments were interpreted using a local MASCOT™ (MASCOT 1.9, Matrix Science, London, UK) server running on a 3 GHz Pentium IV processor. The searches were performed against Swiss-Prot and TrEMBL databases (http://www.expasy.org/sprot/) without any taxonomic nor Mr/p*I* restrictions. One missed cleavage per peptide was allowed, a mass tolerance of 70 ppm was used for the search and some variable modifications were taken into account, such as carbamidomethylation for cysteine and oxidation for methionine.

2.10.2 Nanoscale capillary Liquid Chromatography-Tandem Mass Spectrometry (nanoLC-MS/MS) ✄

Nanoscale capillary liquid chromatography-tandem mass spectrometric (nanoLC-MS/MS) analysis of the tryptic peptides was performed either on a CapLC capillary LC system (Waters) coupled to a hybrid quadrupole orthogonal acceleration TOF tandem MS Q-TOF II (Waters) or on an Agilent 1100 Series capillary LC system coupled to an HCT Plus™ ion trap (Bruker Daltonics). Both instruments were equipped with a nanospray ion source. For the CapLC system, chromatographic separations were conducted on a Pepmap^{TM} C18, 75 µm internal diameter (i.d.) × 15 cm length, RP capillary column (LC Packings, Sunnyvale, CA, USA) with a flow rate of 200 nL/min, accomplished by a pre-column split. An external calibration was performed using a 2 pmol/µL (Glu^{1})-Fibrinopeptide B (from Sigma) solution. For the Agilent 1100 Series capillary LC system, chromatographic separations were conducted on 75 µm i.d. × 15 cm length Zorbax 300SB-C18 column (Agilent Technologies). The gradient profile used consisted of a linear gradient from 95% A (H_2O, 0.05% HCOOH) to 45% B (ACN, 0.05% HCOOH) over 35 min followed by a linear gradient to 95% B for 1 min. Mass data acquisitions were piloted by MassLynx v4 software (Waters) using automatic switching between MS and MS/MS modes for the Q-TOF II sytem and by the ChemStation A.10.02 (Agilent Technologies) and EsquireControl version 5.2 (Bruker Daltonics) softwares for the HCT Plus system.

✄ These experiments have been performed in the lab of Prof. Van Dorsselaer, ECPM, Strasbourg, France by Christine Carapito.

Mass data collected during nanoLC-MS/MS analysis were processed and converted into *.PKL files for the Q-TOF II analysis and into *.MGF for the HCT Plus analysis. These peak lists were submitted to the MASCOT™ search engine and the searches were done with a tolerance on mass measurement of 0.25 Da in MS mode and 0.25 Da in MS/MS mode.

To validate the identifications, the following criteria were used: at least six matching peptides with less then 30 ppm error were required for identifications by PMF and at least two peptides with high quality MS/MS spectra (each peptide presenting a MASCOT ion score higher then 35) were required for nanoLC-MS/MS analysis identifications. For the identifications with two peptides only, the sequences of these peptides were manually checked by *de novo* sequencing of the MS/MS spectra.

2.11 Database searches (Bioinformatic methods)

Bioinformatics involve the use of techniques including applied mathematics, informatics, statistics, computer science, artificial intelligence, chemistry, and biochemistry to solve biological problems usually on the molecular level. In the present study, the bioinformatics methods were used to investigate annotations, sequence alignment and to predict protein-protein interactions.

2.11.1 Annotations

The identified proteins were functionally classified according to their biological functions based on annotations from Swiss-Prot and TrEMBL (http://www.expasy.org/sprot/), *S. pombe* GeneDB (http://www.genedb.org/genedb/pombe/index.jsp) as well as the KEGG *S. pombe* database (http://www.genome.ad.jp/kegg-bin/show_organism?org=spo).

The ExPASy (**Ex**pert **P**rotein **A**nalysis **Sy**stem) proteomics server is dedicated to the analysis of protein sequences and structures as well as 2-D PAGE. The UniProt Knowledgebase consists of UniProtKB/Swiss-Prot and UniProtKB/TrEMBL.
UniProtKB/Swiss-Prot is a curated protein sequence database which strives to provide a high level of annotation, a minimal level of redundancy and high level of integration with other

databases. UniProtKB/TrEMBL is a computer-annotated supplement of Swiss-Prot that contains all the translations of EMBL nucleotide sequence entries not yet integrated in Swiss-Prot.

The *S. pombe* GeneDB contains all *S. pombe* (fission yeast) known and predicted protein coding genes, pseudogenes, transposons, tRNAs, rRNAs, snRNAs, snoRNAs and other known and predicted non-coding RNAs. This database also strives to provide a high level of annotation (http://www.genedb.org/amigo/perl/go.cgi?species_db=GeneDB_Spombe) and high level of integration with other databases.

The KEGG (**K**yoto **E**ncyclopedia of **G**enes and **G**enomes) is a "biological systems" database integrating both molecular building block information and higher-level systemic information. In particular, KEGG PATHWAY maps display the knowledge on the molecular interaction and reaction networks for metabolism, genetic information processing, environmental information processing, cellular processes, and human diseases.
In addition, KEGG GENES is a gene catalogue of all complete genomes and some partial genomes with ortholog annotation (KO assignment), enabling KEGG PATHWAY mapping.

2.11.2 Sequence alignment and prediction of protein-protein interactions

BLAST searches were performed on some proteins with unknown functions. To explore all possibilities, multiple BLAST searches were run for proteins with unknown functions using different combinations of substitution matrices (BLOSUM45, BLOSUM62, BLOSUM80), low-complexity filtering (ON, OFF), gapped alignment (ON, OFF), E-value inclusion threshold (E = 0.001, E = 0.01) and database (Swiss-Prot + TrEMBL, Swiss-Prot alone; http://www.expasy.org/tools/blast/) (Altschul *et al.,* 1997; Pallen *et al.,* 2005).

In addition, Scansite (http://scansite.mit.edu/) searches for motifs within proteins that are likely to be phosphorylated by specific protein kinases or bind to domains such as SH2 domains, 14-3-3 domains or PDZ domains (Obenauer *et al.,* 2003). In this study, the Motif Scan program of Scansite has been used in order to investigate protein-protein binding possibility, *e.g.* 14-3-3 domains.

The program then indicates the percentile ranking of the candidate motif in respect to all potential motifs in proteins of a protein database. When available, percentile scores of some confirmed phosphorylation sites for the kinase of interests or confirmed binding sites of the domain of interest are provided for comparison with the scores of the candidate motifs.

3. **Results**

The two goals of my Ph.D. work were to obtain a global picture of the proteome of the fission yeast *S. pombe* wild type h^{-S} L 972 and to analyze the differential expression of proteins after incubation of the fission yeast with DOC. For the separation of proteins, 2-DE had to be performed. The interpretation of gels were done using PDQuest software (Bio-Rad) and the protein spots were identified by using MS (MALDI-TOF-MS and nanoLC-MS/MS) in collaboration with the group of Dr. Alain Van Dorsselaer. Thereafter, identified proteins were functionally classified according to their biological functions based on annotations from Swiss-Prot and TrEMBL, GeneDB as well as the KEGG database.

In order to address each project separately the results presented in this section as well as the subsequent discussion were divided into independent sections with the following titles:

- 2-D reference map for proteins of the fission yeast *S. pombe* wild type h^{-S} L 972
- Analysis of MR-independent DOC induced effects on the protein pattern of *S. pombe*

3.1 2-D reference map for proteins of the fission yeast **S pombe**

The sequencing of the fission yeast *S. pombe* genome was completed in 2002 (Wood *et al.,* 2002) and thus made it possible to study the intracellular proteome of this yeast. The goal of the first part of my work was to establish a two-dimensional (2-D) reference map for proteins of *S. pombe* wild type h^{-S} L 972. The integrated strategy of 2-DE and MS was used to establish a global picture of the proteome in the fission yeast *S. pombe* (see Figure 3.1). In the present work, the proteome analysis of the fission yeast *S. pombe* wild type h^{-S} L 972 was carried out using 2-DE with a widerange IPG strip of pH 3-10 as well as pH 4-7 with a high solution and high reproducibility. For the second part of my work, these map helped to analyze the differential expression of proteins after incubation of the fission yeast with DOC.
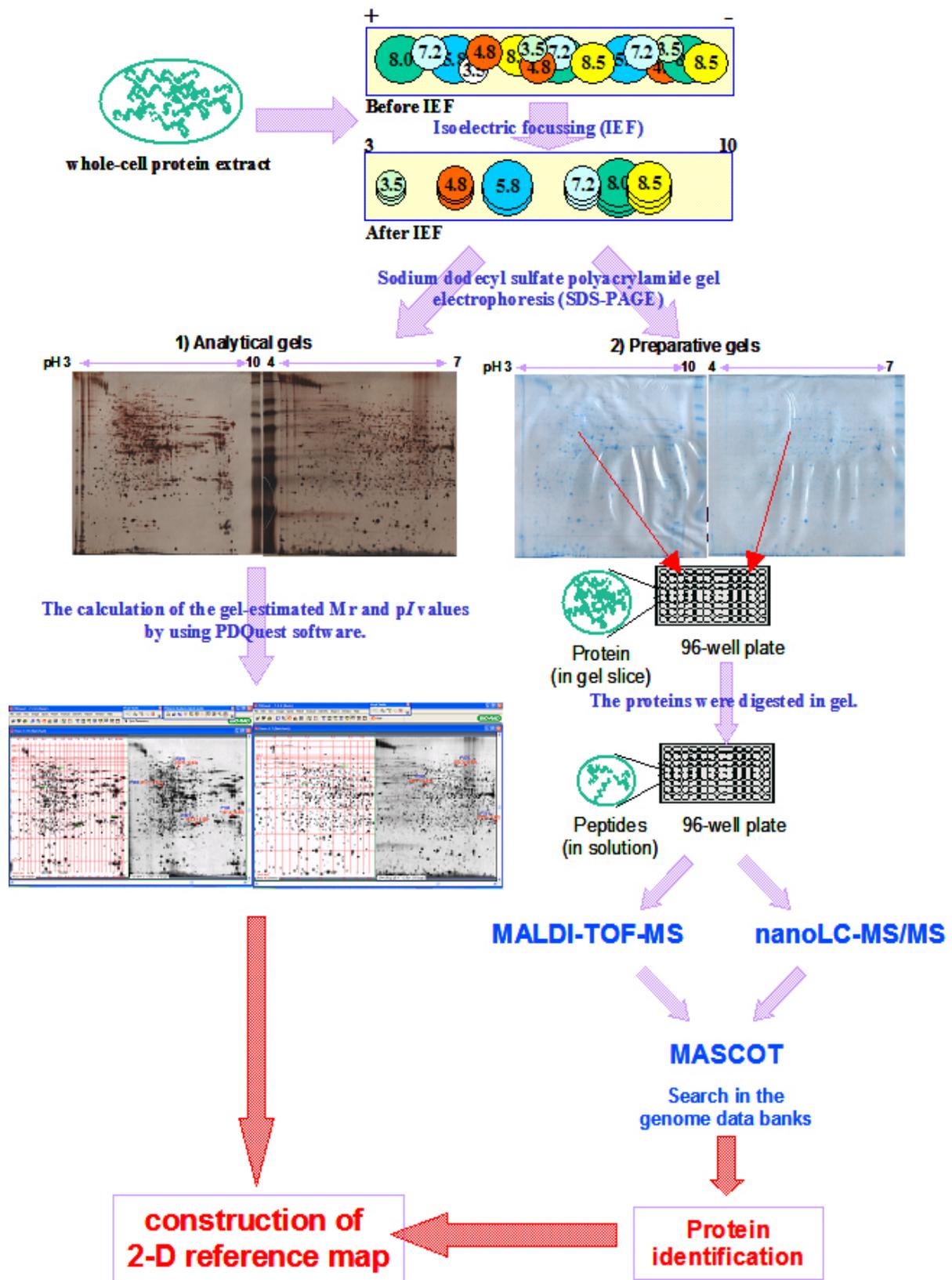
Figure 3.1 Representation of proteomics approach to create a 2-D reference map of *S. pombe*.

3.1.1 Two-dimensional gel electrophoresis (2-DE)

The extracted whole-cell protein mixtures of the fission yeast were quantified by using Ettan 2-D Quant Kit (Amersham Biosciences). To obtain an overview of the protein distribution, the widerange IPG strips (18 cm) of pH 3-10 were used for the first-dimensional separation of the protein mixtures with different amounts of loaded protein (20, 30, 40 or 60 µg proteins / each gel). For the second dimension, SDS-PAGE was run on 12.5% acrylamide gels. After running SDS gel electrophoresis, the separated spots were visualized by silver staining (developing time: 10 min / each gel, see Figure 3.2). By using the widerange IPG strips of pH 3-10, each of 2-DEs with different amounts of loaded protein have been performed at least four times. In particular, more than 1500 protein spots on each silver stained gels (see Figure 3.2D) have been visualized.
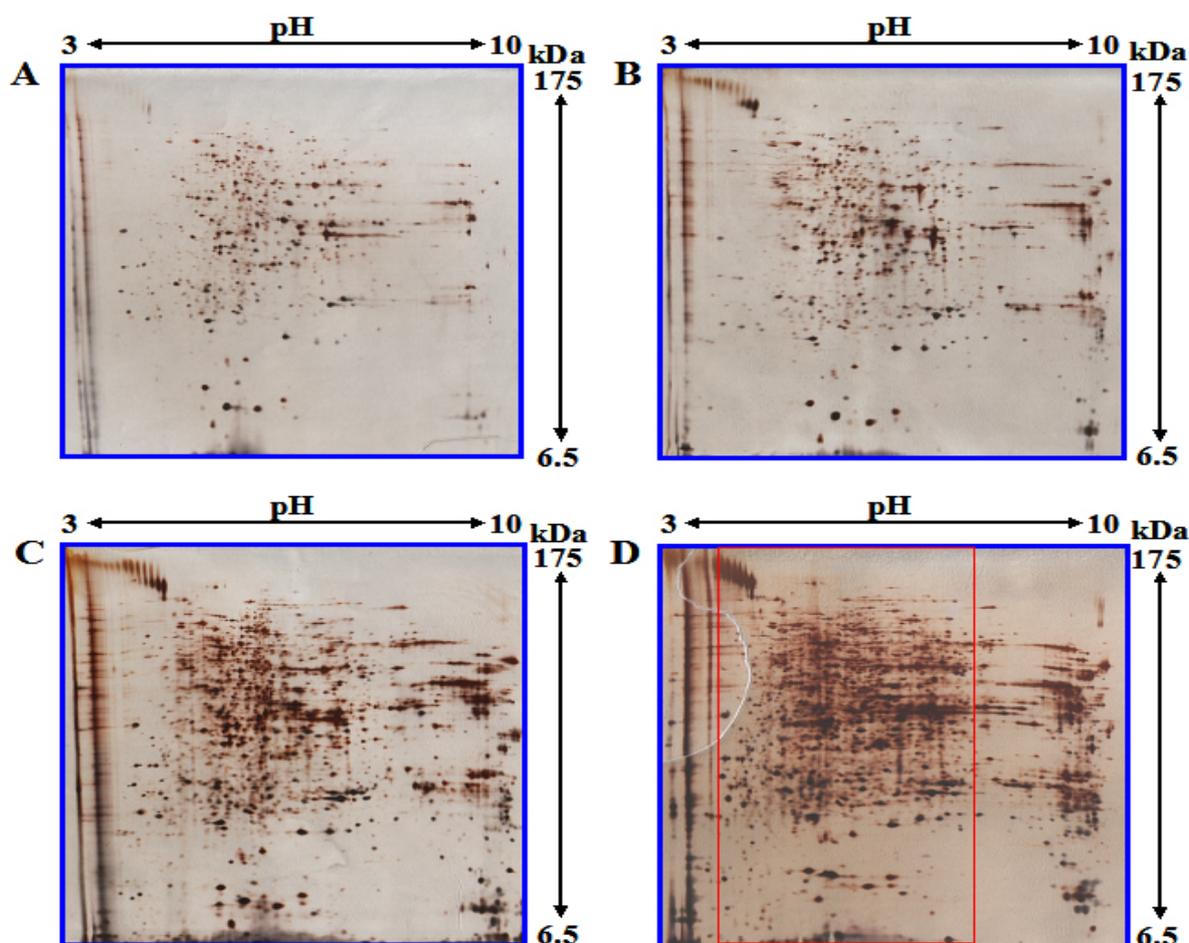
Figure 3.2 2-D gels of the protein mixtures with different amounts of loaded protein. Proteins were separated by IEF using 18 cm IPG strips (pH 3-10), followed by 12.5% SDS–PAGE stained with silver. **A:** 20 µg protein, **B:** 30 µg protein, **C:** 40 µg protein, **D:** 60 µg protein.

To obtain an overview of the protein distribution for preparative gels, the widerange IPG strips (18 cm) of pH 3-10 were used for the first-dimensional separation of the protein mixtures with different amounts of loaded protein (180 or 240 µg protein / gel). For the second dimension, SDS-PAGE was run on 12.5% acrylamide gels. After running SDS-PAGE, the separated spots were visualized by colloidal blue G-250 (see Figure 3.3). By using the widerange IPG strips of pH 3-10, each of 2-DEs with different amounts of loaded protein have been performed at least four times. In particular, more than 800 protein spots on colloidal blue G-250 stained gels (see Figure 3.3B) have been visualized.
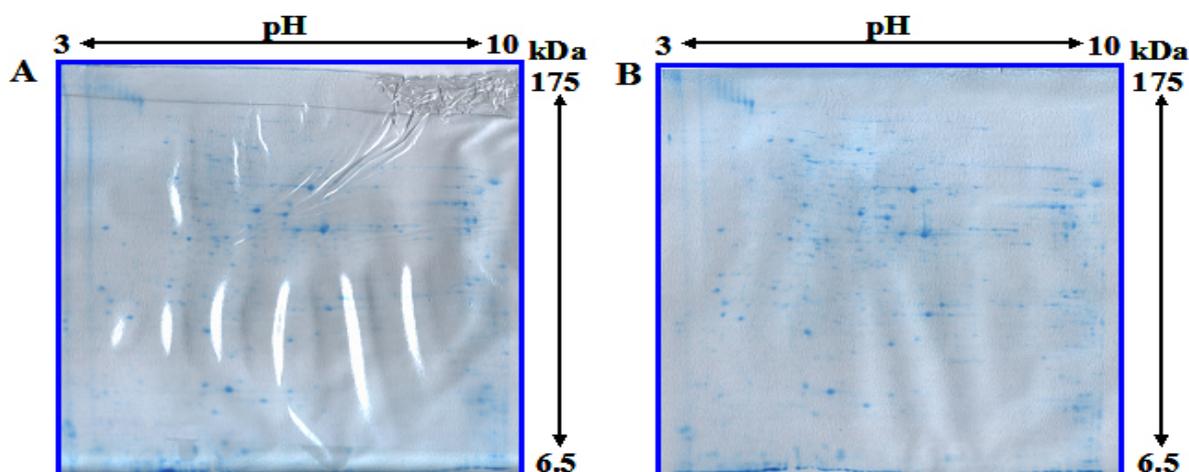
Figure 3.3 2D-gels of the protein mixtures with different amounts of loaded protein. Proteins were separated by IEF using 18 cm IPG strips (pH 3-10), followed by 12.5% SDS−PAGE stained with colloidal blue G 250. **A:** 180 µg protein, **B:** 240 µg protein.

Approximately 80% of the visualized proteins on the 2-D gels using the widerange IPG strips of pH 3-10 are present in the red box range of Figures 3.2D and 3.3B. For a better resolution of the proteins in the range between pH 4 and 7.5 area, there was the need to use another IPG strip. For this, the widerange IPG strips (18 cm) of pH 4-7 were used for the first-dimensional separation of the protein mixtures.

To obtain an overview of the protein distribution for analytical or preparative gels, the widerange IPG strips (18 cm) of pH 4-7 were used for the first-dimensional separation of the protein mixtures with 80 µg protein / gel (for analytical gel) as well as different amounts (for preparative gel: 180 or 240 µg protein / gel). For the second dimension, SDS-PAGE was run on 12.5% acrylamide gels. After SDS gel electrophoresis, the separated spots were visualized by silver staining or colloidal blue G-250. More than 1000 protein spots on silver stained gels (see Figure 3.4A) and more than 500 protein spots on colloidal blue G-250 stained gels (see

Figure 3.4C) has been visualized. By using the widerange IPG strips of pH 4-7, each of 2-DEs have been also performed at least four times.
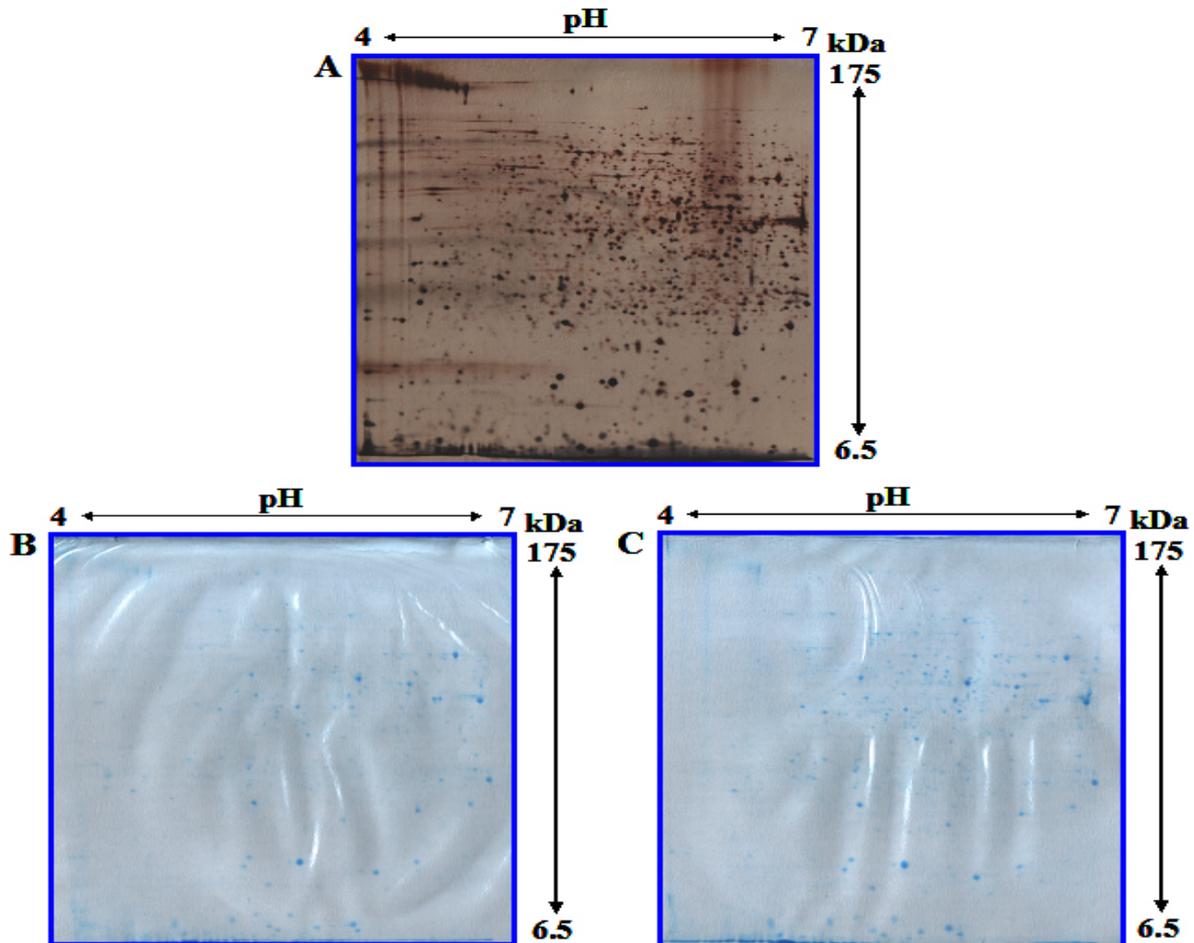
Figure 3.4 2D-gels of the protein mixtures with different amounts of protein loaded onto the gel. Proteins were separated by IEF using 18 cm IPG strips (pH 4-7), followed by 12.5% SDS−PAGE stained with silver (**A:** 80 µg proteins) or colloidal blue G 250 (**B:** 180 µg proteins, **C:** 240 µg proteins).

3.1.2 Protein identifications

For MS analysis, new samples were again resolved by 2-D gels using the widerange pH 3-10 IPG strips and pH 4-7 IPG strips with each one 240 µg protein. 298 colloidal blue G-250 stained spots in the 3-10 pH range from four different gels and 101 spots in the 4-7 pH range from two different gels were excised, destained, and analyzed independently by MALDI-TOF-MS as well as nanoLC-MS/MS analysis. The advantage of the complementarity of these two MS approaches was used to enhance the identification quality.

3.1.2.1 MALDI-TOF-MS

MALDI-TOF-MS measurements were carried out on an Ultraflex^{TM} TOF/TOF (Bruker Daltonics, Bremen, Germany). Monoisotopic peptide masses were assigned and used for databases searches. These files were then fed into the search engine MASCOT (Matrix Science, London, UK). The results were considered as a positive identification when at least four unique peptides from one protein were detected. Moreover, the peptides mass error was limited to 40 ppm.

So far, 295 proteins have been identified by MALDI-TOF-MS. The sequence coverage of the identified proteins ranged from 11% (Probable 5-methyltetrahydropteroyltriglutamate--homocysteine methyltransferase, spot No. 13) to 95% (Guanine nucleotide-binding protein beta subunit-like protein, spot No. 140). The percentage of sequence coverage was calculated by dividing the number of detected amino acids by the actual number of amino acids in the specific protein. Figure 3.5 shows an example of a protein identified as the guanine nucleotide-binding protein beta subunit-like protein (Q10281, GBLP_SCHPO, spot No. 140) by MALDI-TOF-MS.

3.1.2.2 nanoLC-MS/MS

Mass data collected during nanoLC-MS/MS analysis were processed and converted into *.PKL files for the Q-TOF II analysis and into *.MGF for the HCT Plus analysis. These peak lists were submitted to the MASCOT™ search engine. The results were considered as a positive identification when at least two peptides with high quality MS/MS spectra (each peptide presenting a MASCOT ion score higher than 35) for nanoLC-MS/MS analysis identifications were obtained.

A total of 195 proteins are identified by nanoLC-MS/MS. Among these proteins, 126 proteins were already identified by MALDI-TOF-MS. The sequence coverage of the identified proteins ranged from 3% (Elongation factor 2, O14460, EF2_SCHPO, spot No. 361) to 75% (Heat shock protein 16, O14368, HSP16_SCHPO, spot No. 304). Figure 3.6 shows an example of protein identified as 5-methyltetrahydropteroyl-triglutamate--homocysteine methyltransferase (Q9UT19, METE_SCHPO, spot No. 240) by nanoLC-MS/MS. This protein was identified based on the detection of 11 unique peptides covering 15 % of the sequence.

Mascot Search Results

Peptide View

Match to: **GBLP_SCHPO** Score: **250**
Q10281 Guanine nucleotide-binding protein beta subunit-like protein (Receptor of activated protein kinase C)
Found in search of \\Standlone\data\Christine\Sarrebruck\U17997CC\0_D4\1\1Sref\pdata\1\reportfile

Nominal mass (M_r): **34829**; Calculated pI value: **5.43**
NCBI BLAST search of **GBLP_SCHPO** against nr
Unformatted sequence string for pasting into other applications

Taxonomy: Schizosaccharomyces pombe

Variable modifications: Carbamidomethyl (C),N-Acetyl (Protein),Oxidation (M)
Cleavage by Trypsin: cuts C-term side of KR unless next residue is P
Number of mass values searched: **78**
Number of mass values matched: **23**
Sequence Coverage: **95%**

Matched peptides shown in **Bold Red**

```
  1 MPEQLVLRAT LEGHSGWVTS LSTAPENPDI LLSGSRDKSI LLWNLVRDDV
 51 NYGVAQRRLT GHSHFVSDCA LSFDSHYALS ASWDKTIRLW DLEKGECTHQ
101 FVGHTSDVLS VSISPDNRQV VSGSRDKTIK IWNIIGNCKY TITDGGHSDW
151 VSCVRFSPNP DNLTFVSAGW DKAVKVWDLE TFSLRTSHYG HTGYVSAVTI
201 SPDGSLCASG GRDGTLMLWD LNESTHLYSL EAKANINALV FSPNRYWLCA
251 ATGSSIRIFD LETQEKVDEL TVDFVGVGKK SSEPECISLT WSPDGQTLFS
301 GWTDNLIRVW QVTK
```

Show predicted peptides also

Sort Peptides By ⊙Residue Number ○Increasing Mass ○Decreasing Mass

Start - End	Observed	Mr(expt)	Mr(calc)	Delta	Miss	Sequence
2 - 8	854.51	853.50	853.50	0.00	0	EQLVLR
9 - 36	2895.53	2894.52	2894.44	0.08	0	ATLEGHSGWVTSLSTAPENPDILLSGSR
37 - 47	1356.80	1355.79	1355.79	0.00	1	DKSILLWNLVR
39 - 47	1113.70	1112.69	1112.67	0.02	0	SILLWNLVR
48 - 57	1136.55	1135.54	1135.53	0.02	0	DDVNYGVAQR
59 - 85	3038.58	3037.57	3037.37	0.21	0	LTGHSHFVSDCALSFDSHYALSASWDK Carbamidomethyl (C)
89 - 94	803.42	802.41	802.42	-0.01	0	LWDLEK
95 - 118	2642.26	2641.25	2641.22	0.03	0	GECTHQFVGHTSDVLSVSISPDNR Carbamidomethyl (C)
119 - 125	732.38	731.37	731.39	-0.02	0	QVVSGSR
131 - 139	1117.60	1116.59	1116.57	0.02	0	IWNIIGNCK Carbamidomethyl (C)
140 - 155	1852.81	1851.80	1851.82	-0.02	0	YTITDGGHSDWVSCVR Carbamidomethyl (C)
156 - 172	1894.89	1893.88	1893.89	-0.01	0	FSPNPDNLTFVSAGWDK
176 - 185	1265.67	1264.66	1264.65	0.02	0	VWDLETFSLR
186 - 212	2737.31	2736.30	2736.26	0.05	0	TSHYGHTGYVSAVTISPDGSLCASGGR Carbamidomethyl (C)
213 - 233	2452.22	2451.21	2451.16	0.05	0	DGTLMLWDLNESTHLYSLEAK Oxidation (M)
234 - 245	1315.73	1314.72	1314.70	0.02	0	ANINALVFSPNR
246 - 257	1327.68	1326.67	1326.64	0.03	0	YWLCAATGSSIR
246 - 257	1384.68	1383.67	1383.66	0.01	0	YWLCAATGSSIR Carbamidomethyl (C)
258 - 266	1122.59	1121.58	1121.56	0.02	0	IFDLETQEK
258 - 279	2481.33	2480.32	2480.27	0.05	1	IFDLETQEKVDELTVDFVGVGK
267 - 279	1377.74	1376.73	1376.72	0.01	0	VDELTVDFVGVGK
281 - 308	3196.65	3195.64	3195.48	0.16	0	SSEPECISLTWSPDGQTLFSGWTDNLIR Carbamidomethyl (C)
309 - 314	760.42	759.41	759.43	-0.02	0	VWQVTK

Figure 3.5 An example of a protein identified as the guanine nucleotide-binding protein beta subunit-like protein (Q10281, spot No. 140) by MALDI-TOF-MS. 23 of 78 peptides were identified. The protein sequence coverage was 95 %. Complete protein sequence with identified peptide highlighted in **red boldface letters**.

A {MATRIX SCIENCE} **Mascot Search Results**

Peptide View

MS/MS Fragmentation of LLPVYVELIK
Found in gi|19114264, 5-methyltetrahydropteroyltriglutamate--homocystei methyltransferase(ec 2.1.1.14)
[Schizosaccharomyces pombe]
Match to Query 32: 1185.844648 from(593.929600,2+)
From data file \\Q-tof-2\Data\pkl files\Q019411CC.pkl
Monoisotopic mass of neutral peptide Mr(calc): 1185.74
Ions Score: 22 **Expect:** 16
Matches (Bold Red): 19/72 fragment ions using 96 most intense peaks

#	b	b++	b0	b0++	Seq.	y	y++	y*	y*++	y0	y0++	#
1	114.09	57.55			L							10
2	227.18	114.09			L	1073.66	537.33	1056.63	528.82	1055.65	528.33	9
3	324.23	162.62			P	960.58	480.79	943.55	472.28	942.57	471.79	8
4	423.3	212.15			V	863.52	432.27	846.5	423.75	845.51	423.26	7
5	586.36	293.68			Y	764.46	382.73	747.43	374.22	746.44	373.73	6
6	685.43	343.22			V	601.39	301.2	584.37	292.69	583.38	292.19	5
7	814.47	407.74	796.46	398.73	E	502.32	251.67	485.3	243.15	484.31	242.66	4
8	927.55	464.28	909.54	455.28	L	373.28	187.14	356.25	178.63			3
9	1040.64	520.82	1022.63	511.82	I	260.2	130.6	243.17	122.09			2
10					K	147.11	74.06	130.09	65.55			1

B

```
  1 MVKSAVLGFP RIGKNRELKK ATEAYWSGKT SAEELLATAK QLRLEHWKLQ
 51 KAQGVDIIPS NDFSLYDQIM DHSFSFNVIP PRYRLSGLSS LDTYFAMGRG
101 MQRAATADKA AVDVPAGEMV KWFDSNYHFL RPEVSEETDF KLSSTKALDE
151 FLEAKEAGII TRPVLVGPVT YLFIAKAAKG SSIKPIELLP KLLPVYVELI
201 KKLTEAGAEY IQIDEPILTL DLPQEILASY KEAYETLGKI GKLILTTYFG
251 SLQSNADVLK GLPIAGVHVD VVRAPENLDR ALAVLGENQI ISVGVVSGRN
301 IWKTDFQKAT AIIEKAISAV GSERVQVASS SSILHIPHSL SGEDQINPEI
351 KRWFAFAVEK CAELAILTKA ANDGPASVRA ELEANAADCK ARAESPITNV
401 EAVRERQSKV TPQMHERKSP FETRYAKQQA SLKLPLFPTT TIGSFPQTKE
451 IRVTRNRFAK GLISQEEYDA FIRKEISDVV KFQEEVGLDV LVHGEPERND
501 MVQYFGERME GFVFTVNGWV QSYGSRCVRP PIIVGDVYRP APMTVKESQY
551 AQSITSKPMK GMLTAPITIL RWSFPRDDVH DSVQAQQIAL GLRDEVLDLE
601 KAGIKVIQCD EPALREGLPL RRAEWDEYLK WAIDAFRLAT AAVQDDTQIH
651 SHFCYSDFND IFDAIQRLDA DVVSIENSKS DMKLLNVLSR YTSCIGPGLF
701 DIHSPRVPPV SEFKERIDAI VKHVPKDHLW LNPDCGLKTR GWPETTADLK
751 NMIAAAREAR EQYA
```

Figure 3.6 The MS/MS spectrum of one of the matched peptides for spot No. 240 (identified as 5-methyltetrahydropteroyltriglutamate--homocysteine methyltransferase, Q9UT19) and total protein coverage. **A:** an example of a nanoLC MS/MS spectrum, obtained from a capillary LC Q-TOF II analysis, showing the identification of peptide **LLPVYVELIK** (192 – 201). All of the possible b-series (*N*-terminal fragment ions) and y-series ions (*C*-terminal fragment ions) are listed, and those ions that were found in the spectrum are highlighted in **red bold**. The b-series and y-series ions depend upon the amino acid sequence. **B:** Complete protein sequence with identified peptides highlighted in **red boldface letters**. The sequence coverage is 15 %.

3.1.2.3 Summary of both MS approaches

After both MS approaches, the 341 proteins out of 261 spots in the 3-10 pH range 2-D gel were identified at least twice by MALDI-TOF-MS and/or nanoLC-MS/MS analysis (see Figure 3.7A). In addition, the 103 proteins out of 96 spots in the 4-7 pH range 2-D gel were identified at least twice by MALDI-TOF-MS and/or nanoLC-MS/MS analysis (see Figure 3.7B). 42 of 399 analyzed spots could not be identified (37 spots in the 3-10 pH range and 5 spots in the 4-7 pH ranges). In total, 444 proteins out of 356 analyzed spots were identified by both MS approaches in the present study. Interestingly, each one 77 spots on both pH range 2-D gels could be confirmed as the same spots according to a comparison with the identified results of the analyzed spots and the present position on both 2-D gels. Appendix F lists 80 identified proteins out of 77 spots which were resolved by 2-DE in both pH ranges.
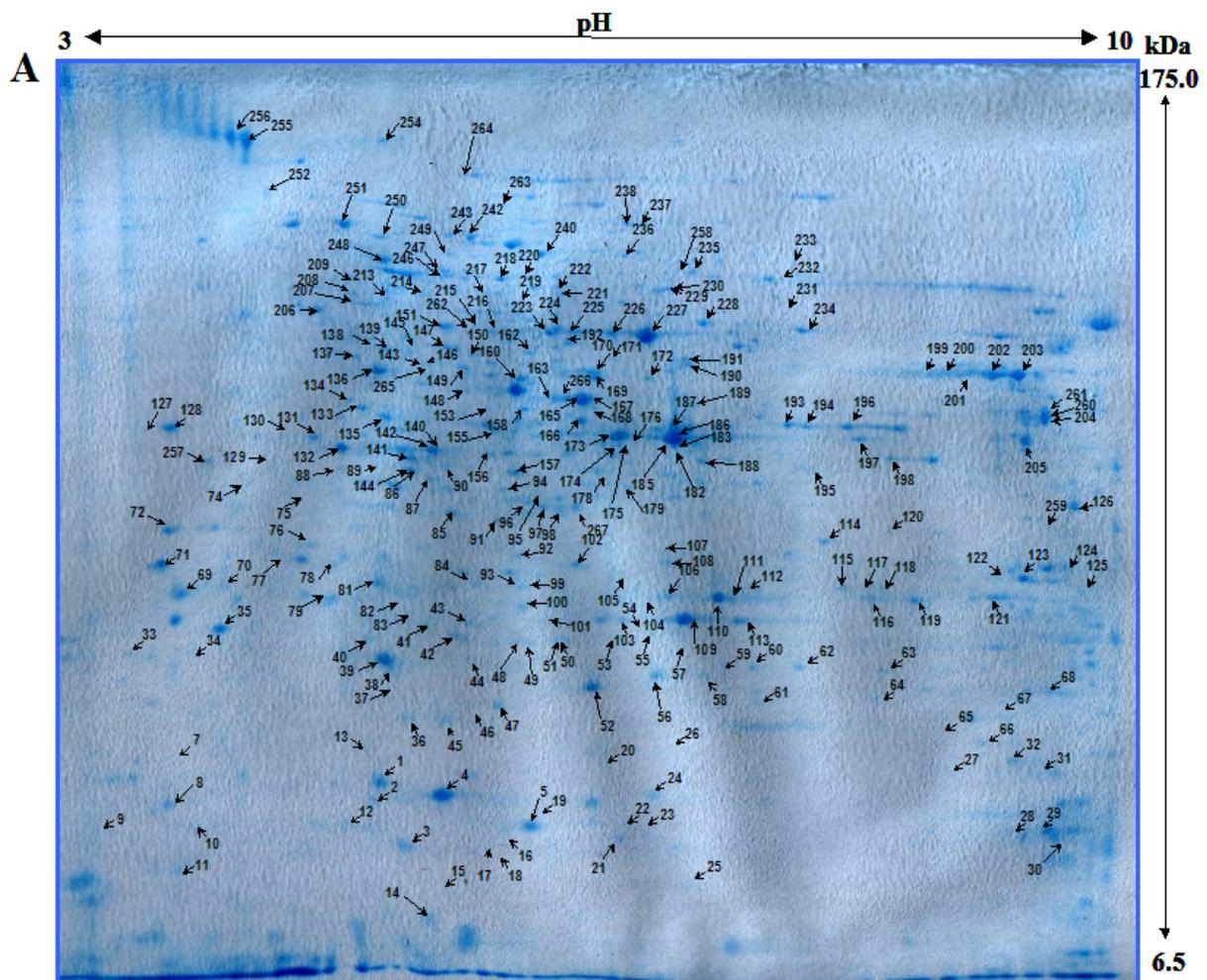
Figure 3.7 2-D reference maps of the *Schizosaccharomyces pombe* proteome. **A:** Proteins were separated by IEF using the 3-10 pH range IPG strips (18 cm), followed by 12.5% SDS–PAGE stained with colloidal blue G-250 (240 µg proteins).
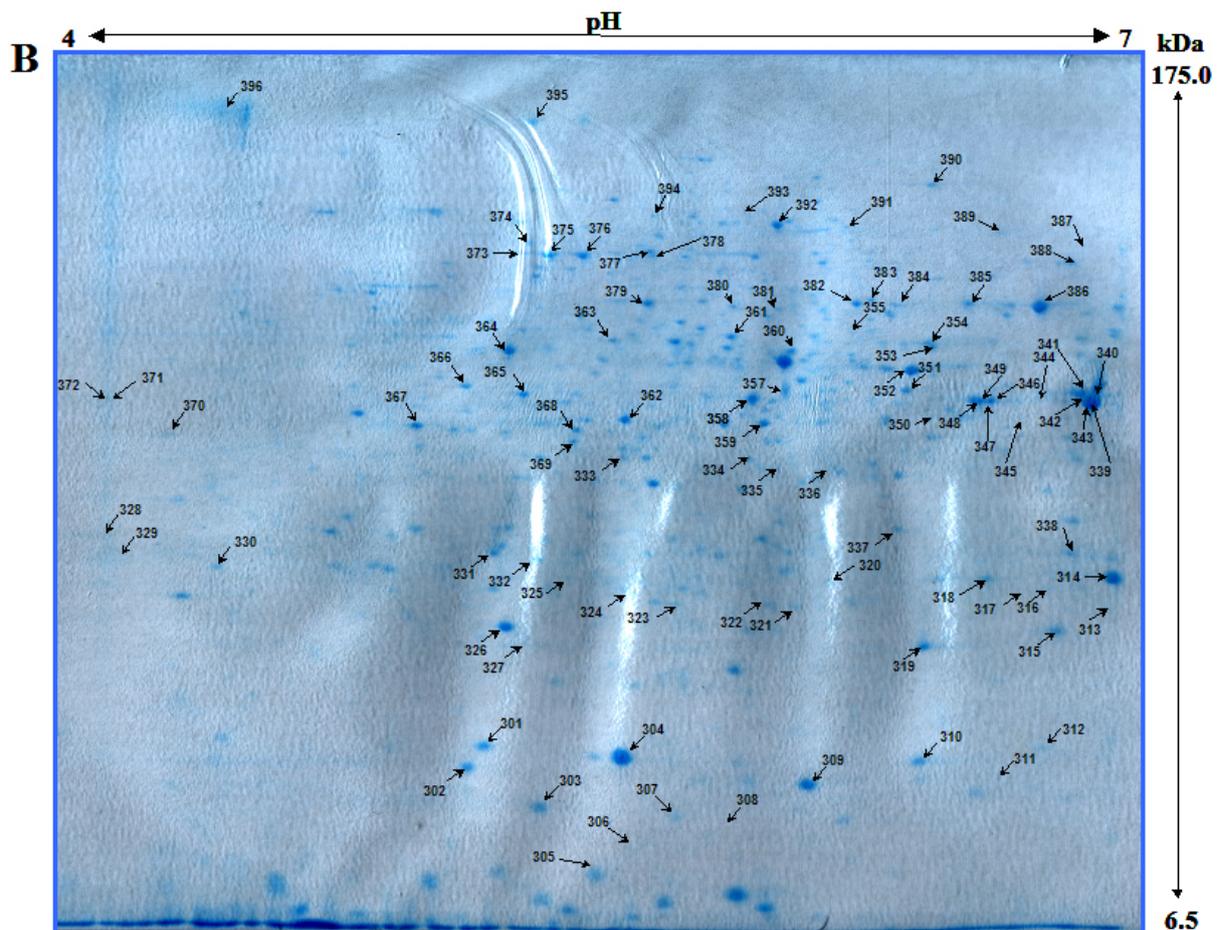
Figure 3.7 continued **B:** Proteins were separated by IEF using the 4-7 pH range IPG strips (18 cm), followed by 12.5% SDS–PAGE stained with colloidal blue G-250 (240 µg proteins). Spots cutted out of the coomassie stained gels for MS analysis are marked with arrows (Hwang *et al.,* 2006).

Table 3.1 lists the 23 identified proteins out of 19 spots resolved by 2-DE only in the 4-7 pH range, their theoretical and gel-estimated Mr and p*I*, the sequence coverages, numbers of matching peptides, and errors (in ppm) obtained by MALDI-TOF-MS as well as nanoLC-MS/MS analysis. Appendix E lists the 261 identified proteins out of 184 spots which were resolved by 2-DE only in the 3-10 pH range. Thus, a total of 364 proteins (representing 157 distinct proteins) have been identified by both MS analyses (Hwang *et al.,* 2006).

Table 3.1 Lists of the 23 identified proteins (*S. pombe*) resolved by 2-DE only in 4-7 pH range (Hwang *et al.*, 2006).

Protein No.	Spot No.[a]	Entry Name [b]	Protein Name [b]	Swiss-Prot Accession Number [b]	identified by	Sequence coverage [c]	Number of peptides[d]	Error in ppm [e]	Theoretical [f]		Gel (4-7) – estimated [g]	
									MW (kDa)	p*I*	MW (kDa)	p*I*
342	339	ADH_SCHPO	Alcohol dehydrogenase	P00332	**MALDI-TOF-MS**	54%	15	7	37.4	6.46	34.9	6.89
343	326	ALF_SCHPO	Fructose-bisphosphate aldolase	P36580	**nanoLC-MS/MS**	8%	2	40	39.6	5.92	21.3	5.31
344	361	EF2_SCHPO	Elongation factor 2	O14460	**nanoLC-MS/MS**	3%	3	57	93.2	6.02	42.8	5.72
345	351	ENO11_SCHPO	Enolase 1-1	P40370	**MALDI-TOF-MS**	37%	14	13	47.4	6.23	36.1	6.19
346	357	ENO11_SCHPO	Enolase 1-1	P40370	**MALDI-TOF-MS**	34%	14	9	47.4	6.23	36.2	5.83
347	310	G3P1_SCHPO	Glyceraldehyde 3-phosphate dehydrogenase 1	P78958	**MALDI-TOF-MS**	36%	12	16	35.9	6.24	14.9	6.26
348	367	IPYR_SCHPO	Inorganic pyrophosphatase	P19117	**MALDI-TOF-MS**	47%	14	11	32.3	5.20	34.2	5.05
349	392	HSP75_SCHPO	Heat shock protein sks2	Q10284	**MALDI-TOF-MS**	27%	12	16	67.2	5.82	66.1	5.81
350	378	HSP75_SCHPO	Heat shock protein sks2	Q10284	**MALDI-TOF-MS**	41%	24	15	67.2	5.82	56.7	5.56
351	340	ILV5_SCHPO	Probable ketol-acid reductoisomerase. mitochondrial [Precursor]	P78827	**MALDI-TOF-MS**	49%	19	28	45.2	9.47	35.5	6.89
352	390	METE_SCHPO	Probable 5-methyltetrahydropteroyltriglutamate--homocysteine methyltransferase	Q9UT19	**MALDI-TOF-MS** **nanoLC-MS/MS**	32% 45%	20 33	26 97	85.3	5.99	80.5	6.28
353	361	METK_SCHPO	S-adenosylmethionine synthetase	O60198	**MALDI-TOF-MS**	57%	18	22	41.8	5.70	42.8	5.72
354	355	O13702_SCHPO	SPAC13F5.03c protein	O13702	**MALDI-TOF-MS**	57%	25	22	49.4	7.23	42.4	5.88
355	344	O13848_SCHPO	SPAC19G12.09 protein	O13848	**MALDI-TOF-MS**	53%	14	16	31.6	6.33	35.1	6.68
356	344	O94315_SCHPO	SPBC215.11c protein	O94315	**MALDI-TOF-MS**	59%	19	16	33.9	6.48	35.1	6.68
357	345	O94315_SCHPO	SPBC215.11c protein	O94315	**MALDI-TOF-MS**	28%	9	28	33.9	6.48	34.1	6.62
358	373	ODO2_SCHPO	Probable dihydrolipoamide succinyltransferase component of 2-DE oxoglutarate dehydrogenase complex. mitochondrial [Precursor]	O94681	**MALDI-TOF-MS**	19%	9	11	49.0	7.55	58.2	5.33
359	310	P25_SCHPO	P25 protein	P30821	**MALDI-TOF-MS** **nanoLC-MS/MS**	46% 43%	8 11	22 42	21.9	6.29	14.9	6.26
360	375	PDC2_SCHPO	Probable pyruvate decarboxylase C1F8.07c	Q92345	**MALDI-TOF-MS**	38%	18	18	64.8	5.71	58.1	5.38
361	376	PDC2_SCHPO	Probable pyruvate decarboxylase C1F8.07c	Q92345	**MALDI-TOF-MS**	39%	22	19	64.8	5.71	57.6	5.44
362	361	PDC2_SCHPO	Probable pyruvate decarboxylase C1F8.07c	Q92345	**MALDI-TOF-MS** **nanoLC-MS/MS**	14% 22%	9 15	15 51	64.8	5.71	42.8	5.72
363	362	PRS6B_SCHPO	26S protease regulatory subunit 6B homolog	O74894	**nanoLC-MS/MS**	11%	4	35	43.6	5.28	34.2	5.52
364	350	TPIS_SCHPO	Triosephosphate isomerase	P07669	**MALDI-TOF-MS**	52%	12	18	27.1	6.61	34.2	6.28

a) Number in Figure 3.7B and 4.1B

b) Entry name and accession number according to Swiss-Prot (http://kr.expasy.org/sprot/)

c) Amino acid sequence coverage for the identified proteins

d) Number of matching peptides according to the MASCOT™ search engine

e) Error in ppm according to the MASCOT™ search engine

f) Theoretical *M*r and p*I* according to protein sequence and Swiss 2-D PAGE database

g) Gel-estimated *M*r and p*I* calculated by analysis of the gel images with PDQuest 7.2.0 software

3.1.2.4 Gel-estimated Mr and pI data (using PDQuest software)

Although the theoretical Mr and p*I* values of the identified proteins can be found due to the database searches, the gel-estimated Mr and p*I* values are also of interest, because post-translational modifications of proteins can regulate the protein functions by causing changes in protein activity, their cellular locations and dynamic interactions with other proteins. Therefore, the various proteins could be presented as multiple spots on 2-D gels.

In this study, so far 58 out of 157 distinct proteins were found in multiple spots (see Table 3.2). The most abundant proteins ($\geq$ 6 spots / one protein) include enolase 1-1 (P40370, 28 spots), glyceraldehyde 3-phosphate dehydrogenase 1 (P78958, 26 spots), fructose-bisphosphate aldolase (P36580, 12 spots), phosphoglycerate kinase (O60101, 11 spots), phosphoglycerate mutase (P36623, 11 spots), probabale ketol-acid reductoisomerase mitochondrial precursor (P36623, 9 spots), alcohol dehydrogenase (P00332, 8 spots), triosephosphate isomerase (P07669, 8 spots), probable heat shock protein ssa2 (O59855, 7 spots), heat shock protein sks2 (Q10284, 7 spots), pyruvate kinase (Q10208, 7 spots), and probable 5-methyl-tetrahydropteroyltriglutamate--homocysteine methyltransferase (Q9UT19, 6 spots). This phenomenon is considered to be caused by PMTs such as phosphorylation, glycosylation, N-acetylation and proteolytic processing (Garrels *et al.,* 1994; Larsen *et al.,* 2001; Meri and Baumann, 2001; Aksu *et al.,* 2002; Hesketh *et al.,* 2002; Mann and Jensen, 2003).

The gel-estimated Mr and p*I* values were determind by using PDQuest software. In order to examine these parameters, the values for a few known proteins have been entered. For three spots (in both pH 3-10 and 4-7 range: protein No. 262, 275 and 321, see Appendix F) and one spot (in pH 3-10 range: protein No. 195, see Appendix E), the gel-estimated Mr and p*I* values were found to be very similar to the theoretical Mr and p*I* values (see Figure 3.8).

Mr and p*I* values of the protein spots on 2-D gels were then estimated by PDQuest (364 identified proteins) and compared with their theoretical masses and p*I* values calculated for the 157 distinct proteins (see Figure 3.9). Overall, values of gel-estimated Mr and their theoretical values show a good correlation. The same is true for the correlation between gel-estimated and theoretical p*I* values. Most discrepancies between gel-estimated and theoretical masses and p*I* seem to result from post-translational proteolytical processing and modifications (Aksu *et al.,* 2002; Hesketh *et al.,* 2002).
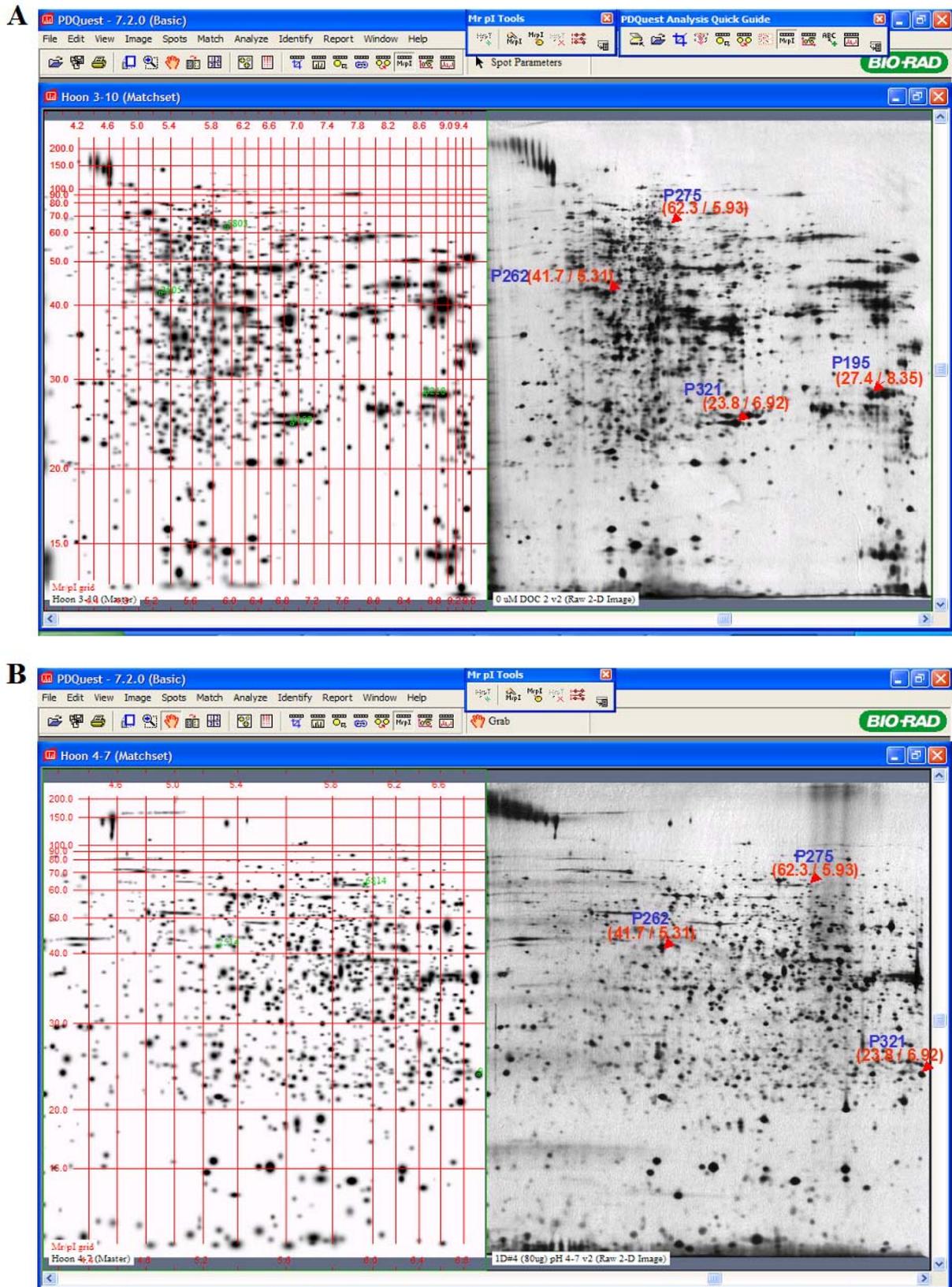
Figure 3.8 The calculation of the gel-estimated Mr and p*I* values using PDQuest software. The gels on the left side are the Master. The gels on the right shown the raw 2-D images. **Blue letters** in the right gels corresponding to protein numbers shown in Appendix E or F. **Red letters** in the right gels indicate Mr and p*I* values. **A:** in the range pH 3-10 gel, **B:** in the range pH 4-7.
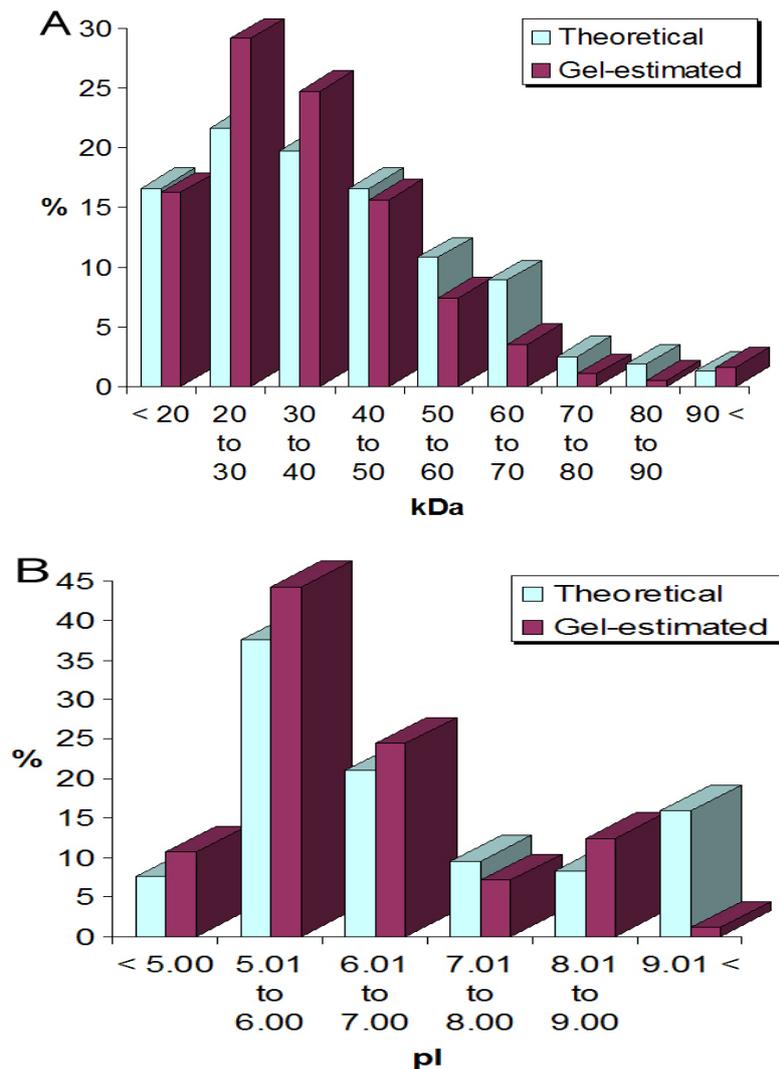
Figure 3.9 Comparison of gel-estimated Mr and p*I* values for the 364 analysed spots with the theoretical calculated Mr and p*I* values of the 157 distinct proteins. **A:** Mr values, **B:** p*I* values (Hwang *et al.,* 2006).

The ribosomal proteins (related to protein synthesis and transcription) with high *pI* values can be easily missed in 2-DE based analysis because the IEF separation step mostly excludes the basic proteins (p*I* > 9.5). However, 16 ribosomal proteins were identified in this study. In addition, two membrane proteins have been identified: a probable mitochondrial import receptor subunit tom40 (O13656, TOM40_SCHPO, spot No. 155), and a probable outer mitochondrial membrane protein porin (Q9P544, VDAC_SCHPO, spot No. 114). The solubilization of membrane proteins is one of the limiting factors of resolution of 2-DE. Generally, membrane proteins are difficult to resolve by ordinary sample preparation methods, and therefore rarely detected by 2-DE. These results point to an efficient resolution of this reference map that has been performed for a global proteome analysis of the fission yeast.

3.1.3 Protein classifications

Based on annotations from Swiss-Prot and TrEMBL, GeneDB as well as the KEGG database, the 157 distinct proteins (364 identified proteins with redundancies) from *S. pombe* were functionally classified according to their biological process. Among these proteins, 41.4% of the proteins (65 distinct proteins) are involved in metabolism (see Figure 3.10). Others are involved in protein synthesis and transcription (12.7%), related to protein folding and associated processing (10.2%), related to cellular transport (8.3%), related to cell rescue, defense and stress (5.1%), involved in the cell organization and biogenesis (4.5%), and finally related to ubiquitin cycle (1.9%) and cell cycle (1.3%) (see Figure 3.10). The entry name of these proteins are shown in Table 3.2.
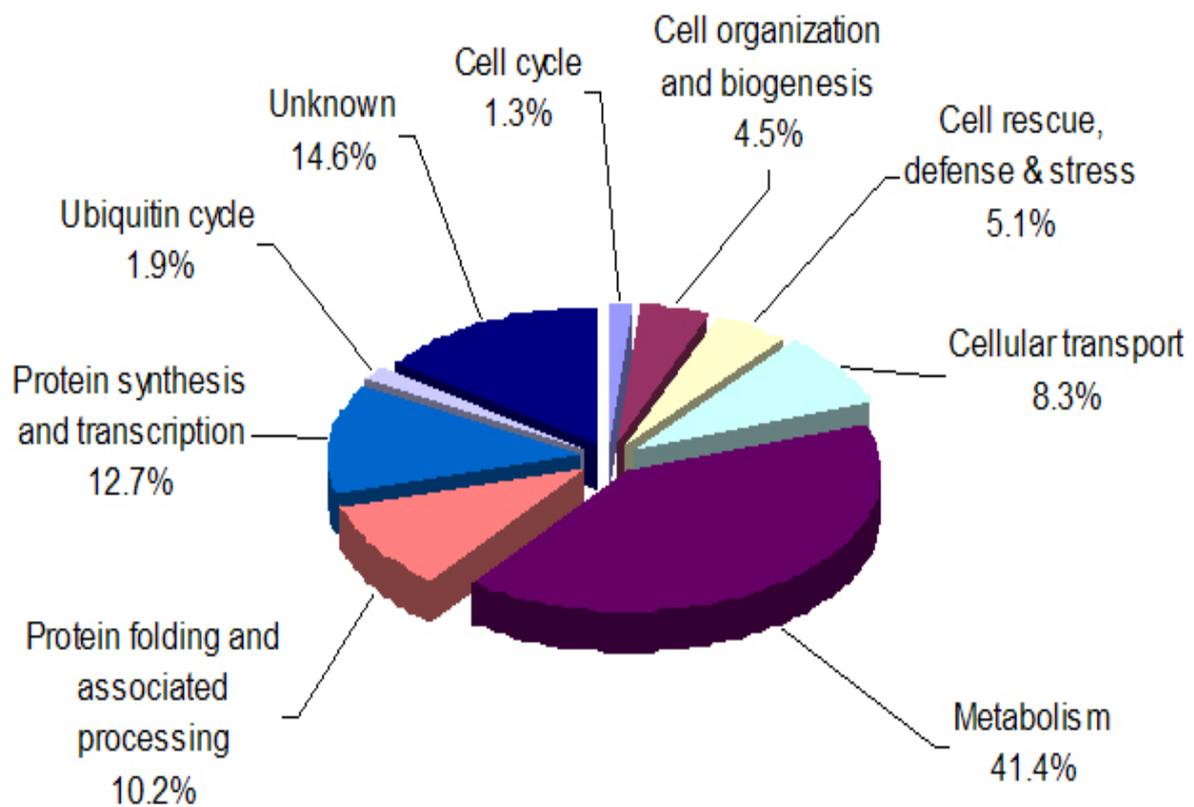
Figure 3.10 Distribution of identified proteins according to their functions. The 157 distinct identified proteins were plotted in a pie chart. The percentages in parentheses were calculated by dividing the number of identified proteins in the group by 157 and by multiplying the dividend by 100.

Table 3.2 The entry names of the identified proteins corresponding to Figure 3.10 were listed based on the their functions.

Functional Calssification [a)		Swiss-Prot Accession Number [b)	Enzyme commission Number [b)	Entry Name [b)	Protein Name [b)	presented as multiple spots
Cell cycle		P42656		RAD24_SCHPO	DNA damage checkpoint protein rad24	3
		P42657		RAD25_SCHPO	DNA damage checkpoint protein rad25	2
Cell organization and biogenesis		Q12702		2ABA_SCHPO	Protein phosphatase PP2A regulatory subunit B	1
		P10989		ACT_SCHPO	Actin	4
		P36621		CAP_SCHPO	Adenylyl cyclase-associated protein	1
		P78929		COFI_SCHPO	Colfilin	2
		Q10281		GBLP_SCHPO	Guanine nucleotide-binding protein beta subunit-like protein	2
		P04688		TBA1_SCHPO	Tubulin alpha-1 chain	1
		Q02088		TPM_SCHPO	Tropomyosin	1
Cell rescue, defense & stress		P55306	EC:1.11.1.6	CATA_SCHPO	Catalase	1
		O59858	EC:1.11.1.9	GPX1_SCHPO	Glutathione peroxidase	2
		P78965	EC:1.8.1.7	GSHR_SCHPO	Glutathione reductase	1
		O74887		O74887_SCHPO	SPCC576.03c protein	3
		P30821		P25_SCHPO	P25 protein	2
		Q11004	EC:5.2.1.8	PPID_SCHPO	40 kDa peptidyl-prolyl cis-trans isomerase	1
		P28758	EC:1.15.1.1	SODC_SCHPO	Superoxide dismutase [Cu-Zn]	2
		Q9UQX0	EC:1.15.1.1	SODM_SCHPO	Superoxide dismutase [Mn]. mitochondrial [Precursor]	2
Cellular transport		P24487	EC:3.6.3.14	ATPA_SCHPO	ATP synthase alpha chain. mitochondrial [Precursor]	1
		P22068	EC:3.6.3.14	ATPB_SCHPO	ATP synthase beta chain. mitochondrial [Precursor]	2
		O94373	EC:3.6.3.14	ATPF_SCHPO	ATP synthase subunit 4. mitocondrial [Precursor]	1
		Q9USP6		CLC1_SCHPO	Clathrin light chain (CLC)	1
		P78790		ETFA_SCHPO	Probable electron transfer flavoprotein alpha-subunit. mitochondrial [Precursor]	1
		P19117	EC:3.6.1.1	IPYR_SCHPO	Inorganic pyrophosphatase	2
		Q09330		MLO3_SCHPO	Protein mlo3	1
		O42932	EC:1.10.2.2	O42932_SCHPO	Qcr6 protein	1
		O13656		TOM40_SCHPO	Probable mitochondrial import receptor subunit tom40	1
		Q09154	EC:1.10.2.2	UCRI_SCHPO	Ubiquinol-cytochrome C reductase iron-sulfur subunit. mitochondrial [Precursor]	1
		P31411	EC:3.6.3.14	VATB_SCHPO	Vacuolar ATP synthase subunit B	1
		Q9P544		VDAC_SCHPO	Probable outer mitochondrial membrane protein porin	1
		Q10499		YDGE_SCHPO	Putative flavoprotein C26F1.14C.	1
Metabolism	Citrate cycle (TCA cycle)	O13966	EC:4.2.1.3	ACON_SCHPO	Aconitate hydratase. mitochondrial [Precursor]	1
		Q10306	EC:2.3.3.1	CISY_SCHPO	Probable citrate synthase. mitochondrial [Precursor]	2
		O13696	EC:1.1.1.41	IDH1_SCHPO	Isocitrate dehydrogenase (NAD) subunit 1, mitochondrial [Precursor]	1
		O14254	EC:1.1.1.42	IDHP_SCHPO	Probable isocitrate dehydrogenase (NADP), mitochondrial [Precursor]	1
		O94681	EC:2.3.1.61	ODO2_SCHPO	Probable dihydrolipoamise succinyltransferase component of 2-oxoglutarate dehydrogenasecomplex. mitochondrial [Precursor]	2
		Q9Y7R8	EC:1.1.1.37	Q9Y7R8_SCHPO	SPCC306.08c protein	2
	Glycolysis / Gluconeogenesis	P00332	EC:1.1.1.1	ADH_SCHPO	Alcohol dehydrogenase	8
		P36580	EC:4.1.2.13	ALF_SCHPO	Fructose-bisphosphate aldolase	12
		P40370	EC:4.2.1.11	ENO11_SCHPO	Enolase 1-1	28
		Q8NKC2	EC:4.2.1.11	ENO12_SCHPO	Enolase 1-2	2
		P78958	EC:1.2.1.12	G3P1_SCHPO	Glyceraldehyde 3-phosphate dehydrogenase 1	26
		O43026	EC:1.2.1.12	G3P2_SCHPO	Glyceraldehyde-3-phosphate dehydrogenase 2	4
		P78917	EC:5.3.1.9	G6PI_SCHPO	Glucose-6-phosphate isomerase	1
		P50521	EC:2.7.1.1	HXK2_SCHPO	Hexokinase 2	1
		Q10208	EC:2.7.1.40	KPYK_SCHPO	Pyruvate kinase	7
		O42873	EC:4.1.1.1	O42873_SCHPO	SPAC3G9.11c protein	3
		Q10489	EC:1.2.4.1	ODPA_SCHPO	Pyruvate dehydrogenase E1 component alpha subunit. mitochondrial [Precursor]	1
		Q92345	EC:4.1.1.1	PDC2_SCHPO	Probable pyruvate decarboxylase C1F8.07c	5
		O60101	EC:2.7.2.3	PGK_SCHPO	Phosphoglycerate kinase	11
		P36623	EC:5.4.2.1	PMGY_SCHPO	Phosphoglycerate mutase	11
		P07669	EC:5.3.1.1	TPIS_SCHPO	Triosephosphate isomerase	8

Table 3.2 continued.

Functional Calssification [a]		Swiss-Prot Accession Number [b]	Enzyme commission Number [b]	Entry Name [b]	Protein Name [b]	presented as multiple spots
Metabolism	**Methionine metabolism**	O13326	EC:2.5.1.49	CYSD_SCHPO	O-acetylhomoserine (Thiol)-lyase	1
		Q9UT19	EC:2.1.1.14	METE_SCHPO	Probable 5-methyltetrahydropteroyltriglutamate--homocysteine methyltransferase	6
		O60198	EC:2.5.1.6	METK_SCHPO	S-adenosylmethionine synthetase	3
		O13639	EC:3.3.1.1	SAHH_SCHPO	Adenosylhomocysteinase	2
	Pentose phosphate pathway	P78812	EC:1.1.1.44	6PGD_SCHPO	6-phosphogluconate dehydrogenase. decarboxylating	3
		Q10242	EC:2.7.1.12	GNTK_SCHPO	Probable gluconokinase	1
		O14105	EC:5.1.3.1	RPE_SCHPO	Ribulose-phosphate 3-epimerase	2
		Q9URM2	EC:2.2.1.1	TKT_SCHPO	Probable transketolase	4
	Purine metabolism	P78825	EC:2.7.1.20	ADK_SCHPO	Adenosine kinase	1
		P33075	EC:2.7.4.3	KAD1_SCHPO	Adenylate kinase	1
		Q9P7G9	EC:2.7.1.25	KAPS_SCHPO	Adenylyl-sulfate kinase	2
		P78937	EC:2.7.7.4	MET3_SCHPO	Sulfate adenylyltransferase	1
	Pyruvate metabolism	Q9UUJ9	EC:3.1.2.1	ACH1_SCHPO	Acetyl-CoA hydrolase	1
		Q9Y823	EC:2.3.3.14	HOSM_SCHPO	Homocitrate synthase. mitochondrial [Precursor]	1
		P40375	EC:1.1.1.38	MAOX_SCHPO	NAD-dependent malic enzyme	5
		Q9UT36	EC:3.1.2.6	Q9UT36_SCHPO	SPAC824.07 protein	1
	Glycerolipid metabolism	O13902	EC:2.7.1.29	DAK1_SCHPO	Dihydroxyacetone kinase 1	3
		O74215	EC:2.7.1.29	DAK2_SCHPO	Dihydroxyacetone kinase 2	1
		O13702	EC:1.5.1.10	O59711_SCHPO	SPBC3B8.03 protein	1
	Other metabolism	Q09755	EC:2.5.1.54	AROF_SCHPO	Putative phospho-2-dehydro-3-deoxyheptonate aldolase	1
		O13990	EC:3.2.1.58	BGL2_SCHPO	Glucan 1.3-beta-glucosidase [Precursor]	1
		P78804	EC:1.4.1.4	DHE4_SCHPO	NADP-specific glutamate dehydrogenase	1
		P36591	EC:1.5.1.3	DYR_SCHPO	Dihydropteridine reductase	1
		O14110	EC:2.6.1.52	GCST_SCHPO	Probable aminomethyltransferase. mitochondrial [Precursor]	1
		O13972	EC:2.1.2.1	GLYD_SCHPO	Probable serine hydroxymethyltransferase. cytosolic	2
		P21696	EC:1.1.1.8	GPD1_SCHPO	Glycerol-3-phosphate dehydrogenase [NAD+] 1	1
		Q09845	EC:1.1.1.8	GPD2_SCHPO	Glycerol-3-phosphate dehydrogenase [NAD+] 2	1
		O14400	EC:1.1.1.86	ILV5_SCHPO	Probable ketol-acid reductoisomerase. mitochondrial [Precursor]	9
		P78827	EC:3.2.1.26	INV1_SCHPO	Invertase [Precursor]	1
		O59852		MMF1_SCHPO	Protein mmf1, mitochondrial [Precursor]	1
		O43003	EC:2.7.7.13	MPG1_SCHPO	Probable mannose-1-phosphate guanyltransferase	1
		O74484	EC:1.1.1.6	O13702_SCHPO	SPAC13F5.03c protein	4
		O59711	EC:4.-.-.-	PDX1_SCHPO	Probable pyridoxin biosynthesis PDX1-like protein	2
		O14027	EC:3.1.1.5	PLB1_SCHPO	Lysophospholipase 1 [Precursor]	2
		P78854	EC:5.4.2.8	PMM_SCHPO	Phosphomannomutase	1
		Q9UTJ2	EC:3.1.3.41	PNPP_SCHPO	4-nitrophenylphosphatase	1
		Q00472	EC:2.7.1.17	Q9C0U6_SCHPO	SPCPJ732.02c protein	1
		Q9C0U6	EC:1.-.-.-	Q9P7B4_SCHPO	SPAC521.03 protein	1
		Q9P7B4	EC:2.6.1.52	SERC_SCHPO	Putative phosphoserine aminotransferase	1
		Q10349		SOU1_SCHPO	Sorbitol utilization protein sou1	1
		Q9Y6Z9	EC:2.5.1.16	SPEE_SCHPO	Spermidine synthase	1
		Q09741	EC:2.7.7.9	UGPA1_SCHPO	Probable UTP--glucose-1-phosphate uridylyltransferase	1
		P78811	EC:3.5.1.5	UREA_SCHPO	Urease	1
		O00084		YA14_SCHPO	Hypothetical protein C13C5.04 in chromosome I	1
Protein folding, modification and destination		Q9P6I2		CPGL_SCHPO	Glutamate carboxypeptidase-like protein	1
		P18253	EC:5.2.1.8	CYPH_SCHPO	Peptidyl-prolyl cis-trans isomerase	2
		O43047		GRPE_SCHPO	GrpE protein homolog. mitochondrial [Precursor]	2
		O14368		HSP16_SCHPO	Heat shock protein 16	3
		Q09864		HSP60_SCHPO	Heat shock protein 60. mitochondrial [Precursor]	1
		Q10265		HSP71_SCHPO	Probable heat shock protein ssa1	2
		O59855		HSP72_SCHPO	Probable heat shock protein ssa2	7
		Q10284		HSP75_SCHPO	Heat shock protein sks2	7
		P41887		HSP90_SCHPO	Heat shock protein 90 homolog	4
		P87147		NACA_SCHPO	Putative nascent polypeptide-associated complex alpha subunit-like protein	2
		Q92371		NACB_SCHPO	Nascent polypeptide-associated complex subunit beta	1

Table 3.2 continued.

Functional Calssification [a]	Swiss-Prot Accession Number [b]	Enzyme commission Number [b]	Entry Name [b]	Protein Name [b]	presented as multiple spots
Protein folding, modification and destination	O74448	EC:5.2.1.8	PIN1_SCHPO	Peptidyl-prolyl cis-trans isomerase pin1	1
	O14313	EC:1.11.1.15	PMP20_SCHPO	Putative peroxiredoxin pmp20	1
	O94273	EC:5.2.1.8	PPIB_SCHPO	Peptidyl-prolyl cis-trans isomerase B [Precursor]	2
	O74894		PRS6B_SCHPO	26S protease regulatory subunit 6B homolog	1
	Q9USI5		STI1_SCHPO	Heat shock protein sti1 homolog	1
Protein synthesis and transcription	P50522	EC:3.6.5.3	EF1A1_SCHPO	Elongation factor 1-alpha-A	4
	Q10119	EC:3.6.5.3	EF1A2_SCHPO	Elongation factor 1-alpha-B/C	5
	O14460		EF2_SCHPO	Elongation factor 2	1
	O14339		RL17A_SCHPO	60S ribosomal protein L17-A	1
	O59794		RL17B_SCHPO	60S ribosomal protein L17-B	1
	P08093		RL2_SCHPO	60S ribosomal protein L2	1
	Q9URX6		RL31_SCHPO	60S ribosomal protein L31	1
	Q92365		RL36A_SCHPO	60S ribosomal protein L36-A	1
	P35679		RL4A_SCHPO	60S ribosomal protein L4-A	1
	P52822		RL5A_SCHPO	60S ribosomal protein L5-A	1
	O13672		RL8_SCHPO	60S ribosomal protein L8	1
	Q9P7P1		RPA8_SCHPO	DNA-directed RNA polymerase I 17 kDa polypeptide	1
	Q9P546		RS0B_SCHPO	40S ribosomal protein S0-B	2
	Q9C0Z7		RS11_SCHPO	40S ribosomal protein S6-B	1
	P79013		RS19A_SCHPO	40S ribosomal protein S11	1
	P58234		RS23_SCHPO	40S ribosomal protein S19-A	1
	P79057		RS24A_SCHPO	40S ribosomal protein S23	1
	O13784		RS24B_SCHPO	40S ribosomal protein S24-A	1
	O59865		RS5A_SCHPO	40S ribosomal protein S24-B	1
	O14277		RS6B_SCHPO	40S ribosomal protein S5-A	1
Ubiquitin cycle	P87167		BUT2_SCHPO	Uba3-binding protein but2	1
	O13685	EC:6.3.2.19	UBC13_SCHPO	Ubiquitin-conjugating enzyme E2 13	1
	P46595	EC:6.3.2.19	UBC4_SCHPO	Ubiquitin-conjugating enzyme E2 4	1
Unknown	P04913		H2B1_SCHPO	Histone H2B-alpha	1
	O13848		O13848_SCHPO	SPAC19G12.09 protein	1
	O42888		O42888_SCHPO	SPBC8E4.04 protein	1
	O74914		O74914_SCHPO	SPCC757.03c protein	1
	O74960		O74960_SCHPO	SPCC736.15 protein	1
	O94315		O94315_SCHPO	SPBC215.11c protein	2
	Q9C1X5		Q9C1X5_SCHPO	SPAP32A8.02 protein	1
	Q9P7G7		Q9P7G7_SCHPO	Ssp1 protein [Fragment]	1
	Q9USU5		Q9USU5_SCHPO	SPBC29A10.08 protein	1
	Q9UT63		Q9UT63_SCHPO	SPAC513.02 protein	1
	P87216		VIP1_SCHPO	Protein vip1	3
	Q09676		YA03_SCHPO	Hypothetical protein C5H10.03 in chromosome I	1
	Q09802		YAAB_SCHPO	Hypothetical protein C22G7.11c in chromosome I	1
	O42914		YBI8_SCHPO	Protein C16A3.08c in chromosome II	1
	Q9URV6		YBL5_SCHPO	Hypothetical protein C106.05c in chromosome II	1
	Q10253		YD25_SCHPO	Hypothetical protein C56F8.05c in chromosome I	1
	Q10494	EC:1.-.-.-	YDG7_SCHPO	Probable oxidoreductase C26F1.07 in chromosome I	1
	O14082		YEAH_SCHPO	Hypothetical protein UNK4.17 in chromosome I	1
	P78890		YEPF_SCHPO	Hypothetical protein C23H3.15C in chromosome I	5
	O94322		YGK3_SCHPO	Hypothetical protein C725.03 in chromosome II	1
	P78833		YHZ8_SCHPO	Hypothetical protein SPBC21B10.08c in chromosome II	3
	Q96WU9		YJO6_SCHPO	Very hypothetical protein PB16A4.06c in chromosome III	1
	SPBC16E9.16c [c]			Hypothetical protein SPBC16E9.16c	2
					364

a) The identified proteins were functionally classified according to their biological functions based on annotations from Swiss-Prot and TrEMBL, *S. pombe* GeneDB as well as the KEGG *S. pombe* database.

b) accession number, enzyme number and protein name according to Swiss-Prot (http://kr.expasy.org/sprot/)

c) Systematic name according to *S.pombe* GeneDB (http://www.genedb.org/genedb/pombe/index.jsp)

14.6% of the identified proteins display unknown functions (see Figure 3.10 and Table 3.2). By performing a BLAST search it was attempted to determine the function of these proteins by using the coresponding sequence information. According to the BLAST search results, some relevant homologies for three proteins with unknown functions were discreted. One protein found in spot No. 82, which was identified by MALDI-TOF-MS as SPCC757.03c protein (O74914, O74914_SCHPO, conserved hypothetical protein), displays 43.7% similarities with the probable chaperone HSP31 in Baker's yeast (*S. cerevisiae*) according to the Blast results (see Figure 3.11A). A second protein out of spot No. 127, which was identified by MALDI-TOF-MS and nanoLC-MS/MS as protein C16A3.08c in chromosome II (O42914, YBI8_SCHPO), shows 28.6% similarities with the suppressor protein STM1 in Baker's yeast (*S. cerevisiae*) according to the Blast results (see Figure 3.11B). Finally, a third protein identified in spot No. 360, which was identified by MALDI-TOF-MS and nanoLC-MS/MS as hypothetical protein C23H3.15c in chromosome I (P78890, YEPF_SCHPO), contains 27% similarities with the stress protein DDR48 (DNA damage-responsive protein 48) in Baker's yeast (*S. cerevisiae*) according to the Blast search (see Figure 3.11C).

A

```
Db AC      Description                                              Score E-value

tr O74914 _SCHPO SPCC757.03c protein [SPCC757.03c] [Schizosacchar... 491 e-138
sp Q04432 HSP31_YEAST Probable chaperone HSP31 [HSP31] [Saccharo... 196 6e-49

CLUSTAL W (1.82) multiple sequence alignment

tr|O74914|O74914_SCHPO     MASEGKVLLVASSYYGPFYPDGMNTGVHFAELLIPYQVFREAGYEVQLTS
sp|Q04432|HSP31_YEAST      -MAPKKVLLALTSYNDVFYSDGAKTGVFVVEALHPFNTFRKEGFEVDFVS
                            :  ****. :** . **.** :***...* * *::.**: *:**::.*

tr|O74914|O74914_SCHPO     ETGKCKFDDHSIKKSALGEVERDAFDNKDNEFWYALKDIKPADKINYKEF
sp|Q04432|HSP31_YEAST      ETGKFGWDEHSLAKDFLNGQDETDFKNKDSDFNKTLAKIKTPKEVNADDY
                           ****  :*:**: *. *. :.  *.***.:*  :* .**...::* .::

tr|O74914|O74914_SCHPO     CIMFIAGGHAAMFDLPHATNLQTLAQQIYASNGVLAAVCHGPVMLPFVDD
sp|Q04432|HSP31_YEAST      QIFFASAGHGTLFDYPKAKDLQDIASEIYANGGVVAAVCHGPAIFDGLTD
                            *:* :.**.::** *:*.:** :*.:***..**:******.::   : *

tr|O74914|O74914_SCHPO     TKSPEGRSVVYGKKVTAFNSTGELVMGVSSALRERNMQDLNSLFREAGAE
sp|Q04432|HSP31_YEAST      KKT--GRPLIEGKSITGFTDVGETILGVDSILKAKNLATVEDVAKKYGAK
                           .*:  **.:: **.:*.*...** ::**.* *: :*:  ::.: :: **:

tr|O74914|O74914_SCHPO     FVDPPTPMSDFTQVDGRIVTGVNPMSAKSTAEAAIKVSQSLRKT
sp|Q04432|HSP31_YEAST      YLAPVGPWDDYSITDGRLVTGVNPASAHSTAVRSIDALKN----
                           :: *  * .*:: .***:****** **:***  :*.. :.
```

Figure 3.11 Sequence alignment of three proteins with unknown functions using CLUSTAL W. **A:** Sequence alignment of SPCC757.03c protein in Fission yeast *S. pombe* and the probable chaperone HSP31 in Baker's yeast (*S. cerevisiae*).

B

```
      Db    AC         Description                                          Score  E-value

      sp    O42914     YBI8_SCHPO Protein C16A3.08c in chromosome II [SPBC16A...  408  e-113
      sp    P39015     STM1_YEAST Suppressor protein STM1 (MPT4 protein) (GU4...   61  4e-08


      CLUSTAL W (1.82) multiple sequence alignment

      sp|O42914|YBI8_SCHPO     MSVASKNLFDLLGEETPAATTTEKKTAASRDKKRSDSPPVPRELVAQSTTSRKRDPNQPT
      sp|P39015|STM1_YEAST     ----MSNPFDLLGNDVEDADVVVLP--------------PKEIVKSNTSSKKADVPPPS
                                 .* *****::.   *  ..              *:*:* ..*:*:* *   *:

      sp|O42914|YBI8_SCHPO     PRERTVNKKADQPRRRQAPQGNEAFAREGKEARANNAAHPVDATGAPSNRRNARARRGR
      sp|P39015|STM1_YEAST     ADP-------SKARKNRPRPSGNEGAIRDKTAGRRNNRSKDVTDSATTK-----KSNTRR
                                 .        .:.*:.* *.***.  *:  .* ** ::  *  :.:..    ::.  *

      sp|O42914|YBI8_SCHPO     EFDRHSQTGRVDTKKATERGWGDLVN-----SAANPDVAENEGNTPSGAQTPAAEEENVK
      sp|P39015|STM1_YEAST     ATDRHSRTGKTDTKKKVNQGWGDDKKELSAEKEAQADAAAEIAEDAAEAEDAGKPKTAQL
                                 ****:**:.**** .::*****  :     . *:.*.* : .: .: *:  ..  :

      sp|O42914|YBI8_SCHPO     TLDEYLSERKSAAKPVGRTVEKLENATKVEKSAPEELFASLKKSASQKKSAAKESKPKKV
      sp|P39015|STM1_YEAST     SLQDYLNQQANNQFNKVPEAKKVELDAERIETAEKEAYVPATKVKNVKSKQLKTKEYLEF
                                 :*::**.::  .       .:*:* .::  ::* :* :.. .*  . *.. * .: :.

      sp|O42914|YBI8_SCHPO     LLDIEQTFTAR-------------PARGGRPNRAPRRGPSET-ASKTQQAPPTLSETDF
      sp|P39015|STM1_YEAST     DATFVESNTRKNFGDRNNNSRNNFNNRRGGRGARKGNNTANATNSANTVQKNRNIDVSNL
                                 : :: * :             ****  *  .. .. * :::* *   .:. :::

      sp|O42914|YBI8_SCHPO     PALA
      sp|P39015|STM1_YEAST     PSLA
                               *:**
```

C

```
      Db    AC         Description                                          Score  E-value
      sp    P78890     YEPF_SCHPO Hypothetical protein C23H3.15c in chromosom...  514  e-145
      sp    P18899     DDR48_YEAST Stress protein DDR48 (DNA damage-responsiv...   55  2e-06


      CLUSTAL W (1.82) multiple sequence alignment

      sp|P78890|YEPF_SCHPO     ------------------------------------------------
      sp|P18899|DDR48_YEAST    GLFDKVKQFANSNNNNNDSGNNNQGDYVTKAENMIGEDRVNQFKSKIGED

      sp|P78890|YEPF_SCHPO     -------MSYQQRANDSMNSAKQYSSSAGAVHNSDEPFSSSGAPQNRNFD
      sp|P18899|DDR48_YEAST    RFDKMESKVRQQFSNTSINDNDSNNNDSYGSNNNDSYGSNNNDSYGSNNN
                                      ** :* *:*. ..  ...: . :*.*.  *... . . * :

      sp|P78890|YEPF_SCHPO     TSYTS-EIPSNSSRAANDMGTDIGSGDPYAGMTSDTKKGFNSVESRKKEQ
      sp|P18899|DDR48_YEAST    DSYGSNNNDSYGSNNDDSYGSSNKKKSSYGSNNDDSYGSSNNNDSYGSNN
                                ** * :  * .*.  :. *:.  . ..*.. ..*:  . *. :*  .::

      sp|P78890|YEPF_SCHPO     SDVRGGD--TSYSRRHDDSSYSSNK----------YSTGGNDSYSSGGRN
      sp|P18899|DDR48_YEAST    NDSYGSNNNDSYGSNNDDSYGSSNKNKSSYGSNNDDSYGSNNDDSYGSSN
                               .*  *.:  **. :*** ****        * *.*: * *. *

      sp|P78890|YEPF_SCHPO     EDYSTSG-------GSYTTDPSRTDDTASYGQSQYNQSRKTTQG-GDYGE
      sp|P18899|DDR48_YEAST    KKKSSYGSSNNDSYGSNNDDSYGSNNNDSYGSNNDDSYGSSNKKKSSYGS
                               :. *: *       ** . *. ::.. ***..: :.  .:.:  ..**.

      sp|P78890|YEPF_SCHPO     DYSQSYPTDTYGSRQKATPSDTVGGGAYDYSSSGSHTHGGSHGTEHRGGS
      sp|P18899|DDR48_YEAST    NNDDSYGSSNNNDSYGSNNDDSYGSSNKNKSSYGSSSNDDSYGSSNNDDS
                               : .:** :.. ..  :. .*: *..  : ** ** ::..*:*:.:...*

      sp|P78890|YEPF_SCHPO     YGNDNTANKTRGAVSSAGYSG---EGYGKGTYATDTTAEAN-------RR
      sp|P18899|DDR48_YEAST    YGSSNKKKSSYGSNNDDSYGSNNDDSYGSSNKKKSSYGSNNDSYGSNND
                               **..*. :.: *: .. .*..   :.**...  ..: ..:*        .

      sp|P78890|YEPF_SCHPO     AATGTRNARTTAQRNAQLAEDEHVSMGDKMKGNMEKMAGKLTRDPELVQK
      sp|P18899|DDR48_YEAST    DSYGSSNKKKSSYGSNNDDSYGSSNNNDSYGSNNDDSYGSSNRNKNSYGS
                                : *: * :.::  . :  .    . .*.  .* :.  *. .*: :   .

      sp|P78890|YEPF_SCHPO     GEDLKTGHHSERY---------------
      sp|P18899|DDR48_YEAST    SNYGSSNNDDSYGSSNRGGRNQYGGDDDY
                               .:  .:.:...
```

Figure 3.11 continued **B:** Sequence alignment of protein C16A3.08c in chromosome II in *S. pombe* and the suppressor protein STM1 in Baker's yeast. **C:** Sequence alignment of hypothetical protein C23H3.15c in chromosome I in *S. pombe* and the stress protein DDR48 (DNA damage-responsive protein 48) in Baker's yeast (Hwang *et al.*, 2006).

Moreover, a protein in spot No. 197 was identified by MALDI-TOF-MS and nanoLC-MS/MS as a probable oxidoreductase C26F1.07 in chromosome I (Q10494, YDG7_SCHPO). This protein displays similarities to the alcohol dehydrogenase [NADP+] in humans, mice, pigs and rats according to the BLAST search (see Figure 3.12A).

The aldoketo reductase family (Bohren *et al.,* 1989; Bruce *et al.,* 1994) contains a number of structurally and functionally related NADPH-dependent oxidoreductases as well as some other proteins. These proteins possess three known consensus patterns that are specific to this family of proteins.

YDG7_SCHPO also belongs to the aldoketo reductase family and exhibits the aldo-keto reductase family signature 1 (aldoketo reductase 1, PS00798) and 2 (aldoketo reductase 2, PS00062). Additionally, this protein presents a high homology with the aldo-keto reductase family signature 3 (aldoketo reductase 3, PS00063). This protein was identified by nanoLC-MS/MS (based on the detection of 24 peptides covering 57% of the sequence) and three times by MALDI-TOF-MS (based on the detection of 23 peptides covering 69%, 21 peptides covering 73%, or 20 peptides covering 57% of the sequence) so that we could confirm the 3 consensus patterns. Only partially overlapping amino acid sequence coverage was obtained, comparing the triple MALDI-TOF-MS analysis and the nanoLC-MS/MS analysis. 13 peptides (47% of the total sequence) were detected by all MS analyses. The 79% amino acid sequence coverage of this protein obtained from the combination of all MS analyses is shown in Figure 3.12B, along with a list of all the identified peptides. Finally, it was confirmed that the aldoketo reductase 1 signature (located in the N-terminal section of this protein family: G-[FY]-R-[HSAL]-[LIVMF]-D-[STAGCL]-[AS]-x(5)-[EQ]-x(2)-[LIVMCA]-G) and 6 amino acids of the C-terminal region of the aldoketo reductase 2 signature (it is located in the central section: [LIVMFY]-x(8)-{L}-[KREQ]-{K}-[LIVM]-G-[LIVM]-[SC]-N-[FY]) have been confirmed from all MS analyses.

The aldoketo reductase 3 signature (it is located in the C-terminal: [LIVM]-[PAIV]-[KR]-[ST]-{EPQG}-x(3)-R-{SVAF}-x-[GSTAEQK]-[NSL]-x(2)-[LIVMFA]) is centered on a lysine residue whose chemical modification, in aldose and aldehyde reductases, affects the catalytic efficiency. The amino acid sequence, which is similar to the aldoketo reductase family signature 3, has also been confirmed.

A

Db	AC	Description	Score	E-value
sp	Q10494	YDG7_SCHPO Probable oxidoreductase C26F1.07 in chromos...	616	e-175
sp	P14550	AK1A1_HUMAN Alcohol dehydrogenase [NADP+] (EC 1.1.1.2)...	229	1e-58
sp	Q9JII6	AK1A1_MOUSE Alcohol dehydrogenase [NADP+] (EC 1.1.1.2)...	224	2e-57
sp	P50578	AK1A1_PIG Alcohol dehydrogenase [NADP+] (EC 1.1.1.2) (...	222	1e-56
sp	P51635	AK1A1_RAT Alcohol dehydrogenase [NADP+] (EC 1.1.1.2) (...	221	2e-56

CLUSTAL W (1.82) multiple sequence alignment

```
sp|Q10494|YDG7_SCHPO.      MSAEQKYFENAQNVHFTLADGSKIPGLGLGTWRSEPNQTKNAVKTALQY
sp|P14550|AK1A1_HUMAN.     -----------AASCVLLHTGQKMPLIGLGTWKSEPGQVKAAVKYALSV
sp|Q9JII6|AK1A1_MOUSE.     -----------TASSVLLHTGQKMPLIGLGTWKSEPGQVKAAIKHALSA
sp|P50578|AK1A1_PIG.       -----------AASCVLLHTGQKMPLIGLGTWKSEPGQVKAAIKYALTV
sp|P51635|AK1A1_RAT.       -----------TASSVLLHTGQKMPLIGLGTWKSEPGQVKAAIKYALSV
                                      . *   *.*:* :*****:***.*.* *:* **
```

                    ALDOKETO_REDUCTASE_family signature 1
```
sp|Q10494|YDG7_SCHPO.      GYRHIDAAAIYGNEDEVGDGIKESG-----VPRKDIWVTSKLWCNAHAPEA
sp|P14550|AK1A1_HUMAN.     GYRHIDCAAIYGNEPEIGEALKEDVGPGKAVPREELFVTSKLWNTKHHPED
sp|Q9JII6|AK1A1_MOUSE.     GYRHIDCASVYGNETEIGEALKESVGSGKAVPREELFVTSKLWNTKHHPED
sp|P50578|AK1A1_PIG.       GYRHIDCAAIYGNELEIGEALTETVGPGKAVPREELFVTSKLWNTKHHPED
sp|P51635|AK1A1_RAT.       GYRHIDCASVYGNETEIGEALKESVGAGKAVPREELFVTSKLWNTKHHPED
                           ******.*::**** *:*:.:.*      ***::::****** . * **
```

ALDOKETO_REDUCTASE_1
G - [FY] - R - [HSAL] - [LIVMF] - D - [STAGCL] - [AS] - x(5) - [EQ] - x(2) - [LIVMCA] - G

```
sp|Q10494|YDG7_SCHPO.      VPKALEKTLKDLKLDYLDEYLIHWPVSFKTGEDKFPKDKDGNLIYEKNPI
sp|P14550|AK1A1_HUMAN.     VEPALRKTLADLQLEYLDLYLMHWPYAFERGDNPFPKNADGTICYDSTHY
sp|Q9JII6|AK1A1_MOUSE.     VEPALRKTLADLQLEYLDLYLMHWPYAFERGDNPFPKNADGTVRYDSTHY
sp|P50578|AK1A1_PIG.       VEPALRKTLADLQLEYLDLYLMHWPYAFERGDNPFPKNADGTIRYDATHY
sp|P51635|AK1A1_RAT.       VEPAVRKTLADLQLEYLDLYLMHWPYAFERGDNPFPKNADGTVKYDSTHY
                           *  *:.*** **:*:*** **:*** *:: ***: **.: *:  .
```

                    ALDOKETO_REDUCTASE_family signature 2
```
sp|Q10494|YDG7_SCHPO.      EETWKAMEKLLETGKVRHIGLSNFNDTNLERILKVAKVKPAVHQMELHPF
sp|P14550|AK1A1_HUMAN.     KETWKALEALVAKGLVQALGLSNFNSRQIDDILSVASVRPAVLQVECHPY
sp|Q9JII6|AK1A1_MOUSE.     KETWKALEVLVAKGLVKALGLSNFNSRQIDDVLSVASVRPAVLQVECHPY
sp|P50578|AK1A1_PIG.       KDTWKALEALVAKGLVRALGLSNFSSRQIDDVLSVASVRPAVLQVECHPY
sp|P51635|AK1A1_RAT.       KETWKALEALVAKGLVKALGLSNFSSRQIDDVLSVASVRPAVLQVECHPY
                           ::****:* *: .* *: :*****.. ::: :*.**.*:*** *:* **:
```

ALDOKETO_REDUCTASE_2
[LIVMFY] - x(8) - {L} - [KREQ] - {K} - [LIVM] - G - [LIVM] - [SC] - N - [FY]

```
sp|Q10494|YDG7_SCHPO.      LPQTEFVEKHKKLGIHVTAYSPFGNQNTIYES-KIPKLIEHETIQKIAKS
sp|P14550|AK1A1_HUMAN.     LAQNELIAHCQARGLEVTAYSPLGSSDRAWRDPDEPVLLEEPVVLALAEK
sp|Q9JII6|AK1A1_MOUSE.     LAQNELIAHCHARGLEVTAYSPLGSSDRAWRHPDEPVLLEEPVVLALAEK
sp|P50578|AK1A1_PIG.       LAQNELIAHCQARGLEVTAYSPLGSSDRAWRDPNEPVLLEEPVVQALAEK
sp|P51635|AK1A1_RAT.       LAQNELIAHCQARGLEVTAYSPLGSSDRAWRHPDEPVLLEEPVVLALAEK
                           *.*.*::  : :   *:.*******:*..:  :.   * *:*. .:  :*:.
```

                              ALDOKETO_REDUCTASE_family signature 3
```
sp|Q10494|YDG7_SCHPO.      KGEGVTGATIAVSWAITRGTSVIPKSVNEQRIKSNFKYIPLTK--EDMDE
sp|P14550|AK1A1_HUMAN.     YGR--SPAQILLRWQVQRKVICIPKSITPSRILQNIKVFDFTFSPEEMKQ
sp|Q9JII6|AK1A1_MOUSE.     HGR--SPAQILLRWQVQRKVICIPKSINPSRILQNIQVFDFTFSPEEMKQ
sp|P50578|AK1A1_PIG.       YNR--SPAQILLRWQVQRKVICIPKSVTPSRIPQNIQVFDFTFSPEEMKQ
sp|P51635|AK1A1_RAT.       HGR--SPAQILLRWQVQRKVICIPKSITPSRILQNIQVFDFTFSPEEMKQ
                           .. : * * : * : * . ****:. .** .*:: : :*   *:*.:
```

ALDOKETO_REDUCTASE_3
[LIVM] - [PAIV] - [KR] - [ST] - {EPQG} - x(3) - R - {SVAF} - x - [GSTAEQK] - [NSL] - x(2) - [LIVMFA]

```
sp|Q10494|YDG7_SCHPO.      INSIGIRARFNQATFSNEPVFAGLEDGRT--------
sp|P14550|AK1A1_HUMAN.     LNALNKNWRYIVPMLTVDGKRVPRDAGHPLYPFNDPY
sp|Q9JII6|AK1A1_MOUSE.     LDALNKNWRYIVPMITVDGKRVPRDAGHPLYPFNDPY
sp|P50578|AK1A1_PIG.       LDALNKNLRFIVPMLTVDGKRVPRDAGHPLYPFNDPY
sp|P51635|AK1A1_RAT.       LDALNKNWRYIVPMITVDGKRVPRDAGHPLYPFNDPY
                           ::::. . *:  . :: :   . : *:.
```

Figure 3.12 Multiple sequence alignment of YDG7_SCHPO partially overlapping amino acid sequence coverage with aldoketo reductase family signatures and using CLUSTAL W. **A:** YDG7_SCHPO (Q10494, spot No. 197) shows similarities with alcohol dehydrogenase [NADP+] in humans, mice, pigs and rats according to the BLAST search. Moreover, these proteins possess the aldo/keto reductase family signature 1, 2 and 3. These sequences are marked with grey boxes**.**

B
```
  1 MSAEQKYFEN AQNVHFTLAD GSKIPGLGLG TWRSEPNQTK NAVKTALQYG
```

Aldoketo_Reductase_1
```
 51 YRHIDAAAIY GNEDEVGDGI KESGVPRKDI WVTSKLWCNA HAPEAVPKAL
```

```
101 EKTLKDLKLD YLDEYLIHWP VSFKTGEDKF PKDKDGNLIY EKNPIEETWK
```

Aldoketo_Reductase_2
```
151 AMEKLLETGK VRHIGLSNFN DTNLERILKV AKVKPAVHQM ELHPFLPQTE
```

```
201 FVEKHKKLGI HVTAYSPFGN QNTIYESKIP KLIEHETIQK IAKSKGEGVT
```

the region is similar to the Aldoketo_Reductase_3
```
251 GATIAVSWAI TRGTSVIPKS VNEQRIKSNF KYIPLTKEDM DEINSIGIRA
```

```
301 RFNQATFSNE PVFAGLEDGR T
```

Sequence coverage percentages:

First MALDI-TOF-MS : 69%

Second MALDI-TOF-MS : 73%

Third MALDI-TOF-MS : 57%

NanoLC-MS/MS : 57%

Total : 79%

Figure 3.12 continued **B:** Peptides identified by MALDI-TOF-MS or nanoLC-MS/MS are shown in **red boldface letters** and in **blue boldface letters** when identified by both techniques. The aldoketo reductase family signature 1, 2 and a very similar to the aldoketo reductase family signature 3 of YDG7_SCHPO are marked with grey boxes (Hwang *et al.,* 2006)**.**

3.1.4 Summary of the proteome analysis of S. pombe

Two extensive 2-D reference maps (pH 3-10 and pH 4-7) for the proteome analysis of the fission yeast *S. pombe* wild h^{-S} L 972 were created. A total of 364 proteins (representing 157 distinct proteins) have been identified by using MALDI-TOF-MS as well as nanoLC-MS/MS. These proteins were functionally classified according to their biological process. Therefore, the present reference maps provide a very useful information for the second part of my work using *S. pombe* as a model organism to study the effect of steroid hormones on the yeast proteome.

3.2 Analysis of MR-independent DOC induced effects on the protein pattern of S. pombe

Currently, 2-DE is the most often used technique for obtaining a global picture of the expression levels of a proteome under various conditions. As mentional in the introduction, *S. pombe* does not contain nuclear steroid receptors making it possible to investigate the receptor-independent actions of different kinds of steroid hormones on the protein pattern. Steroid hormones act as chemical messengers in many species and target tissues to produce both genomic actions, and non-genomic actions. In a previous study of our group, Böhmer *et al.* (Böhmer *et al.,* 2006) recently reported the MR-independent action of aldosterone on the protein level in *S. pombe*. In the first part of the present work, a well resolved 2-D reference map of *S. pombe* has been established (Hwang *et al.,* 2006).

The goal of second part of this work was to analyze the MR-independent action of DOC, which is a potent MR agonist. The differentially expressed proteins by DOC were separated by 2-DE and analyzed by using PDQuest software. Both MS techniques were used for establishing the reference map and were also used to identify the differential expression of proteins (see Figure 3.13). The identified proteins may be specifically associated with non-genomic actions and might be new targets for the development of drugs against mineralocorticoid-caused heart disease.

3.2.1 Analysis of differentially expressed proteins after incubation with DOC

Since *S. pombe* is not a natural target cell for DOC, the incubation time and suitable DOC concentrations should be considered. As previously described, non-genomic effects are *inter alia* characterized by a rapid onset of action. The rapidity varies in most cases from seconds to minutes. As the fission yeast does not contain nuclear steroid receptors, it is not necessary to apply a short time limit to induce a non-genomic effect. In a previous study of our group, an incubation time of 3.5 h was used to assure that the steroid can enter the cell and induce changes to the protein pattern in *S. pombe* (Böhmer *et al.,* 2006). Taking this into accout, an incubation time of 3.5 h was also used in the present study.
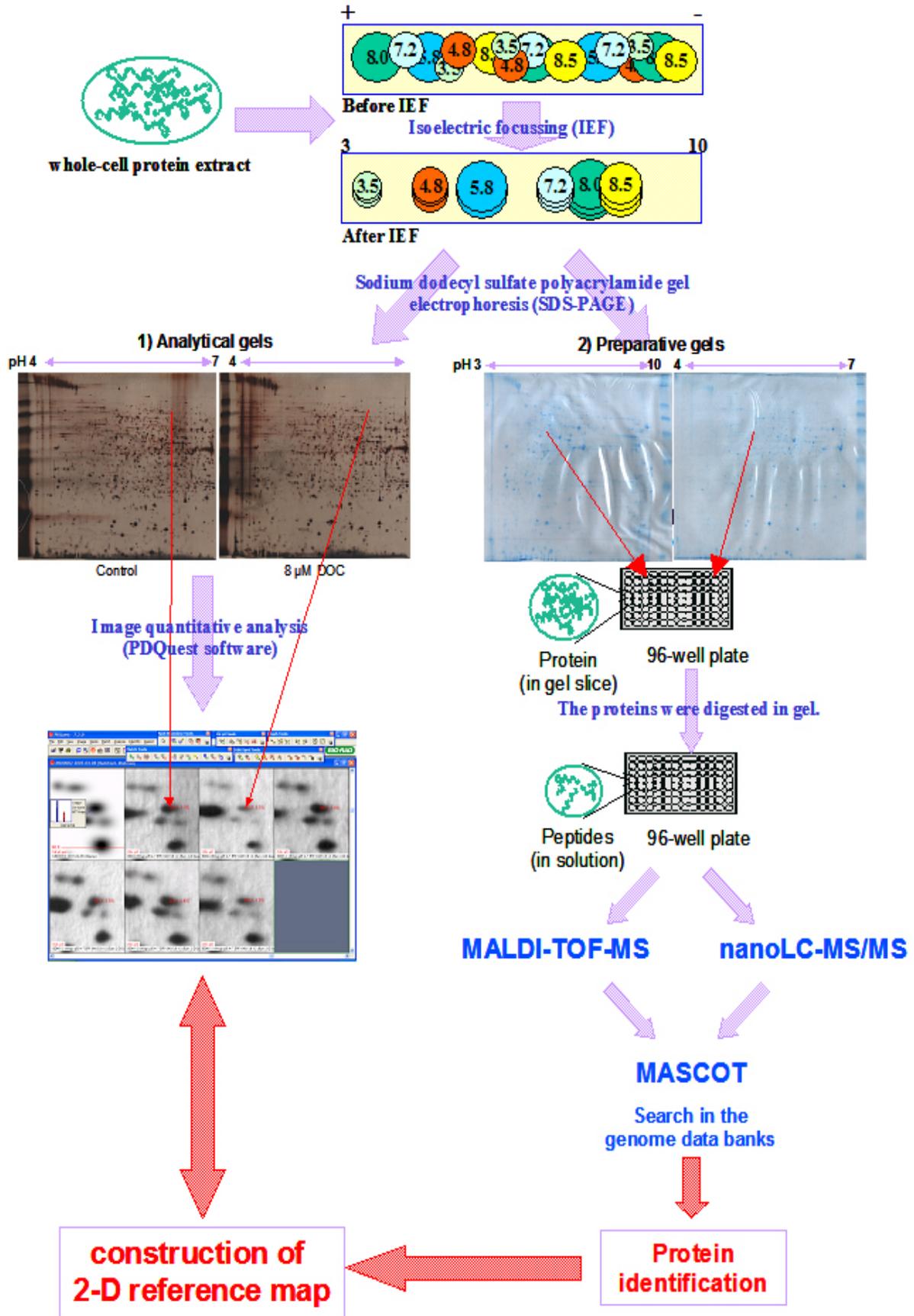
Figure 3.13 Representation of proteomics approach to identify differential protein pattern.

In a previous study, the metabolism of DOC was investigated in A6 cells with serum-free culture media containing 2.5 µM (^{3}H) DOC (Matsuzaki *et al.,* 1995). Additionally, hydroxylase activity assays in COS-1 cells (Cao and Bernhardt, 1999) have been performed in our group using between 1 and 5 µM DOC. Aldosterone-induced changes of the protein patterns using one dimensional electrophoresis with [^{35}S]-methionine labeled proteins in *S. pombe* was investigated with culture media containing only 8 µM aldosterone (Böhmer *et al.,* 2006). DOC can be converted to corticosterone and finally to aldosterone. The appropriate concentration of DOC applied to *S. pombe* could be considered to be on a micromolar level (less than 10 µM), since this concentration is regarded to induce unspecific effects (Falkenstein *et al.,* 2000).

Moreover, for aldosterone and corticosterone concentration of 8 µM have been determind as suitable for induction of MR-independent protein patterns using a combination of 2-DE and MS in *S. pombe* (Böhmer *et al.,* 2006). This finding was recently underlined by a new study (Bureik *et al.,* 2005) in which the human MR and GR were cloned and expressed in *S. pombe.* Thus, DOC concentration of 8 µM has been determind as suitable for induction of MR-independent effects in *S. pombe.*

10 mL of the main cultured cells were incubated with 8 µM DOC and without DOC for 3.5 h at 32°C and 185 rpm. Each experiment contained always two control samples (just ethanol of same volume) as well as two 8 µM DOC treated sample. The extracted whole-cell protein mixtures were quantified by using the Ettan 2-D Quant Kit (Amersham Biosciences). Protein preparation, separations and visualizations were performed due to the optimized 2-DE conditions obtained in the first part work. After 2-DEs using the widerange pH 3-10 IPG strips, more than 1500 protein spots on silver stained gels of all samples have been visualized. Each 2-DEs with different samples have been performed at least four times. Figure 3.14 shows the silver stained 2-D gels using the widerange pH 3-10 IPG strips under four different condition (control sample and 8 µM DOC treated sample; 60 µg protein / gel).

To find the differentially expressed proteins due to DOC, the scanned gel images were analyzed using PDQuest software. After comparsion, a remarkable difference between the control and 8 µM DOC treated samples is displayed.
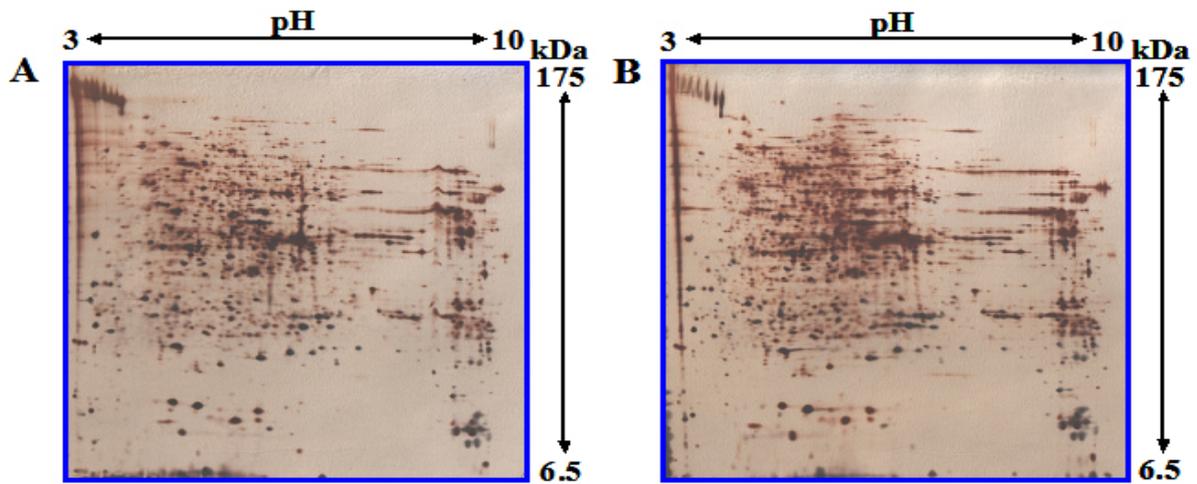
Figure 3.14 2-D gels of the protein mixtures treated with different concentrations of DOC. Proteins were separated by IEF using 18 cm IPG strips (pH 3-10), followed by 12.5% SDS–PAGE stained with silver. **A:** Control sample, **B:** 8 µM DOC treated sample.

As shown in the reference map (in the range pH 3-10) produced in the first part of my work, a comparison of different intensities was difficult because of many protein spots presented in the area between pH 4 and 7.5 on the 2-D gel when using the widerange 3-10 IPG strips. Thereby, the silver stained 2-D gels using the widerange pH 4-7 IPG strips were used to compare the protein spots in this range.

When using in the widerange pH 4-7 IPG strips more than 1000 protein spots on silver stained gels of all samples have been visualized. Figure 3.15 shows the silver stained 2-D gels using the widerange pH 4-7 IPG strips with two different conditions (control sample and 8 µM DOC treated sample; 80 µg protein / gel).
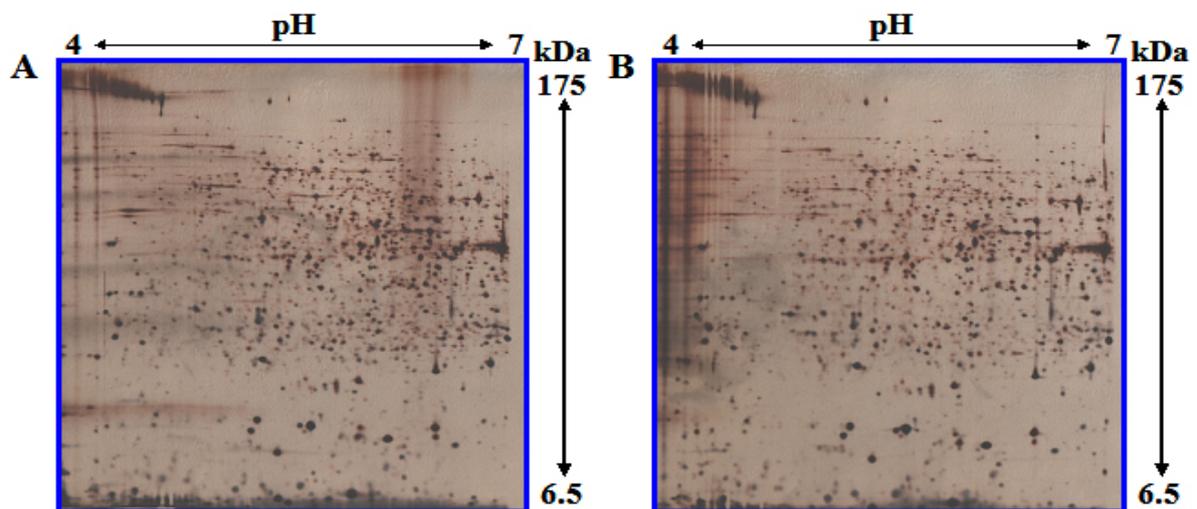
Figure 3.15 The expression of proteins on 2-D gels by two different conditions (**A:** control sample, **B:** 8 µM DOC) in the fission yeast *S. pombe*.

Thus, proteins extracted from two samples (control and 8 µM DOC) were resolved by 2-DE using 18 cm-long IPG strips in the range of 3-10 as well as 4-7 forming each of two groups (control sample and 8 µM DOC treated sample). Each 2-DEs using 18 cm-long IPG strips in the range of 3-10 as well as 4-7 forming each of two groups (control sample and 8 µM DOC treated sample) have been performed at least four times. Thereafter, spot quantification using PDQuest was performed with control and 8 µM DOC treated samples.

3.2.2 Spot Quantification using PDQuest

As shown above, 2-D gels using the strips of pH range 4-7 were used to compare the different intensities of all spots in this area. 2-D gels using the widerange pH 3-10 IPG strips were used only to compare the different intensities of the all spots in the area above pH 7 or below pH 4. The size and orientation of each gel image were adjusted with the cropping and rotating tools in the image menu. After spot detection, a matchset (composed of the Gaussian and filtered gel images) was created. The spot-matching and analysis was performed on the Gaussian spots. To compare the different intensities of the protein spots on the 2-D gels, two groups with quintuplicate gels were created by using the replicate groups function of PDQuest software. They were named as "Control" and "DOC" (8 µM DOC treated samples). The data analysis can be performed on each gel individually or on the set of quintuplicate gels grouped together. The differentially visualized spots in at least four out of five gels were selected and used to calculate the average differences in protein expression.

Under the applied conditions, a total of 42 spots were found to be significantly different between the two groups (at least 2 fold: see Figure 3.16). 33 spots were detected from 2-D gels with a pH 4-7 range and 9 spots (pH > 7) from 2-D gels with a pH range 3-10. Of these spots, 26 spots are significantly decreased in intensity while 16 spots are increased.
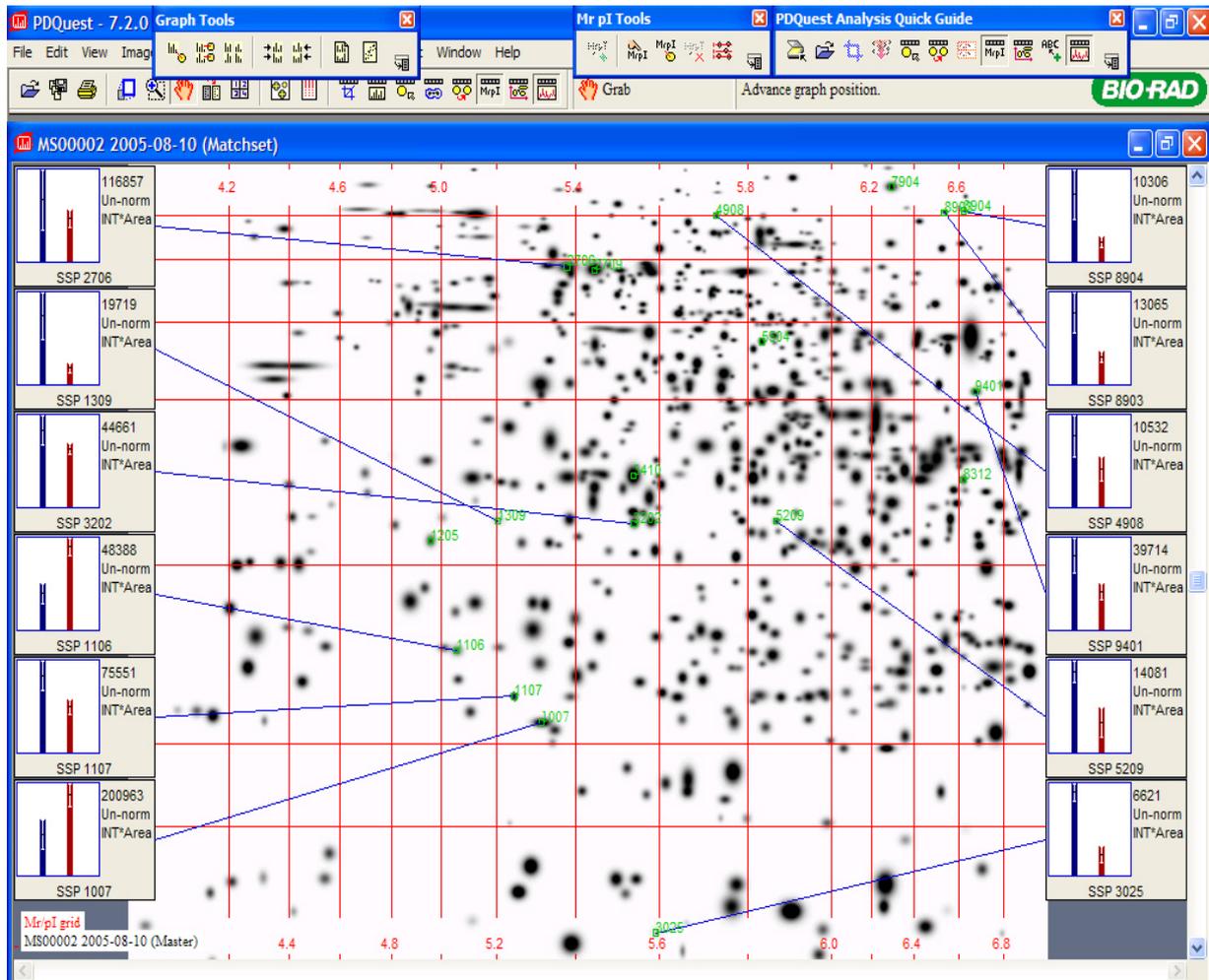
Figure 3.16 Some of the differentially visualized spots between each groups on the master gel with the range pH 4-7. Control, blue color in bar chart; DOC, red color in bar chart.

3.2.3 Mass spectrometry analyses

For MS analysis, proteins extracted from two samples (control and 8 µM DOC: 240 µg proteins / gel) were also resolved by 2-D gels using the widerange pH 3-10 IPG strips as well as pH 4-7 IPG strips. After colloidal blue G-250 staining, 6 spots in the 3-10 pH range and 23 spots in the 4-7 pH range were excised, destained and analyzed independently by MALDI-TOF-MS as well as nanoLC-MS/MS approaches. Thereafter, 27 spots could be identified through both MS approaches, whereas 2 spots could not be identified (1 spot in the 3-10 pH range and 1 spot in the 4-7 pH range). Among 27 analyzed spots, 22 spots contained only a single protein. In 5 spots more than two proteins were identified. Normally, the presence of multiple proteins in a spot could make an interpretation of the differential approach very difficult. However, it seems to be possible to put an interpretation on the presence of two

proteins in a spot (No. 11: vip1 and rad24, see Table 3.3) identified together. Thus, it can be stated that 24 proteins out of 23 spots have been differentially regulated (18 spots were obtained from 2-D gel with a pH 4-7 range and 5 spots (pH > 7) from 2-D gel with a pH range 3-10: see Figure 3.17).
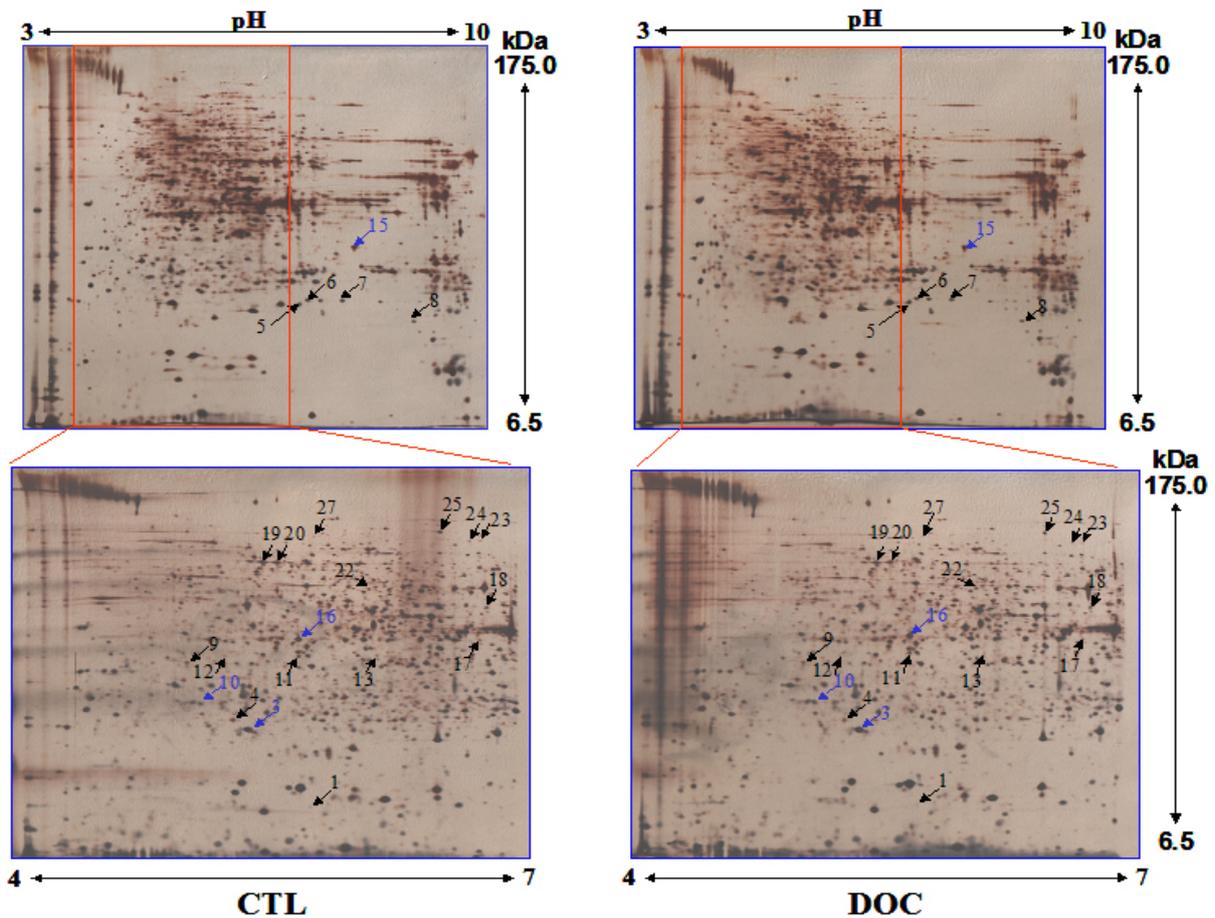
Figure 3.17 Representative proteome analysis of DOC-dependent differential protein patterns in the fission yeast *S. pombe* wild type h^{-S} L 972. Proteins were separated by IEF using 18 cm IPG strips (pH 3-10 or 4-7), followed by 12.5% SDS–PAGE and gels were stained with silver (60 or 80 µg protein). 19 spots that were repressed by DOC are indicated by **black arrows**, 4 spots (spot No. 3, 10, 15 and 16) that were enhanced by DOC are indicated by **blue arrows** (see Table 3.3). CTL, control; DOC, 8 µM DOC treated sample.

20 proteins were found in 19 spots which show a repressed intensity (see Figure 3.18) and 4 proteins (spot No. 3, 10, 15 and 16) exhibit enhanced intensity due to DOC treatment (see Figure 3.19). The list of differentially regulated proteins is shown in Table 3.3. As illustrated, both MALDI-TOF MS and nanoLC-MS/MS analysis have been performed in order to be able to increase the coverage percentage of the identified proteins and take advantage of the

complementarity of the two ionization techniques. Among these proteins, 12 proteins were identified by both MS approaches.
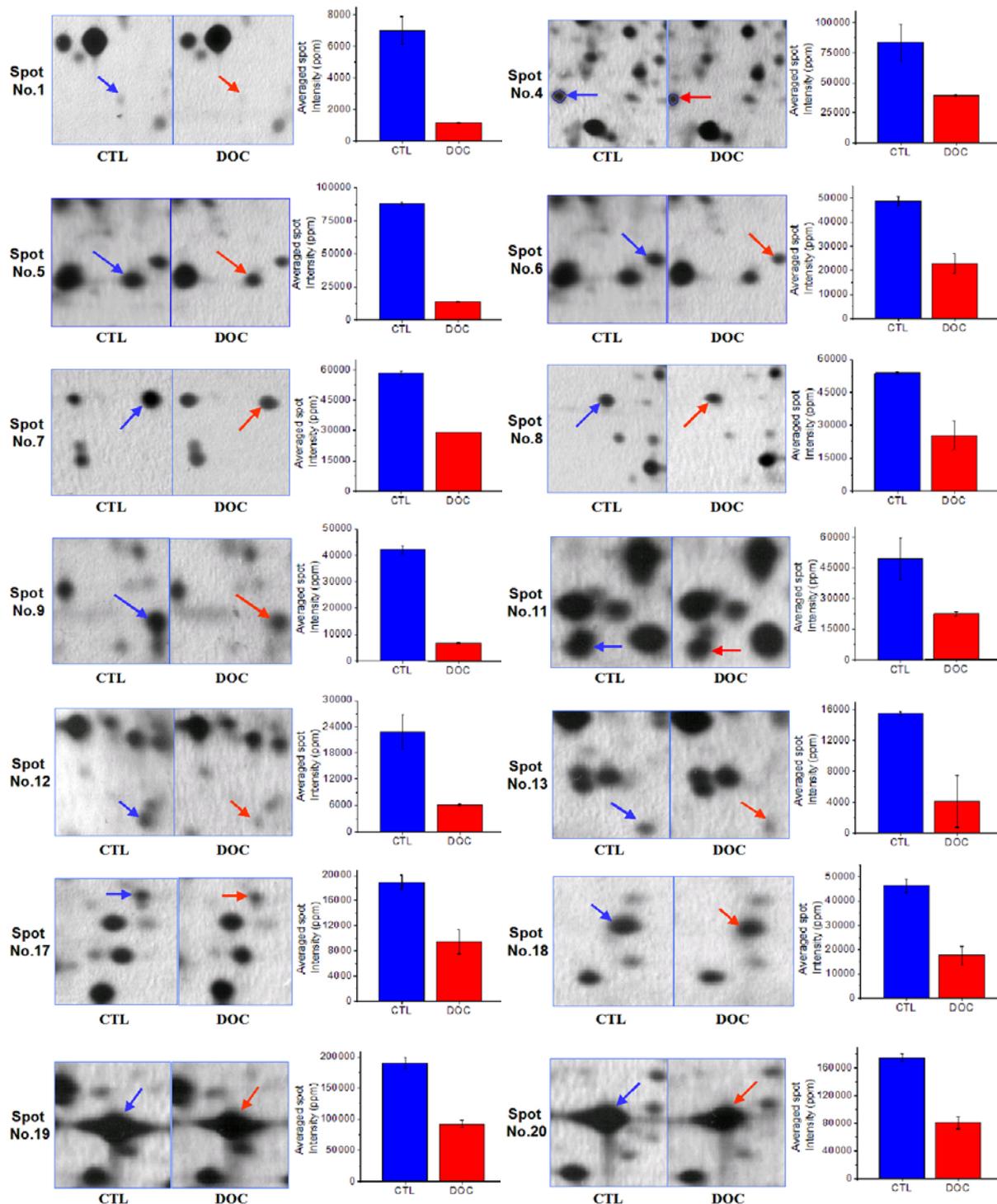
Figure 3.18 Twenty proteins were found in 19 spots which show decreased intensity due to DOC compared to the control in the 2-DE. CTL, control; DOC, 8 µM DOC treated sample. To be continued in the next page.
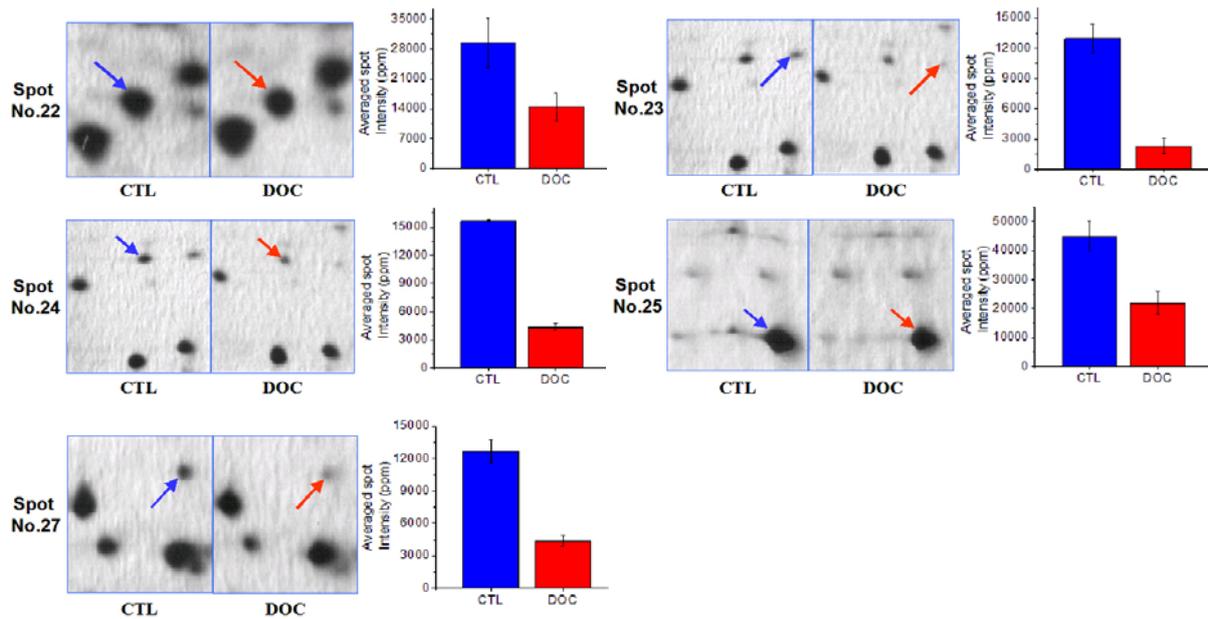
Figure 3.18 continued. CTL, control; DOC, 8 µM DOC treated sample. All determinations were done in triplicates, and values given were calculated from at least two different experiments.
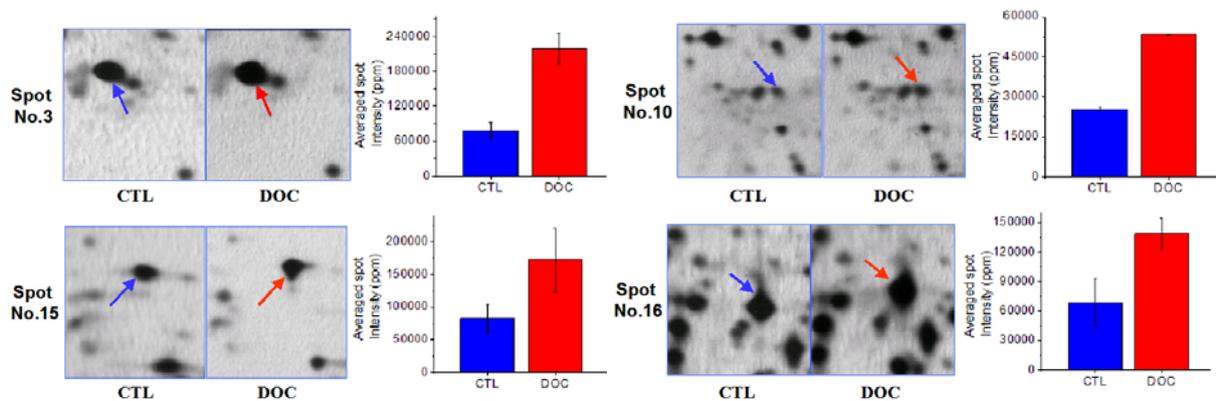
Figure 3.19 Four proteins are upregulated due to DOC compared to the control in the 2-DE. CTL, control; DOC, 8 µM DOC treated sample. All determinations were done in triplicates, and values given were calculated from at least two different experiments.

Table 3.3 List of differentially regulated proteins by DOC.

Regulation	SSP [a]	Spot No. [b]	Entry Name [c]	Protein Name [c]	Swiss-Prot Accession Number [c]	identified by	Sequence coverage [d]	Number of peptides [e]	Theoretical [f]		Gel-estimated [g]	
									MW (kDa)	pI	MW (kDa)	pI
Down	3025 [h]	1	COFI_SCHPO	Cofilin	P78929	nanoLC-MS/MS	60%	5	15.6	5.60	13.6	5.76
Down	1107 [h]	4	6PGD_SCHPO	6-phosphogluconate dehydrogenase, decarboxylating	P78812	MALDI-TOF-MS	20%	9	53.7	6.73	22.1	5.31
Down	9401 [h]	18				MALDI-TOF-MS nanoLC-MS/MS	46% 29%	23 12			41.3	6.69
Down	6107	5	G3P1_SCHPO	Glyceraldehyde 3-phosphate dehydrogenase 1	P78958	MALDI-TOF-MS	28%	10	35.9	6.24	20.5	7.03
Down	6109	6				MALDI-TOF-MS nanoLC-MS/MS	26% 16%	10 5			21.1	7.15
Down	7105	7	SODM_SCHPO	Superoxide dismutase [Mn], mitochondrial [Precursor]	Q9UQX0	MALDI-TOF-MS nanoLC-MS/MS	69% 40%	10 9	24.3	9.12	21.6	7.66
Down	8001	8	GPX1_SCHPO	Glutathione peroxidase	O59858	MALDI-TOF-MS	36%	8	18.1	8.35	18.1	8.59
Down	1205	9	MAOX_SCHPO	NAD-dependent malic enzyme	P40375	MALDI-TOF-MS nanoLC-MS/MS	30% 10%	21 7	62.5	5.68	32.7	4.64
Down	1309 [h]	12				MALDI-TOF-MS nanoLC-MS/MS	29% 15%	23 8			33.1	5.30
Down	3202 [h]	11	VIP1_SCHPO	Protein vip1	P87216	MALDI-TOF-MS nanoLC-MS/MS	74% 59%	15 11	27.5	5.54	32.8	5.54
			RAD24_SCHPO	DNA damage checkpoint protein rad24	P42656	nanoLC-MS/MS	30%	6	30.0	4.66		
Down	5209 [h]	13	KPYK_SCHPO	Pyruvate kinase	Q10208	MALDI-TOF-MS	32%	15	55.5	8.18	32.4	5.93
Down	3410	17	O94315_SCHPO	SPBC215.11c protein	O94315	MALDI-TOF-MS	28%	9	33.9	6.48	34.1	6.62
Down	9401	19	PDC2_SCHPO	Probable pyruvate decarboxylase C1F8.07c	Q92345	MALDI-TOF-MS	38%	18	64.8	5.71	58.1	5.38
Down	2706 [h]	20				MALDI-TOF-MS	39%	22			57.6	5.44
Down	2709	22	ENO12_SCHPO	Enolase 1-2	Q8NKC2	MALDI-TOF-MS	57%	25	47.8	5.73	46.8	5.81
Down	5504	23	TKT_SCHPO	Probable transketolase	Q9URM2	MALDI-TOF-MS	46%	30	75.1	6.33	72.0	6.62
Down	8904 [h]	24				MALDI-TOF-MS nanoLC-MS/MS	47% 30%	35 17			71.7	6.51
Down	8903 [h]	25	METE_SCHPO	Probable 5-methyltetrahydropteroyltriglutamate--homocysteine methyltransferase	Q9UT19	MALDI-TOF-MS nanoLC-MS/MS	32% 45%	20 33	85.3	5.99	80.5	6.28
Down	4908 [h]	27	HSP75_SCHPO	Heat shock protein sks2	Q10284	MALDI-TOF-MS	12%	7	67.2	5.82	69.0	5.63
Up	1007 [h]	3	O74887_SCHPO	SPCC576.03c protein	O74887	MALDI-TOF-MS nanoLC-MS/MS	70% 50%	11 13	21.2	5.37	21.3	5.36
Up	1106 [h]	10	ENO11_SCHPO	Enolase 1-1	P40370	MALDI-TOF-MS nanoLC-MS/MS	15% 31%	7 9	47.4	6.23	24.4	5.04
Up	7209	15	VDAC_SCHPO	Probable outer mitochondrial membrane protein porin	Q9P544	MALDI-TOF-MS nanoLC-MS/MS	78% 13%	13 4	29.7	7.10	28.7	7.82
Up	3410	16	GBLP_SCHPO	Guanine nucleotide-binding protein beta subunit-like protein	Q10281	MALDI-TOF-MS nanoLC-MS/MS	67% 69%	16 20	34.9	5.43	35.6	5.53

a) Number according to PDQuest 7.2.0 software

b) Number in Figure 3.17 – 3.19

c) Entry name, protein name and accession number according to Swiss-Prot (http://kr.expasy.org/sprot/)

d) Amino acid sequence coverage for the identified proteins

e) Number of matching peptides according to the MASCOT™ search engine

f) Theoretical Mr and pI according to protein sequence and Swiss 2-D PAGE database

g) Gel-estimated Mr and pI calculated by analysis of the gel images with PDQuest 7.2.0 software

h) Number in Figure 3.16

3.2.4 Protein classifications

Using the approach of the protein classifications according to their biological function applied in the first part of my work, a total of 19 distinct proteins with redundancies (24 identified proteins) were functionally classified. Among these proteins, 9 distinct proteins are involved in glycolysis (spot No. 5, 6, 10, 13 and 22) or other metabolic process (spot No. 4, 9, 12, 18, 19, 20, 23, 24 and 25). 5 distinct proteins are related to protein folding and associated processing (spot No. 27), to cellular transport (spot No. 15) or to cell rescue, defense and stress (spot No. 3, 7, and 8). 3 distinct proteins involved in the cell organization and biogenesis (spot No. 1 and 16) or cell cycle (spot No. 11). Two proteins display unknown function. Figure 3.20 display the functional classification of these proteins.
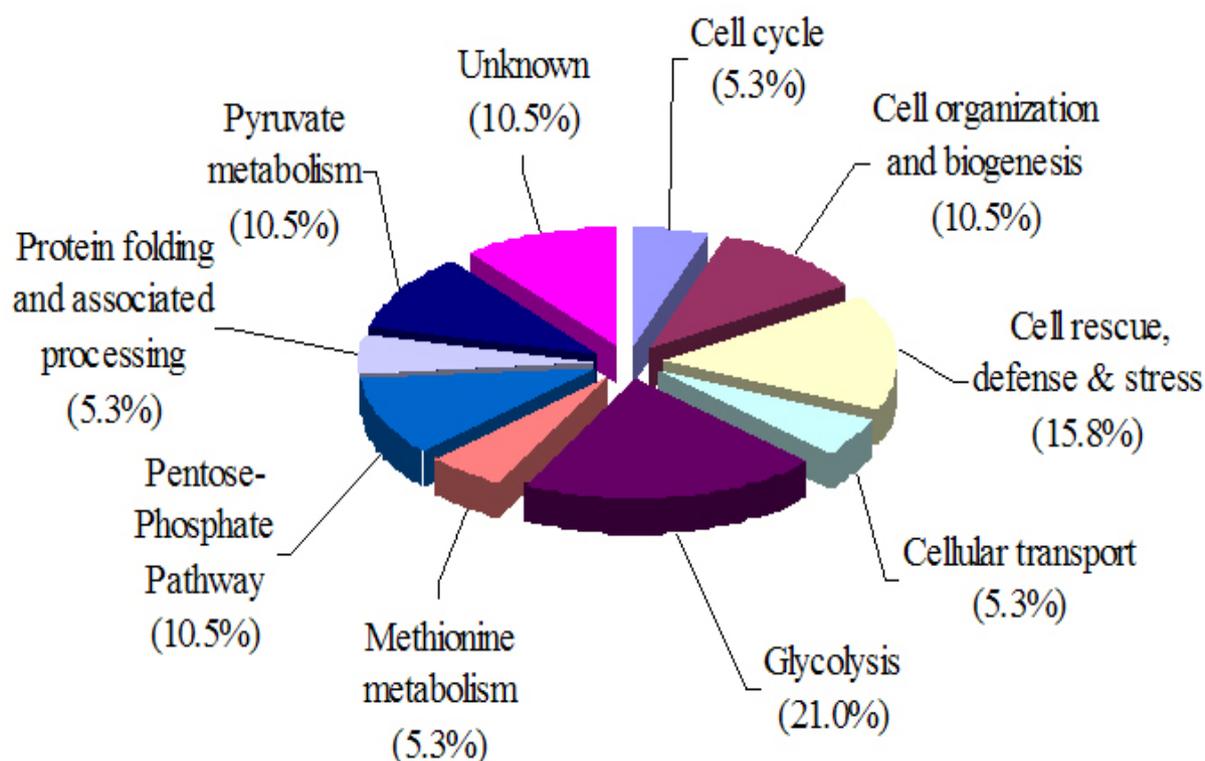
Figure 3.20 Distribution of identified proteins according to their biological function. The 19 identified distinct proteins were plotted in a pie chart. The percentages in parentheses were calculated by dividing the number of identified proteins in the group by 19 and by multiplying the dividend by 100.

Due to a possible specific action of DOC-affected proteins, the 19 were subdivided into four groups: metabolism, non-genomic actions through PKC pathway, oxidative stress and unknown. Table 3.4 and Figure 3.21 display the subdivisional classification of these proteins.

Table 3.4 Functional classification according to a specific possible action of DOC-affected proteins.

Subclass	Regulation	Entry Name [a]	Protein Name [a]	Biological Process [b]	Molecular Function [b]
Metabolism	Down	6PGD_SCHPO	6-phosphogluconate dehydrogenase, decarboxylating	pentose-phosphate shunt, oxidative branch / glucose metabolism	phosphogluconate dehydrogenase (decarboxylating) activity
	Up	ENO11_SCHPO	Enolase 1-1	carbohydrate metabolism / generation of precursor metabolites and energy / glycolysis	phosphopyruvate hydratase activity / magnesium ion binding
	Down	ENO12_SCHPO	Enolase 1-2	carbohydrate metabolism / generation of precursor metabolites and energy / glycolysis	magnesium ion binding / phosphopyruvate hydratase activity
	Down	G3P1_SCHPO	Glyceraldehyde 3-phosphate dehydrogenase 1	carbohydrate metabolism / generation of precursor metabolites and energy / glycolysis	glyceraldehyde-3-phosphate dehydrogenase (phosphorylating) activity
	Down	KPYK_SCHPO	Pyruvate kinase	carbohydrate metabolism / generation of precursor metabolites and energy / glycolysis / purine nucleotide metabolism	pyruvate kinase activity / magnesium ion binding
	Down	MAOX_SCHPO	NAD-dependent malic enzyme	amino acid metabolism / pyruvate metabolism / carbohydrate catabolism / generation of precursor metabolites and energy / main pathways of carbohydrate metabolism / malate metabolism	malate dehydrogenase (oxaloacetate-decarboxylating) activity
	Down	METE_SCHPO	Probable 5-methyltetrahydropteroyltriglutamate--homocysteine methyltransferase	cysteine metabolism / methionine metabolism / methionine biosynthesis	5-methyltetrahydropteroyltriglutamate-homocysteine S-methyltransferase activity
	Down	PDC2_SCHPO	Probable pyruvate decarboxylase C1F8.07c	pyruvate metabolism	pyruvate decarboxylase activity
	Down	TKT_SCHPO	Probable transketolase	pentose-phosphate shunt, non-oxidative branch	transketolase activity / calcium ion binding
Non-genomic actions through PKC pathway	Down	COFI_SCHPO	Cofilin	actin filament depolymerization	actin binding
	Up	GBLP_SCHPO	Guanine nucleotide-binding protein beta subunit-like protein	conjugation with cellular fusion / meiosis / actin cytoskeleton organization and biogenesis / cell wall organization and biogenesis / translation / regulation of meiosis / protein localization / intracellular signaling cascade	protein binding / ribosome binding / protein binding
	Down	RAD24_SCHPO	DNA damage checkpoint protein rad24	DNA damage checkpoint / protein localization / cell cycle / meiosis / DNA repair	protein binding / protein domain specific binding
	Down	VIP1_SCHPO	Protein vip1		RNA binding
Oxidative stress	Down	GPX1_SCHPO	Glutathione peroxidase	sulfur metabolism / response to stress / response to oxidative stress	glutathione peroxidase activity
	Down	HSP75_SCHPO	Heat shock protein sks2	response to stress / protein biosynthesis / protein folding / response to unfolded protein	heat shock protein activity / ATP binding
	Up	O74887_SCHPO	SPCC576.03c protein <Thioredoxin peroxidase>	unknow	peroxidase activity
	Down	SODM_SCHPO	Superoxide dismutase [Mn], mitochondrial [Precursor]	superoxide metabolism / response to stress	manganese superoxide dismutase activity / manganese ion binding
	Up	VDAC_SCHPO	Probable outer mitochondrial membrane protein porin	ion transport / mitochondrion organization and biogenesis / aerobic respiration / anion transport	voltage-dependent ion-selective channel activity
Unknown	Down	O94315_SCHPO	SPBC215.11c protein	unknow	oxidoreductase activity

a) Entry name, protein name and accession number according to Swiss-Prot (http://kr.expasy.org/sprot/)

b) Biological process and molecular function according to S. pombe Gene DB
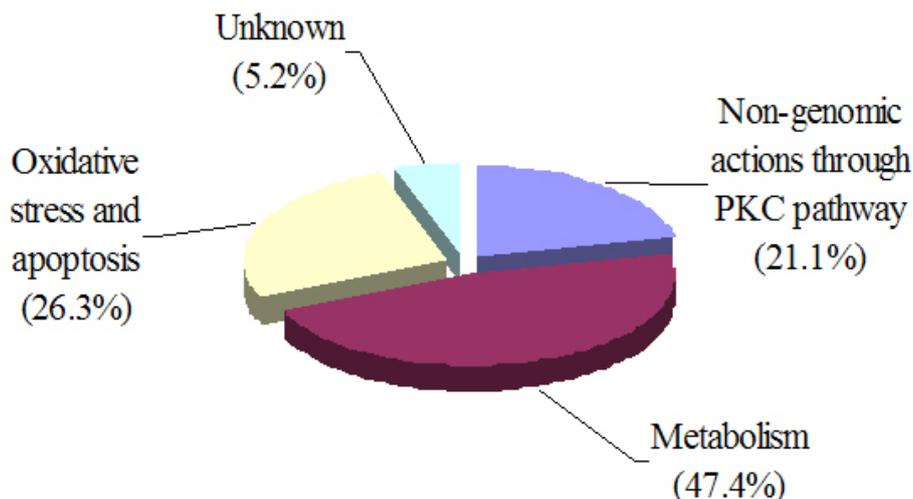
Figure 3.21 The subdivision of a specific possible action of DOC-affected proteins. The 19 identified distinct proteins were plotted in a pie chart. The percentages in parentheses were calculated by dividing the number of identified proteins in the subdivisional group by 19 and by multiplying the dividend by 100.

Nine distinct proteins regulated by DOC are involved in the primary metabolism. Of these proteins, five proteins were identified in two different spots in each case (with different gel-estimated Mr and pI's): 6-phosphogluconate dehydrogenase, decarboxylating (P78812, spot No. 4 and 18), glyceraldehyde 3-phosphate dehydrogenase 1 (P78958, spot No. 5 and 6), NAD-dependent malic enzyme (P40375, spot No. 9 and 12), probable pyruvate decarboxylase C1F8.07c (Q92345, spot No. 19 and 20) and probale transketolase (Q9URM2, spot No. 23 and 24). The multiple spots on 2-D gels were considered to be due to post-translational modifications (Meri and Baumann, 2001; Hesketh *et al.,* 2002; Mann and Jensen, 2003).

Five differentially regulated proteins may be connected to oxidative stress: including manganese superoxide dismutase mitochondrial precursor, glutathione peroxidase, SPCC576.03c protein (thioredoxin peroxidase), probable outer mitochondrial membrane protein porin and heat shock protein sks2.

Moreover, four distinct proteins may be associated with non-genomic actions through the PKC pathway. These include cofilin, DNA damage checkpoint protein rad24, guanine nucleotide-binding protein beta subunit-like protein and protein vip1. Interestingly, two proteins in spot No. 11 were identified by MALDI-TOF-MS and/or nanoLC-MS/MS. These proteins are the DNA damage checkpoint protein rad24 (P42656, rad24) and protein vip1

(P87216, vip1). The rad24 is a member of the 14-3-3 protein family and is related to cell cycle. 14-3-3 proteins are found to represent a family of regulatory proteins which are ubiquitously expressed in eukaryotic tissues (Fu *et al.,* 2000). In *S. pombe*, two 14-3-3 genes (rad24+ and rad25+) have been identified which serve as checkpoint controls to ensure that DNA damage has been repaired before mitosis begins (Ishii and Kurachi, 2002). Rad24 is the human 14-3-3 protein epsilon homologous (see Figure 3.22). The 14-3-3 proteins possess two highly conserved regions that are specific to this family of proteins: the first signature pattern is a peptide of 11 residues (14-3-3 protein signature 1, PS00796, [RA]-N-L-[LIV]-S-[VG]-[GA]-Y-[KN]-N-[IVA]) located in the N-terminal section; the second, a 20 amino acid region (14-3-3 protein signature 2, PS00797, Y-K-[DE]-[SG]-T-L-I-[IML]-Q-L-[LF]-[RHC]-D-N-[LF]-T-[LS]-W-[TANS]-[SAD]) is located in the C-terminal section. At the moment, it is known that the 14-3-3 protein family can interact with more than 200 different, mostly phosphorylated proteins (van Heusden and Steensma, 2006).

```
 Db     AC        Description                                    Score  E-value

 sp     P42656    RAD24_SCHPO DNA damage checkpoint protein rad24 [rad24...  525  e-148

 sp     P62258    1433E_HUMAN 14-3-3 protein epsilon (14-3-3E) [YWHAE] [...  354  2e-96
```

CLUSTAL W (1.82) multiple sequence alignment

```
                                           PS00796; 14-3-3 proteins signature 1
sp|P42656|RAD24_SCHPO    MSTTSREDAVYLAKLAEQAERYEGMVENMKSVASTDQELTVEERNLLSVA
sp|P62258|1433E_HUMAN    --MDDREDLVYQAKLAEQAERYDEMVESMKKVAGMDVELTVEERNLLSVA
                           .*** ** **********: ***.**.**. * *************

sp|P42656|RAD24_SCHPO    YKNVIGARRASWRIVSSIEQKEESKGNTAQVELIKEYRQKIEQELDTICQ
sp|P62258|1433E_HUMAN    YKNVIGARRASWRIISSIEQKEENKGGEDKLKMIREYRQMVETELKLICC
                         **************:********.**.   :::*:**** :* **. **

sp|P42656|RAD24_SCHPO    DILTVLEKHLIPNAASAESKVFYYKMKGDYYRYLAEFAVGEKRQHSADQS
sp|P62258|1433E_HUMAN    DILDVLDKHLIPAANTGESKVFYYKMKGDYHRYLAEFATGNDRKEAAENS
                         *** **:***** * :.*************:*******.*:.*:.:*::*

sp|P42656|RAD24_SCHPO    LEGYKAASEIATAELAPTHPIRLGLALNFSVFYYEILNSPDRACYLAKQA
sp|P62258|1433E_HUMAN    LVAYKAASDIAMTELPPTHPIRLGLALNFSVFYYEILNSPDRACRLAKAA
                         * .*****:** :**.************************** *** *

                          PS00797; 14-3-3 proteins signature 2
sp|P42656|RAD24_SCHPO    FDEAISELDSLSEESYKDSTLIMQLLRDNLTLWTSDAEYSAAAAGGNTEG
sp|P62258|1433E_HUMAN    FDDAIAELDTLSEESYKDSTLIMQLLRDNLTLWTSDMQGDGEEQ--NKEA
                         **:**:***:*************************** : ..    *.*.

sp|P42656|RAD24_SCHPO    AQENAPSNAPEGEAEPKADA
sp|P62258|1433E_HUMAN    LQDVEDENQ----------
                          *:   .*
```

Figure 3.22 Sequence alignment between Rad24 and the human 14-3-3 protein epsilon. The 14-3-3 proteins signature 1 and 2 are marked with **grey boxes.**

The function of vip1 has not yet been identified. However, the protein vip1 includes a RNA Recognition Motif (RRM) domain. This domain is found in many eukaryotic proteins and is not only involved in RNA recognition but also in protein–protein interaction (Maris *et al.,* 2005). Therefore, BLAST search against a mammalian database with this protein sequences was performed to try to predict function. According to the BLAST search results, some relevant homologies for protein vip1 have been found. It displays at least a weak similarities with the platelet-activating factor acetylhydrolase IB alpha subunit (PAFAH alpha, Lissencephaly-1 protein, LIS1, in *Bos taurus, Homo sapiens and Mus musculus*). In addition, Jungbluth (Jungbluth, 2000) assumed that the protein vip1 could be a p53-antigen-homolog. Stavridi *et al.* (Stavridi *et al.,* 2001) reported that the 14-3-3 protein epsilon binds to the C-terminus of p53. Between p53 and vip1, a section with high homology in the C-terminal area exists. Terefore, it may be possible that vip1 and rad24 bind to each other and were for this reason identified together.

Summarizing, a total of 42 spots from silver stained gels displaying significant intensity differences between the samples treated with DOC and control samples (at least 2 fold) could be detected using specific Analysis Sets in PDQuest. Of these spots, 24 proteins out of 23 spots have been identified (18 spots were obtained from 2-D gel with a pH 4-7 range and 5 spots (pH > 7) from 2-D gel with a pH range 3-10). Four of these spots show an at least 2-fold increased intensity in the DOC-treated samples, 19 show an at least 2-fold decreased intensity in the control samples. It was possible to attribute functions to 17 out of 19 distinct identified proteins. For one protein a function can be suggested due to homology search. Of these proteins, four distinct proteins seem to be associated with non-genomic actions through the PKC pathway.

4. Discussion and Outlook

4.1 Reference maps of the fission yeast S. pombe *wild type h*$^{-S}$ *L 972*

4.1.1 The fission yeast Schizosaccharomyces pombe

Schizosaccharomyces pombe (*S. pombe*) was first isolated from east African millet beer more than 100 years ago. It was called fission yeast, since it was observed to reproduce by fission alone, with no budding like that seen in the brewer's yeast *S. cerevisiae*. *S. pombe* started to become the subject of more intensive experimentation in the 1950s. It attracted interest from cell biologists because this yeast is a single-celled free-living archiascomycete fungus sharing many features with cells of more complicated eukaryotes. The 13.8 Mb genome of *S. pombe* containing three chromosomes (Smith *et al.,* 1987) together with a 20 kb mitochondrial genome (Lang *et al.,* 1987) was the sixth completely sequenced genome among eukaryotes (Wood *et al.,* 2002), officially putting *S. pombe* into the post-genomic era. Even though *S. pombe* has a similar size of the genome as *S. cerevisiae*, it has the smallest number of open reading frames (ORFs) among eukaryotes (4824), compared to 6200 ORFs in *S. cerevisiae* (Goffeau *et al.,* 1996).

S. pombe can be as easily cultured and manipulated as budding yeast. It attracted interest from cell biologists because its cell division is more typical for most eukaryotes and is distinct from that of the budding yeasts. The amount of genes in the fission yeast (about 5000 different ORFs for proteins) is considerably lower than that in the human (about 23,000). It contains many genes and regulatory mechanisms, which are close to those of mammals (Wood *et al.,* 2002). From a scientific point of view, the fission yeast is a powerful model system in the study of numerous biological processes of eukaryotic cells such as cell cycle, mitosis and meiosis (Fantes, 2000), DNA repair and recombination (Davis and Smith, 2001), and the analysis of checkpoint controls important for genome stability (Humphrey, 2000), metabolism or regulatory cascades.

Since the major signaling pathways and cellular processes involved in cellular response to cytotoxic agents are conserved between yeasts and mammalian cells, these simple eukaryotic systems have been shown to be excellent models for the identification of molecular as well as cellular mechanisms of sensitivity to antitumor drugs.

Thus, analyzing its proteome will be of greatest help for the use of this interesting yeast in model studies and biotechnological applications.

4.1.2 Proteomics

It is apparent that the paradigm of 'one gene encoding a single protein' is no longer applicable because of differential RNA processing such as alternative RNA splicing, *trans*-splicing RNA events, overlapping transcription events, etc. (Labrador *et al.*, 2001). The end result of these processes includes post-translational protein modifications resulting in multiple protein products for a single encoded gene. Thus, a major challenge in modern biology is to understand the expression, function, and regulation of the entire set of proteins encoded by an organism. Proteomic methods and techniques were developed to measure the expression of different proteins in a proteome, modifications and interaction of proteins that occur due to changes in the proteome during the developmental process, disease-state or exposure to an external stimulus. Proteomics itself is best viewed as a continuum of strategies that can be used to bridge the experimental gaps between the classical reductionist approaches of biochemistry and the global information coming from bioinformatics and mRNA expression studies (McDonald and Yates, 2000).

2-DE is now a widely used approach for proteome analysis. By resolving the same protein mixture on multiple of these narrow range 2-DEs, the total number of resolvable spots should increase (Corthals *et al.*, 2000). Not only the resolving power of these gels has increased, but also their reproducibility has allowed comparison between gels. Based on the speed and sensitivity with which the separated proteins by 2-DE can be identified, MS has become an important essential technology for proteomics (Yates, 1998).

The two most common types of ionization techniques are MALDI (Karas and Hillenkamp, 1988) and ESI (Fenn *et al.*, 1989). MALDI creates ions by using a small nitrogen laser (at 337 nm) and is mostly applied to the analysis of peptides. ESI is the method of choice for determining molecular weight of proteins, as MALDI results in broad peaks and low sensitivity for proteins above about 30 kDa. Moreover, ESI is performed in combination with high-performance liquid chromatography (LC). LC-MS/MS combines efficient separations of biological materials and sensitive identification of the individual components by MS. In a

typical LC-MS/MS experiment, the analyte is eluted from a reversed-phase column to separate the peptides by hydrophobicity, and is ionized and transferred with high efficiency into the mass spectrometer for analysis. LC-MS/MS can be used alone or in combination with one-dimensional electrophoresis or 2-DE, immunoprecipitation, or other protein purification techniques.

The major advantage of 2-DE coupled with various MS technologies is that they enable the simultaneous separation, visualization and identification of hundreds of unknown proteins at different modification states, *e.g.* the discovery of more than 100 proteins altered during apoptosis (Thiede and Rudel, 2004). The technology has successfully been applied to gain more information on the protein profile of simple organisms such as *S. cerevisiae* (Garrels *et al.,* 1994), *Escherichia coli* (VanBogelen *et al.,* 1997), and *Candida albicans* (Hernandez *et al.,* 2004).

Quite recently, a 2-D reference map for cytosolic proteins of *S. pombe* ed665 with 149 proteins (representing 97 distinct proteins) was constructed by Sun *et al.* (Sun *et al.*, 2005). This 2-D reference map is, however, still incomplete. In case of *S. cerevisiae*, the proteome analysis has since then been up-dated several times (Perrot *et al.*, 1999; Pardo *et al.*, 2000; Wildgruber *et al.*, 2002; Hazbun *et al.*, 2003; Breci *et al.*, 2005).

The benefit of 2-D reference maps is that it can provide much information such as the expression, function and regulation of proteins, and a survey of proteins affected during different physiological processes. The setup of a 2-D reference map (VanBogelen *et al.*, 1997; Jungblut *et al.*, 2000; Regula *et al.*, 2000; Buttner *et al.*, 2001; Schaffer *et al.*, 2001) will provide an important feature for the understanding of simple organisms physiology. It will also help in the characterization of stimuli, regulations and post-translational modifications of proteins. The increasing evidence of regulated post-translational modification points out the important role of this physiological process. These modifications will undoubtedly become an important research area, which will expand with the development of highly sensitive MS methods for the analysis of the modification on 2-D gel separated proteins.

In particular, *S. pombe* is a highly interesting organism for various purposes and can be used as an excellent model system for the expression of heterogeneous proteins from higher eukaryotes because it resembles higher eukaryotes in various aspects. Thus, the 2-D reference

map for the proteome of *S. pombe* may be relevant to obtain a better understanding of molecular as well as cellular mechanisms in humans.

4.1.3 2-D reference maps and protein identifications

In the first part of this work, a global proteome analysis of the fission yeast *S. pombe* wild type h^{-S} L 972 has been performed. It was possible to produce 2-D gels with a high resolution and high reproducibility. More than 1500 protein spots on silver stained gels using pH 3–10 IPG strips (see Figure 4.1A) and more than 800 protein spots on colloidal blue G-250 stained gels (see Figure 3.5A) were visualized. Since the majority of the spots has been observed in the range between pH 4 and 7.5, the widerange IPG strips of pH 4-7 have been used additionally in order to gain a higher resolution by stretching the protein pattern in the first dimension. The use of the widerange IPG strips of pH 3-10 as well as 4-7 provied on proteome profile displaying hundreds of overlapping proteins that are impossible to detect and identify. In order to detect proteins of low abundance, it is crucial to simplify these protein profiles so that individual spots can be visualized. This simplifies the computer aided image analysis and allows the visualization and identification of more proteins. Thereby, more than 1000 protein spots on silver stained gels using pH 4–7 IPG strip (see Figure 4.1B) and more than 500 protein spots on colloidal blue G-250 stained gels (see Figure 3.5B) were visualized.

298 spots in the 3-10 pH range and 101 spots in the 4-7 pH range were excised and analyzed independently by MALDI-TOF-MS and/or nanoLC-MS/MS analysis. Among these spots, 42 spots could not been identified by both MS techniques (37 spots in the 3-10 pH range and 5 spots in the 4-7 pH ranges). 341 proteins out of 261 spots in the 3-10 pH range were identified. In addition, 103 proteins out of 96 spots in the 4-7 pH range were identified. So far, 444 proteins out of 356 analyzed spots were identified by both MS approaches in the present study. Interestingly, 77 spots on both pH range 2-D gels could be confirmed as the same spots according to a comparison with the results of the analyzed spots and the present position on both 2-D gels. Therefore, overlapping IPG strips could be used successfully for acidic and neutral p*I* proteins. Appendix F lists 80 identified proteins out of 77 spots which were resolved by 2-DE in both pH ranges.
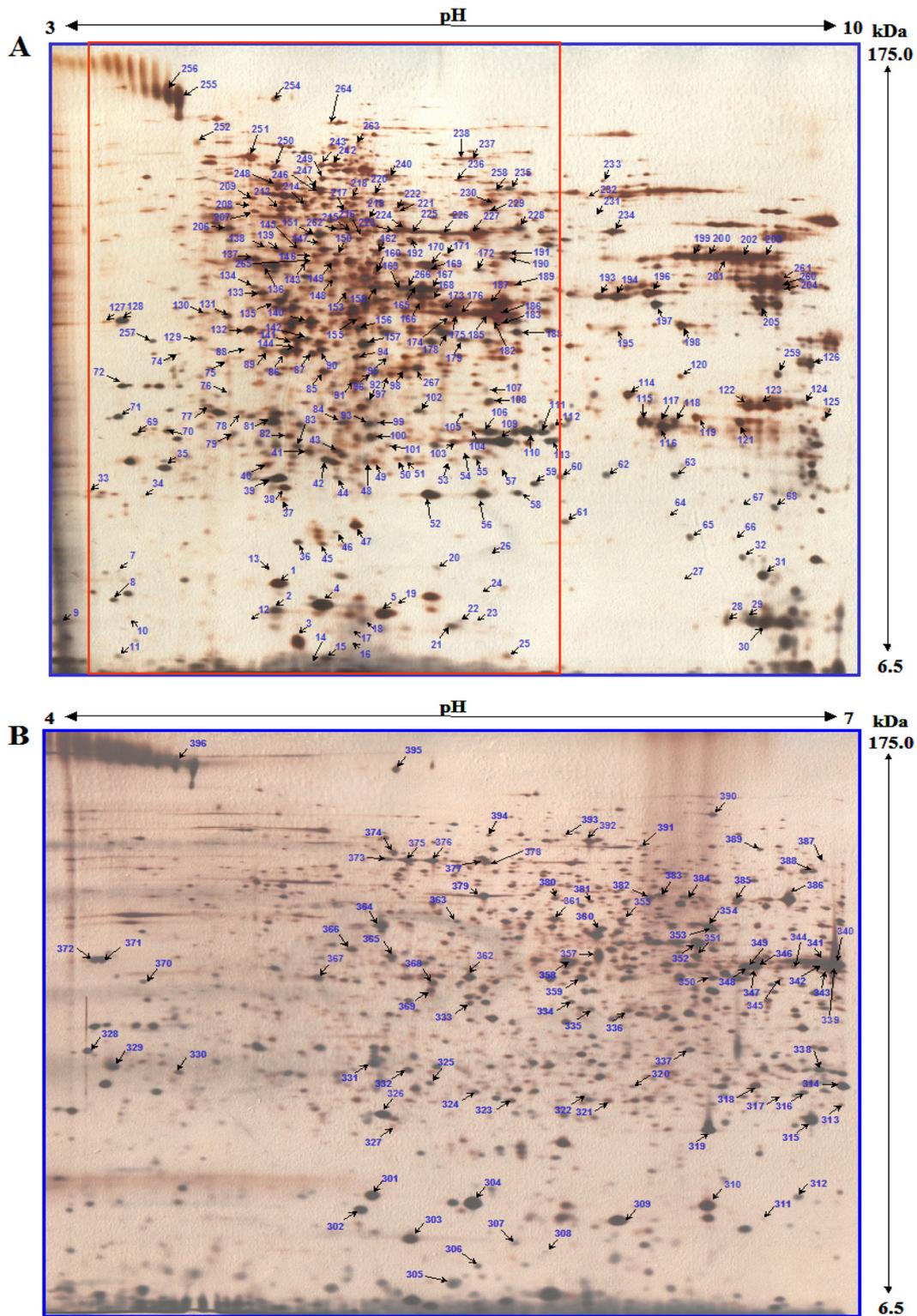
Figure 4.1 2-D reference maps of the *Schizosaccharomyces pombe* proteome. **(A, B)** Proteins were separated by IEF using 18 cm IPG strips (**A:** pH 3-10, **B:** pH 4-7), followed by 12.5% SDS–PAGE stained with silver (**A:** 40 µg proteins, **B:** 80 µg proteins). Two hundred and sixty-one proteins were resolved only in the range pH 3-10 by 2-DE and were identified by MS (see Appendix E). Eighty proteins were resolved by 2-DE and identified in both ranges, pH 3-10 and pH 4-7 (see Appendix F). Twenty-three proteins were identified only in the range pH 4-7 (see Table 3.1). Spot cut out of the coomassie stained gels for MS analysis are marked with arrows (Hwang *et al.,* 2006).

The use of the two techniques allowed us to increase the sequence coverage for some identified proteins and thus take advantage of the complementarity of the two ionization techniques. Figure 4.2 shows as an example of a protein identified by both MS approaches a probable 5-methyltetra-hydropteroyltriglutamate--homocysteine methyltransferase (Q9UT19, spot No. 390). This protein was identified based on the detection of 20 peptides covering 32% of the sequence by MALDI-TOF-MS (see Figure 4.2A) and based on the detection of 33 peptides covering 45% of the sequence by nanoLC-MS/MS (see Figure 4.2B). Only partially overlapping amino acid sequence coverage was obtained when comparing the MALDI-TOF-MS analysis and the nanoLC-MS/MS analysis. Thirteen peptides (22% of the total sequence) were detected by both techniques. Thus, the total percentage of the amino acid sequence covered for a given protein was usually higher than the sequence covered by either method alone. The 56% amino acid sequence coverage of this protein obtained from both MS analysis is shown in Figure 4.2C, along with a list of all the identified peptides.

A **Mascot Search Results**
Protein View

Match to: METE_SCHPO Score: 164
5-methyltetrahydropteroyltriglutamate--homocystei methyltransferase (ec 2.1.1.14) [Schizosaccharomyces pombe]
Found in search of \\Winframe\Users\ChristineC\Sarrebruck\reportfile\Spot 118

Nominal mass (M_r): 85286; Calculated pI value: 5.99
NCBI BLAST search of METE_SCHPO against nr
Unformatted sequence string for pasting into other applications

Taxonomy: Schizosaccharomyces pombe

Variable modifications: Carbamidomethyl (C), N-Acetyl (Protein), Oxidation (M)
Cleavage by Trypsin: cuts C-term side of KR unless next residue is P
Number of mass values searched: 42
Number of mass values matched: 20
Sequence Coverage: 32%

Show predicted peptides also

Sort Peptides By   ⊙ Residue Number   ○ Increasing Mass   ○ Decreasing Mass

Start	-	End	Observed	Mr(expt)	Mr(calc)	Delta	Miss	Sequence
4	-	11	846.49	845.48	845.48	0.01	0	SAVLGFPR
85	-	99	1633.80	1632.79	1632.78	0.01	0	LSGLSSLDTYFAMGR Oxidation (M)
156	-	176	2257.31	2256.30	2256.32	-0.02	0	EAGIITRPVLVGPVTYLFIAK
261	-	273	1331.82	1330.81	1330.77	0.04	0	GLPIAGVHVDVVR
281	-	299	1882.10	1881.09	1881.07	0.02	0	ALAVLGENQIISVGVVSGR
370	-	379	957.49	956.48	956.47	0.02	0	AANDGPASVR
393	-	404	1285.71	1284.70	1284.67	0.04	0	AESPITNVEAVR
410	-	417	1013.51	1012.50	1012.48	0.03	0	VTPQMHER Oxidation (M)
418	-	424	864.47	863.46	863.45	0.01	1	KSPFETR
425	-	433	1036.54	1035.53	1035.57	-0.04	1	YAKQQASLK
461	-	473	1540.78	1539.77	1539.56	0.02	0	GLISQEEYDAFIR
482	-	498	1952.99	1951.98	1951.96	0.02	0	FQEEVGLDVLVHGEPER
499	-	508	1274.59	1273.58	1273.54	0.04	0	NDMVQYFGER Oxidation (M)
527	-	546	2211.10	2210.09	2210.21	-0.11	0	CVRPPIIVGDVYRPAPMTVK
561	-	571	1201.74	1200.73	1200.69	0.04	0	GMLTAPITILR Oxidation (M)
577	-	593	1864.97	1863.96	1863.94	0.02	0	DDVHDSVQAQQIALGLR
606	-	615	1200.64	1199.63	1199.60	0.04	0	VIQCDEPALR Carbamidomethyl (C)
631	-	637	878.46	877.45	877.44	0.01	0	WAIDAFR
684	-	690	814.47	813.46	813.51	-0.04	0	LLNVLSR
691	-	706	1819.89	1819.88	1818.87	0.01	0	YTSCIGPGLFDIHSPR Carbamidomethyl (C)

Figure 4.2 An example of a protein identified as probable 5-methyltetra-hydropteroyltriglutamate-homocysteine methyltransferase (spot 390) by MALDI-TOF-MS and nanoLC-MS/MS. **A:** This protein was identified based on the detection of 20 peptides covering 32 % of the sequence by MALDI-TOF-MS.

B {MATRIX SCIENCE} Mascot Search Results

Protein View

```
Match to: gi|19114264 Score: 961
5-methyltetrahydropteroyltriglutamate--homocystei methyltransferase(ec 2.1.1.14) [Schizosaccharomyces pombe]
Found in search of \\Q-tof-2\Data\pkl files\Q019412CC.pkl

Nominal mass (Mr): 85286; Calculated pI value: 5.99
NCBI BLAST search of gi|19114264 against nr
Unformatted sequence string for pasting into other applications

Taxonomy: Schizosaccharomyces pombe
Links to retrieve other entries containing this sequence from NCBI Entrez:
gi|6014428 from Schizosaccharomyces pombe
gi|30913128 from Schizosaccharomyces pombe
gi|7489994 from Schizosaccharomyces pombe

Variable modifications: Carbamidomethyl (C),N-Acetyl (Protein),Oxidation (M)
Cleavage by Trypsin: cuts C-term side of KR unless next residue is P
Sequence Coverage: 45%
```

[Show predicted peptides also]

[Sort Peptides By] ⦿Residue Number ○Increasing Mass ○Decreasing Mass

```
Start - End   Observed  Mr(expt)  Mr(calc)  Delta  Miss Sequence
    4 -  11    423.79    845.56    845.48   0.09    0  SAVLGFPR  (Ions score 7)
   30 -  40    567.36   1132.70   1132.60   0.10    0  TSAEELLATAK  (Ions score 63)
   85 -  99    809.49   1616.96   1616.79   0.18    0  LSGLSSLDTYFAMGR  (Ions score 29)
   85 -  99    817.48   1632.94   1632.78   0.16    0  LSGLSSLDTYFAMGR  Oxidation (M)  (Ions score 48)
  147 - 155    518.32   1034.62   1034.53   0.09    0  ALDEFLEAK  (Ions score 48)
  156 - 176    753.18   2256.53   2256.32   0.21    0  EAGIITRPVLVGPVTYLFIAK  (Ions score 28)
  192 - 201    593.93   1185.85   1185.74   0.11    0  LLPVYVELIK  (Ions score 11)
  203 - 231   1082.99   3245.94   3245.70   0.25    0  LTEAGAEYIQIDEPILTLDLPQEILASYK  (Ions score 10)
  243 - 260    661.76   1982.26   1982.07   0.18    0  LILTTYFGSLQSNADVLK  (Ions score 4)
  243 - 260    992.13   1982.24   1982.07   0.17    0  LILTTYFGSLQSNADVLK  (Ions score 41)
  281 - 299    941.63   1881.24   1881.07   0.17    0  ALAVLGENQIISVGVVSGR  (Ions score 59)
  353 - 360    499.31    996.61    996.51   0.11    0  WFAFAVEK  (Ions score 26)
  361 - 369    509.84   1017.66   1017.55   0.11    0  CAELAILTK  Carbamidomethyl (C)  (Ions score 56)
  393 - 404    643.40   1284.79   1284.67   0.12    0  AESPITNVEAVR  (Ions score 50)
  434 - 449    583.38   1747.12   1746.96   0.16    0  LPLFPTTTIGSFPQTK  (Ions score 12)
  434 - 449    874.56   1747.11   1746.96   0.16    0  LPLFPTTTIGSFPQTK  (Ions score 66)
  482 - 498    651.72   1952.15   1951.96   0.18    0  FQEEVGLDVLVHGEPER  (Ions score 39)
  499 - 508    629.84   1257.67   1257.54   0.12    0  NDMVQYFGER  (Ions score 47)
  499 - 508    637.84   1273.67   1273.54   0.13    0  NDMVQYFGER  Oxidation (M)  (Ions score 24)
  509 - 526   1040.58   2079.15   2078.95   0.20    0  MEGFVFTVNGWVQSYGSR  Oxidation (M)  (Ions score 12)
  561 - 571    593.42   1184.82   1184.70   0.12    0  GMLTAPITILR  (Ions score 27)
  561 - 571    601.41   1200.81   1200.69   0.12    0  GMLTAPITILR  Oxidation (M)  (Ions score 54)
  577 - 593    622.38   1864.12   1863.94   0.18    0  DDVHDSVQAQQIALGLR  (Ions score 36)
  594 - 601    480.80    959.59    959.48   0.11    0  DEVLDLEK  (Ions score 28)
  606 - 615    600.87   1199.72   1199.60   0.12    0  VIQCDEPALR  Carbamidomethyl (C)  (Ions score 32)
  623 - 630    527.30   1052.59   1052.48   0.11    0  AEWDEYLK  (Ions score 7)
  631 - 637    439.77    877.53    877.44   0.09    0  WAIDAFR  (Ions score 31)
  668 - 679    645.39   1288.76   1288.65   0.11    0  LDADVVSIENSK  (Ions score 64)
  684 - 690    407.80    813.59    813.51   0.08    0  LLNVLSR  (Ions score 27)
  691 - 706    607.35   1819.04   1818.87   0.17    0  YTSCIGPGLFDIHSPR  Carbamidomethyl (C)  (Ions score 41)
  727 - 738    734.43   1466.84   1466.70   0.15    0  DHLWLNPDCGLK  Carbamidomethyl (C)  (Ions score 4)
  727 - 738    489.95   1466.83   1466.70   0.13    0  DHLWLNPDCGLK  Carbamidomethyl (C)  (Ions score 14)
  741 - 750    559.35   1116.68   1116.55   0.13    0  GWPETTADLK  (Ions score 20)
```

C

```
  1  MVKSAVLGFP RIGKNRELKK ATEAYWSGKT SAEELLATAK QLRLEHWKLQ
 51  KAQGVDIIPS NDFSLYDQIM DHSFSFNVIP PRYRLSGLSS LDTYFAMGRG
101  MQRAATADKA AVDVPAGEMV KWFDSNYHFL RPEVSEETDF KLSSTKALDE
151  FLEAKEAGII TRPVLVGPVT YLFIAKAAKG SSIKPIELLP KLLPVYVELI
201  KKLTEAGAEY IQIDEPILTL DLPQEILASY KEAYETLGKI GKLILTTYFG
251  SLQSNADVLK GLPIAGVHVD VVRAPENLDR ALAVLGENQI ISVGVVSGRN
301  IWKTDFQKAT AIIEKAISAV GSERVQVASS SSILHIPHSL SGEDQINPEI
351  KRWFAFAVEK CAELAILTKA ANDGPASVRA ELEANAADCK ARAESPITNV
401  EAVRERQSKV TPQMHERKSP FETRYAKQQA SLKLPLFPTT TIGSFPQTKE
451  IRVTRNRFAK GLISQEEYDA FIRKEISDVV KFQEEVGLDV LVHGEPERND
501  MVQYFGERME GFVFTVNGWV QSYGSRCVRP PIIVGDVYRP APMTVKESQY
551  AQSITSKPMK GMLTAPITIL RWSFPRDDVH DSVQAQQIAL GLRDEVLDLE
601  KAGIKVIQCD EPALREGLPL RRAEWDEYLK WAIDAFRLAT AAVQDDTQIH
651  SHFCYSDFND IFDAIQRLDA DVVSIENSKS DMKLLNVLSR YTSCIGPGLF
701  DIHSPRVPPV SEFKERIDAI VKHVPKDHLW LNPDCGLKTR GWPETTADLK
751  NMIAAAREAR EQYA
```

Sequence coverage percentages:

MALDI-TOF-MS : **32%**
NanoLC-MS/MS : **45%**
Total : **56%**

Figure 4.2 continued. **B:** This protein was also identified based on the detection of 33 peptides covering 45 % of the sequence by nanoLC-MS/MS. **C:** Identified peptides are shown in **blue boldface letters** for MALDI-TOF-MS analysis, **red boldface letters** for nanoLC-MS/MS analysis and ***boldface italic letters*** for both analysis.

A total of 364 proteins (representing 157 distinct proteins, *e.g.* isoforms) has been identified by both MS methods (Hwang *et al.,* 2006). Among the 364 identified proteins, 126 proteins were identified by both MS approaches. In parallel to peptide-mass mapping (PMM) experiments performed by MALDI-TOF-MS, the identity of some proteins was confirmed by amino acid sequence analysis of several of their tryptic peptides by nanoLC-MS/MS analysis. The identification of 117 new distinct proteins on a 2-D reference map of this yeast compared to the first 2-D reference map constructed by Sun *et al* that showed 149 proteins (97 distinct proteins) (Sun *et al.*, 2005) was performed.

4.1.4 Protein classifications

The objective of Gene Ontology (GO) is to provide controlled vocabularies for the description of the three ontologies (biological process, cellular component and molecular function) of gene products. In particular, *S. pombe* has at least one GO annotation for 98.3% of its genes (excluding annotations to unknown terms), greater than the current percentage coverage for any other organism. Approximately 65% (3225 gene products) have at least one annotation to each of the three ontologies (Aslett and Wood, 2006). Only 82 genes considered likely to be protein-coding have no known function. In contrast, *S. cerevisiae* has more gene products assigned to at least one term in all three ontologies (3460), but also a greater number of genes with unknown function (596).

Based on GO annotations from several databases, the identified proteins were functionally classified according to their biological function (see Figure 3.10 and Table 3.2). Of 157 distinct proteins, 65 proteins are involved in metabolism. Others are involved in protein synthesis and transcription (20 proteins), related to protein folding and associated processing (16 proteins), related to cellular transport (13 proteins), related to cell rescue, defense and stress (8 proteins), involved in the cell organization and biogenesis (7 proteins), and finally related to ubiquitin cycle (3 proteins) and cell cycle (2 proteins).

Hesketh *et al.* (Hesketh *et al.,* 2002) reported that proteins annotated as functioning in primary metabolic pathways were highly represented on the proteome map of *Streptomyces coelicolor* with 60% or more of the enzymes assigned to glycolysis, the tricarboxylic acid cycle and the pentose phosphate metabolism. In addition, Perrot *et al.* (Perrot *et al.,* 1999) identified 43% of the enzymes involved in the primary metabolic pathways on the proteome map of

S. cerevisiae. According to GO annotation for *S. pombe* (see http://www.ebi.ac.uk/integr8/ GOAnalysisPage.do?orgProteomeID=78), 43.9% of all predicted proteins are involved in metabolism. The present study gave quite similar results with 41.4% of identified proteins (65 proteins) involved in metabolism (see Figure 3.10). Sun *et al.* (Sun *et al.*, 2005) also reported that 41.2% of the identified proteins are involved in metabolism on the first proteome map of *S. pombe*.

The knowledge on the molecular interaction and reaction networks for the metabolism can be displayed through KEGG PATHWAY maps. Therefore, 65 identified distinct *S. pombe* proteins were subdivided according to KEGG PATHWAY maps. Among these proteins, 15 proteins are involved in glycolysis and gluconeogenesis (see Figure 4.4). Others are involved in citrate cycle (TCA cycle: 6 proteins; see Figure 4.3), in methionine metabolism (4 proteins), in pentose phosphate pathway (4 proteins), in pyruvate metabolism (4 proteins), in purine metabolism (4 proteins), in glycerolipid metabolism (3 proteins) and in other metabolism (25 proteins). Figrue 4.3 displays schematically the proteins of *S. pombe* involved in the citrate cycle (TCA cycle) according to the KEGG database.
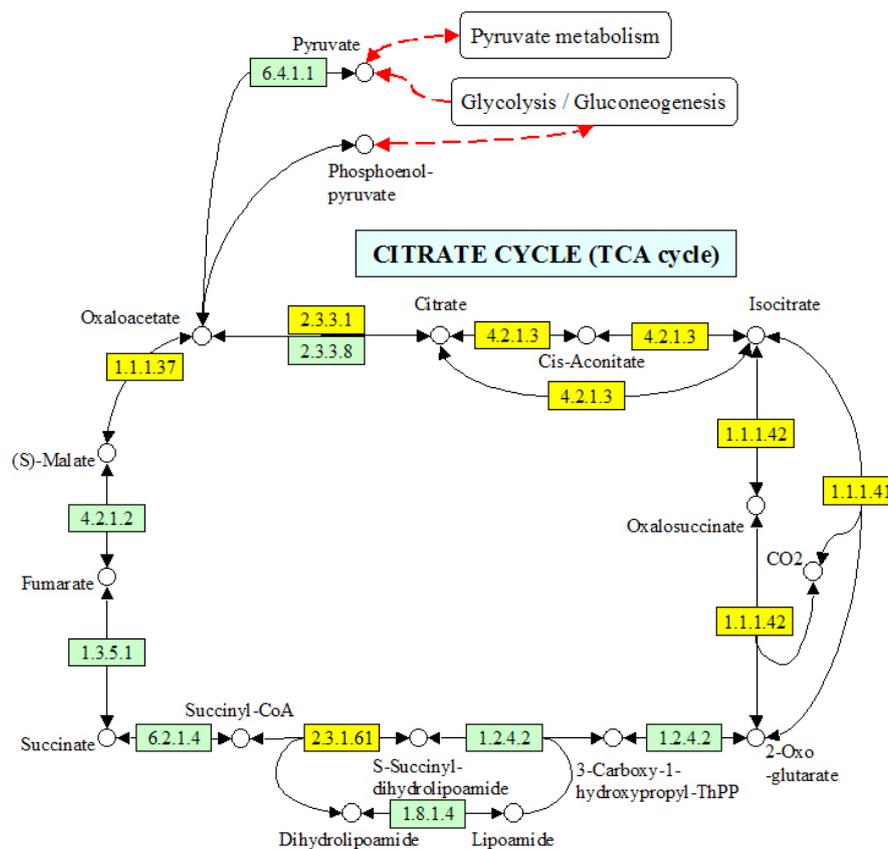
Figure 4.3 Schmatic representation of *S. pombe* proteins involved in the citrate cycle (TCA cycle). Six identified distinct proteins observed on the 2-D reference map are marked by yellow boxes. Numbers in the box are designated enzyme commission (EC) number for the corresponding enzyme.

Figrue 4.4 displays schematically the proteins of *S. pombe* involved in glycolysis and gluconeogenesis according to the KEGG PATHWAY.
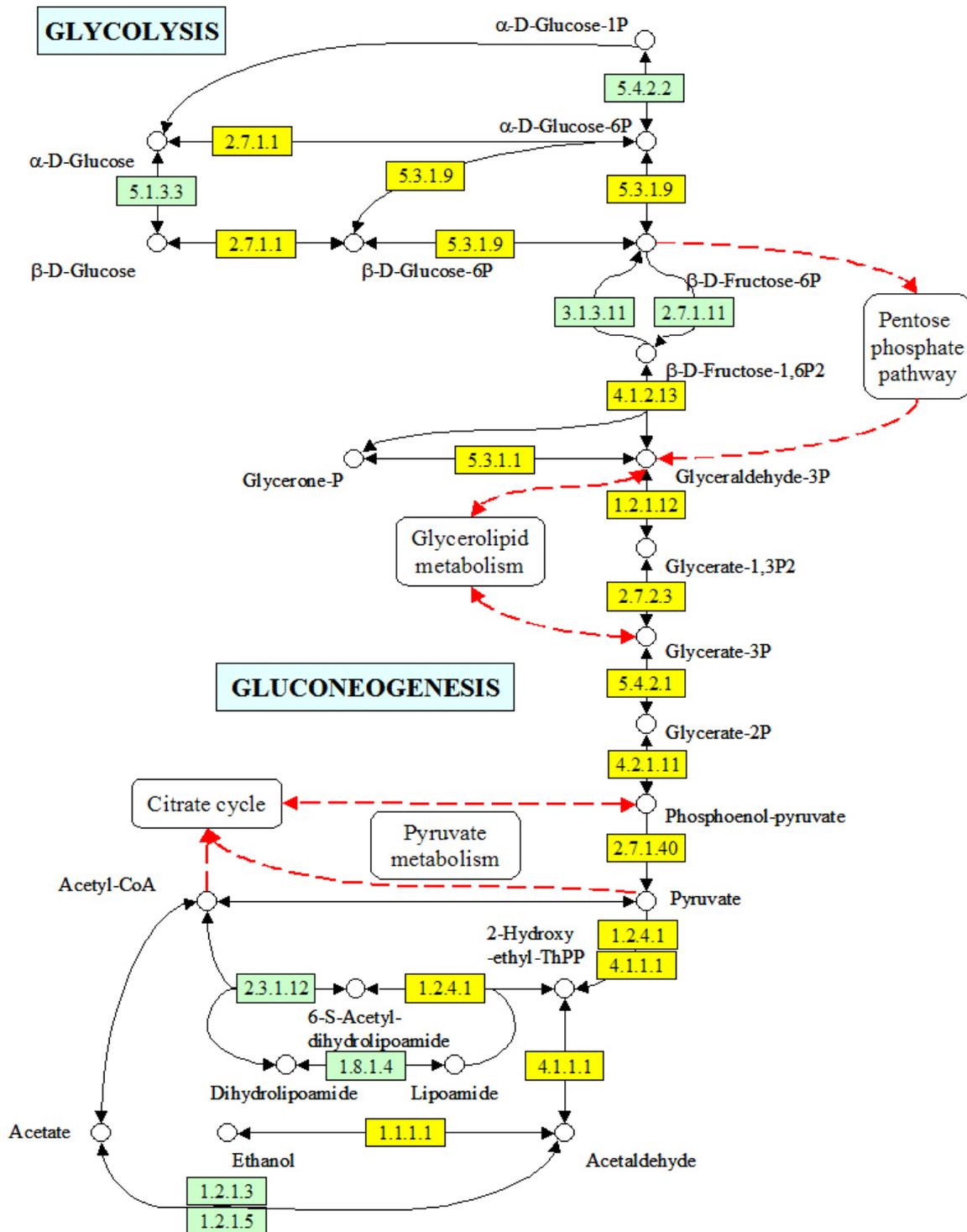
Figure 4.4 Schmatic representation of the *S. pombe* proteins involved in glycolysis and gluconeogenesis. 15 identified distinct proteins observed on the 2-D reference map of *S. pombe* are indicated by yellow boxes. Numbers in the box are designated enzyme commission (EC) number for the corresponding enzyme.

One of the greatest strengths of 2-DE is the ability to resolve proteins that have undergone some form of post-translational modification. This resolution is possible in 2-DE because many types of protein modifications confer a difference in charge as well as a change in the mass on the protein.

The presence of multiple spots on 2-D gels is considered to be due to post-translational modifications or proteolytic processing (Garrels *et al.,* 1994; Larsen *et al.,* 2001; Meri and Baumann, 2001; Hesketh *et al.,* 2002; Mann and Jensen, 2003). Larsen *et al.* (Larsen *et al.,* 2001) reported that a total of 11 spots in *S. cerevisiae* were found to be processed forms of enolase 2 by a combination of 2-DE and MS.

In this study, 58 out of 157 distinct proteins were found in multiple spots (see Table 3.2). The most abundant proteins ($\geq$ 6 spots / one protein) include enolase 1-1 (P40370, EC:4.2.1.11, 28 spots), glyceraldehyde 3-phosphate dehydrogenase 1 (P78958, EC:1.2.1.12, 26 spots), fructose-bisphosphate aldolase (P36580, EC:4.1.2.13, 12 spots), phosphoglycerate kinase (O60101, EC:2.7.2.3, 11 spots), phosphoglycerate mutase (P36623, EC:5.4.2.1, 11 spots), probabale ketol-acid reductoisomerase (P78827, EC:1.1.1.86, 9 spots), alcohol dehydrogenase (P00332, EC:1.1.1.1, 8 spots), triosephosphate isomerase (P07669, EC:5.3.1.1, 8 spots), pyruvate kinase (Q10208, EC:2.7.1.40, 7 spots), and probable 5-methyltetrahydropteroyl-triglutamate--homocysteine methyltransferase (Q9UT19, EC:2.1.1.14, 6 spots). These proteins are mainly involved in metabolism. Sun *et al.* (Sun *et al.*, 2005) also found some proteins with multiple spots. The most abundant proteins ($\geq$ 4 spots / one protein) include heat shock protein sks2 (10 spots), enolase 1-1 (EC:4.2.1.11, 7 spots), probable heat shock protein ssa2 (7 spots), fructose-bisphosphate aldolase (EC:4.1.2.13, 5 spots), thioredoxin peroxidase (4 spots) and phosphoglycerate kinase (EC:2.7.2.3, 4 spots). Lewis *et al*. reported that a single phosphoprotein will appear as multiple spots on a 2-D gel (Lewis *et al*., 2000).

Furthermore, 23 distinct proteins with unknown functions were identified in our 2-D reference map (see Figure 3.10 and Table 3.2). Among these proteins, interesting homologies for three of these proteins could be found through a BLAST search against a yeast database. The first protein, SPCC757.03c protein (O74914, spot No. 82) shows similarities with the probable chaperone HSP31 (Q04432, HSP31_YEAST). The sequences of the both proteins have 43.7% identity (see Figure 3.11A). Its function is a probable protease and it may act as a chaperone. The second protein, SPBC16A3.08c protein (O42914, spot No. 127) presents similarities with the suppressor protein STM1 (P39015, STM1_YEAST). The sequences of both proteins have 28.6% identity (see Figure 3.11B). Its function may be to act with CDC13 to control telomere

length homeostasis and to be involved in the control of the apoptosis-like cell death. The third protein, hypothetical protein C23H3.15C in chromosome I (P78890, spot No. 360) shows similarities with the stress protein DDR48 (DNA damage-responsive protein 48, P18899, DDR48_YEAST). Both sequences have 26% identity (see Figure 3.11C). The stress protein DDR48 may be implicated in one or possibly more pathways of mutagenesis in yeast.

Bohren *et al*. (Bohren et al., 1989) reported that the aldoketo reductase family includes a number of related monomeric NADPH-dependent oxidoreductases, such as aldehyde reductase, aldose reductase, rho crystallin, and many others. The protein in spot No. 197 was identified as a probable oxidoreductase C26F1.07 in chromosome I (Q10494). Description of the similarity (sequence or structural) of this protein with other proteins indicate that it belongs to the aldoketo reductase family. This protein not only possesses the aldoketo reductase 1 and 2 domains but also an amino acid sequence closely related to the aldoketo reductase 3 domain. In this study, the aldoketo reductase 1, 2 and an amino acid sequence closely related to the aldoketo reductase 3 have been confirmed via MALDI-TOF-MS as well as nanoLC-MS/MS. According to the BLAST search, this protein displayed similarities with the alcohol dehydrogenase [NADP+] in human, mouse, pig and rat (see Figure 3.12).

It is important to identify proteins with so far unknown functions since they may exhibit unique roles for the growth of *S. pombe*, which now can be tested using different growth conditions and noxes. Further experiments are needed to explore their functions and involvements in *S. pombe*.

In conclusion, the creation of 2-D reference maps of the *S. pombe* proteome with more than 1500 protein spots on silver stained gels in the 3-10 pH range and more than 1000 protein spots on silver stained gels in the 4-7 pH range was very successful. So far, a total of 364 proteins (representing 157 distinct proteins) have been identified. In this study, 117 distinct proteins on a 2-D reference map of this yeast were newly found when compared with the first 2-D reference map (Sun *et al*., 2005). The 2-D reference maps are intended to serve as a useful reference for future studies on the actions of different kinds of physiological conditions and states of this yeast. Thus, the 2-D reference map of *S. pombe* seems to be a powerful tool for future studies to elucidate the biological role of a variety of proteins under different conditions.

4.2 Analysis of MR independent DOC induced effects on the protein pattern of S. pombe

Steroid hormones are involved in almost all physiological processes in the human body including conception, intrautrine fetal development, bone maturation, immune system regulation, water and electrolyte homeostasis, and central nervous system activity. Alterations of steroid hormone biosynthesis and metabolism seem to be involved in the pathogenesis of several diseases (Auchus and Miller, 2001). These include endocrinological syndromes (*e.g.* apparent mineralocorticoid excess syndrome (AMES), congenital adrenal hyperplasia (CAH), various forms of pseudohermaphroditism) and different tumors (*e.g.* breast and prostate carcinoma). According to the classic genomic theory of action, steroid hormones bind to specific receptors and exert positive or negative effects on the expression of target genes (Beato *et al.,* 1996; Beato and Klug, 2000). In addition, very rapid non-genomic effects of steroids that are clearly incompatible with the genomic model mainly affecting intracellular signaling have been widely recognized. These non-genomic steroid actions are likely to be transmitted via specific membrane receptors and involve conventional second messenger cascades, including phospholipase C (Civitelli *et al.,* 1990), phosphoinositide turnover (Morley *et al.,* 1992; Morelli *et al.,* 1993), intracellular pH (Jenis *et al.,* 1993; Wehling *et al.,* 1996), free intracellular calcium (de Boland and Norman, 1990; Wehling *et al.,* 1990), and PKC (Sylvia *et al.,* 1993). Finally, the rapid signaling pathways can result in genomic effects ("crosstalk" between non-genomic and genomic action). These rapid effects are likely to be mediated through receptors with pharmacological properties distinct from those of the intracellular steroid receptors.

Although rapid responses of steroid hormones have been described on all biological levels from intracellular signaling to human physiology, it is obvious that many aspects of rapid non-genomic action still require continuous intensive research, because essential clues for their understanding are still lacking.

Abnormalities of mineralocorticoid synthesis as well as metabolism profoundly affect the regulation of electrolyte and water balance and of blood pressure. Mineralocorticoids play a role in some physiological disorders (Connell *et al.,* 2001) and have been related to severe heart failure (Pitt *et al.,* 1999; Ramires *et al.,* 2000; Nussberger, 2003). The most important mineralocorticoids are aldosterone and DOC. It has been found that a high aldosterone level is

not only linked to hypertension, but also plays a role in the development of congestive heart failure. The mechanisms of these changes are poorly understood yet (Brilla, 2000).

DOC binds to the MR with high affinity (DOC = corticosterone $\geq$ aldosterone = cortisol), and circulates at concentrations comparable to aldosterone. MR are found in both Na^+ transporting epithelia (*e.g.* kidney, colon) and nonepithelial tissues (*e.g.* heart, brain) (Funder, 2005). Severe DOC excess as is seen in 17α- and 11β-hydroxylase deficiencies causes hypertension, and moderate DOC overproduction in late pregnancy is also associated with hypertension. In addition, elevated levels of DOC causes Cushing's syndrome (Yasuda *et al.,* 1993) and can be involved in the generation of adrenal tumors (adenomas or carcinomas) (Egoshi *et al.,* 1998; Pitt *et al.,* 1999), whereas low levels of DOC may be the cause for the AMES, hypotension and hyperkalemia (Ghulam *et al.,* 2003).

Recently, Böhmer *et al.* (Böhmer *et al.,* 2006) used a proteomic approach to identify MR-independent effects of aldosterone in *S. pombe,* a nuclear receptor-free system. Thereby, 38 protein spots displaying significant intensity difference between samples treated with aldosterone and control samples could be detected. 11 proteins have been successfully identified, which may represent newly identified players of aldosterone-induced action.

The mechanism of the non-genomic action of DOC is still unknown. Thus, to the best of our knowledge, this study is the first work that succeeded in showing and identifying non-genomic DOC effects on the protein level in a completely nuclear receptor-free system. Therefore, it can be postulated that DOC displays at least part of its so-called non-genomic action in this receptor-free system by modulating gene expression.

4.2.1 The identification of differential regulated proteins by DOC

To investigate the MR-independent DOC induced effects on the protein pattern, the 2-D reference map of the *S. pombe* proteome (Hwang *et al.,* 2006) has been used. In this analysis, 24 cellular proteins (representing 19 distinct proteins) out of 23 spots were found to be differentially regulated by DOC. Among these proteins, four different proteins may be associated with non-genomic actions through the PKC pathway. These include cofilin, DNA damage checkpoint protein rad24, guanine nucleotide-binding protein beta subunit-like protein and protein vip1. Nine proteins were involved in primary metabolism. One of these proteins, glyceraldehyde-3-phosphate dehydrogenase 1, may also play a relevant role in

cytoskeleton assembly. Three of these proteins, enolase 1-1, enolase 1-2 and NAD-dependent malic enzyme, may be also associated with the osmotic regulation. Finally five proteins responsed to oxidative stress. One protein was identified with unknown function.

4.2.2 The differentially identified proteins involved in non-genomic actions through the PKC pathway (spot No. 1, 11 and 16)

The extracellular signals (hormones, neurotransmitters and growth factors) bind to cell surface membrane receptors, which may be divided into three main groups/families: coupled with GTP-binding regulatory proteins (GPCR), ionic channels, and tyrosine kinases. The hormone binding to steroid specific receptors at the cell surface represents the first step in a complicated sequence of molecular events transmitting the signal into the cell interior and initiating the ultimate physiological response.

In the guanine nucleotide binding protein (G protein) mediated pathway (Gilman, 1987), the hormone binding induces conformational change of the receptor molecule, which induces dissociation of the trimeric G protein-complex (non-active) into the free (active) Gα and Gβγ subunits. The length of the G protein signal is controlled by the duration of the GTP-bound alpha subunit, which can be regulated by a regulator of G protein signalling (RGS) proteins or by covalent modifications (Chen and Manning, 2001). The cycle is completed by the hydrolysis of alpha subunit-bound GTP to GDP, resulting in the reassociation of the alpha and beta/gamma subunits and their binding to the receptor, which terminates the signal (Svoboda *et al.,* 2004).

As previously discussed, non-genomic effects generated by steroids appear to be mediated by a mechanism not depending on the activation of nuclear receptors (Marcinkowska and Wiedlocha, 2002) and are able to activate G proteins (Rosner *et al.,* 1999) and PKC (Kelly *et al.,* 1999). PKCs are thought to play an important role in carcinogenesis and regulate various cellular processes including mitogenesis, cell adhesion, apoptosis, angiogenesis, invasion, and metastasis (Gopalakrishna and Jaken, 2000).

In this study, 4 proteins regulated by DOC have been identified, which may be specifically associated with non-genomic actions through the PKC pathway. Three out of these proteins,

cofilin (P78929, cof1/adf1, spot No. 1), DNA damage checkpoint protein rad24 (P42656, rad24, spot No. 11) and protein vip1 (P87216, vip1, spot No. 11), are downregulated after DOC treatment compared to the control (see Figure 3.18), whereas the G protein beta subunit-like protein (Q10281, rkp1/cpc2, spot No. 16) is upregulated (see Figure 3.19). Figure 4.5 summarizes schematically a possible connection between these proteins discussed below in more detail.
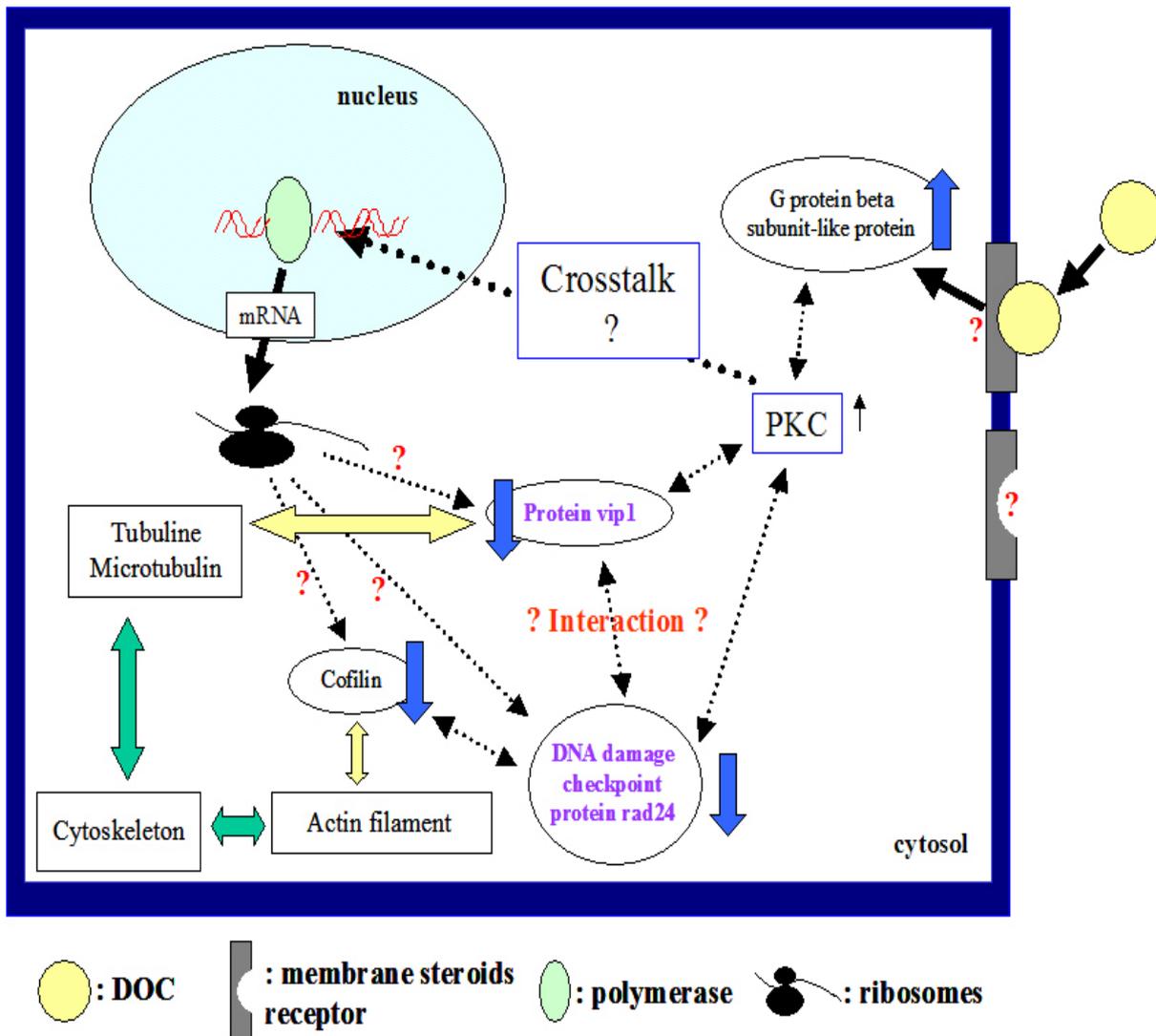
Figure 4.5 Schematic representation of the DOC-induced non-genomic actions observed by comparative proteomics on 2-DE in *S. pombe.* Four proteins may be specifically associated with non-genomic actions through the PKC pathway. These include cofilin, DNA damage checkpoint protein rad24, protein vip1 and G proteins beta subunit-like protein. Thus, the influence of DOC on these proteins points towards a possible function in structure remodeling. The decrease or increase in the protein spot intensity as seen on 2-D gels is indicated with **blue arrows**.

4.2.2.1 G protein beta subunit-like protein (Q10281, rkp1/cpc2, spot No. 16)

The intensity of spot No. 16 is upregulated after incubation with DOC compared to the control (see Figure 3.19). The protein in this spot was identified as the G protein beta subunit-like protein according to MALDI-TOF-MS and nanoLC-MS/MS (see Table 3.3). It consists of 314 amino acid residues, including seven WD-40 repeats (also known as WD or beta-transducin repeats), which are short 40 amino acid motifs, often terminating in a Trp-Asp (W-D) dipeptide (van der Voorn and Ploegh, 1992). WD-repeat proteins comprise a large family found in all eukaryotes and are implicated in a variety of functions ranging from signal transduction and transcription regulation to cell cycle control and apoptosis. The underlying common function of all WD-repeat proteins is the coordination of multi-protein complex assemblies, where the repeating units serve as a rigid scaffold for protein interactions.

G proteins are a family of membrane-associated proteins that couple extracellularly-activated integral-membrane receptors to intracellular effectors. G proteins are composed of three subunits (alpha, beta and gamma) which associate as a trimer at the inner face of the plasma membrane (Preininger and Hamm, 2004). In particular, four different G protein beta subunits have been identified in mammals, and some have also been identified in certain invertebrate species. Beta subunits contain around 340 amino acids, with apparent molecular weights of 35-36 kDa. The sequences display tandem WD-40 repeat domains. Their sequences are highly conserved between species, implying that they perform a fundamentally important role in the organisation of G protein linked systems (Duronio *et al.*, 1992). G proteins and their receptors form one of the most prevalent signalling systems in mammalian cells, regulating systems as diverse as sensory perception, cell growth and hormonal regulation (Roberts and Waelbroeck, 2004).

Won *et al*. (Won *et al.,* 2001) reported that G protein beta subunit-like protein (rkp1/cpc2) may function as a receptor for PKC, Pck2, in the regulation of actin cytoskeleton organization during cell wall synthesis and morphogenesis of *S. pombe*. PKC is a family of phospholipid dependent serine/threonine kinases, which are activated by many extracellular signals. PKCs are regulated by a variety of lipid secondary messengers and suggested to play a fundamental role in cell signaling mechanisms leading to the proliferation and mitogenesis of cells, apoptosis, platelet activation, remodeling of the actin cytoskeleton, modulation of ion channels, and secretion.

It has long been believed that the biological effects of steroid hormones are mediated by receptors associated with the plasma membrane as well as located inside of target cells. The fission yeast *S. pombe* does not contain nuclear steroid receptors and a membrane receptor for DOC is still unknown. Taken together, it can be carefully proposed that non-genomic effect of DOC might be mediated by G-protein coupled receptor (see Figure 4.5).

4.2.2.2 Spot No. 11: rad24 and vip1

The intensity of spot No. 11 is downregulated due to the action of DOC compared to the control (see Figure 3.18). First identification with MALDI-TOF-MS resulted in protein vip1 (P87216, VIP1_SCHPO, vip1) (see Table 3.3). To confirm this result, nanoLC-MS/MS has been performed. Interestingly, nanoLC-MS/MS confirmed protein vip1 and identified in addition DNA damage checkpoint protein rad24 (P42656, RAD24_SCHPO, rad24) (see Table 3.3). In general, the identification of more than one protein per spot is a problem in this kind of differential analysis, since it remains unclear whether both proteins or just one of the proteins are responsible for the spot intensity differences. However, in this case, it could be possible interpreted that protein vip1 can be one of the binding partners of the DNA damage checkpoint protein rad24, which would provide a very interesting explanation for the identification of the two proteins in spot 11. In the following, both proteins and their possible connections are discussed in more detail.

4.2.2.2.1 DNA damage checkpoint protein rad24 (P42656, rad24)

The DNA damage checkpoint protein rad24, which is a member of the 14-3-3 protein family, is characterised by 270 amino acid residues, including two 14-3-3 proteins signatures. Yeast 14-3-3 proteins are involved in the response to DNA damage. During the cell cycle, DNA is replicated and segregated equally into two daughter cells. Genetic studies of the fission yeast *S. pombe* have identified two genes, rad24 and rad25, that are required for the DNA damage checkpoint before mitosis is attempted (Ford *et al.,* 1994). Their function is essential for cell proliferation. Later, it was shown that overexpression of *rad24* and *rad25* reduced mating and sporulation in homothallic *S. pombe* cells (Ozoe *et al.,* 2002).

The 14-3-3 proteins (Morrison, 1994; Aitken, 1995; Xiao *et al.,* 1995) are a family of closely related acidic homodimeric proteins of about 30 kDa which were first identified as a brain-enriched protein in 1967 (Moore and Perez, 1967). Subsequently, it was found that they are present not only in a wide variety of different mammalian tissues (Aitken, 1995) but also in all eukaryotic organisms: including *Xenopus* (Martens *et al.,* 1992), *Drosophila* (Swanson and Ganguly, 1992), *Caenorhabditis elegans* (Wang and Shakes, 1994), the budding yeast *S. cerevisiae* (van Heusden *et al.,* 1995), and many different mammalian and plant species (Aitken *et al.,* 1992). In almost every known organism, multiple (at least two) isoforms of 14-3-3 have been observed: in mammals seven isoforms plus their phosphorylated versions have been identified. Within a eukaryotic cell, 14-3-3 is largely found in the cytoplasmic compartment. However, 14-3-3 proteins can also be detected at the plasma membrane and in intracellular organelles such as the nucleus and the golgi apparatus (Celis *et al.,* 1990; Leffers *et al.,* 1993; Freed *et al.,* 1994; Fanger *et al.,* 1998; Garcia-Guzman *et al.,* 1999).

The first function ascribed to 14-3-3 protein was activation of neurotransmitter synthesis (Ichimura *et al.,* 1987). Subsequently, 14-3-3 was found to regulate or inhibit the activity of PKC (Aitken *et al.,* 1990; Toker *et al.,* 1990). Aitken *et al.* (Aitken, 1996) implicated 14-3-3 as a novel type of dimeric scaffold proteins that modulate interactions between kinases and other signalling proteins. Today, 14-3-3 is regarded as a multifunctional protein, like calmodulin, which binds to a variety of cellular proteins and modulates their function. Muslin *et al.* (Muslin *et al.,* 1996) reported that target protein phosphorylation is important for 14-3-3 binding via a novel phosphoserine sequence motif. 14-3-3 proteins recognize three consensus motifs containing either a phosphorylated serine (pS) or threonine (pT) residue, which is present in most known 14-3-3 binding partners (Aitken, 1996; Rittinger *et al.,* 1999; Fu *et al.,* 2000). They include RSXpSXP (mode 1) (Muslin *et al.,* 1996), RXY/FXpSXP (mode 2) (Yaffe *et al.,* 1997) and pS/T [X(1-2)]-COOH (-COOH being the C-terminus: mode 3) (Ganguly *et al.,* 2005) (X representing any amino acid, and pS phosphoserine).

The 14-3-3 proteins play a key role in signal transduction pathways and the cell cycle, including signal transduction, apoptotic cell death, and cell cycle control. In many but not all cases, 14-3-3 proteins bind to the phosphorylated forms of these proteins. The binding partners are involved in almost every cellular process. In mammals, specific isoforms of 14-3-3 appear in the cerebrospinal fluid (CSF) of patients with Creutzfeldt-Jakob disease (CJD), sheep with scrapie and cows with bovine spongiform encephalopathy (BSE). 14-3-3 proteins also participate in complexes present in such neurodegenerative disorders as

Alzheimer's and Parkinson's disease. Neurofibrillary tangles of Alzheimer's disease brains contain 14-3-3 proteins (Layfield *et al.,* 1996) and 14-3-3 isoforms *β*, *γ*, *ε*, and *η* are present in the CSF of patients with CJD. Now with precise knowledge of the isoforms, a test can be made applicable to the differential diagnosis of a wide range of such diseases.

Mammalian and yeast 14-3-3 isoforms show a preference in dimerisation with specific partners in *vivo*, with important implications for the role of 14-3-3 in the formation of signalling complexes. Tanaka *et al.* (Tanaka *et al.,* 2000) reported that rad24 is essential for the proliferation of diploid cells in fission yeast. Recent genome-wide studies on yeast strains with impaired 14-3-3 function support the participation of 14-3-3 proteins in numerous yeast cellular processes (van Heusden and Steensma, 2006).

4.2.2.2.2 Protein vip1 (P87216, vip1, spot No. 11)

The protein vip1 is characterised by 257 amino acid residues, including a RNA recognition motif (RRM) domain. The RRM domin is found in many eukaryotic proteins and is not only involved in RNA recognition but also in protein-protein interaction (Maris *et al.,* 2005). Jungbluth (Jungbluth, 2000) postulated an association of vip1 to the cytoskeleton due to similarities in the central domain between vip1 and proteins of the myosin family and Lissencephaly-1 (LIS1) protein (L13385). On the basis of findings in cold-shock experiments using green fluorescence protein (GFP)-labeled vip1, the possible participation of this protein in a reconstitution of a functional microtubuli-framework is corroborated (Jungbluth, 2000). Recently, Böhmer *et al.* (Böhmer *et al.,* 2006) reported that the protein vip1 was also downregulated by aldosterone and corticosterone. Thus, these results are pointing towards an interesting possible physiological mode of action of this new cohesive player of mineralocorticoid action.

The peptide sequence of protein vip1 displays at least weak similarities with the platelet-activating factor acetylhydrolase (PAFAH) IB alpha subunit (PAFAH alpha, Lissencephaly-1 protein, LIS1, in *Bos taurus, Homo sapiens and Mus musculus*) according to the Blast results against a mammalian database. The PAFAH have been suggested to participate in targeting cytoplasmatic dynein to microtubule plus ends, thereby playing an essential role in dynein-mediated microtubule sliding. It interacts with dynein and dynactin (for example see: http://ca.expasy.org/cgi-bin/niceprot.pl?P43033). The PAFAH has been the target of many

clinical studies in several disorders associated with inflammation and oxidative reactions: including arthritis, sepsis, lung injury and vascular disease. In addition, Pritchard *et al.* (Pritchard, 1987) reported that PAFAH is associated *in vivo* with different subspecies of high-density lipoprotein (HDL). The HDL functions to account for the antiatherogenic effect including participation in reverse cholesterol transport, protection against endothelial dysfunction, and inhibition of oxidative stress. Observational studies provide overwhelming evidence that low HDL-cholesterol is an independent risk factor for coronary heart disease.

4.2.2.2.3 Binding possibility between rad24 and vip1

As shown above, vip1 was down-regulated by mineralocorticoids including aldosterone, corticosterone (Böhmer *et al.,* 2006) and, as shown in the present work, by DOC. However, the effective function of *vip1* in *S. pombe* has not yet been identified.

The rad24 is the human 14-3-3 protein epsilon homolog. The 14-3-3 epsilon protein (P62258) is a multifunctional regulator involved in cell-cycle control (checkpoint) and signal transduction, and is an inhibitor of apoptosis through inhibiting the activation of p38 MAP kinase. Until now, at least seven binding partners have been found for the *S. pombe* 14-3-3 proteins rad24 and rad25 (see Table 4.2). As in higher eukaryotes, the fission yeast binding partners are very diverse, again supporting the notion that yeast 14-3-3 proteins participate in many different processes.

According to the results of this examination, it is likely to assume that protein vip1 may be a new binding partner of the 14-3-3 family. Thus, the possible connections between these proteins will be discussed in more detail.

First of all, the 14-3-3 protein epsilon, the rad24 homolog, binds to the C-terminus of p53. Jungbluth *et al.* (see: http://www.ebi.ac.uk/cgi-bin/expasyfetch?Y13635) assumed that the protein vip1 is a p53-related protein from fission yeast. According to the BLAST search results, a section with high homology in the C-terminal area exists between p53 and vip1. Therefore, it could be possible that vip1 and rad24 bind each other which could explain that these proteins were identified together. Moreover, Waterman *et al.* (Waterman *et al.,* 1998) reported that *de*-phosphorylation of serine 376 of the p53 tumour-suppressor protein can lead

to the creation of an interaction motif. This in turn increased the affinity of p53 for sequence-specific DNA.

Table 4.2 *S. pombe* proteins physically interacting with 14-3-3 proteins (van Heusden and Steensma, 2006).

Protein	14-3-3 isoform*	Description	Reference
Cdc25	24	Protein phosphatase involved in mitosis	(Zeng and Piwnica-Worms, 1999)
Chk1	24, 25	Protein kinase required for proper cell cycle arrest in response to DNA damage	(Chen *et al.,* 1999)
Plc1	24, 25	Phospholipase C	(Andoh *et al.,* 1998)
Mei2	24	Meiotic regulator	(Sato *et al.,* 2002)
Ste11	24	High mobility group transcription factor	(Kitamura *et al.,* 2001; Qin *et al.,* 2003)
Clp1	24	Protein phosphatase involved in cell cycle regulation	(Mishra *et al.,* 2005)
Byr2	24, 25	Mitogen-activated protein kinase kinase kinase (MAPKKK) involved in sexual development	(Ozoe *et al.,* 2002)

24, rad24; 25, rad25

Secondly, the interaction between vip1 and rad24 can be mediated due to the RRM domain of vip1. This domain is found in many eukaryotic proteins and is not only involved in RNA recognition but also in protein–protein interaction (Maris *et al.,* 2005). Sato *et al.* (Sato *et al.,* 2002) reported that the regulation of the *S. pombe* Mei2 protein by 14-3-3 proteins involves a different mechanism. Mei2 is involved in the switch from mitosis to meiosis and its ability to bind to specific RNA species is essential for the initiation of meiosis. During mitosis, Mei2 is phosphorylated and bound to rad24, thus masking the RRM on Mei2p and inhibiting meiosis. Under meiotic conditions Mei2 becomes dephosphorylated, the binding to rad24 is lost and Mei2 binds to RNA (see Figure 4.6). Therefore, it could be possible that vip1 is phosphorylated and bound to rad24 thus masking the RRM on vip1p.

Another possibility is that the gene for 14-3-3 protein epsilon is located in a chromosomal region, 17p13.3, that contains genes implicated in the Miller-Dieker syndrome (MDS) (Chong *et al.,* 1997). This syndrome is associated with LIS1, which draws an additional interesting connection. On the basis of the BLAST search results, the 14-3-3 protein epsilon displays at least weak similarities with the platelet-activating factor acetylhydrolase IB alpha subunit (PAFAH alpha, LIS1).
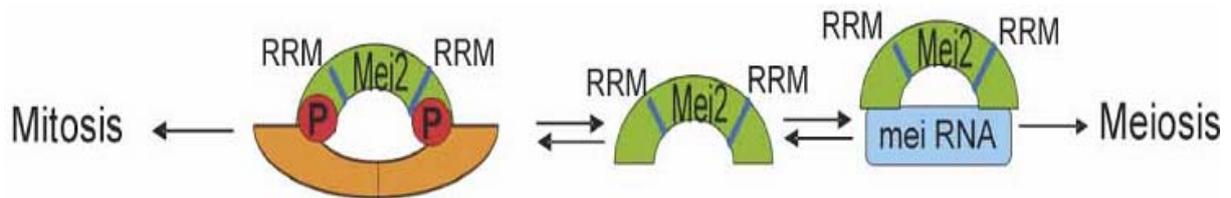
Figure 4.6 The regulation of the *S. pombe* Mei2 protein by 14-3-3 proteins involves a different mechanism. 14-3-3 proteins (dimers) are indicated in orange (Sato *et al.,* 2002).

In addition, in order to investigate the binding possibility of both proteins, the Motif Scan program of Scansite (http://scansite.mit.edu/) (Obenauer *et al.,* 2003) has been used, which can find a pS or pT residue for phosphospecific binding domains (such as 14-3-3 domains). Thereby, three possible sites in protein vip1 being able to bind with 14-3-3 domains, T247, S177 and T239 (see Figure 4.7), have been detected.

Taken together, it can be proposed that protein vip1 might, however, be a new binding partner of the 14-3-3 family (see Figure 4.5). Further investigations are needed to confirm this hypothesis and to explore the functions and binding possibility of both proteins in *S. pombe*.

Phosphoserine/threonine binding group (pST_bind)				
14-3-3 Mode 1			Gene Card **YWHAZ**	
Site	Score	Percentile	Sequence	SA
T247	0.4933	1.216 %	APAEKEP**T**APTTESK	1.997
14-3-3 Mode 1			Gene Card **YWHAZ**	
Site	Score	Percentile	Sequence	SA
S177	0.5645	2.492 %	DKLNRTS**S**LVSTYFH	0.487
14-3-3 Mode 1			Gene Card **YWHAZ**	
Site	Score	Percentile	Sequence	SA
T239	0.6322	4.772 %	SPASSTP**T**APAEKEP	1.165

Figure 4.7 *Motif Scan*'s output Table. For the 14-3-3 motif family details about the best matching domain motif and the position of the site in the query are shown. The score, percentile and sequence of the site are indicated.

4.2.2.3 Cofilin (P78929, cof1/adf1, spot No. 1)

The intensity of spot No. 1 is downregulated due to treatment with DOC compared with the control (see Figure 3.18). In this spot, cofilin was identified with nanoLC-MS/MS (see Table

3.3). This protein is characterised by 137 amino acid residues, including the actin-depolymerizing factor (ADF) homology domain. Cofilin controls reversible actin polymerization and depolymerization in a pH-sensitive manner (Yonezawa *et al.,* 1985; Hawkins *et al.,* 1993). It has the ability to bind G- and F-actin in a 1:1 ratio of cofilin to actin (Nishida *et al.,* 1984). The ADF/cofilin-family proteins are conserved low-molecular-weight actin-modulating proteins in eukaryotic cells. Gohla and Bokoch (Gohla and Bokoch, 2002) report the exciting discovery of a new, rather unusual activator of cofilin, a member of the ADF/cofilin family known to be ubiquitous and a potent regulator of actin dynamics in all eukaryotes. The dynamics of actin assembly and disassembly is essential for most cellular processes that involve movement, and cofilin is the major calcium-independent regulator of this dynamics (Bamburg and Wiggan, 2002). Nakano and Mabuchi (Nakano and Mabuchi, 2006a) reported that the actin-capping protein controls turnover of actin together with cdc3 and adf1 in *S. pombe*. Nakano and Mabuchi (Nakano and Mabuchi, 2006b) also reported that adf1 is required for formation and maintenance of the contractile ring during cytokinesis in fission yeast. Furthermore, Gohla and Bokoch (Gohla and Bokoch, 2002) reported that 14-3-3 regulates actin dynamics by stabilizing phosphorylated cofilin. Therefore, it could be inferred that rad24 may regulate actin dynamics by stabilizing phosphorylated cofilin (see Figure 4.5).

4.2.2.4 Summary of the differential identified proteins involved in non-genomic actions through the PKC pathway (spot No. 1, 11 and 16)

As previously discussed, non-genomic effects generated by steroids appear to be mediated by a mechanism not depending on the activation of nuclear receptors (Marcinkowska and Wiedlocha, 2002) and are able to activate PKC (Kelly *et al.,* 1999) and G proteins (Rosner *et al.,* 1999). PKCs are thought to play an important role in carcinogenesis and regulate various cellular processes including mitogenesis, cell adhesion, apoptosis, angiogenesis, invasion, and metastasis (Gopalakrishna and Jaken, 2000).

G protein beta subunit-like protein (rkp1/cpc2) may be a receptor for PKC in the regulation of actin cytoskeleton organization during cell wall synthesis and morphogenesis. Cofilin is expressed in virtually all eukaryotic cells. The dynamics of actin assembly and disassembly is essential for most cellular processes that involve movement, and cofilin is the major calcium-independent regulator of this dynamics (Bamburg and Wiggan, 2002). Altered levels of phosphorylated cofilin may be associated with the reorganization of the actin cytoskeleton.

Cofilin is encoded by cof1 in *S. pombe*, and is essential for cell viability (Palmgren *et al.,* 2002). Moreover, PKC is clearly regulated by 14-3-3 proteins (Ishii and Kurachi, 2002). It could be shown, that phosphorylated cofilin interacts with members of the 14-3-3 family (Gohla and Bokoch, 2002). It is tempting to postulate that there could be a pathway starting from the PKC regulating rad24 which itself regulates cofilin and *vice versa*.

In addition, due to the similarities of the central domain of vip1 to proteins of the myosine-family and LIS1-protein (L13385), a connection of protein vip1 to the cytoskeleton has been postulated (Jungbluth, 2000). Ali *et al.* (Ali *et al.,* 1994) reported that desensitization of the platelet-activating factor receptor was accompanied by phosphorylation, which was partially blocked by PKC inhibitors. It could therefore be hypothesized that the PKC regulates vip1 which is associated with cytoskeleton regulation.

Aldosterone excess might lead to a detrimental effect on cardiovascular functions, characterized by severe hypertension and development of cardiac fibrosis (Brilla and Weber, 1992; Young *et al.*, 1994). These effects can be mimicked by the administration of the mineralocorticoid DOC, but not by the glucocorticoid corticosterone (Young *et al.*, 1994). It has also been reported that aldosterone synthesis and secretion occur in the heart, suggesting that this local renin-angiotensin-aldosterone system (RAAS) could exert specific autocrine or paracrine effects on the cardiovascular system (Silvestre *et al.*, 1998; Delcayre and Silvestre, 1999). In addition, elevated levels of DOC cause adrenal tumors (adenomas or carcinomas) (Egoshi *et al.,* 1998; Pitt *et al.,* 1999). DOC-secreting tumors cause primary aldosteronism-like symptoms, show low plasma aldosterone but very high DOC levels (Ghulam *et al.,* 2003).

Taken together, the fact that these proteins are influenced by DOC points towards a possible function of the steroid in structure remodeling. Thus, it is tempting to propose that DOC-induced non-genomic actions in *S. pombe* may be mediated by the PKC pathway (see Figure 4.5).

4.2.3 The differentially regulated proteins involved in metabolism

As shown in the first part of this work, 41.4% of the identified proteins on the 2-D reference map of *S. pombe* are involved in the primary metabolic pathways (Hwang *et al.,* 2006). In the differential analysis part, it has been found that nine enzymes involved in the metabolism

were differentially regulated by DOC (see Figure 3.21). Among these proteins, four enzymes are involved in glycolysis (spot No. 5, 6, 10, 13 and 22). Two enzymes are involved in pyruvate metabolism (spot No. 9, 12, 19 and 20). Others are involved in pentose-phosphate pathway (2 enzymes; spot No. 4, 18, 23, and 24) and methionine metabolism (1 enzyme; spot No. 25). This demonstrates that DOC causes fundamental changes in the over all metabolism of a cell. Figure 4.8 summarizes schematically a possible connection between these proteins and glucose metabolism of a cell. Therefore, these proteins and their functions are discussed in more detail.
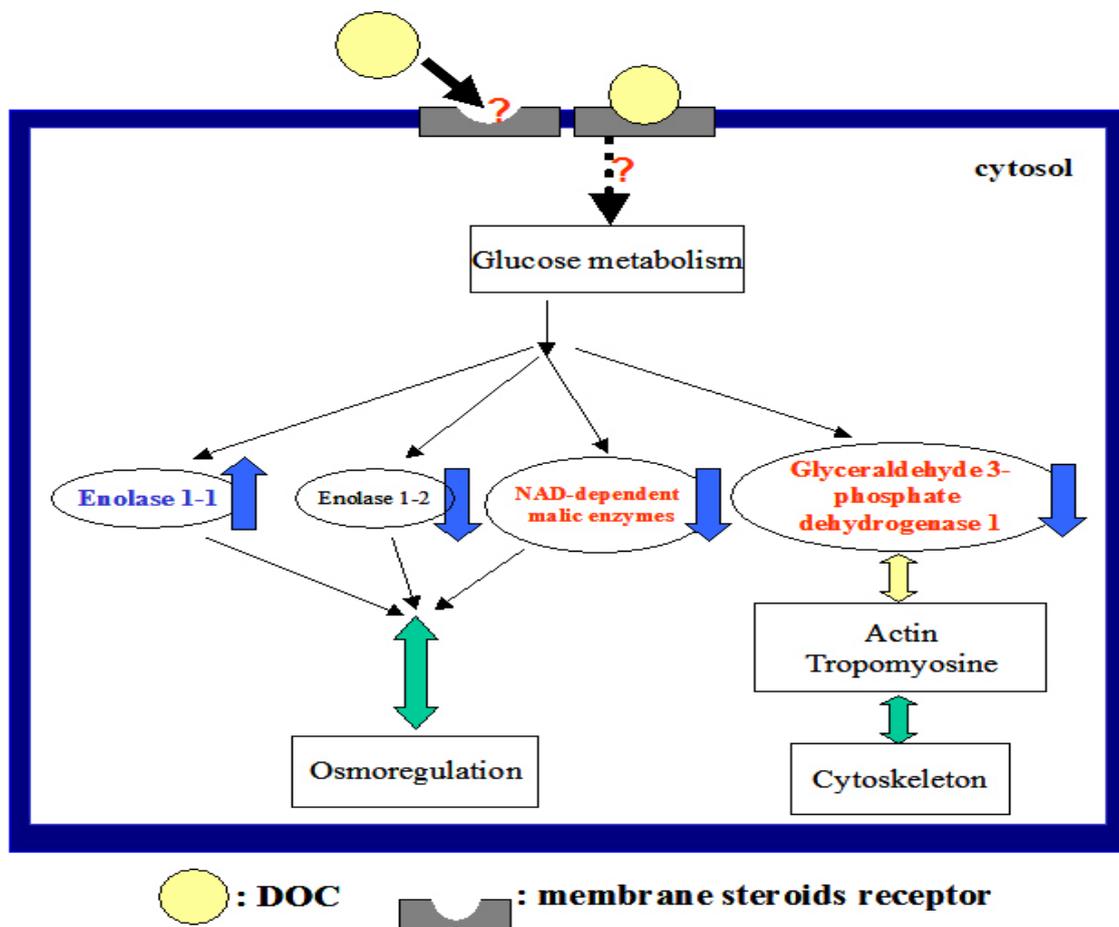
Figure 4.**8** Schematic representation of the four differentially regulated proteins due to the action of DOC involved in metabolism as observed by comparative proteomics on 2-DE in *S. pombe*. Glyceraldehyde-3-phosphate dehydrogenase 1 is a glycolytic enzyme and may also play a relevant role in cytoskeleton assembly. In addition, two enolases and the NAD-dependent malic enzyme, involved in primary metabolism, may be associated with the osmotic regulation. The decrease or increase in the protein spot intensity as seen on 2-D gels is indicated with **blue arrows**.

4.2.3.1 Glycolysis (spot No. 5, 6, 10, 13 and 22)

Glycolysis is the most ubiquitious pathway in the energy metabolism, occurring in almost every living cell. It is the sequence of reactions that converts glucose into pyruvate with the concomitant production of a relatively small amount of ATP. Atkins *et al.* (Atkins *et al.*, 2001) reported that alterations in glucose uptake and metabolism in vascular smooth muscle cells may participate in the contractile abnormalities characteristic of certain forms of hypertension. The pathway of glycolysis can be divided into 2 separate phases. The first is the chemical priming phase requiring energy in form of ATP, and the second is considered the energy-yielding phase. In particular, the second phase of glucose metabolism features the energy-yielding glycolytic reactions that produce ATP and NADH. It was found that four enzymes were differentially regulated in the second phase of glucose metabolism by DOC. These include glyceraldehyde-3-phosphate dehydrogenase 1, enolase 1-1, enolase 1-2 and pyruvate kinase.

The protein in spot No. 5 and 6 is downregulated due to DOC compared to the control (see Figure 3.18). In both spots, the glyceraldehyde-3-phosphate dehydrogenase 1 (P78958, tdh1/gpd1, GAPDH, EC:1.2.1.12) was identified with MALDI-TOF-MS (spot No. 5; see Table 3.3) and both MS results (spot No. 6; see Table 3.3). The theoretical molecular weight and *pI* of this protein is 53.7 kDa / p*I* 6.73. These two spots differed with regard to their position in the 2-D gels. Spot No. 5 was located around p*I* 7.03, and spot No. 6 was close to p*I* 7.15 with respective molecular weights of about 20.5 and 21.1 kDa. It could be possible that protein modification are primary induced by DOC which may have affected the *pI* and the molecular weight of this protein. Recently, Böhmer *et al.* (Böhmer *et al.*, 2006) reported that GAPDH 1 was downregulated due to aldosterone and corticosterone. In addition, it was possible to show that GAPDH is also regulated by aldosterone in a mammalian system (HCT116 cells) (Böhmer *et al.*, 2006).

This protein is involved in the beginning of the second phase glycolysis. The highly conserved GAPDH plays an important role in glycolysis and gluconeogenesis. Interestingly, many glycolytic proteins have functions in addition to their roles in glycolysis. Thus, GAPDH is a versatile protein with multiple functions. It binds to several proteins and nucleic acids, phosphorylates proteins and takes part in nuclear export of RNA, DNA repair and apoptosis (Sirover, 1999). Dugaiczyk *et al.* (Dugaiczyk *et al.*, 1983) found that GAPDH binds to actin and tropomyosin. Thus, this protein may play a relevant role in cytoskeleton assembly. By

showing that this enzyme is affected by DOC, a third protein (in addition to rad24 and vip1) with a possible connection to cytoskeletal organization has been identified (see Figure 4.8).

The protein in spot No. 10 was identified as the enolase 1-1 (P40370, eno101, EC:4.2.1.11) according to both MS results and is upregulated due to the action of DOC compared with the control (see Figure 3.19). In contrast, the protein in spot No. 22 was identified as the enolase 1-2 (Q8NKC2, eno102, EC:4.2.1.11) according to the MALDI-TOF-MS result and is downregulated due to DOC compared with the control (see Figure 3.18). Enolase (2-phospho-D-glycerate hydrolase) is an abundant cytosolic protein and an essential glycolytic enzyme that catalyses the interconversion of 2-phosphoglycerate and phosphoenolpyruvate. The enolase reaction is the first step in gluconeogenesis, which is also part of the glycolytic pathway. Genetic studies of the fission yeast *S. pombe* have identified two genes, eno101 and eno102, that are required for this step. The bakers' yeast also has two enolase genes. Although they both function as glycolytic enzymes, eno2 is essential, whereas eno1 is non-essential (McAlister and Holland, 1982). Recently, Decker and Wickner (Decker and Wickner, 2006) reported that enolase from *S. cerevisiae* participates in vacuole fusion by distinct mechanisms. A small portion of enolase is bound to vacuoles. The vacuole fusion and fission in *S pombe* affects an osmotic response dependent on mitogen-activated protein kinases (Bone *et al.,* 1998). Thus, it can be proposed that enolase regulation by DOC points towards a possible function in osmotic regulation of this steroid (see Figure 4.8).

The final reaction of aerobic glycolysis is catalyzed by the highly regulated enzyme pyruvate kinase. In spot No. 13, a pyruvate kinase (Q10208, pyk1, PK, EC:2.7.1.40) was identified according to the MALDI-TOF-MS result and is downregulated due to the DOC action compared with the control (see Figure 3.18). Pyruvate kinase from fission yeast is a dimeric protein. It catalyzes the conversion of phosphoenol-pyruvate to pyruvate (Lal *et al.,* 1991), in a reaction that yields an ATP molecule. ATP is the major energy source for several metabolic reactions that occur during inflammation. However, pyruvate kinase might also exhibit a protective function by producing excess pyruvate, which is an antioxidant (Peshavaria and Day, 1991). Pyruvate is known to protect cells against the oxidative damage caused by O_2 and H_2O_2. Although pyruvate kinase is a rate-controlling glycolytic enzyme and is also involved in fundamental processes such as cell proliferation, differentiation, tumor formation and apoptosis (Mazurek *et al.,* 1997; Mazurek *et al.,* 1999), the role of the DOC-mediated effects is still unknown.

4.2.3.2. Pyruvate metabolism (spot No. 9, 12, 19 and 20)

The NAD-dependent malic enzyme (P40375, mae2, NAD-ME, EC:1.1.1.38, spot No. 9 and 12) has been identified with both MS techniques and is involved in pyruvate metabolism. It is downregulated due to DOC compared with the control (see Figure 3.18). Another protein was identified as a probable pyruvate decarboxylase C1F8.07c (Q92345, EC:4.1.1.1, spot No. 19 and 20) according to the MALDI-TOF-MS results. This protein is involved in pyruvate metabolism and is downregulated due to DOC compared with the control (see Figure 3.18).

The two spots identified as NAD-ME differed with regard to their position in the 2-D gels. The theoretical molecular weight and *pI* of this protein is 62.5 kDa / p*I* 5.68. Spot No. 9 was located around p*I* 4.64, and spot No. 12 was close to p*I* 5.30 with molecular weights of about 32.7 kDa and 33.1 kDa, respectively. In addition, two spots identified as a probable pyruvate decarboxylase C1F8.07c also differed with regard to their position in the 2-D gels. The theoretical molecular weight and *pI* of this protein is 64.8 kDa / p*I* 5.71. Spot No. 19 was located around p*I* 5.38, and spot No. 12 was close to p*I* 5.44 with molecular weights of about 58.1 kDa and 57.6 kDa, respectively. As observed in the case of GAPDH 1, DOC may have affected the *pI* and the molecular weight of these proteins, too.

The NAD-ME from *S. pombe* catalyzes the oxidative decarboxylation of L-malate to pyruvate and CO_2, a reaction important in a number of metabolic pathways. In *S. pombe*, the NAD-ME plays an important role in maintaining the redox balance under aerobic conditions (Viljoen *et al.,* 1999). Expression of the ME gene (*mae2*) seems to be regulated *inter alia* in response to osmotic stress conditions (Groenewald and Viljoen-Bloom, 2001) transmitted by the stress-activated protein kinase pathway (Toone *et al.*, 1998; Groenewald and Viljoen-Bloom, 2001). It is well known that mineralocorticoids regulate the water and electrolyte homoestasis in the human body, thereby playing a major role in osmoregulation. Recently, Böhmer *et al.* (Böhmer *et al.,* 2006) reported that the NAD-ME was downregulated due to aldosterone action and might be associated with the osmotic regulation. In higher eukaryotes, regulation often involves the participation of hormones, as shown, for example, by the insulin-dependent ME regulation in rat H-35 cells (Barroso and Santisteban, 1999). The finding that the NAD-ME is influenced by DOC points also towards a possible function of this protein in osmotic regulation (see Figure 4.8).

Pyruvate decarboxylase (PDC) catalyzes the thiamine pyrophosphate- and magnesium-dependent decarboxylation of pyruvate to acetaldehyde with release of carbon dioxide. PDC exhibits cooperativity with respect to pyruvate, an effect which is enhanced by phosphate. PDC is widely distributed in fungi and plants, but not commonly found in bacteria or animals (Furey *et al.,* 1998). It is common for eukaryotes to have multiple PDC genes, although there are only a few examples in which regulation and function are well understood. Most research has focused on ethanol production in plants and yeasts. Thus, the role of the DOC-mediated effects is not yet clear.

4.2.3.3. Other metabolic pathways (spot No. 4, 18, 23, 24 and 25)

The protein found in spot No. 4 and 18 is downregulated due to DOC compared with the control (see Figure 3.18). It has been identified as the 6-phosphogluconate dehydrogenase, decarboxylating (P78812, EC:1.1.1.44) according to the MALDI-TOF-MS result (spot No. 4; see Table 3.3) and both MS results (spot No. 18; see Table 3.3). The spots No. 23 and 24 are also downregulated due to DOC compared to the control (see Figure 3.18). In these two spots has been identified a probable transketolase (Q9URM2, TK, EC:2.2.1.1) according to MALDI-TOF-MS result (spot No. 23; see Table 3.3) and both MS result (spot No. 24; see Table 3.3). These two enzymes are involved in the oxidative part of the pentose-phosphate pathway.

Two spots identified as 6-phosphogluconate dehydrogenase, decarboxylating also differed with regard to their position in the 2-D gels. The theoretical molecular weight and *pI* of this protein is 53.7 kDa / p*I* 6.73. Spot No. 4 was located around p*I* 5.31, and spot No. 18 was close to p*I* 6.69 with respective molecular weights of about 22.1 kDa and 41.3 kDa. In addition, two spots identified as a probable transketolase also differed with regard to their position in the 2-D gels. The theoretical molecular weight and *pI* of this protein is 75.1 kDa / p*I* 6.33. Spot No. 23 was located around p*I* 6.62, and spot No. 24 was close to p*I* 6.51 with respective molecular weights of about 72.0 kDa and 71.7 kDa. As observed in the case of GAPDH 1, DOC may have affected the *pI* and the molecular weight of these proteins, too.

The pentose phosphate pathway is the major source of NADPH required for reductive biosynthesis, and is the source of ribose-5-phosphate required in nucleotide biosynthesis. NADPH is also the substrate for superoxide production by the respiratory burst NADPH oxidase (Pick *et al.,* 1989). The pentose-phosphate pathway of *S. pombe* can act as a route for

the breakdown of sugars such as glucose or pentoses. 6-phosphogluconate dehydrogenase from *S. pombe* is tetrameric having a subunit mass of 38 kDa and it catalyzes the NADP(+)-linked oxidative decarboxylation of 6-phosphogluconate by an equilibrium random mechanism with two independent binding sites, namely one site for the nicotinamide coenzyme, NADP+/NADPH, and another site for 6-phosphogluconate-D-ribulose-5-phosphate and for CO_2 (Tsai and Chen, 1998). Transketolase catalyzes the transfer of two carbon units between sugars in the pentose phosphate pathway (Kochetov, 2001). Wood *et al.* (Wood *et al.,* 2002) reported that 50 genes associated with human diseases like cystic fibrosis, diabetes or cancer have been identified in *S. pombe*. In particular, it is known that transketolase associates with the Wernicke Korsakoff syndrome (Wood *et al.,* 2002).

In addition, one enzyme differentially regulated by DOC has been identified which is involved in the methionine metabolism. The probable 5-methyltetrahydro-pteroyltriglutamate--homocysteine methyltransferase (Q9UT19, met26) was identified with both MS techniques and is downregulated due to the action of DOC (see Figure 3.18; spot No. 25). It catalyzes the biosynthesis of methionine from homocysteine in *S. pombe*.

It remains unclear by now why the three proteins discussed in this chapter are influenced by DOC. Further studies will help to clearify this question.

4.2.4 Oxidative stress (spot No. 3, 7, 8, 15 and 27)

Oxidative stress that generates reactive oxygen species (ROS) can be highly toxic causing damage to proteins, lipids and DNA, and cell death. These damage can be mitigated by DNA repair enzymes, lipases, proteases and other enzymes. Several enzymes play a role in antioxidant defence mechanisms. These include ROS scavenger enzymes such as superoxide dismutase (SOD), catalase and glutathione peroxidase (Martindale and Holbrook, 2002). ROS are not only toxic but play an important role in cellular signalling and in the regulation of gene expression. Oxidative stress has been implicated in a wide variety of disease processes including diabetes, pulmonary fibrosis, and neurodegenerative disorders and is believed to be a major factor in aging (Finkel and Holbrook, 2000). In addition, angiotensin II-induced hypertension is associated with increased vascular superoxide production. The effects of low-renin hypertension on vascular ROS production remain unclear. Furthermore, the role of ROS

in vascular function and hypertension in low-renin hypertension is undefined. In this study, 5 proteins involved in the oxidative stress have been found.

The protein in spot No. 7 was identified as the manganese superoxide dismutase mitochondrial precursor (Q9UQX0, sod2, EC:1.15.1.1) according to both MS techniques and is downregulated due to DOC compared with the control (see Figure 3.18). The protein in spot No. 8 was identified as the glutathione peroxidase (O59858, gpx1, EC:1.11.1.9) according to the MALDI-TOF-MS result and is downregulated due to DOC compared with the control (see Figure 3.18).

SOD belongs to an ubiquitous family of enzymes that function to efficiently catalyze the dismutation of superoxide anions. The SODs are the first and most important line of antioxidant enzyme defense systems against ROS. In detail, manganese SOD has been localized in mitochondria of aerobic cells and has been shown to play a major role in promoting cellular differentiation and tumorgenesis (St Clair *et al.,* 1994). The most abundant peroxidase is the glutathione peroxidase which is present in both the cytosol and mitochondria. This enzyme has the transition metal selenium at its active site and uses reduced glutathione as a substrate to transfer electrons to H_2O_2 thereby converting it into two molecules of water. In the absence of glutathione peroxidases, it is expected that glutathione would be oxidized slower and this could have a consequence in cell signaling.

In addition, the protein in spot No. 3 was identified as the SPCC576.03c protein (O74887, tpx1, thioredoxin peroxidase) according to the both MS results and is upregulated due to DOC compared with the control (see Figure 3.19). Thioredoxin could be another important component to maintain mitochondrial activity intact. This is because it is known that oxidative stress and decreases in glutathione content lead to the oxidation of thioredoxin *in vivo* (Kuge *et al.,* 2001). The increase of thioredoxin peroxidases leads to the suggestion that thioredoxin can be oxidized faster.

Interestingly, sod2 and gpx1 is downregulated due to DOC, whereas tpx1 is upregulated due to DOC. It remains unclear by now why the three proteins are differently influenced by DOC.

It is well known that the mitochondrion is the site of oxidative phosphorylation in eukaryotes. Eukaryotic porins are membrane proteins that form aqueous channels in the cell membrane and the mitochondrial outer membrane. The protein in spot No. 15 was identified as the

probable outer mitochondrial membrane protein porin (Q9P544) according to the both MS results and is upregulated due to DOC compared with the control (see Figure 3.19). The mitochondrial outer membrane pore was first characterized by Marco Colombini as a voltage dependent anion channel (Colombini, 1979). The voltage dependent anion channel plays an important role in coordination of communication. A substantial aspect of this management is a transient formation of complexes with other proteins. The complexes between the outer mitochondrial membrane pore and the adenine nucleotide translocase were associated with energy metabolism and apoptosis. It has been observed that contact sites contained cytochrome *c* (Vyssokikh and Brdiczka, 2003). One major pathway of apoptosis involves the release of cytochrome *c* from mitochondria (Kluck *et al.,* 1997; Yang *et al.,* 1997).

In addition, it is found that one protein regulated by DOC is involved in protein folding. In spot No. 27, the heat shock protein sks2 (Q10284, sks2/hsc1) was identified according to the MALDI-TOF-MS result which is downregulated due to DOC compared with the control (see Figure 3.18). The heat shock proteins are expressed in normal cells but their expression is enhanced by a number of different stresses including heat and ischaemia. They play important roles in chaperoning the folding of other proteins and in protein degradation. The heat shock protein sks2 (HSP75_SCHPO) belongs to the heat shock protein 70 family. Heat shock protein 70 chaperones comprise a set of abundant cellular machines that assist a large variety of protein folding processes in almost all cellular compartments. It has been shown that heat shock protein 70 can inhibit apoptosis in a caspase independent manner (Jaattela *et al.,* 1998). This is likely to involve the ability of heat shock protein 70 to inhibit the c-Jun N-terminal kinase which plays a key role in inducing apoptotic cell death in response to specific stimuli (Gabai *et al.,* 2000; Park *et al.,* 2001).

Summarizing, 5 proteins to be regulated by DOC have been found, which are connected to oxidative stress. As for the three proteins discussed in 4.2.3, the reason why these proteins are influenced is yet not known.

4.2.5 Summary and Outlook

Taken together, effects on the protein pattern in the fission yeast *S. pombe* in response to DOC treatment have been demonstrated in this study. 24 cellular proteins (representing 19

distinct proteins) out of 23 spots were found to be differentially regulated by DOC. Among these proteins, four proteins affected may be associated with non-genomic actions through the PKC pathway. These include cofilin, DNA damage checkpoint protein rad24, G protein beta subunit-like protein and protein vip1. These proteins display a possible function in structure remodeling. In particular, it is proposed that protein vip1 may be a new binding partner of the 14-3-3 protein family. GAPDH 1, involved in primary metabolism, may also play a relevant role in cytoskeleton assembly. Enolase 1-1, enolase 1-2 and NAD-dependent malic enzyme, involved in primary metabolism, may be associated with the osmotic regulation. Other proteins differentially affected by DOC are involved in the primary metabolism or are related to oxidative stress. It is noteworthy to mention that some protein differentially regulated by DOC, such as protein vip1, NAD-dependent malic enzyme and GAPDH 1, are also modulated in a similar way by aldosterone treatment of *S. pombe* (Böhmer *et al.,* 2006). This indicates a more general effect of mineralocorticoids on these proteins and the pathway they are connected with.

In further studies, RT-PCR and western blot analysis should be used to confirm differential expression in mammalian system. Furthermore, the validated proteins could be used as a starting point to identify interaction partners by the two-hybrid system (*in vivo*) and BIAcore measurements (*in vitro*). These studies will help to better understand the way steroids are effecting the fission yeast and other eukaryotic cells in a non-MR mediated way.

5. References

Aitken A (1995) 14-3-3 proteins on the MAP. Trends Biochem Sci 20:95-97.

Aitken A (1996) 14-3-3 and its possible role in co-ordinating multiple signalling pathways. Trends Cell Biol 6:341-347.

Aitken A, Ellis CA, Harris A, Sellers LA, Toker A (1990) Kinase and neurotransmitters. Nature 344:594.

Aitken A, Collinge DB, van Heusden BP, Isobe T, Roseboom PH, Rosenfeld G, Soll J (1992) 14-3-3 proteins: a highly conserved, widespread family of eukaryotic proteins. Trends Biochem Sci 17:498-501.

Aksu S, Scheler C, Focks N, Leenders F, Theuring F, Salnikow J, Jungblut PR (2002) An iterative calibration method with prediction of post-translational modifications for the construction of a two-dimensional electrophoresis database of mouse mammary gland proteins. Proteomics 2:1452-1463.

Ali H, Richardson RM, Tomhave ED, DuBose RA, Haribabu B, Snyderman R (1994) Regulation of stably transfected platelet activating factor receptor in RBL-2H3 cells. Role of multiple G proteins and receptor phosphorylation. J Biol Chem 269:24557-24563.

Altschul SF, Madden TL, Schaffer AA, Zhang J, Zhang Z, Miller W, Lipman DJ (1997) Gapped BLAST and PSI-BLAST: a new generation of protein database search programs. Nucleic Acids Res 25:3389-3402.

Anderson NG, Anderson NL (1996) Twenty years of two-dimensional electrophoresis: past, present and future. Electrophoresis 17:443-453.

Andoh T, Kato T, Jr., Matsui Y, Toh-e A (1998) Phosphoinositide-specific phospholipase C forms a complex with 14-3-3 proteins and is involved in expression of UV resistance in fission yeast. Mol Gen Genet 258:139-147.

Aslett M, Wood V (2006) Gene Ontology annotation status of the fission yeast genome: preliminary coverage approaches 100%. Yeast 23:913-919.

Atkins KB, Johns D, Watts S, Clinton Webb R, Brosius FC, 3rd (2001) Decreased vascular glucose transporter expression and glucose uptake in DOCA-salt hypertension. J Hypertens 19:1581-1587.

Auchus RJ, Miller WL (2001) The principles, pathways and enzymes of human steroidogenesis. In: Endocrinology (de Groot LJ, Jameson JL, eds), pp 1616-1631. Philadelphia: W.B. Saunders.

Bamburg JR, Wiggan OP (2002) ADF/cofilin and actin dynamics in disease. Trends Cell Biol 12:598-605.

Barroso I, Santisteban P (1999) Insulin-induced early growth response gene (Egr-1) mediates a short term repression of rat malic enzyme gene transcription. J Biol Chem 274:17997-18004.

Beato M, Klug J (2000) Steroid hormone receptors: an update. Hum Reprod Update 6:225-236.

Beato M, Truss M, Chavez S (1996) Control of transcription by steroid hormones. Ann N Y Acad Sci 784:93-123.

Biglieri EG, Kater CE (1991) Mineralocorticoids in congenital adrenal hyperplasia. J Steroid Biochem Mol Biol 40:493-499.

Blum H, Beier, H., and Goss, H.J., (1987) Improved silver staining of plant proteins, RNA and DNA in polyacrylamide gels. Electrophoresis 8:93-99.

Böhmer S, Carapito C, Wilzewski B, Leize E, Van Dorsselaer A, Bernhardt R (2006) Analysis of aldosterone induced differential receptor-independent protein patterns using 2Delectrophoresis and mass spectrometry. Biological Chemistry 387:917-929.

Bohren KM, Bullock B, Wermuth B, Gabbay KH (1989) The aldo-keto reductase superfamily. cDNAs and deduced amino acid sequences of human aldehyde and aldose reductases. J Biol Chem 264:9547-9551.

Bone N, Millar JB, Toda T, Armstrong J (1998) Regulated vacuole fusion and fission in Schizosaccharomyces pombe: an osmotic response dependent on MAP kinases. Curr Biol 8:135-144.

Breci L, Hattrup E, Keeler M, Letarte J, Johnson R, Haynes PA (2005) Comprehensive proteomics in yeast using chromatographic fractionation, gas phase fractionation, protein gel electrophoresis, and isoelectric focusing. Proteomics 5:2018-2028.

Brilla CG, Weber KT (1992) Mineralocorticoid excess, dietary sodium, and myocardial fibrosis. J Lab Clin Med 120:893-901.

Brilla CG (2000) Aldosterone and myocardial fibrosis in heart failure. Herz 25:299-306.

Bruce NC, Willey DL, Coulson AF, Jeffery J (1994) Bacterial morphine dehydrogenase further defines a distinct superfamily of oxidoreductases with diverse functional activities. Biochem J 299:805-811.

Brunner D, Nurse P (2000) New concepts in fission yeast morphogenesis. Philos Trans R Soc Lond B Biol Sci 355:873-877.

Bureik M, Schiffler B, Hiraoka Y, Vogel F, Bernhardt R (2002) Functional expression of human mitochondrial CYP11B2 in fission yeast and identification of a new internal electron transfer protein, etp1. Biochemistry 41:2311-2321.

Bureik M, Bruck N, Hubel K, Bernhardt R (2005) The human mineralocorticoid receptor only partially differentiates between different ligands after expression in fission yeast. FEMS Yeast Res 5:627-633.

Burt VL, Whelton P, Roccella EJ, Brown C, Cutler JA, Higgins M, Horan MJ, Labarthe D (1995) Prevalence of hypertension in the US adult population. Results from the Third National Health and Nutrition Examination Survey, 1988-1991. Hypertension 25:305-313.

Buttner K, Bernhardt J, Scharf C, Schmid R, Mader U, Eymann C, Antelmann H, Volker A, Volker U, Hecker M (2001) A comprehensive two-dimensional map of cytosolic proteins of Bacillus subtilis. Electrophoresis 22:2908-2935.

Cao PR, Bernhardt R (1999) Interaction of CYP11B1 (cytochrome P-45011 beta) with CYP11A1 (cytochrome P-450scc) in COS-1 cells. Eur J Biochem 262:720-726.

Celis JE, Gesser B, Rasmussen HH, Madsen P, Leffers H, Dejgaard K, Honore B, Olsen E, Ratz G, Lauridsen JB, et al. (1990) Comprehensive two-dimensional gel protein databases offer a global approach to the analysis of human cells: the transformed amnion cells (AMA) master database and its link to genome DNA sequence data. Electrophoresis 11:989-1071.

Chen CA, Manning DR (2001) Regulation of G proteins by covalent modification. Oncogene 20:1643-1652.

Chen L, Liu TH, Walworth NC (1999) Association of Chk1 with 14-3-3 proteins is stimulated by DNA damage. Genes Dev 13:675-685.

Chong SS, Pack SD, Roschke AV, Tanigami A, Carrozzo R, Smith AC, Dobyns WB, Ledbetter DH (1997) A revision of the lissencephaly and Miller-Dieker syndrome critical regions in chromosome 17p13.3. Hum Mol Genet 6:147-155.

Civitelli R, Kim YS, Gunsten SL, Fujimori A, Huskey M, Avioli LV, Hruska KA (1990) Nongenomic activation of the calcium message system by vitamin D metabolites in osteoblast-like cells. Endocrinology 127:2253-2262.

Collett-Solberg PF (2001) Congenital adrenal hyperplasia: from genetics and biochemistry to clinical practice, Part 1. Clin Pediatr (Phila) 40:1-16.

Colombini M (1979) A candidate for the permeability pathway of the outer mitochondrial membrane. Nature 279:643-645.

Conn JW (1955) Presidential address. I. Painting background. II. Primary aldosteronism, a new clinical syndrome. J Lab Clin Med 45:3-17.

Connell JM, Fraser R, Davies E (2001) Disorders of mineralocorticoid synthesis. Best Pract Res Clin Endocrinol Metab 15:43-60.

Corthals GL, Wasinger VC, Hochstrasser DF, Sanchez JC (2000) The dynamic range of protein expression: a challenge for proteomic research. Electrophoresis 21:1104-1115.

Curnow KM, Mulatero P, Emeric-Blanchouin N, Aupetit-Faisant B, Corvol P, Pascoe L (1997) The amino acid substitutions Ser288Gly and Val320Ala convert the cortisol producing enzyme, CYP11B1, into an aldosterone producing enzyme. Nat Struct Biol 4:32-35.

Davis L, Smith GR (2001) Meiotic recombination and chromosome segregation in Schizosaccharomyces pombe. Proc Natl Acad Sci U S A 98:8395-8402.

de Boland AR, Norman AW (1990) Influx of extracellular calcium mediates 1,25-dihydroxyvitamin D3-dependent transcaltachia (the rapid stimulation of duodenal Ca2+ transport). Endocrinology 127:2475-2480.

Decker BL, Wickner WT (2006) Enolase activates homotypic vacuole fusion and protein transport to the vacuole in yeast. J Biol Chem 281:14523-14528. Epub 12006 Mar 14524.

Delcayre C, Silvestre JS (1999) Aldosterone and the heart: towards a physiological function? Cardiovasc Res 43:7-12.

Dostal DE, Hunt RA, Kule CE, Bhat GJ, Karoor V, McWhinney CD, Baker KM (1997) Molecular mechanisms of angiotensin II in modulating cardiac function: intracardiac effects and signal transduction pathways. J Mol Cell Cardiol 29:2893-2902.

Drury PL (1985) Disorders of mineralocorticoid activity. Clin Endocrinol Metab 14:175-202.

Dugaiczyk A, Haron JA, Stone EM, Dennison OE, Rothblum KN, Schwartz RJ (1983) Cloning and sequencing of a deoxyribonucleic acid copy of glyceraldehyde-3-phosphate dehydrogenase messenger ribonucleic acid isolated from chicken muscle. Biochemistry 22:1605-1613.

Duronio RJ, Gordon JI, Boguski MS (1992) Comparative analysis of the beta transducin family with identification of several new members including PWP1, a nonessential gene of Saccharomyces cerevisiae that is divergently transcribed from NMT1. Proteins 13:41-56.

Egoshi K, Masai M, Nagao K, Ito H (1998) 11-Deoxycorticosterone-producing adrenocortical carcinoma. Urol Int 61:251-253.

Falkenstein E, Tillmann HC, Christ M, Feuring M, Wehling M (2000) Multiple actions of steroid hormones--a focus on rapid, nongenomic effects. Pharmacol Rev 52:513-556.

Fanger GR, Widmann C, Porter AC, Sather S, Johnson GL, Vaillancourt RR (1998) 14-3-3 proteins interact with specific MEK kinases. J Biol Chem 273:3476-3483.

Fantes PB, J. (2000) The Yeast Nucleus. Oxford: Oxford Univ. Press.

Fardella CE, Miller WL (1996) Molecular biology of mineralocorticoid metabolism. Annu Rev Nutr 16:443-470.

Fardella CE, Rodriguez H, Hum DW, Mellon SH, Miller WL (1995) Artificial mutations in P450c11AS (aldosterone synthase) can increase enzymatic activity: a model for low-renin hypertension? J Clin Endocrinol Metab 80:1040-1043.

Fardella CE, Rodriguez H, Montero J, Zhang G, Vignolo P, Rojas A, Villarroel L, Miller WL (1996) Genetic variation in P450c11AS in Chilean patients with low renin hypertension. J Clin Endocrinol Metab 81:4347-4351.

Fardella CE, Mosso L, Gomez-Sanchez C, Cortes P, Soto J, Gomez L, Pinto M, Huete A, Oestreicher E, Foradori A, Montero J (2000) Primary hyperaldosteronism in essential hypertensives: prevalence, biochemical profile, and molecular biology. J Clin Endocrinol Metab 85:1863-1867.

Fenn JB, Mann M, Meng CK, Wong SF, Whitehouse CM (1989) Electrospray ionization for mass spectrometry of large biomolecules. Science 246:64-71.

Finkel T, Holbrook NJ (2000) Oxidants, oxidative stress and the biology of ageing. Nature 408:239-247.

Ford JC, al-Khodairy F, Fotou E, Sheldrick KS, Griffiths DJ, Carr AM (1994) 14-3-3 protein homologs required for the DNA damage checkpoint in fission yeast. Science 265:533-535.

Fountoulakis M, Cairns N, Lubec G (1999) Increased levels of 14-3-3 gamma and epsilon proteins in brain of patients with Alzheimer's disease and Down syndrome. J Neural Transm Suppl 57:323-335.

Freed E, Symons M, Macdonald SG, McCormick F, Ruggieri R (1994) Binding of 14-3-3 proteins to the protein kinase Raf and effects on its activation. Science 265:1713-1716.

Freel EM, Connell JM (2004) Mechanisms of hypertension: the expanding role of aldosterone. J Am Soc Nephrol 15:1993-2001.

Frey FJ, Odermatt A, Frey BM (2004) Glucocorticoid-mediated mineralocorticoid receptor activation and hypertension. Curr Opin Nephrol Hypertens 13:451-458.

Fu H, Subramanian RR, Masters SC (2000) 14-3-3 proteins: structure, function, and regulation. Annu Rev Pharmacol Toxicol 40:617-647.

Funder JW (2005) Mineralocorticoid receptors: distribution and activation. Heart Fail Rev 10:15-22.

Furey W, Arjunan P, Chen L, Sax M, Guo F, Jordan F (1998) Structure-function relationships and flexible tetramer assembly in pyruvate decarboxylase revealed by analysis of crystal structures. Biochim Biophys Acta 1385:253-270.

Gabai VL, Yaglom JA, Volloch V, Meriin AB, Force T, Koutroumanis M, Massie B, Mosser DD, Sherman MY (2000) Hsp72-mediated suppression of c-Jun N-terminal kinase is implicated in development of tolerance to caspase-independent cell death. Mol Cell Biol 20:6826-6836.

Ganguly S, Weller JL, Ho A, Chemineau P, Malpaux B, Klein DC (2005) Melatonin synthesis: 14-3-3-dependent activation and inhibition of arylalkylamine N-acetyltransferase mediated by phosphoserine-205. Proc Natl Acad Sci U S A 102:1222-1227. Epub 2005 Jan 1211.

Garcia-Guzman M, Dolfi F, Russello M, Vuori K (1999) Cell adhesion regulates the interaction between the docking protein p130(Cas) and the 14-3-3 proteins. J Biol Chem 274:5762-5768.

Garrels JI, Futcher B, Kobayashi R, Latter GI, Schwender B, Volpe T, Warner JR, McLaughlin CS (1994) Protein identifications for a Saccharomyces cerevisiae protein database. Electrophoresis 15:1466-1486.

Ghulam A, Vantyghem MC, Wemeau JL, Boersma A (2003) Adrenal minerlocorticoids pathway and its clinical applications. Clin Chim Acta 330:99-110.

Gilman AG (1987) G proteins: transducers of receptor-generated signals. Annu Rev Biochem 56:615-649.

Goffeau A, Barrell BG, Bussey H, Davis RW, Dujon B, Feldmann H, Galibert F, Hoheisel JD, Jacq C, Johnston M, Louis EJ, Mewes HW, Murakami Y, Philippsen P, Tettelin H, Oliver SG (1996) Life with 6000 genes. Science 274:546, 563-547.

Gohla A, Bokoch GM (2002) 14-3-3 regulates actin dynamics by stabilizing phosphorylated cofilin. Curr Biol 12:1704-1710.

Gomez-Sanchez EP, Gomez-Sanchez CE (1992) Central hypertensinogenic effects of glycyrrhizic acid and carbenoxolone. Am J Physiol 263:E1125-1130.

Gopalakrishna R, Jaken S (2000) Protein kinase C signaling and oxidative stress. Free Radic Biol Med 28:1349-1361.

Gordon RD, Stowasser M, Tunny TJ, Klemm SA, Rutherford JC (1994) High incidence of primary aldosteronism in 199 patients referred with hypertension. Clin Exp Pharmacol Physiol 21:315-318.

Graves PR, Haystead TA (2002) Molecular biologist's guide to proteomics. Microbiol Mol Biol Rev 66:39-63; table of contents.

Groenewald M, Viljoen-Bloom M (2001) Factors involved in the regulation of the Schizosaccharomyces pombe malic enzyme gene. Curr Genet 39:222-230.

Gutz H, Heslot, H., Leupold, U. and Loprieno, N. (1974). New York, London: Plenum Press.

Hagan IM, Petersen J (2000) The microtubule organizing centers of Schizosaccharomyces pombe. Curr Top Dev Biol 49:133-159.

Hanash SM, Madoz-Gurpide J, Misek DE (2002) Identification of novel targets for cancer therapy using expression proteomics. Leukemia 16:478-485.

Haseroth K, Gerdes D, Berger S, Feuring M, Gunther A, Herbst C, Christ M, Wehling M (1999) Rapid nongenomic effects of aldosterone in mineralocorticoid-receptor-knockout mice. Biochem Biophys Res Commun 266:257-261.

Hawkins M, Pope B, Maciver SK, Weeds AG (1993) Human actin depolymerizing factor mediates a pH-sensitive destruction of actin filaments. Biochemistry 32:9985-9993.

Hayashi E, Kuramitsu Y, Okada F, Fujimoto M, Zhang X, Kobayashi M, Iizuka N, Ueyama Y, Nakamura K (2005) Proteomic profiling for cancer progression: Differential display analysis for the expression of intracellular proteins between regressive and progressive cancer cell lines. Proteomics 5:1024-1032.

Hazbun TR, Malmstrom L, Anderson S, Graczyk BJ, Fox B, Riffle M, Sundin BA, Aranda JD, McDonald WH, Chiu CH, Snydsman BE, Bradley P, Muller EG, Fields S, Baker D, Yates JR, 3rd, Davis TN (2003) Assigning function to yeast proteins by integration of technologies. Mol Cell 12:1353-1365.

Hernandez R, Nombela C, Diez-Orejas R, Gil C (2004) Two-dimensional reference map of Candida albicans hyphal forms. Proteomics 4:374-382.

Herskowitz I (1995) MAP kinase pathways in yeast: for mating and more. Cell 80:187-197.

Hesketh AR, Chandra G, Shaw AD, Rowland JJ, Kell DB, Bibb MJ, Chater KF (2002) Primary and secondary metabolism, and post-translational protein modifications, as portrayed by proteomic analysis of Streptomyces coelicolor. Mol Microbiol 46:917-932.

Humphrey T (2000) DNA damage and cell cycle control in Schizosaccharomyces pombe. Mutat Res 451:211-226.

Hwang KH, Carapito C, Böhmer S, Leize E, Van Dorsselaer A, Bernhardt R (2006) Proteome analysis of Schizosaccharomyces pombe by two-dimensional gel electrophoresis and mass spectrometry. Proteomics 6:4115 - 4129.

Ichimura T, Isobe T, Okuyama T, Yamauchi T, Fujisawa H (1987) Brain 14-3-3 protein is an activator protein that activates tryptophan 5-monooxygenase and tyrosine 3-monooxygenase in the presence of Ca2+,calmodulin-dependent protein kinase II. FEBS Lett 219:79-82.

Ishii M, Kurachi Y (2002) The 14-3-3 protein as a novel regulator of ion channel localisation. J Physiol 545:2.

Jaattela M, Wissing D, Kokholm K, Kallunki T, Egeblad M (1998) Hsp70 exerts its anti-apoptotic function downstream of caspase-3-like proteases. Embo J 17:6124-6134.

Jenis LG, Lian JB, Stein GS, Baran DT (1993) 1 alpha,25-dihydroxyvitamin D3-induced changes in intracellular pH in osteoblast-like cells modulate gene expression. J Cell Biochem 53:234-239.

Jungblut PR, Bumann D, Haas G, Zimny-Arndt U, Holland P, Lamer S, Siejak F, Aebischer A, Meyer TF (2000) Comparative proteome analysis of Helicobacter pylori. Mol Microbiol 36:710-725.

Jungbluth A (2000) Funktionelle Charakterisierung des vip1-Proteins der Spalthefe Schizosaccharomyces pombe. In. Saarbrücken: Universität des Saarlandes.

Kannel WB (2000) Elevated systolic blood pressure as a cardiovascular risk factor. Am J Cardiol 85:251-255.

Karas M, Hillenkamp F (1988) Laser desorption ionization of proteins with molecular masses exceeding 10,000 daltons. Anal Chem 60:2299-2301.

Kaufmann R (1995) Matrix-assisted laser desorption ionization (MALDI) mass spectrometry: a novel analytical tool in molecular biology and biotechnology. J Biotechnol 41:155-175.

Kelly MJ, Lagrange AH, Wagner EJ, Ronnekleiv OK (1999) Rapid effects of estrogen to modulate G protein-coupled receptors via activation of protein kinase A and protein kinase C pathways. Steroids 64:64-75.

Kishimoto I, Garbers DL (1997) Physiological regulation of blood pressure and kidney function by guanylyl cyclase isoforms. Curr Opin Nephrol Hypertens 6:58-63.

Kitamura K, Katayama S, Dhut S, Sato M, Watanabe Y, Yamamoto M, Toda T (2001) Phosphorylation of Mei2 and Ste11 by Pat1 kinase inhibits sexual differentiation via ubiquitin proteolysis and 14-3-3 protein in fission yeast. Dev Cell 1:389-399.

Klose J (1975) Protein mapping by combined isoelectric focusing and electrophoresis of mouse tissues. A novel approach to testing for induced point mutations in mammals. Humangenetik 26:231-243.

Kluck RM, Bossy-Wetzel E, Green DR, Newmeyer DD (1997) The release of cytochrome c from mitochondria: a primary site for Bcl-2 regulation of apoptosis. Science 275:1132-1136.

Kochetov GA (2001) Functional flexibility of the transketolase molecule. Biochemistry (Mosc) 66:1077-1085.

Kuge S, Arita M, Murayama A, Maeta K, Izawa S, Inoue Y, Nomoto A (2001) Regulation of the yeast Yap1p nuclear export signal is mediated by redox signal-induced reversible disulfide bond formation. Mol Cell Biol 21:6139-6150.

Labrador M, Mongelard F, Plata-Rengifo P, Baxter EM, Corces VG, Gerasimova TI (2001) Protein encoding by both DNA strands. Nature 409:1000.

Lal SK, Johnson S, Conway T, Kelley PM (1991) Characterization of a maize cDNA that complements an enolase-deficient mutant of Escherichia coli. Plant Mol Biol 16:787-795.

Lang BF, Cedergren R, Gray MW (1987) The mitochondrial genome of the fission yeast, Schizosaccharomyces pombe. Sequence of the large-subunit ribosomal RNA gene, comparison of potential secondary structure in fungal mitochondrial large-subunit rRNAs and evolutionary considerations. Eur J Biochem 169:527-537.

Larsen MR, Larsen PM, Fey SJ, Roepstorff P (2001) Characterization of differently processed forms of enolase 2 from Saccharomyces cerevisiae by two-dimensional gel electrophoresis and mass spectrometry. Electrophoresis 22:566-575.

Latif C, Harvey SH, O'Connell MJ (2001) Ensuring the stability of the genome: DNA damage checkpoints. ScientificWorldJournal 1:684-702.

Lavoie JL, Sigmund CD (2003) Minireview: overview of the renin-angiotensin system--an endocrine and paracrine system. Endocrinology 144:2179-2183.

Layfield R, Fergusson J, Aitken A, Lowe J, Landon M, Mayer RJ (1996) Neurofibrillary tangles of Alzheimer's disease brains contain 14-3-3 proteins. Neurosci Lett 209:57-60.

Leffers H, Madsen P, Rasmussen HH, Honore B, Andersen AH, Walbum E, Vandekerckhove J, Celis JE (1993) Molecular cloning and expression of the transformation sensitive epithelial marker stratifin. A member of a protein family that has been involved in the protein kinase C signalling pathway. J Mol Biol 231:982-998.

Lewis TS, Hunt JB, Aveline LD, Jonscher KR, Louie DF, Yeh JM, Nahreini TS, Resing KA, Ahn NG (2000) Identification of novel MAP kinase pathway signaling targets by functional proteomics and mass spectrometry. Mol Cell 6:1343-1354.

Lifton RP, Gharavi AG, Geller DS (2001) Molecular mechanisms of human hypertension. Cell 104:545-556.

Lifton RP, Dluhy RG, Powers M, Rich GM, Cook S, Ulick S, Lalouel JM (1992) A chimaeric 11 beta-hydroxylase/aldosterone synthase gene causes glucocorticoid-remediable aldosteronism and human hypertension. Nature 355:262-265.

Losel R, Wehling M (2003) Nongenomic actions of steroid hormones. Nat Rev Mol Cell Biol 4:46-56.

Mann M, Talbo G (1996) Developments in matrix-assisted laser desorption/ionization peptide mass spectrometry. Curr Opin Biotechnol 7:11-19.

Mann M, Jensen ON (2003) Proteomic analysis of post-translational modifications. Nat Biotechnol 21:255-261.

Mantero F, Lucarelli G (2000) Aldosterone antagonists in hypertension and heart failure. Ann Endocrinol (Paris) 61:52-60.

Marcinkowska E, Wiedlocha A (2002) Steroid signal transduction activated at the cell membrane: from plants to animals. Acta Biochim Pol 49:735-745.

Maris C, Dominguez C, Allain FH (2005) The RNA recognition motif, a plastic RNA-binding platform to regulate post-transcriptional gene expression. Febs J 272:2118-2131.

Marks R, Barlow JW, Funder JW (1982) Steroid-induced vasoconstriction: glucocorticoid antagonist studies. J Clin Endocrinol Metab 54:1075-1077.

Martens GJ, Piosik PA, Danen EH (1992) Evolutionary conservation of the 14-3-3 protein. Biochem Biophys Res Commun 184:1456-1459.

Martindale JL, Holbrook NJ (2002) Cellular response to oxidative stress: signaling for suicide and survival. J Cell Physiol 192:1-15.

Matsuzaki K, Arai T, Miyazaki T, Yasuda K (1995) Formation of 6 beta-OH-deoxycorticosterone from deoxycorticosterone by A6 cells. Steroids 60:457-462.

Mazurek S, Michel A, Eigenbrodt E (1997) Effect of extracellular AMP on cell proliferation and metabolism of breast cancer cell lines with high and low glycolytic rates. J Biol Chem 272:4941-4952.

Mazurek S, Weisse G, Wust G, Schafer-Schwebel A, Eigenbrodt E, Friis RR (1999) Energy metabolism in the involuting mammary gland. In Vivo 13:467-477.

McAlister L, Holland MJ (1982) Targeted deletion of a yeast enolase structural gene. Identification and isolation of yeast enolase isozymes. J Biol Chem 257:7181-7188.

McDonald WH, Yates JR, 3rd (2000) Proteomic tools for cell biology. Traffic 1:747-754.

Meri S, Baumann M (2001) Proteomics: posttranslational modifications, immune responses and current analytical tools. Biomol Eng 18:213-220.

Merril CR, Dunau ML, Goldman D (1981) A rapid sensitive silver stain for polypeptides in polyacrylamide gels. Anal Biochem 110:201-207.

Mishra M, Karagiannis J, Sevugan M, Singh P, Balasubramanian MK (2005) The 14-3-3 protein rad24p modulates function of the cdc14p family phosphatase clp1p/flp1p in fission yeast. Curr Biol 15:1376-1383.

Moneva MH, Gomez-Sanchez CE (2002) Pathophysiology of adrenal hypertension. Semin Nephrol 22:44-53.

Moore BW, Perez VJ (1967) Specific proteins of the nervous system. In: Physiological and Biochemical Aspects of Nervous Integration (Carlson FD, ed), pp 343-359. MA: Prentice Hall Inc: The Marine Biological Laboratory, Woods Hole.

Morelli S, de Boland AR, Boland RL (1993) Generation of inositol phosphates, diacylglycerol and calcium fluxes in myoblasts treated with 1,25-dihydroxyvitamin D3. Biochem J 289:675-679.

Moreno S, Klar A, Nurse P (1991) Molecular genetic analysis of fission yeast Schizosaccharomyces pombe. Methods Enzymol 194:795-823.

Morley P, Whitfield JF, Vanderhyden BC, Tsang BK, Schwartz JL (1992) A new, nongenomic estrogen action: the rapid release of intracellular calcium. Endocrinology 131:1305-1312.

Morrison D (1994) 14-3-3: modulators of signaling proteins? Science 266:56-57.

Moser BA, Russell P (2000) Cell cycle regulation in Schizosaccharomyces pombe. Curr Opin Microbiol 3:631-636.

Mosterd A, D'Agostino RB, Silbershatz H, Sytkowski PA, Kannel WB, Grobbee DE, Levy D (1999) Trends in the prevalence of hypertension, antihypertensive therapy, and left ventricular hypertrophy from 1950 to 1989. N Engl J Med 340:1221-1227.

Muslin AJ, Tanner JW, Allen PM, Shaw AS (1996) Interaction of 14-3-3 with signaling proteins is mediated by the recognition of phosphoserine. Cell 84:889-897.

Must A, Spadano J, Coakley EH, Field AE, Colditz G, Dietz WH (1999) The disease burden associated with overweight and obesity. Jama 282:1523-1529.

Nakano K, Mabuchi I (2006a) Actin-capping protein is involved in controlling organization of actin cytoskeleton together with ADF/cofilin, profilin and F-actin crosslinking proteins in fission yeast. Genes Cells 11:893-905.

Nakano K, Mabuchi I (2006b) Actin-depolymerizing protein Adf1 is required for formation and maintenance of the contractile ring during cytokinesis in fission yeast. Mol Biol Cell 17:1933-1945.

Nakao K, Itoh H, Saito Y, Mukoyama M, Ogawa Y (1996) The natriuretic peptide family. Curr Opin Nephrol Hypertens 5:4-11.

Nguyen AN, Ikner AD, Shiozaki M, Warren SM, Shiozaki K (2002) Cytoplasmic localization of Wis1 MAPKK by nuclear export signal is important for nuclear targeting of Spc1/Sty1 MAPK in fission yeast. Mol Biol Cell 13:2651-2663.

Nishida E, Maekawa S, Sakai H (1984) Cofilin, a protein in porcine brain that binds to actin filaments and inhibits their interactions with myosin and tropomyosin. Biochemistry 23:5307-5313.

Norman AW, Mizwicki MT, Norman DP (2004) Steroid-hormone rapid actions, membrane receptors and a conformational ensemble model. Nat Rev Drug Discov 3:27-41.

Nurse P (2000) A long twentieth century of the cell cycle and beyond. Cell 100:71-78.

Nussberger J (2003) Investigating mineralocorticoid hypertension. J Hypertens Suppl 21:S25-30.

Obenauer JC, Cantley LC, Yaffe MB (2003) Scansite 2.0: Proteome-wide prediction of cell signaling interactions using short sequence motifs. Nucleic Acids Res 31:3635-3641.

O'Farrell PH (1975) High resolution two-dimensional electrophoresis of proteins. J Biol Chem 250:4007-4021.

Ozoe F, Kurokawa R, Kobayashi Y, Jeong HT, Tanaka K, Sen K, Nakagawa T, Matsuda H, Kawamukai M (2002) The 14-3-3 proteins Rad24 and Rad25 negatively regulate Byr2 by affecting its localization in Schizosaccharomyces pombe. Mol Cell Biol 22:7105-7119.

Pallen MJ, Beatson SA, Bailey CM (2005) Bioinformatics, genomics and evolution of non-flagellar type-III secretion systems: a Darwinian perspective. FEMS Microbiol Rev 29:201-229.

Palmgren S, Vartiainen M, Lappalainen P (2002) Twinfilin, a molecular mailman for actin monomers. J Cell Sci 115:881-886.

Pandey A, Mann M (2000) Proteomics to study genes and genomes. Nature 405:837-846.

Pardo M, Ward M, Bains S, Molina M, Blackstock W, Gil C, Nombela C (2000) A proteomic approach for the study of Saccharomyces cerevisiae cell wall biogenesis. Electrophoresis 21:3396-3410.

Park HS, Lee JS, Huh SH, Seo JS, Choi EJ (2001) Hsp72 functions as a natural inhibitory protein of c-Jun N-terminal kinase. Embo J 20:446-456.

Pascoe L, Curnow KM, Slutsker L, Connell JM, Speiser PW, New MI, White PC (1992) Glucocorticoid-suppressible hyperaldosteronism results from hybrid genes created by unequal crossovers between CYP11B1 and CYP11B2. Proc Natl Acad Sci U S A 89:8327-8331.

Pearce D, Bhargava A, Cole TJ (2003) Aldosterone: its receptor, target genes, and actions. Vitam Horm 66:29-76.

Pennisi E (2003) Bioinformatics. Gene counters struggle to get the right answer. Science 301:1040-1041.

Perego P, Jimenez GS, Gatti L, Howell SB, Zunino F (2000) Yeast mutants as a model system for identification of determinants of chemosensitivity. Pharmacol Rev 52:477-492.

Perrot M, Sagliocco F, Mini T, Monribot C, Schneider U, Shevchenko A, Mann M, Jeno P, Boucherie H (1999) Two-dimensional gel protein database of Saccharomyces cerevisiae (update 1999). Electrophoresis 20:2280-2298.

Peshavaria M, Day IN (1991) Molecular structure of the human muscle-specific enolase gene (ENO3). Biochem J 275:427-433.

Peters J, Hampf M, Peters B, Bernhardt R (1998) Molekularbiologie, Klinik und Therapie steroidbedingter Hypertonien. In: Handbuch der Molekularen Medizin: Herz-Kreislauf-Erkrankungen (Ganten D, Ruckpaul K, eds), pp 413-452. Berlin: Springer-Verlag.

Pick E, Kroizman T, Abo A (1989) Activation of the superoxide-forming NADPH oxidase of macrophages requires two cytosolic components--one of them is also present in certain nonphagocytic cells. J Immunol 143:4180-4187.

Pitt B, Zannad F, Remme WJ, Cody R, Castaigne A, Perez A, Palensky J, Wittes J (1999) The effect of spironolactone on morbidity and mortality in patients with severe heart failure. Randomized Aldactone Evaluation Study Investigators. N Engl J Med 341:709-717.

Preininger AM, Hamm HE (2004) G protein signaling: insights from new structures. Sci STKE 2004:re3.

Pritchard PH (1987) The degradation of platelet-activating factor by high-density lipoprotein in rat plasma. Effect of ethynyloestradiol administration. Biochem J 246:791-794.

Qin J, Kang W, Leung B, McLeod M (2003) Ste11p, a high-mobility-group box DNA-binding protein, undergoes pheromone- and nutrient-regulated nuclear-cytoplasmic shuttling. Mol Cell Biol 23:3253-3264.

Ramires FJ, Mansur A, Coelho O, Maranhao M, Gruppi CJ, Mady C, Ramires JA (2000) Effect of spironolactone on ventricular arrhythmias in congestive heart failure secondary to idiopathic dilated or to ischemic cardiomyopathy. Am J Cardiol 85:1207-1211.

Reaven GM (1988) Banting lecture 1988. Role of insulin resistance in human disease. Diabetes 37:1595-1607.

Regula JT, Ueberle B, Boguth G, Gorg A, Schnolzer M, Herrmann R, Frank R (2000) Towards a two-dimensional proteome map of Mycoplasma pneumoniae. Electrophoresis 21:3765-3780.

Remacle JE, Albrecht G, Brys R, Braus GH, Huylebroeck D (1997) Three classes of mammalian transcription activation domain stimulate transcription in Schizosaccharomyces pombe. Embo J 16:5722-5729.

Rittinger K, Budman J, Xu J, Volinia S, Cantley LC, Smerdon SJ, Gamblin SJ, Yaffe MB (1999) Structural analysis of 14-3-3 phosphopeptide complexes identifies a dual role for the nuclear export signal of 14-3-3 in ligand binding. Mol Cell 4:153-166.

Roberts DJ, Waelbroeck M (2004) G protein activation by G protein coupled receptors: ternary complex formation or catalyzed reaction? Biochem Pharmacol 68:799-806.

Rodriguez-Gabriel MA, Russell P (2005) Distinct signaling pathways respond to arsenite and reactive oxygen species in Schizosaccharomyces pombe. Eukaryot Cell 4:1396-1402.

Rosner W, Hryb DJ, Khan MS, Nakhla AM, Romas NA (1999) Androgen and estrogen signaling at the cell membrane via G-proteins and cyclic adenosine monophosphate. Steroids 64:100-106.

Sakai RR, McEwen BS, Fluharty SJ, Ma LY (2000) The amygdala: site of genomic and nongenomic arousal of aldosterone-induced sodium intake. Kidney Int 57:1337-1345.

Sato M, Watanabe Y, Akiyoshi Y, Yamamoto M (2002) 14-3-3 protein interferes with the binding of RNA to the phosphorylated form of fission yeast meiotic regulator Mei2p. Curr Biol 12:141-145.

Schaeffer HJ, Weber MJ (1999) Mitogen-activated protein kinases: specific messages from ubiquitous messengers. Mol Cell Biol 19:2435-2444.

Schaffer S, Weil B, Nguyen VD, Dongmann G, Gunther K, Nickolaus M, Hermann T, Bott M (2001) A high-resolution reference map for cytoplasmic and membrane-associated proteins of Corynebacterium glutamicum. Electrophoresis 22:4404-4422.

Sernia C, Zeng T, Kerr D, Wyse B (1997) Novel perspectives on pituitary and brain angiotensinogen. Front Neuroendocrinol 18:174-208.

Sheppard KE (2003) Corticosteroid receptors, 11 beta-hydroxysteroid dehydrogenase, and the heart. Vitam Horm 66:77-112.

Sheppard KE, Autelitano DJ (2002) 11Beta-hydroxysteroid dehydrogenase 1 transforms 11-dehydrocorticosterone into transcriptionally active glucocorticoid in neonatal rat heart. Endocrinology 143:198-204.

Silvestre JS, Robert V, Heymes C, Aupetit-Faisant B, Mouas C, Moalic JM, Swynghedauw B, Delcayre C (1998) Myocardial production of aldosterone and corticosterone in the rat. Physiological regulation. J Biol Chem 273:4883-4891.

Sipiczki M (2000) Where does fission yeast sit on the tree of life? Genome Biol 1:REVIEWS1011. Epub 2000 Aug 1014.

Sirover MA (1999) New insights into an old protein: the functional diversity of mammalian glyceraldehyde-3-phosphate dehydrogenase. Biochim Biophys Acta 1432:159-184.

Smith CL, Matsumoto T, Niwa O, Klco S, Fan JB, Yanagida M, Cantor CR (1987) An electrophoretic karyotype for Schizosaccharomyces pombe by pulsed field gel electrophoresis. Nucleic Acids Res 15:4481-4489.

St Clair DK, Oberley TD, Muse KE, St Clair WH (1994) Expression of manganese superoxide dismutase promotes cellular differentiation. Free Radic Biol Med 16:275-282.

Stavridi ES, Chehab NH, Malikzay A, Halazonetis TD (2001) Substitutions that compromise the ionizing radiation-induced association of p53 with 14-3-3 proteins also compromise the ability of p53 to induce cell cycle arrest. Cancer Res 61:7030-7033.

Stewart PM (1999) Mineralocorticoid hypertension. Lancet 353:1341-1347.

Stoll D, Templin MF, Schrenk M, Traub PC, Vohringer CF, Joos TO (2002) Protein microarray technology. Front Biosci 7:c13-32.

Sun N, Jang J, Lee S, Kim S, Lee S, Hoe KL, Chung KS, Kim DU, Yoo HS, Won M, Song KB (2005) The first two-dimensional reference map of the fission yeast, Schizosaccharomyces pombe proteins. Proteomics 5:1574-1579.

Svoboda P, Teisinger J, Novotny J, Bourova L, Drmota T, Hejnova L, Moravcova Z, Lisy V, Rudajev V, Stohr J, Vokurkova A, Svandova I, Durchankova D (2004) Biochemistry of transmembrane signaling mediated by trimeric G proteins. Physiol Res 53:S141-152.

Swanson KD, Ganguly R (1992) Characterization of a Drosophila melanogaster gene similar to the mammalian genes encoding the tyrosine/tryptophan hydroxylase activator and protein kinase C inhibitor proteins. Gene 113:183-190.

Switzer RC, 3rd, Merril CR, Shifrin S (1979) A highly sensitive silver stain for detecting proteins and peptides in polyacrylamide gels. Anal Biochem 98:231-237.

Sylvia VL, Schwartz Z, Schuman L, Morgan RT, Mackey S, Gomez R, Boyan BD (1993) Maturation-dependent regulation of protein kinase C activity by vitamin D3 metabolites in chondrocyte cultures. J Cell Physiol 157:271-278.

Tanaka Y, Okuzaki D, Yabuta N, Yoneki T, Nojima H (2000) Rad24 is essential for proliferation of diploid cells in fission yeast. FEBS Lett 472:254-258.

Templin MF, Stoll D, Schrenk M, Traub PC, Vohringer CF, Joos TO (2002) Protein microarray technology. Trends Biotechnol 20:160-166.

Thiede B, Rudel T (2004) Proteome analysis of apoptotic cells. Mass Spectrom Rev 23:333-349.

Toker A, Ellis CA, Sellers LA, Aitken A (1990) Protein kinase C inhibitor proteins. Purification from sheep brain and sequence similarity to lipocortins and 14-3-3 protein. Eur J Biochem 191:421-429.

Toone WM, Jones N (1998) Stress-activated signalling pathways in yeast. Genes Cells 3:485-498.

Toone WM, Kuge S, Samuels M, Morgan BA, Toda T, Jones N (1998) Regulation of the fission yeast transcription factor Pap1 by oxidative stress: requirement for the nuclear export factor Crm1 (Exportin) and the stress-activated MAP kinase Sty1/Spc1. Genes Dev 12:1453-1463.

Tryoen-Toth P, Richert S, Sohm B, Mine M, Marsac C, Van Dorsselaer A, Leize E, Florentz C (2003) Proteomic consequences of a human mitochondrial tRNA mutation beyond the frame of mitochondrial translation. J Biol Chem 278:24314-24323. Epub 22003 Apr 24324.

Tsai CS, Chen Q (1998) Purification and kinetic characterization of 6-phosphogluconate dehydrogenase from Schizosaccharomyces pombe. Biochem Cell Biol 76:637-644.

van der Voorn L, Ploegh HL (1992) The WD-40 repeat. FEBS Lett 307:131-134.

van Heusden GP, Steensma HY (2006) Yeast 14-3-3 proteins. Yeast 23:159-171.

van Heusden GP, Griffiths DJ, Ford JC, Chin AWTF, Schrader PA, Carr AM, Steensma HY (1995) The 14-3-3 proteins encoded by the BMH1 and BMH2 genes are essential in the yeast Saccharomyces cerevisiae and can be replaced by a plant homologue. Eur J Biochem 229:45-53.

VanBogelen RA, Abshire KZ, Moldover B, Olson ER, Neidhardt FC (1997) Escherichia coli proteome analysis using the gene-protein database. Electrophoresis 18:1243-1251.

Vierstraete E, Cerstiaens A, Baggerman G, Van den Bergh G, De Loof A, Schoofs L (2003) Proteomics in Drosophila melanogaster: first 2D database of larval hemolymph proteins. Biochem Biophys Res Commun 304:831-838.

Viljoen M, Volschenk H, Young RA, van Vuuren HJ (1999) Transcriptional regulation of the Schizosaccharomyces pombe malic enzyme gene, mae2. J Biol Chem 274:9969-9975.

Vyssokikh MY, Brdiczka D (2003) The function of complexes between the outer mitochondrial membrane pore (VDAC) and the adenine nucleotide translocase in regulation of energy metabolism and apoptosis. Acta Biochim Pol 50:389-404.

Wang W, Shakes DC (1994) Isolation and sequence analysis of a Caenorhabditis elegans cDNA which encodes a 14-3-3 homologue. Gene 147:215-218.

Wasinger VC, Cordwell SJ, Cerpa-Poljak A, Yan JX, Gooley AA, Wilkins MR, Duncan MW, Harris R, Williams KL, Humphery-Smith I (1995) Progress with gene-product mapping of the Mollicutes: Mycoplasma genitalium. Electrophoresis 16:1090-1094.

Waterman MJ, Stavridi ES, Waterman JL, Halazonetis TD (1998) ATM-dependent activation of p53 involves dephosphorylation and association with 14-3-3 proteins. Nat Genet 19:175-178.

Wehling M, Kasmayr J, Theisen K (1990) Aldosterone influences free intracellular calcium in human mononuclear leukocytes in vitro. Cell Calcium 11:565-571.

Wehling M, Bauer MM, Ulsenheimer A, Schneider M, Neylon CB, Christ M (1996) Nongenomic effects of aldosterone on intracellular pH in vascular smooth muscle cells. Biochem Biophys Res Commun 223:181-186.

Wehling M (1997) Specific, nongenomic actions of steroid hormones. Annu Rev Physiol 59:365-393.

Wildgruber R, Reil G, Drews O, Parlar H, Gorg A (2002) Web-based two-dimensional database of Saccharomyces cerevisiae proteins using immobilized pH gradients from pH 6 to pH 12 and matrix-assisted laser desorption/ionization-time of flight mass spectrometry. Proteomics 2:727-732.

Widmann C, Gibson S, Jarpe MB, Johnson GL (1999) Mitogen-activated protein kinase: conservation of a three-kinase module from yeast to human. Physiol Rev 79:143-180.

Wilkins MR, Sanchez JC, Gooley AA, Appel RD, Humphery-Smith I, Hochstrasser DF, Williams KL (1996) Progress with proteome projects: why all proteins expressed by a genome should be identified and how to do it. Biotechnol Genet Eng Rev 13:19-50.

Williams GH, Fisher ND (1997) Genetic approach to diagnostic and therapeutic decisions in human hypertension. Curr Opin Nephrol Hypertens 6:199-204.

Wilm M, Mann M (1996) Analytical properties of the nanoelectrospray ion source. Anal Chem 68:1-8.

Wilm M, Shevchenko A, Houthaeve T, Breit S, Schweigerer L, Fotsis T, Mann M (1996) Femtomole sequencing of proteins from polyacrylamide gels by nano-electrospray mass spectrometry. Nature 379:466-469.

Won M, Park SK, Hoe KL, Jang YJ, Chung KS, Kim DU, Kim HB, Yoo HS (2001) Rkp1/Cpc2, a fission yeast RACK1 homolog, is involved in actin cytoskeleton organization through protein kinase C, Pck2, signaling. Biochem Biophys Res Commun 282:10-15.

Wood V, Gwilliam R, Rajandream MA, Lyne M, Lyne R, Stewart A, Sgouros J, Peat N, Hayles J, Baker S, Basham D, Bowman S, Brooks K, Brown D, Brown S, Chillingworth T, Churcher C, Collins M, Connor R, Cronin A, Davis P, Feltwell T, Fraser A, Gentles S, Goble A, Hamlin N, Harris D, Hidalgo J, Hodgson G, Holroyd S, Hornsby T, Howarth S, Huckle EJ, Hunt S, Jagels K, James K, Jones L, Jones M, Leather S, McDonald S, McLean J, Mooney P, Moule S,

Mungall K, Murphy L, Niblett D, Odell C, Oliver K, O'Neil S, Pearson D, Quail MA, Rabbinowitsch E, Rutherford K, Rutter S, Saunders D, Seeger K, Sharp S, Skelton J, Simmonds M, Squares R, Squares S, Stevens K, Taylor K, Taylor RG, Tivey A, Walsh S, Warren T, Whitehead S, Woodward J, Volckaert G, Aert R, Robben J, Grymonprez B, Weltjens I, Vanstreels E, Rieger M, Schafer M, Muller-Auer S, Gabel C, Fuchs M, Dusterhoft A, Fritzc C, Holzer E, Moestl D, Hilbert H, Borzym K, Langer I, Beck A, Lehrach H, Reinhardt R, Pohl TM, Eger P, Zimmermann W, Wedler H, Wambutt R, Purnelle B, Goffeau A, Cadieu E, Dreano S, Gloux S, et al. (2002) The genome sequence of Schizosaccharomyces pombe. Nature 415:871-880.

Xiao B, Smerdon SJ, Jones DH, Dodson GG, Soneji Y, Aitken A, Gamblin SJ (1995) Structure of a 14-3-3 protein and implications for coordination of multiple signalling pathways. Nature 376:188-191.

Yaffe MB, Rittinger K, Volinia S, Caron PR, Aitken A, Leffers H, Gamblin SJ, Smerdon SJ, Cantley LC (1997) The structural basis for 14-3-3:phosphopeptide binding specificity. Cell 91:961-971.

Yang J, Liu X, Bhalla K, Kim CN, Ibrado AM, Cai J, Peng TI, Jones DP, Wang X (1997) Prevention of apoptosis by Bcl-2: release of cytochrome c from mitochondria blocked. Science 275:1129-1132.

Yasuda G, Shionoiri H, Hayashi S, Umemura S, Ikeda Y, Ishii M (1993) Cushing's disease: evaluation of mineralocorticoid-induced hypertension. Intern Med 32:784-788.

Yates JR, 3rd (1998) Mass spectrometry and the age of the proteome. J Mass Spectrom 33:1-19.

Yonezawa N, Nishida E, Sakai H (1985) pH control of actin polymerization by cofilin. J Biol Chem 260:14410-14412.

Young M, Fullerton M, Dilley R, Funder J (1994) Mineralocorticoids, hypertension, and cardiac fibrosis. J Clin Invest 93:2578-2583

Young MJ, Funder JW (2002) Mineralocorticoid receptors and pathophysiological roles for aldosterone in the cardiovascular system. J Hypertens 20:1465-1468.

Zeng Y, Piwnica-Worms H (1999) DNA damage and replication checkpoints in fission yeast require nuclear exclusion of the Cdc25 phosphatase via 14-3-3 binding. Mol Cell Biol 19:7410-7419.

Zhou BB, Elledge SJ (2000) The DNA damage response: putting checkpoints in perspective. Nature 408:433-439.

Appendix

A. Publications resulting from this work

i) Manuscripts

1. "Proteome analysis of *Schizosaccharomyces pombe* by two-dimensional gel electrophoresis and mass spectrometry"
   Hwang KH, Böhmer S, Carapito C, Leize E, Van Dorsselaer A, Bernhardt R,
   Proteomics, Vol. 6, Issue.14, pp. 4115–4129, (2006)

2. "Analysis of mineralocorticoid receptor independent effects of 11-deoxycorticosterone on the protein patterns in *Schizosaccharomyces pombe*"
   Hwang KH, Böhmer S, Carapito C, Leize E, Van Dorsselaer A, Bernhardt R,
   in preparation

B. Contributions to international meetings

i) Presentations

1. Seminar of the European Graduiertenkolleg 532 "Physical Methods for the Structural Investigation of New Materials"
   Achern, in Germany, 4th December 2003
   „Analysis of Deoxycorticosterone (DOC) dependent differential protein patterns analysed by using 2D-Electrophoresis"
   Hwang KH

2. International Conference of the European Graduiertenkolleg 532 "Physical Methods for the Structural Investigation of New Materials"
   Saarbrücken, in Germany, 12th November 2004
   „Proteomics in *Schizosaccharomyces pombe*; Analysis of 11-deoxycorticosterone (DOC) and aldosterone dependent differential protein patterns"
   Hwang KH, Böhmer S, Carapito C, Leize E, Van Dorsselaer A, Bernhardt R

ii) Poster

1   International Conference of the European Graduiertenkolleg 532 "Physical Methods for the Structural Investigation of New Materials"

    Saarbrücken, in Germany, 11th-12th November 2004

    „Proteomics in *Schizosaccharomyces pombe*; Analysis of 11-deoxycorticosterone (DOC) and aldosterone dependent differential protein patterns"

    <u>Hwang KH</u>, Böhmer S, Carapito C, Leize E, Van Dorsselaer A, Bernhardt R

2   Conference for Biotechnology, BioPerspectives 2005

    Rhein-Main-Hallen, Wiesbaden, Germany, 10.05. - 12.05.2005

    „Proteomics in *Schizosaccaromyces pombe*; Analysis of 11-deoxycorticosterone (DOC) and aldosterone dependent differential protein patterns"

    <u>Hwang KH</u>, Böhmer S, Carapito C, Leize E, Van Dorsselaer A, Bernhardt R

3   2nd Summer-School in Proteomic Basics

    Kloster Neustift, Brixen/Bressalone, Süd-Tirol, Italien, 31.07. - 06.08.2005

    „Proteomics in *Schizosaccaromyces pombe*; Analysis of 11-deoxycorticosterone (DOC) and aldosterone dependent differential protein patterns"

    <u>Hwang KH</u>, Böhmer S, Carapito C, Leize E, Van Dorsselaer A, Bernhardt R

C. Protein marker composition
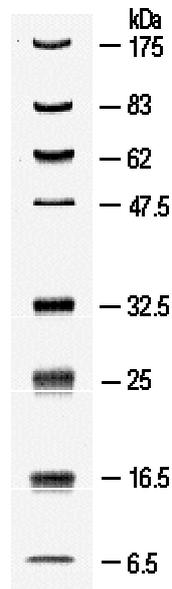
10-20% SDS-PAGE

Effective Size Range: 6 kDa to 175 kDa

Protein	Source	Mr (kDa)
MBP-β-galactosidase	*E.coli*	175.0
MBP-paramyosin	*E.coli*	83.0
MBP-CBD	*E.coli*	62.0
Aldolase	rabbit muscle	47.5
Triosephosphate isomerase	*E.coli*	32.5
β-Lactoglobulin A	bovine milk	25.0
Lysozyme	chicken egg white	16.5
Aprotinin	bovine lung	6.5

Concentration: 0.1 mg/ml to 0.2 mg/ml

Composition of the used pre-stained SDS-gelelectrophoresis protein marker (New England BioLabs)

D. Stock solution for EMM Medium

All Stock solution would autoclave und stored at 4°C.

Salt Stock (x50)		
Amount [g/L]	Contents	Final Concentration
52.5	$MgCl_2 \cdot 6H_2O$	0.26 M
0.735	$CaCl_2 \cdot 2H_2O$	4.99 mM
50.0	KCl	0.67 M
2.0	Na_2SO_4	14.10 mM

Vitamin Stock (x1000)		
Amount [g/L]	Contents	Final Concentration
1.0	Na Pantothenate	4.20 mM
10.0	Nicotinic Acid	81.20 mM
10.0	Inositol	55.50 mM
10.0	Biotin	40.80 μM

Mineral Stock (x10,000)		
Amount [g/L]	Contents	Final Concentration
5.0	H_3BO_3	80.90 mM
4.0	$MnSO_4$	23.70 mM
4.0	$ZnSO_4 \cdot 7H_2O$	13.90 mM
2.0	$FeCl_2 \cdot 6H_2O$	7.40 mM
0.4	H2MOO4 H2O	2.47 mM
1.0	KI	6.02 mM
0.4	$CuSO_4 \cdot 5H_2O$	1.60 mM
10.0	Citric Acid	47.60 mM

Appendix E List of identified *S. pombe* proteins by MALDI-TOF-MS and/or nanoLC-MS/MS (only in the 3-10 *pI* range) (Hwang *et al.,* 2006)

Protein No.[a]	Spot No.[a]	Entry Name[b]	Protein Name[b]	Swiss-Prot Accession Number[b]	identified by	Sequence coverage[c]	Number of peptides[d]	Error in ppm[e]	Theoretical[f] MW (kDa)	pI	Gel (3-10) – estimated[g] MW (kDa)	pI
1	214	2ABA_SCHPO	Protein phosphatase PP2A regulatory subunit B	Q12702	nanoLC-MS/MS	29%	11	46	52.8	5.41	54.0	5.49
2	40	6PGD_SCHPO	Fragment of the 6-phosphogluconate dehydrogenase. decarboxylating	P78812	MALDI-TOF-MS	20%	9	25	53.7	6.73	22.1	5.31
3	172	6PGD_SCHPO	6-phosphogluconate dehydrogenase. decarboxylating	P78812	MALDI-TOF-MS nanoLC-MS/MS	46% 29%	23 12	26 53	53.7	6.73	41.3	6.69
4	228	6PGD_SCHPO	6-phosphogluconate dehydrogenase. decarboxylating	P78812	MALDI-TOF-MS nanoLC-MS/MS	41% 11%	22 5	21 34	53.7	6.73	49.0	6.99
5	235	ACH1_SCHPO	Acetyl-CoA hydrolase	Q9UUJ9	MALDI-TOF-MS nanoLC-MS/MS	26% 13%	14 6	12 109	57.9	6.35	59.0	6.93
6	259	ACON_SCHPO	Aconitate hydratase. mitochondrial [Precursor]	O13966	MALDI-TOF-MS	28%	25	21	84.9	8.08	31.2	8.89
7	134	ACT_SCHPO	Actin	P10989	MALDI-TOF-MS nanoLC-MS/MS	44% 50%	19 15	19 56	41.8	5.31	39.3	5.19
8	146	ACT_SCHPO	Actin	P10989	MALDI-TOF-MS	31%	11	14	41.8	5.31	43.3	5.54
9	148	ACT_SCHPO	Actin	P10989	MALDI-TOF-MS nanoLC-MS/MS	50% 32%	23 11	18 86	41.8	5.31	40.3	5.64
10	18	ADH_SCHPO	Alcohol dehydrogenase	P00332	nanoLC-MS/MS	20%	5	77	37.4	6.46	14.2	5.82
11	68	ADH_SCHPO	Alcohol dehydrogenase	P00332	nanoLC-MS/MS	18%	6	92	37.4	6.46	19.9	8.88
12	186	ADH_SCHPO	Alcohol dehydrogenase	P00332	MALDI-TOF-MS	59%	18	9	37.4	6.46	38.0	6.88
13	195	ADH_SCHPO	Alcohol dehydrogenase	P00332	MALDI-TOF-MS nanoLC-MS/MS	40% 28%	14 9	17 41	37.4	6.46	35.3	7.72
14	94	ALF_SCHPO	Fructose-bisphosphate aldolase	P36580	MALDI-TOF-MS	35%	9	8	39.6	5.92	32.5	5.77
15	98	ALF_SCHPO	Fructose-bisphosphate aldolase	P36580	MALDI-TOF-MS	30%	6	21	39.6	5.92	31.5	6.08
16	163	ALF_SCHPO	Fructose-bisphosphate aldolase	P36580	MALDI-TOF-MS	39%	9	10	39.6	5.92	39.3	6.02
17	166	ALF_SCHPO	Fructose-bisphosphate aldolase	P36580	MALDI-TOF-MS	41%	10	19	39.6	5.92	38.3	6.20
18	167	ALF_SCHPO	Fructose-bisphosphate aldolase	P36580	MALDI-TOF-MS	65%	18	8	39.6	5.92	39.3	6.28
19	178	ALF_SCHPO	Fructose-bisphosphate aldolase	P36580	MALDI-TOF-MS	39%	9	11	39.6	5.92	34.8	6.45
20	266	ALF_SCHPO	Fructose-bisphosphate aldolase	P36580	MALDI-TOF-MS nanoLC-MS/MS	55% 6%	15 2	20 8	39.6	5.92	39.3	6.11
21	267	ALF_SCHPO	Fructose-bisphosphate aldolase	P36580	MALDI-TOF-MS nanoLC-MS/MS	33% 18%	8 5	21 27	39.6	5.92	31.5	6.20
22	105	AROF_SCHPO	Putative phospho-2-dehydro-3-deoxyheptonate aldolase	Q09755	nanoLC-MS/MS	12%	3	80	39.8	6.31	26.9	6.59
23	31	ATPA_SCHPO	ATP synthase alpha chain. mitochondrial [Precursor]	P24487	nanoLC-MS/MS	6%	3	81	58.6	9.18	16.3	8.80
24	132	ATPB_SCHPO	ATP synthase beta chain. mitochondrial [Precursor]	P22068	nanoLC-MS/MS	6%	3	49	56.9	5.72	34.9	5.16
25	206	ATPB_SCHPO	ATP synthase beta chain. mitochondrial [Precursor]	P22068	MALDI-TOF-MS nanoLC-MS/MS	51% 26%	22 9	16 43	56.9	5.72	48.4	4.99
26	189	BGL2_SCHPO	Glucan 1.3-beta-glucosidase [Precursor]	O13990	MALDI-TOF-MS nanoLC-MS/MS	63% 23%	13 11	14 135	35.4	6.35	39.9	6.95
27	7	NACB_SCHPO	Nascent polypeptide-associated complex subunit beta	Q92371	MALDI-TOF-MS	64%	8	23	16.2	5.95	16.3	4.20
28	256	BUT2_SCHPO	Uba3-binding protein but2	P87167	nanoLC-MS/MS	5%	3	21	43.6	9.13	145.9	4.50
29	190	CAP_SCHPO	Adenylyl cyclase-associated protein	P36621	nanoLC-MS/MS	5%	2	39	60.2	6.39	43.1	6.89

Appendix E continued

Protein No.	Spot No.[a)]	Entry Name [b)]	Protein Name [b)]	Swiss-Prot Accession Number [b)]	identified by	Sequence coverage [c)]	Number of peptides[d)]	Error in ppm [e)]	Theoretical [f)]		Gel (3-10) – estimated [g)]	
									MW (kDa)	p*I*	MW (kDa)	p*I*
30	189	CISY_SCHPO	Probable citrate synthase. mitochondrial [Precursor]	Q10306	MALDI-TOF-MS nanoLC-MS/MS	30% 22%	13 12	15 29	53.0	7.75	39.9	6.95
31	190	CISY_SCHPO	Probable citrate synthase. mitochondrial [Precursor]	Q10306	MALDI-TOF-MS nanoLC-MS/MS	43% 42%	22 20	16 34	53.0	7.75	43.1	6.89
32	213	CPGL_SCHPO	Glutamate carboxypeptidase-like protein	Q9P6I2	MALDI-TOF-MS nanoLC-MS/MS	40% 37%	19 15	28 39	52.6	5.27	53.2	5.36
33	78	PPID_SCHPO	40 kDa peptidyl-prolyl cis-trans isomerase	Q11004	MALDI-TOF-MS nanoLC-MS/MS	23% 35%	9 10	9 42	40.2	8.05	26.6	5.10
34	29	CYPH_SCHPO	Peptidyl-prolyl cis-trans isomerase	P18253	MALDI-TOF-MS nanoLC-MS/MS	57% 45%	12 9	8 58	17.4	8.81	14.4	8.71
35	30	CYPH_SCHPO	Peptidyl-prolyl cis-trans isomerase	P18253	MALDI-TOF-MS nanoLC-MS/MS	57% 28%	10 5	17 56	17.4	8.81	14.2	8.81
36	171	CYSD_SCHPO	O-acetylhomoserine (Thiol)-lyase	O13326	MALDI-TOF-MS nanoLC-MS/MS	39% 11%	14 5	9 35	46.4	6.05	43.5	6.40
37	221	DAK1_SCHPO	Dihydroxyacetone kinase 1	O13902	MALDI-TOF-MS nanoLC-MS/MS	35% 31%	24 17	10 105	62.3	5.93	52.7	5.98
38	222	DAK1_SCHPO	Dihydroxyacetone kinase 1	O13902	MALDI-TOF-MS nanoLC-MS/MS	27% 7%	16 4	20 24	62.3	5.93	53.3	5.98
39	249	DAK2_SCHPO	Dihydroxyacetone kinase 2	O74215	nanoLC-MS/MS	16%	7	87	62.1	5.50	61.6	5.57
40	71	DHE4_SCHPO	NADP-specific glutamate dehydrogenase	P78804	nanoLC-MS/MS	9%	3	42	48.8	7.14	26.1	4.19
41	221	DYR_SCHPO	Dihydropteridine reductase	P36591	nanoLC-MS/MS	8%	3	96	51.5	6.15	52.7	5.98
42	61	EF1A1_SCHPO	Elongation factor 1-alpha-A	P50522	MALDI-TOF-MS	21%	9	15	49.7	9.12	20.1	7.35
43	126	EF1A1_SCHPO	Elongation factor 1-alpha-A	P50522	MALDI-TOF-MS nanoLC-MS/MS	29% 21%	13 10	12 32	49.7	9.12	32.2	9.34
44	205	EF1A1_SCHPO	Elongation factor 1-alpha-A	P50522	MALDI-TOF-MS	43%	18	15	49.7	9.12	37.9	8.75
45	260	EF1A1_SCHPO	Elongation factor 1-alpha-A	P50522	MALDI-TOF-MS	35%	14	17	49.7	9.12	39.9	8.88
46	28	EF1A2_SCHPO	Elongation factor 1-alpha-B/C	Q10119	nanoLC-MS/MS	18%	6	32	49.7	9.12	14.4	8.55
47	30	EF1A2_SCHPO	Elongation factor 1-alpha-B/C	Q10119	nanoLC-MS/MS	16%	5	46	49.7	9.12	14.2	8.81
48	61	EF1A2_SCHPO	Fragment of the elongation factor 1-alpha-B/C	Q10119	MALDI-TOF-MS	33%	11	23	49.7	9.12	20.1	7.35
49	115	EF1A2_SCHPO	Elongation factor 1-alpha-B/C	Q10119	nanoLC-MS/MS	20%	9	39	49.7	9.12	25.9	7.91
50	261	EF1A2_SCHPO	Elongation factor 1-alpha-B/C	Q10119	MALDI-TOF-MS	20%	6	10	49.7	9.12	40.2	8.88
51	50	ENO11_SCHPO	Enolase 1-1	P40370	MALDI-TOF-MS	24%	9	5	47.4	6.23	22.5	6.03
52	63	ENO11_SCHPO	N-terminal fragment of the enolase 1-1	P40370	MALDI-TOF-MS nanoLC-MS/MS	30% 20%	14 9	19 69	47.4	6.23	21.6	8.17
53	79	ENO11_SCHPO	Enolase 1-1	P40370	MALDI-TOF-MS nanoLC-MS/MS	15% 31%	7 9	14 24	47.4	6.23	24.4	5.04
54	84	ENO11_SCHPO	C-terminal fragment of the enolase 1-1	P40370	MALDI-TOF-MS	29%	11	15	47.4	6.23	25.5	5.70
55	85	ENO11_SCHPO	Enolase 1-1	P40370	MALDI-TOF-MS nanoLC-MS/MS	39% 36%	15 10	13 44	47.4	6.23	31.2	5.60
56	92	ENO11_SCHPO	Enolase 1-1	P40370	MALDI-TOF-MS	51%	23	15	47.4	6.23	27.9	5.84
57	93	ENO11_SCHPO	Enolase 1-1	P40370	MALDI-TOF-MS nanoLC-MS/MS	31% 22%	12 8	21 30	47.4	6.23	25.4	5.84
58	100	ENO11_SCHPO	Enolase 1-1	P40370	MALDI-TOF-MS nanoLC-MS/MS	23% 18%	10 7	10 21	47.4	6.23	24.1	5.86
59	103	ENO11_SCHPO	Enolase 1-1	P40370	MALDI-TOF-MS nanoLC-MS/MS	37% 29%	14 11	22 79	47.4	6.23	23.8	6.51

Appendix E continued

Protein No.	Spot No.[a]	Entry Name [b]	Protein Name [b]	Swiss-Prot Accession Number [b]	identified by	Sequence coverage [c]	Number of peptides[d]	Error in ppm [e]	Theoretical [f] MW (kDa)	pI	Gel (3-10) – estimated [g] MW (kDa)	pI
60	107	ENO11_SCHPO	N-terminal fragment of the Enolase 1-1	P40370	**MALDI-TOF-MS**	25%	13	13	47.4	6.23	29.1	6.76
61	108	ENO11_SCHPO	N-terminal fragment of the Enolase 1-1	P40370	**MALDI-TOF-MS**	25%	11	19	47.4	6.23	27.8	6.80
62	112	ENO11_SCHPO	Enolase 1-1	P40370	**MALDI-TOF-MS**	17%	8	4	47.4	6.23	25.3	7.27
63	168	ENO11_SCHPO	Enolase 1-1	P40370	**MALDI-TOF-MS**	38%	16	10	47.4	6.23	38.6	6.27
64	192	ENO11_SCHPO	Enolase 1-1	P40370	**MALDI-TOF-MS**	38%	11	11	47.4	6.23	45.8	6.10
65	193	ENO11_SCHPO	Enolase 1-1	P40370	**MALDI-TOF-MS**	50%	18	25	47.4	6.23	38.6	7.59
66	87	ETFA_SCHPO	Probable electron transfer flavoprotein alpha-subunit. mitochondrial [Precursor]	P78790	**nanoLC-MS/MS**	6%	3	86	36.4	7.03	32.8	5.54
67	25	G3P1_SCHPO	Glyceraldehyde 3-phosphate dehydrogenase 1	P78958	**MALDI-TOF-MS**	18%	5	14	35.9	6.24	12.5	6.96
68	31	G3P1_SCHPO	Glyceraldehyde 3-phosphate dehydrogenase 1	P78958	**MALDI-TOF-MS** **nanoLC-MS/MS**	31% 21%	12 17	17 89	35.9	6.24	16.3	8.80
69	47	G3P1_SCHPO	Glyceraldehyde 3-phosphate dehydrogenase 1	P78958	**MALDI-TOF-MS**	32%	9	15	35.9	6.24	18.7	5.78
70	58	G3P1_SCHPO	C-terminal fragment of the Glyceraldehyde 3-phosphate dehydrogenase 1	P78958	**MALDI-TOF-MS**	34%	13	23	35.9	6.24	20.5	7.03
71	59	G3P1_SCHPO	Glyceraldehyde 3-phosphate dehydrogenase 1	P78958	**MALDI-TOF-MS** **nanoLC-MS/MS**	26% 16%	10 5	16 41	35.9	6.24	21.1	7.15
72	60	G3P1_SCHPO	Glyceraldehyde 3-phosphate dehydrogenase 1	P78958	**nanoLC-MS/MS**	7%	2	52	35.9	6.24	21.5	7.33
73	86	G3P1_SCHPO	Glyceraldehyde 3-phosphate dehydrogenase 1	P78958	**MALDI-TOF-MS** **nanoLC-MS/MS**	59% 40%	20 11	16 33	35.9	6.24	32.9	5.40
74	91	G3P1_SCHPO	Glyceraldehyde 3-phosphate dehydrogenase 1	P78958	**MALDI-TOF-MS**	54%	15	11	35.9	6.24	30.0	5.76
75	111	G3P1_SCHPO	Glyceraldehyde 3-phosphate dehydrogenase 1	P78958	**MALDI-TOF-MS**	40%	13	14	35.9	6.24	24.7	7.22
76	115	G3P1_SCHPO	Glyceraldehyde 3-phosphate dehydrogenase 1 (phosphorylating)	P78958	**nanoLC-MS/MS**	39%	11	39	35.9	6.24	25.9	7.91
77	116	G3P1_SCHPO	Glyceraldehyde 3-phosphate dehydrogenase 1 (phosphorylating)	P78958	**MALDI-TOF-MS**	42%	15	14	35.9	6.24	25.2	8.07
78	117	G3P1_SCHPO	Glyceraldehyde 3-phosphate dehydrogenase 1	P78958	**MALDI-TOF-MS** **nanoLC-MS/MS**	35% 38%	13 13	16 98	35.9	6.24	26.3	8.07
79	118	G3P1_SCHPO	Glyceraldehyde 3-phosphate dehydrogenase 1 (phosphorylating)	P78958	**MALDI-TOF-MS** **nanoLC-MS/MS**	40% 39%	12 12	18 11	35.9	6.24	25.4	8.17
80	119	G3P1_SCHPO	Glyceraldehyde 3-phosphate dehydrogenase 1 (phosphorylating)	P78958	**MALDI-TOF-MS** **nanoLC-MS/MS**	35% 35%	13 11	18 11	35.9	6.24	26.4	8.32
81	123	G3P1_SCHPO	Glyceraldehyde 3-phosphate dehydrogenase 1	P78958	**MALDI-TOF-MS** **nanoLC-MS/MS**	47% 46%	16 14	12 67	35.9	6.24	27.7	8.75
82	124	G3P1_SCHPO	Glyceraldehyde 3-phosphate dehydrogenase 1	P78958	**MALDI-TOF-MS** **nanoLC-MS/MS**	50% 35%	16 13	10 25	35.9	6.24	28.0	9.26
83	183	G3P1_SCHPO	Glyceraldehyde 3-phosphate dehydrogenase 1	P78958	**MALDI-TOF-MS**	63%	22	20	35.9	6.24	36.3	6.89
84	27	G3P2_SCHPO	Glyceraldehyde-3-phosphate dehydrogenase 2	O43026	**MALDI-TOF-MS** **nanoLC-MS/MS**	26% 21%	10 7	21 10	35.7	7.69	16.1	8.24
85	55	G3P2_SCHPO	Glyceraldehyde-3-phosphate dehydrogenase 2	O43026	**MALDI-TOF-MS**	26%	8	11	35.7	7.69	22.7	6.71
86	120	G3P2_SCHPO	Glyceraldehyde-3-phosphate dehydrogenase 2	O43026	**nanoLC-MS/MS**	4%	2	44	35.7	7.69	30.9	8.20
87	198	G3P2_SCHPO	Glyceraldehyde-3-phosphate dehydrogenase 2	O43026	**MALDI-TOF-MS** **nanoLC-MS/MS**	62% 38%	22 12	10 27	35.7	7.69	35.7	8.20
88	104	G6PI_SCHPO	Glucose-6-phosphate isomerase	P78917	**MALDI-TOF-MS** **nanoLC-MS/MS**	33% 23%	21 12	14 71	60.9	5.97	25.2	6.64
89	160	GBLP_SCHPO	Guanine nucleotide-binding protein beta subunit-like protein	Q10281	**nanoLC-MS/MS**	20%	4	39	34.9	5.43	41.2	5.88

Appendix E continued

Protein No.	Spot No.[a]	Entry Name [b]	Protein Name [b]	Swiss-Prot Accession Number [b]	identified by	Sequence coverage [c]	Number of peptides[d]	Error in ppm [e]	Theoretical [f]		Gel (3-10) – estimated [g]	
									MW (kDa)	p*I*	MW (kDa)	p*I*
90	199	GCST_SCHPO	Probable aminomethyltransferase. mitochondrial [Precursor]	O14110	**MALDI-TOF-MS** **nanoLC-MS/MS**	44% 54%	17 13	19 53	42.4	8.85	43.5	8.27
91	67	GLYD_SCHPO	C-terminal fragment of the probable serine hydroxymethyltransferase. cytosolic	O13972	**MALDI-TOF-MS** **nanoLC-MS/MS**	19% 19%	8 10	22 113	51.9	7.66	19.8	8.65
92	234	GLYD_SCHPO	Probable serine hydroxymethyltransferase. cytosolic	O13972	**MALDI-TOF-MS** **nanoLC-MS/MS**	40% 45%	20 22	14 67	51.9	7.66	48.1	7.68
93	103	GNTK_SCHPO	Probable gluconokinase	Q10242	**nanoLC-MS/MS**	18%	3	83	21.6	6.31	23.8	6.51
94	137	GPD1_SCHPO	Glycerol-3-phosphate dehydrogenase [NAD+] 1	P21696	**MALDI-TOF-MS**	66%	24	20	42.0	5.25	42.7	5.19
95	137	GPD2_SCHPO	Glycerol-3-phosphate dehydrogenase [NAD+] 2	Q09845	**nanoLC-MS/MS**	52%	19	37	40.9	7.91	42.7	5.19
96	65	GPX1_SCHPO	Glutathione peroxidase	O59858	**MALDI-TOF-MS** **nanoLC-MS/MS**	63% 46%	10 7	5 69	18.1	8.35	18.2	8.28
97	66	GPX1_SCHPO	Glutathione peroxidase	O59858	**MALDI-TOF-MS**	36%	8	30	18.1	8.35	18.1	8.59
98	24	GRPE_SCHPO	GrpE protein homolog. mitochondrial [Precursor]	O43047	**nanoLC-MS/MS**	33%	5	28	25.3	7.73	15.8	6.75
99	231	GSHR_SCHPO	Glutathione reductase	P78965	**MALDI-TOF-MS** **nanoLC-MS/MS**	22% 32%	9 12	6 46	50.0	6.90	53.6	7.54
100	17	H2B1_SCHPO	Histone H2B-alpha	P04913	**nanoLC-MS/MS**	9%	2	96	13.7	10.07	13.6	5.76
101	147	HOSM_SCHPO	Homocitrate synthase. mitochondrial [Precursor]	Q9Y823	**MALDI-TOF-MS** **nanoLC-MS/MS**	50% 19%	21 7	18 59	46.3	5.69	45.3	5.56
102	1	HSP16_SCHPO	Heat shock protein 16	O14368	**nanoLC-MS/MS**	20%	2	41	16.0	5.72	15.8	5.37
103	250	HSP71_SCHPO	Probable heat shock protein ssa1	Q10265	**nanoLC-MS/MS**	34%	21	56	70.0	5.13	66.9	5.33
104	265	HSP71_SCHPO	Probable heat shock protein ssa1	Q10265	**MALDI-TOF-MS**	21%	11	37	70.0	5.13	42.3	5.55
105	145	HSP72_SCHPO	Probable heat shock protein ssa2	O59855	**MALDI-TOF-MS** **nanoLC-MS/MS**	38% 26%	27 18	14 52	70.1	5.13	44.3	5.45
106	146	HSP72_SCHPO	Probable heat shock protein ssa2	O59855	**MALDI-TOF-MS** **nanoLC-MS/MS**	38% 28%	25 17	25 35	70.1	5.13	43.3	5.54
107	214	HSP72_SCHPO	Probable heat shock protein ssa2	O59855	**MALDI-TOF-MS** **nanoLC-MS/MS**	45% 32%	31 22	17 37	70.1	5.13	54.0	5.49
108	250	HSP72_SCHPO	Probable heat shock protein ssa2	O59855	**MALDI-TOF-MS** **nanoLC-MS/MS**	55% 35%	32 23	17 56	70.1	5.13	66.9	5.33
109	251	HSP72_SCHPO	Probable heat shock protein ssa2	O59855	**MALDI-TOF-MS**	25%	14	24	70.1	5.13	72.1	5.13
110	262	HSP72_SCHPO	Probable heat shock protein ssa2	O59855	**MALDI-TOF-MS** **nanoLC-MS/MS**	40% 27%	29 19	10 36	70.1	5.13	48.5	5.66
111	147	HSP75_SCHPO	Heat shock protein sks2	Q10284	**nanoLC-MS/MS**	23%	13	32	67.2	5.82	45.3	5.56
112	249	HSP75_SCHPO	Heat shock protein sks2	Q10284	**MALDI-TOF-MS** **nanoLC-MS/MS**	28% 29%	17 12	17 93	67.2	5.82	61.6	5.57
113	208	HSP90_SCHPO	Heat shock protein 90 homolog	P41887	**MALDI-TOF-MS** **nanoLC-MS/MS**	29% 10%	22 7	21 43	80.6	4.89	54.5	5.16
114	209	HSP90_SCHPO	Heat shock protein 90 homolog	P41887	**MALDI-TOF-MS** **nanoLC-MS/MS**	34% 9%	25 6	10 41	80.6	4.89	55.9	5.17
115	242	HSP90_SCHPO	Heat shock protein 90 homolog	P41887	**nanoLC-MS/MS**	6%	4	17	80.6	4.89	69.0	5.63
116	252	HSP90_SCHPO	Heat shock protein 90 homolog	P41887	**MALDI-TOF-MS** **nanoLC-MS/MS**	31% 23%	23 17	25 53	80.6	4.89	80.3	4.75
117	162	HXK2_SCHPO	Hexokinase 2	P50521	**MALDI-TOF-MS** **nanoLC-MS/MS**	35% 45%	17 18	11 37	50.9	5.89	43.8	5.87
118	124	IDH1_SCHPO	Isocitrate dehydrogenase (NAD) subunit 1, mitochondrial [Precursor]	O13696	**nanoLC-MS/MS**	9%	3	19	38.8	7.71	28.0	9.26
119	202	IDHP_SCHPO	Probable isocitrate dehydrogenase (NADP), mitochondrial [Precursor]	O14254	**MALDI-TOF-MS** **nanoLC-MS/MS**	54% 39%	26 18	16 98	47.3	8.86	43.4	8.65

Appendix E continued

Protein No.	Spot No.[a]	Entry Name [b]	Protein Name [b]	Swiss-Prot Accession Number [b]	identified by	Sequence coverage [c]	Number of peptides[d]	Error in ppm [e]	Theoretical [f] MW (kDa)	pI	Gel (3-10) – estimated [g] MW (kDa)	pI
120	46	ILV5_SCHPO	Probable ketol-acid reductoisomerase. mitochondrial [Precursor]	P78827	MALDI-TOF-MS	30%	12	13	45.2	9.47	18.3	5.67
121	118	ILV5_SCHPO	Probable ketol-acid reductoisomerase. mitochondrial [Precursor]	P78827	MALDI-TOF-MS nanoLC-MS/MS	41% 41%	15 15	16 14	45.2	9.47	25.4	8.17
122	121	ILV5_SCHPO	Probable ketol-acid reductoisomerase. mitochondrial [Precursor]	P78827	MALDI-TOF-MS nanoLC-MS/MS	17% 29%	6 10	18 30	45.2	9.47	26.0	8.61
123	133	ILV5_SCHPO	Probable ketol-acid reductoisomerase. mitochondrial [Precursor]	P78827	MALDI-TOF-MS	65%	30	22	45.2	9.47	38.8	5.25
124	193	ILV5_SCHPO	Probable ketol-acid reductoisomerase. mitochondrial [Precursor]	P78827	MALDI-TOF-MS nanoLC-MS/MS	64% 53%	28 19	10 91	45.2	9.47	38.6	7.59
125	194	ILV5_SCHPO	Probable ketol-acid reductoisomerase. mitochondrial [Precursor]	P78827	nanoLC-MS/MS	13%	4	21	45.2	9.47	38.6	7.72
126	196	ILV5_SCHPO	Probable ketol-acid reductoisomerase. mitochondrial [Precursor]	P78827	MALDI-TOF-MS nanoLC-MS/MS	59% 53%	28 20	16 41	45.2	9.47	38.9	7.97
127	256	INV1_SCHPO	Invertase [Precursor]	O59852	nanoLC-MS/MS	10%	5	24	64.4	4.94	145.9	4.50
128	101	KAD1_SCHPO	Adenylate kinase	P33075	MALDI-TOF-MS	37%	9	14	24.4	6.14	23.6	5.95
129	48	KAPS_SCHPO	Adenylyl-sulfate kinase	Q9P7G9	MALDI-TOF-MS	42%	8	18	22.7	6.23	22.4	5.83
130	95	KPYK_SCHPO	Pyruvate kinase	Q10208	MALDI-TOF-MS	32%	15	19	55.5	8.18	32.4	5.93
131	119	KPYK_SCHPO	Pyruvate kinase	Q10208	MALDI-TOF-MS nanoLC-MS/MS	26% 21%	20 10	13 19	55.5	8.18	26.4	8.32
132	121	KPYK_SCHPO	Pyruvate kinase	Q10208	MALDI-TOF-MS nanoLC-MS/MS	28% 8%	17 4	17 40	55.5	8.18	26.0	8.61
133	122	KPYK_SCHPO	Pyruvate kinase	Q10208	MALDI-TOF-MS	17%	8	9	55.5	8.18	27.6	8.56
134	123	KPYK_SCHPO	Pyruvate kinase	Q10208	MALDI-TOF-MS nanoLC-MS/MS	28% 26%	17 14	15 58	55.5	8.18	27.7	8.75
135	125	KPYK_SCHPO	Pyruvate kinase	Q10208	MALDI-TOF-MS	21%	9	15	55.5	8.18	26.4	9.55
136	146	KPYK_SCHPO	Pyruvate kinase	Q10208	nanoLC-MS/MS	19%	8	82	55.5	8.18	43.3	5.54
137	75	MAOX_SCHPO	NAD-dependent malic enzyme	P40375	MALDI-TOF-MS nanoLC-MS/MS	30% 10%	21 7	19 40	62.5	5.68	32.0	4.99
138	89	MAOX_SCHPO	NAD-dependent malic enzyme	P40375	MALDI-TOF-MS nanoLC-MS/MS	29% 15%	23 8	12 40	62.5	5.68	33.1	5.30
139	117	MAOX_SCHPO	NAD-dependent malic enzyme	P40375	nanoLC-MS/MS	6%	3	96	62.5	5.68	26.3	8.07
140	218	MAOX_SCHPO	NAD-dependent malic enzyme	P40375	MALDI-TOF-MS nanoLC-MS/MS	43% 21%	29 13	14 48	62.5	5.68	56.1	5.74
141	219	MAOX_SCHPO	NAD-dependent malic enzyme	P40375	MALDI-TOF-MS	38%	27	16	62.5	5.68	50.6	5.83
142	229	MET3_SCHPO	Sulfate adenylyltransferase	P78937	MALDI-TOF-MS nanoLC-MS/MS	49% 16%	25 8	22 62	54.8	6.62	53.0	6.75
143	13	METE_SCHPO	Probable 5-methyltetrahydropteroyltriglutamate--homocysteine methyltransferase	Q9UT19	MALDI-TOF-MS	11%	8	21	85.3	5.99	16.4	5.33
144	233	METE_SCHPO	Probable 5-methyltetrahydropteroyltriglutamate--homocysteine methyltransferase	Q9UT19	MALDI-TOF-MS nanoLC-MS/MS	18% 18%	14 13	23 32	85.3	5.99	61.5	7.60
145	240	METE_SCHPO	Probable 5-methyltetrahydropteroyltriglutamate--homocysteine methyltransferase	Q9UT19	nanoLC-MS/MS	15%	11	93	85.3	5.99	62.3	5.93
146	242	METE_SCHPO	Probable 5-methyltetrahydropteroyltriglutamate--homocysteine methyltransferase	Q9UT19	nanoLC-MS/MS	7%	5	21	85.3	5.99	69.0	5.63
147	263	METE_SCHPO	Probable 5-methyltetrahydropteroyltriglutamate--homocysteine methyltransferase	Q9UT19	MALDI-TOF-MS nanoLC-MS/MS	32% 17%	26 13	18 39	85.3	5.99	80.3	5.76

Appendix E continued

Protein No.	Spot No.[a]	Entry Name [b]	Protein Name [b]	Swiss-Prot Accession Number [b]	identified by	Sequence coverage [c]	Number of peptides[d]	Error in ppm [e]	Theoretical [f]		Gel (3-10) – estimated [g]	
									MW (kDa)	p*I*	MW (kDa)	p*I*
148	148	METK_SCHPO	S-adenosylmethionine synthetase	O60198	MALDI-TOF-MS	18%	8	26	41.8	5.70	40.3	5.64
149	160	METK_SCHPO	S-adenosylmethionine synthetase	O60198	nanoLC-MS/MS	14%	4	42	41.8	5.70	41.2	5.88
150	33	MLO3_SCHPO	Protein mlo3	Q09330	MALDI-TOF-MS nanoLC-MS/MS	74% 29%	18 5	15 96	21.8	10.21	20.5	4.00
151	15	MMF1_SCHPO	Protein mmf1, mitochondrial [Precursor]	O43003	MALDI-TOF-MS	67%	11	18	17.5	9.41	12.4	5.62
152	24	MPG1_SCHPO	Probable mannose-1-phosphate guanyltransferase	O74484	nanoLC-MS/MS	7%	2	21	39.7	6.02	15.8	6.75
153	130	O42873_SCHPO	SPAC3G9.11c protein	O42873	MALDI-TOF-MS nanoLC-MS/MS	27% 26%	15 12	16 54	62.7	5.45	36.6	4.83
154	215	O42873_SCHPO	SPAC3G9.11c protein	O42873	nanoLC-MS/MS	15%	7	69	62.7	5.45	47.6	5.72
155	217	O42873_SCHPO	SPAC3G9.11c protein	O42873	MALDI-TOF-MS nanoLC-MS/MS	49% 22%	25 11	21 71	62.7	5.45	53.2	5.69
156	188	O42888_SCHPO	SPBC8E4.04 protein	O42888	MALDI-TOF-MS	48%	16	18	36.6	6.61	34.9	7.00
157	3	O74887_SCHPO	SPCC576.03c protein	O74887	nanoLC-MS/MS	23%	4	25	21.2	5.37	13.1	5.47
158	82	O74914_SCHPO	SPCC757.03c protein	O74914	MALDI-TOF-MS	39%	10	10	26.7	5.42	24.2	5.42
159	138	O74960_SCHPO	SPCC736.15 protein	O74960	MALDI-TOF-MS nanoLC-MS/MS	40% 32%	17 10	7 45	39.8	5.24	44.5	5.28
160	36	PPIB_SCHPO	Peptidyl-prolyl cis-trans isomerase	O94273	MALDI-TOF-MS	52%	12	27	22.2	5.58	17.8	5.47
161	45	PPIB_SCHPO	Peptidyl-prolyl cis-trans isomerase	O94273	MALDI-TOF-MS	61%	10	16	22.2	5.58	17.7	5.60
162	247	ODO2_SCHPO	Probable dihydrolipoamise succinyltransferase component of 2-oxoglutarate dehydrogenasecomplex. mitochondrial [Precursor]	O94681	MALDI-TOF-MS	36%	16	20	49.0	7.55	58.9	5.54
163	191	ODPA_SCHPO	Pyruvate dehydrogenase E1 component alpha subunit. mitochondrial [Precursor]	Q10489	nanoLC-MS/MS	43%	11	10	45.1	8.34	43.8	6.90
164	77	NACA_SCHPO	Putative nascent polypeptide-associated complex alpha subunit-like protein	P87147	MALDI-TOF-MS nanoLC-MS/MS	64% 72%	12 13	20 90	18.8	5.00	27.1	4.86
165	149	PDC2_SCHPO	Probable pyruvate decarboxylase C1F8.07c	Q92345	nanoLC-MS/MS	14%	7	23	64.8	5.71	42.7	5.65
166	157	PDX1_SCHPO	Probable pyridoxin biosynthesis PDX1-like protein	O14027	MALDI-TOF-MS	58%	30	17	31.4	5.92	33.7	5.82
167	37	PGK_SCHPO	C-terminal fragment of the phosphoglycerate kinase	O60101	MALDI-TOF-MS	21%	7	28	44.0	8.33	20.1	5.40
168	38	PGK_SCHPO	Phosphoglycerate kinase	P60101	MALDI-TOF-MS	41%	17	30	44.0	8.33	20.7	5.40
169	42	PGK_SCHPO	C-terminal fragment of the Phosphoglycerate kinase	O60101	MALDI-TOF-MS	44%	19	21	44.0	8.33	22.5	5.61
170	43	PGK_SCHPO	C-terminal fragment of the Phosphoglycerate kinase	O60101	MALDI-TOF-MS	43%	16	13	44.0	8.33	23.1	5.67
171	68	PGK_SCHPO	Phosphoglycerate kinase	O60101	nanoLC-MS/MS	25%	9	85	44.0	8.33	19.9	8.88
172	133	PGK_SCHPO	Phosphoglycerate kinase	O60101	MALDI-TOF-MS	36%	16	26	44.0	8.33	38.8	5.25
173	194	PGK_SCHPO	Phosphoglycerate kinase	O60101	MALDI-TOF-MS nanoLC-MS/MS	63% 56%	24 21	16 27	44.0	8.33	38.6	7.72
174	200	PGK_SCHPO	Phosphoglycerate kinase	O60101	MALDI-TOF-MS nanoLC-MS/MS	61% 60%	23 23	13 84	44.0	8.33	43.4	8.42
175	201	PGK_SCHPO	Phosphoglycerate kinase	O60101	MALDI-TOF-MS nanoLC-MS/MS	75% 63%	27 24	13 72	44.0	8.33	43.5	8.52
176	203	PGK_SCHPO	Phosphoglycerate kinase	O60101	MALDI-TOF-MS	76%	30	15	44.0	8.33	43.5	8.75
177	204	PGK_SCHPO	Phosphoglycerate kinase	O60101	MALDI-TOF-MS	41%	14	23	44.0	8.33	39.3	8.87

Appendix E continued

Protein No.	Spot No.[a)]	Entry Name [b)]	Protein Name [b)]	Swiss-Prot Accession Number [b)]	identified by	Sequence coverage [c)]	Number of peptides[d)]	Error in ppm [e)]	Theoretical [f)] MW (kDa)	pI	Gel (3-10) – estimated [g)] MW (kDa)	pI
178	63	PIN1_SCHPO	Peptidyl-prolyl cis-trans isomerase pin1	O74448	nanoLC-MS/MS	16%	2	68	19.8	7.92	21.6	8.17
179	255	PLB1_SCHPO	Lysophospholipase 1 [Precursor]	P78854	MALDI-TOF-MS	14%	8	18	67.1	4.74	137.8	4.60
180	23	PMGY_SCHPO	Phosphoglycerate mutase	P36623	MALDI-TOF-MS	47%	8	10	23.8	6.92	14.1	6.71
181	32	PMGY_SCHPO	Phosphoglycerate mutase	P36623	MALDI-TOF-MS nanoLC-MS/MS	61% 55%	17 14	27 84	23.8	6.92	17.2	8.66
182	55	PMGY_SCHPO	Phosphoglycerate mutase	P36623	MALDI-TOF-MS	51%	9	18	23.8	6.92	22.7	6.71
183	64	PMGY_SCHPO	Phosphoglycerate mutase	P36623	MALDI-TOF-MS nanoLC-MS/MS	52% 55%	10 11	26 63	23.8	6.92	19.6	8.13
184	68	PMGY_SCHPO	Phosphoglycerate mutase	P36623	MALDI-TOF-MS nanoLC-MS/MS	66% 56%	18 14	11 108	23.8	6.92	19.9	8.88
185	101	PMGY_SCHPO	Phosphoglycerate mutase	P36623	MALDI-TOF-MS	56%	10	19	23.8	6.92	23.6	5.95
186	113	PMGY_SCHPO	Phosphoglycerate mutase	P36623	MALDI-TOF-MS nanoLC-MS/MS	81% 45%	22 11	22 40	23.8	6.92	23.9	7.26
187	83	PMM_SCHPO	Phosphomannomutase	Q9UTJ2	nanoLC-MS/MS	12%	2	35	29.2	5.25	23.5	5.46
188	90	PNPP_SCHPO	4-nitrophenylphosphatase	Q00472	MALDI-TOF-MS	38%	10	8	32.8	5.58	33.0	5.58
189	220	Q9C0U6_SCHPO	SPCPJ732.02c protein	Q9C0U6	MALDI-TOF-MS nanoLC-MS/MS	23% 28%	12 15	9 77	61.6	5.77	57.3	5.87
190	202	Q9C1X5_SCHPO	SPAP32A8.02 protein	Q9C1X5	nanoLC-MS/MS	7%	2	49	31.8	5.79	43.4	8.65
191	67	Q9P7B4_SCHPO	SPAC521.03 protein	Q9P7B4	nanoLC-MS/MS	16%	4	122	28.1	6.01	19.8	8.65
192	101	Q9P7G7_SCHPO	Ssp1 protein [Fragment]	Q9P7G7	MALDI-TOF-MS	28%	6	24	25.1	5.81	23.6	5.95
193	33	RPA8_SCHPO	DNA-directed RNA polymerase I 17 kDa polypeptide	Q9P7P1	nanoLC-MS/MS	8%	2	56	17.0	6.23	20.5	4.00
194	108	Q9UT36_SCHPO	SPAC824.07 protein	Q9UT36	MALDI-TOF-MS	33%	7	20	28.5	6.41	27.8	6.80
195	122	SOU1_SCHPO	Sorbitol utilization protein sou1	Q9Y6Z9	nanoLC-MS/MS	20%	4	55	27.4	8.61	27.6	8.56
196	20	Q9Y7R8_SCHPO	SPCC306.08c protein	Q9Y7R8	MALDI-TOF-MS	27%	7	18	35.8	8.90	16.5	6.36
197	179	Q9Y7R8_SCHPO	SPCC306.08c protein	Q9Y7R8	nanoLC-MS/MS	14%	4	131	35.8	8.90	34.1	6.57
198	74	RAD24_SCHPO	DNA damage checkpoint protein rad24	P42656	MALDI-TOF-MS nanoLC-MS/MS	53% 56%	15 14	11 68	30.1	4.66	29.4	4.49
199	87	RAD24_SCHPO	DNA damage checkpoint protein rad24	P42656	nanoLC-MS/MS	23%	7	128	30.1	4.66	32.8	5.54
200	144	RAD24_SCHPO	DNA damage checkpoint protein rad24	P42656	nanoLC-MS/MS	30%	8	127	30.1	4.66	32.9	5.46
201	129	RAD25_SCHPO	DNA damage checkpoint protein rad25	P42657	nanoLC-MS/MS	45%	13	40	30.4	4.78	34.1	4.80
202	257	RAD25_SCHPO	DNA damage checkpoint protein rad25	P42657	nanoLC-MS/MS	16%	4	129	30.4	4.78	33.9	4.44
203	34	RL17A_SCHPO	60S ribosomal protein L17-A	O14339	MALDI-TOF-MS	51%	13	19	20.8	10.36	20.2	4.38
204	35	RL17B_SCHPO	60S ribosomal protein L17-B	O59794	MALDI-TOF-MS nanoLC-MS/MS	48% 26%	10 5	14 85	20.8	10.33	21.9	4.53
205	72	RL2_SCHPO	60S ribosomal protein L2	P08093	MALDI-TOF-MS	49%	12	20	27.1	10.86	29.4	4.23
206	9	RL31_SCHPO	60S ribosomal protein L31	Q9URX6	MALDI-TOF-MS	55%	9	13	13.3	10.24	14.1	3.80
207	11	RL36A_SCHPO	60S ribosomal protein L36-A	Q92365	MALDI-TOF-MS	61%	12	20	11.3	11.85	12.4	4.20

Appendix E continued

Protein No.	Spot No.[a]	Entry Name [b]	Protein Name [b]	Swiss-Prot Accession Number [b]	identified by	Sequence coverage [c]	Number of peptides[d]	Error in ppm [e]	Theoretical [f] MW (kDa)	Theoretical [f] pI	Gel (3-10) – estimated [g] MW (kDa)	Gel (3-10) – estimated [g] pI
208	69	RL4A_SCHPO	60S ribosomal protein L4-A	P35679	nanoLC-MS/MS	28%	7	110	39.8	10.78	24.3	4.32
209	12	RL5A_SCHPO	60S ribosomal protein L5-A	P52822	MALDI-TOF-MS	30%	7	18	33.5	9.08	14.2	5.15
210	7	RL8_SCHPO	60S ribosomal protein L8	O13672	MALDI-TOF-MS	42%	13	30	28.5	10.35	16.3	4.20
211	3	RPE_SCHPO	Ribulose-phosphate 3-epimerase	O14105	nanoLC-MS/MS	11%	2	20	25.2	5.53	13.1	5.47
212	41	RPE_SCHPO	Ribulose-phosphate 3-epimerase	O14105	nanoLC-MS/MS	11%	2	35	25.2	5.53	23.1	5.52
213	127	RS0B_SCHPO	40S ribosomal protein S0-B	Q9P546	nanoLC-MS/MS	11%	3	115	31.4	4.95	35.7	4.10
214	131	RS0B_SCHPO	40S ribosomal protein S0-B	Q9P546	MALDI-TOF-MS nanoLC-MS/MS	32% 32%	11 9	6 53	31.4	4.95	36.3	4.99
215	7	RS11_SCHPO	40S ribosomal protein S11	P79013	MALDI-TOF-MS	67%	12	30	17.5	10.37	16.3	4.20
216	10	RS19A_SCHPO	40S ribosomal protein S19-A	P58234	MALDI-TOF-MS	53%	13	25	16.2	9.71	14.3	4.28
217	8	RS23_SCHPO	40S ribosomal protein S23	P79057	MALDI-TOF-MS	62%	9	25	15.7	10.32	15.1	4.17
218	8	RS24A_SCHPO	40S ribosomal protein S24-A	O13784	MALDI-TOF-MS	60%	11	14	15.3	10.93	15.1	4.17
219	8	RS24B_SCHPO	40S ribosomal protein S24-B	O59865	MALDI-TOF-MS	62%	13	27	15.4	10.92	15.1	4.17
220	37	RS5A_SCHPO	40S ribosomal protein S5-A	O14277	MALDI-TOF-MS	31%	6	14	22.2	9.91	20.1	5.40
221	69	RS6B_SCHPO	40S ribosomal protein S6-B	Q9C0Z7	nanoLC-MS/MS	41%	7	109	27.5	10.77	24.3	4.32
222	109	PMGY_SCHPO	Phosphoglycerate mutase	P36623	MALDI-TOF-MS	76%	20	20	23.8	6.92	23.8	6.92
223	49	SAHH_SCHPO	Adenosylhomocysteinase	O13639	MALDI-TOF-MS	13%	6	24	47.4	5.61	22.4	5.87
224	150	SAHH_SCHPO	Adenosylhomocysteinase	O13639	MALDI-TOF-MS nanoLC-MS/MS	43% 7%	19 3	9 45	47.4	5.61	43.5	5.65
225	19	SODC_SCHPO	Superoxide dismutase [Cu-Zn]	P28758	MALDI-TOF-MS	68%	6	27	15.9	5.80	14.9	6.03
226	60	SODM_SCHPO	Superoxide dismutase [Mn]. mitochondrial [Precursor]	Q9UQX0	MALDI-TOF-MS nanoLC-MS/MS	59% 24%	9 4	9 39	24.3	9.12	21.5	7.33
227	62	SODM_SCHPO	Superoxide dismutase [Mn]. mitochondrial [Precursor]	Q9UQX0	MALDI-TOF-MS nanoLC-MS/MS	77% 40%	12 9	22 37	24.3	9.12	21.6	7.66
228	209	TBA1_SCHPO	Tubulin alpha-1 chain	P04688	MALDI-TOF-MS	27%	12	15	51.2	4.97	55.9	5.17
229	190	TKT_SCHPO	Probable transketolase	Q9URM2	nanoLC-MS/MS	14%	7	31	75.2	6.33	43.1	6.89
230	191	TKT_SCHPO	C-terminal fragment of the Probable transketolase	Q9URM2	MALDI-TOF-MS nanoLC-MS/MS	40% 31%	19 16	9 12	75.2	6.33	43.8	6.90
231	237	TKT_SCHPO	Probable transketolase	Q9URM2	MALDI-TOF-MS	46%	30	21	75.2	6.33	72.0	6.62
232	238	TKT_SCHPO	Probable transketolase	Q9URM2	MALDI-TOF-MS nanoLC-MS/MS	47% 30%	35 17	15 26	75.2	6.33	71.7	6.51
233	155	TOM40_SCHPO	Probable mitochondrial import receptor subunit tom40	O13656	MALDI-TOF-MS	37%	13	17	37.6	5.90	36.2	5.78
234	81	TPIS_SCHPO	Triosephosphate isomerase	P07669	MALDI-TOF-MS	68%	13	20	27.1	6.61	25.7	5.34
235	104	TPIS_SCHPO	Triosephosphate isomerase	P07669	nanoLC-MS/MS	17%	3	61	27.1	6.61	25.2	6.64
236	110	TPIS_SCHPO	Triosephosphate isomerase	P07669	MALDI-TOF-MS	93%	22	17	27.1	6.61	24.9	7.08
237	111	TPIS_SCHPO	Triosephosphate isomerase	P07669	MALDI-TOF-MS	77%	19	18	27.1	6.61	24.7	7.22

Appendix E continued

Protein No.	Spot No.[a]	Entry Name [b]	Protein Name [b]	Swiss-Prot Accession Number [b]	identified by	Sequence coverage [c]	Number of peptides[d]	Error in ppm [e]	Theoretical [f]		Gel (3-10) – estimated [g]	
									MW (kDa)	p*I*	MW (kDa)	p*I*
238	179	TPIS_SCHPO	Triosephosphate isomerase	P07669	**MALDI-TOF-MS** **nanoLC-MS/MS**	80% 47%	17 12	19 145	27.1	6.61	34.1	6.57
239	35	TPM_SCHPO	Tropomyosin	Q02088	**MALDI-TOF-MS** **nanoLC-MS/MS**	86% 45%	18 8	30 102	19.0	4.63	21.9	4.53
240	21	UBC4_SCHPO	Ubiquitin-conjugating enzyme E2 4	P46595	**MALDI-TOF-MS** **nanoLC-MS/MS**	47% 38%	6 3	20 35	16.5	6.40	13.9	6.50
241	22	UBC13_SCHPO	Ubiquitin-conjugating enzyme E2 13	O13685	**nanoLC-MS/MS**	22%	3	64	16.9	6.74	14.2	6.57
242	232	UGPA1_SCHPO	Probable UTP--glucose-1-phosphate uridylyltransferase	P78811	**MALDI-TOF-MS** **nanoLC-MS/MS**	25% 12%	13 6	22 36	56.4	7.04	56.6	7.49
243	264	UREA_SCHPO	Urease	O00084	**MALDI-TOF-MS** **nanoLC-MS/MS**	17% 17%	13 11	15 45	91.2	5.56	102.1	5.62
244	207	VATB_SCHPO	Vacuolar ATP synthase subunit B	P31411	**MALDI-TOF-MS** **nanoLC-MS/MS**	64% 25%	29 13	14 49	55.8	5.19	52.5	5.19
245	114	VDAC_SCHPO	Probable outer mitochondrial membrane protein porin	Q9P544	**MALDI-TOF-MS** **nanoLC-MS/MS**	78% 13%	13 4	28 32	29.6	7.10	28.7	7.82
246	257	VIP1_SCHPO	Protein vip1	P87216	**MALDI-TOF-MS**	69%	16	25	27.5	5.54	33.9	4.44
247	99	YA03_SCHPO	Hypothetical protein C5H10.03 in chromosome I	Q09676	**MALDI-TOF-MS**	74%	15	12	24.7	5.77	25.7	5.89
248	76	YA14_SCHPO	Hypothetical protein C13C5.04 in chromosome I	Q09686	**MALDI-TOF-MS**	64%	17	12	28.0	5.05	28.6	5.01
249	142	YD25_SCHPO	Hypothetical protein C56F8.05c in chromosome I	Q10253	**MALDI-TOF-MS**	57%	19	18	32.7	5.55	34.1	5.51
250	197	YDG7_SCHPO	Probable oxidoreductase C26F1.07 in chromosome I	Q10494	**MALDI-TOF-MS** **nanoLC-MS/MS**	73% 55%	21 16	13 74	36.2	7.78	37.8	8.00
251	139	YEAH_SCHPO	Hypothetical protein UNK4.17 in chromosome I	O14082	**MALDI-TOF-MS**	59%	23	17	45.6	5.31	44.1	5.35
252	153	YEPF_SCHPO	Hypothetical protein C23H3.15C in chromosome I	P78890	**MALDI-TOF-MS**	64%	16	18	34.7	5.86	38.9	5.71
253	57	YEPF_SCHPO	Hypothetical protein C23H3.15C in chromosome I	P78890	**MALDI-TOF-MS**	31%	8	19	34.7	5.86	22.0	6.91
254	88	YEPF_SCHPO	Hypothetical protein C23H3.15c in chromosome I	P78890	**MALDI-TOF-MS** **nanoLC-MS/MS**	40% 23%	9 5	15 70	34.7	5.86	33.1	5.14
255	158	YEPF_SCHPO	Hypothetical protein C23H3.15C in chromosome I	P78890	**MALDI-TOF-MS**	74%	22	19	34.7	5.86	39.5	5.88
256	102	YGK3_SCHPO	Hypothetical protein C725.03 in chromosome II	O94322	**MALDI-TOF-MS** **nanoLC-MS/MS**	82% 30%	19 7	18 94	29.3	6.11	26.8	6.20
257	44	YHZ8_SCHPO	Hypothetical protein SPBC21B10.08c in chromosome II	P78833	**MALDI-TOF-MS**	64%	9	15	21.8	5.65	21.4	5.67
258	83	YHZ8_SCHPO	Hypothetical protein SPBC21B10.08c in chromosome II	P78833	**nanoLC-MS/MS**	67%	7	30	21.8	5.65	23.5	5.46
259	26	YJO6_SCHPO	Very hypothetical protein PB16A4.06c in chromosome III	Q96WU9	**MALDI-TOF-MS**	50%	6	11	14.4	7.87	17.3	6.83
260	149	SPBC16E9.16c [h]	Hypothetical protein SPBC16E9.16c		**MALDI-TOF-MS** **nanoLC-MS/MS**	17% 6%	12 3	24 110	74.1	6.41	42.7	5.65
261	265	SPBC16E9.16c [h]	Hypothetical protein SPBC16E9.16c		**MALDI-TOF-MS** **nanoLC-MS/MS**	27% 9%	19 6	26 133	74.1	6.41	42.3	5.55

a) Number in figure 3.7A and 4.1A

b) Entry name, protein name and accession number according to Swiss-Prot (http://kr.expasy.org/sprot/)

c) Amino acid sequence coverage for the identified proteins

d) Number of matching peptides according to the MASCOT™ search engine

e) Error in ppm according to the MASCOT™ search engine

f) Theoretical *M*r and p*I* according to protein sequence and Swiss 2-D PAGE database

g) Gel-estimated *M*r and p*I* calculated by analysis of the gel images with PDQuest 7.2.0 software

h) Systematic name according to *S.pombe* GeneDB (http://www.genedb.org/genedb/pombe/index.jsp)

Appendix F Lists of the 80 identified proteins (*S. pombe*) resolved by 2-DE in both 3-10 *pI* and 4-7 *pI* ranges (Hwang *et al.,* 2006).

Protein No.	Spot No.[a]	Entry Name [b]	Protein Name [b]	Swiss-Prot Accession Number [b]	identified by	Sequence coverage [c]	Number of peptides[d]	Error in ppm [e]	Theoretical [f] MW (kDa)	Theoretical [f] p*I*	Gel (4-7) – estimated [g] MW (kDa)	Gel (4-7) – estimated [g] p*I*
262	136 364	ACT_SCHPO	Actin	P10989	MALDI-TOF-MS nanoLC-MS/MS	57% 45%	21 13	12 45	41.7	5.31	41.7	5.31
263	187 341	ADH_SCHPO	Alcohol dehydrogenase	P00332	MALDI-TOF-MS	59%	17	13	37.4	6.46	35.5	6.80
264	94 334	ADH_SCHPO	Alcohol dehydrogenase	P00332	MALDI-TOF-MS	30%	10	9	37.4	6.46	32.0	5.77
265	49 321	ADH_SCHPO	Alcohol dehydrogenase	P00332	MALDI-TOF-MS	27%	6	6	37.4	6.46	22.5	5.85
266	133 366	ADK_SCHPO	Adenosine kinase	P78825	MALDI-TOF-MS	46%	13	15	36.7	5.26	37.2	5.19
267	156 359	ALF_SCHPO	Fructose-bisphosphate aldolase	P36580	MALDI-TOF-MS	39%	12	23	39.6	5.92	34.2	5.79
268	81 331	ALF_SCHPO	N-terminal fragment of the Fructose-bisphosphate aldolase	P36580	MALDI-TOF-MS	39%	14	12	39.6	5.92	26.2	5.28
269	165 352	ALF_SCHPO	Fructose-bisphosphate aldolase	P36580	MALDI-TOF-MS	76%	18	17	39.6	5.92	38.5	6.20
270	48 322	ATPF_SCHPO	ATP synthase subunit 4. mitocondrial [Precursor]	O94373	MALDI-TOF-MS	51%	14	21	26.7	8.65	23.1	5.80
271	230 388	CATA_SCHPO	Catalase	P55306	MALDI-TOF-MS	64%	33	28	58.3	6.39	54.9	6.78
272	257 370	CLC1_SCHPO	Clathrin light chain (CLC)	Q9USP6	MALDI-TOF-MS nanoLC-MS/MS	30% 44%	7 9	6 126	25.9	4.61	33.9	4.37
273	3 303	COFI_SCHPO	Colfilin	P78929	MALDI-TOF-MS nanoLC-MS/MS	67% 60%	10 8	26 13	15.6	5.60	13.1	5.39
274	17 307	COFI_SCHPO	Colfilin	P78929	nanoLC-MS/MS	42%	4	106	15.6	5.60	12.9	5.63
275	240 391	DAK1_SCHPO	Dihydroxyacetone kinase 1	O13902	MALDI-TOF-MS nanoLC-MS/MS	29% 51%	16 30	12 81	62.3	5.93	62.3	5.93
276	173 349	ENO11_SCHPO	Enolase 1-1	P40370	MALDI-TOF-MS	42%	16	13	47.4	6.23	35.1	6.44
277	227 386	ENO11_SCHPO	Enolase 1-1	P40370	MALDI-TOF-MS nanoLC-MS/MS	68% 50%	33 31	13 96	47.4	6.23	47.5	6.65
278	226 385	ENO11_SCHPO	Enolase 1-1	P40370	MALDI-TOF-MS	58%	23	17	47.4	6.23	47.2	6.39
279	224 383	ENO11_SCHPO	Enolase 1-1	P40370	MALDI-TOF-MS	51%	22	13	47.4	6.23	48.2	6.02
280	135 365	ENO11_SCHPO	Enolase 1-1	P40370	MALDI-TOF-MS	45%	19	10	47.4	6.23	35.9	5.33
281	54 317	ENO11_SCHPO	Enolase 1-1	P40370	MALDI-TOF-MS	33%	11	7	47.4	6.23	23.0	6.62
282	176 346	ENO11_SCHPO	Enolase 1-1	P40370	MALDI-TOF-MS	38%	16	9	47.4	6.23	34.6	6.50
283	225 384	ENO11_SCHPO	Enolase 1-1	P40370	MALDI-TOF-MS	48%	19	7	47.4	6.23	47.9	6.15
284	174 348	ENO11_SCHPO	Enolase 1-1	P40370	MALDI-TOF-MS	42%	17	18	47.4	6.23	34.7	6.39
285	223 382	ENO11_SCHPO	Enolase 1-1	P40370	MALDI-TOF-MS	57%	21	12	47.4	6.23	47.7	5.97
286	258 387	ENO11_SCHPO	Enolase 1-1	P40370	MALDI-TOF-MS nanoLC-MS/MS	38% 19%	14 7	15 98	47.4	6.23	57.6	6.83
287	216 381	ENO12_SCHPO	Enolase 1-2	Q8NKC2	MALDI-TOF-MS	60%	25	13	47.9	5.73	46.8	5.81
288	215 380	ENO12_SCHPO	Enolase 1-2	Q8NKC2	MALDI-TOF-MS nanoLC-MS/MS	64%	28	27	47.9	5.73	47.6	5.72
289	182 343	G3P1_SCHPO	Glyceraldehyde 3-phosphate dehydrogenase 1	P78958	MALDI-TOF-MS	72%	24	15	35.9	6.24	34.6	6.82
290	56 315	G3P1_SCHPO	C-terminal fragment of the Glyceraldehyde 3-phosphate dehydrogenase 1	P78958	MALDI-TOF-MS	40%	16	18	35.9	6.24	20.8	6.77

Appendix F continued

Protein No.	Spot No.[a]	Entry Name [b]	Protein Name [b]	Swiss-Prot Accession Number [b]	identified by	Sequence coverage [c]	Number of peptides[d]	Error in ppm [e]	Theoretical [f] MW (kDa)	Theoretical [f] pI	Gel (4-7) – estimated [g] MW (kDa)	Gel (4-7) – estimated [g] pI
291	141 368	G3P1_SCHPO	Glyceraldehyde 3-phosphate dehydrogenase 1	P78958	MALDI-TOF-MS	59%	19	17	35.9	6.24	33.8	5.44
292	175 347	G3P1_SCHPO	Glyceraldehyde 3-phosphate dehydrogenase 1	P78958	MALDI-TOF-MS	62%	18	13	35.9	6.24	34.5	6.45
293	55 316	G3P1_SCHPO	Glyceraldehyde 3-phosphate dehydrogenase 1	P78958	MALDI-TOF-MS	40%	14	16	35.9	6.24	23.3	6.73
294	96 335	G3P1_SCHPO	Glyceraldehyde 3-phosphate dehydrogenase 1	P78958	MALDI-TOF-MS	59%	20	20	35.9	6.24	31.3	5.81
295	185 342	G3P1_SCHPO	Glyceraldehyde 3-phosphate dehydrogenase 1	P78958	MALDI-TOF-MS	37%	7	19	35.9	6.24	35.0	6.79
296	155 358	G3P1_SCHPO	Glyceraldehyde 3-phosphate dehydrogenase 1	P78958	MALDI-TOF-MS	30%	8	13	35.9	6.24	35.5	5.77
297	140 362	GBLP_SCHPO	Guanine nucleotide-binding protein beta subunit-like protein	Q10281	MALDI-TOF-MS nanoLC-MS/MS	95% 69%	23 20	23 31	34.9	5.43	34.2	5.52
298	83 325	GRPE_SCHPO	GrpE protein homolog. mitochondrial [Precursor]	O43047	MALDI-TOF-MS	26%	5	13	25.3	7.73	24.2	5.43
299	4 304	HSP16_SCHPO	Heat shock protein 16	O14368	MALDI-TOF-MS nanoLC-MS/MS	89% 75%	14 24	19 39	16.0	5.72	15.1	5.53
300	2 302	HSP16_SCHPO	Heat shock protein 16	O14368	MALDI-TOF-MS	87%	14	24	16.0	5.72	14.7	5.23
301	248 374	HSP60_SCHPO	Heat shock protein 60. mitochondrial [Precursor]	Q09864	MALDI-TOF-MS nanoLC-MS/MS	64% 34%	36 17	12 77	62.2	5.76	60.2	5.34
302	246 377	HSP72_SCHPO	Probable heat shock protein ssa2	O59855	MALDI-TOF-MS	26%	13	23	70.1	5.13	57.9	5.56
303	242 393	HSP75_SCHPO	N-terminal fragment of the heat shock protein sks2	Q10284	MALDI-TOF-MS	22%	12	29	67.2	5.82	67.5	5.75
304	37 327	HSP75_SCHPO	Heat shock protein sks2	Q10284	MALDI-TOF-MS	12%	7	17	67.2	5.82	20.3	5.34
305	82 332	HSP75_SCHPO	Heat shock protein sks2	Q10284	MALDI-TOF-MS	18%	9	14	67.2	5.82	25.5	5.38
306	15 306	ILV5_SCHPO	C terminal fragment of the probable ketol-acid reductoisomerase. mitochondrial [Precursor]	P78827	MALDI-TOF-MS	32%	13	26	45.2	9.47	11.8	5.55
307	132 367	IPYR_SCHPO	Inorganic pyrophosphatase	P19117	MALDI-TOF-MS nanoLC-MS/MS	60% 42%	20 15	14 59	32.3	5.20	34.2	5.05
308	51 320	KAPS_SCHPO	Adenylyl-sulfate kinase	Q9P7G9	MALDI-TOF-MS	51%	9	18	22.7	6.23	23.8	5.91
309	169 353	O13702_SCHPO	SPAC13F5.03c protein	O13702	MALDI-TOF-MS	57%	25	17	49.4	7.23	40.8	6.28
310	143 363	O13702_SCHPO	SPAC13F5.03c protein	O13702	MALDI-TOF-MS	34%	12	13	49.4	7.23	42.3	5.50
311	170 354	O13702_SCHPO	SPAC13F5.03c protein	O13702	MALDI-TOF-MS	53%	22	16	49.4	7.23	41.5	6.26
312	128 371	O42932_SCHPO	Qcr6 protein	O42932	MALDI-TOF-MS	55%	20	16	24.3	4.41	35.8	4.21
313	151 379	O59711_SCHPO	SPBC3B8.03 protein	O59711	MALDI-TOF-MS	39%	17	13	49.9	5.41	48.3	5.56
314	39 326	O74887_SCHPO	SPCC576.03c protein	O74887	MALDI-TOF-MS nanoLC-MS/MS	72% 50%	11 13	9 31	21.2	5.37	21.3	5.31
315	16 308	O74887_SCHPO	SPCC576.03c protein	O74887	MALDI-TOF-MS	29%	4	16	21.2	5.37	12.5	5.70
316	52 319	P25_SCHPO	P25 protein	P30821	MALDI-TOF-MS	58%	10	27	21.9	6.29	20.0	6.26
317	69 329	NACA_SCHPO	Putative nascent polypeptide-associated complex alpha subunit-like protein	P87147	nanoLC-MS/MS	25%	6	96	18.8	5.00	25.8	4.25
318	24 312	PDC2_SCHPO	Probable pyruvate decarboxylase C1F8.07c	Q92345	nanoLC-MS/MS	15%	12	31	64.8	5.71	15.6	6.59
319	97 336	PDX1_SCHPO	Probable pyridoxin biosynthesis PDX1-like protein	O14027	MALDI-TOF-MS	40%	17	7	31.4	5.92	31.2	5.90

Appendix F continued

Protein No.	Spot No.[a]	Entry Name[b]	Protein Name[b]	Swiss-Prot Accession Number[b]	identified by	Sequence coverage[c]	Number of peptides[d]	Error in ppm[e]	Theoretical[f] MW (kDa)	Theoretical[f] pI	Gel (4-7) – estimated[g] MW (kDa)	Gel (4-7) – estimated[g] pI
320	256 396	PLB1_SCHPO	Lysophospholipase 1 [Precursor]	P78854	nanoLC-MS/MS	25%	13	32	67.1	4.74	15.9	4.50
321	109 314	PMGY_SCHPO	Phosphoglycerate mutase	P36623	MALDI-TOF-MS	83%	23	10	23.8	6.92	23.8	6.92
322	53 318	PMGY_SCHPO	Phosphoglycerate mutase	P36623	MALDI-TOF-MS	80%	19	18	23.8	6.92	23.9	6.49
323	22 311	PMGY_SCHPO	Phosphoglycerate mutase	P36623	MALDI-TOF-MS nanoLC-MS/MS	50% 51%	11 10	11 61	23.8	6.92	14.2	6.53
324	1 301	PMP20_SCHPO	Putative peroxiredoxin pmp20	O14313	MALDI-TOF-MS nanoLC-MS/MS	87% 62%	10 10	20 29	16.7	5.18	15.5	5.28
325	254 395	Q9USU5_SCHPO	SPBC29A10.08 protein	Q9USU5	MALDI-TOF-MS	19%	9	21	50.6	5.32	145.0	5.35
326	102 337	Q9UT63_SCHPO	SPAC513.02 protein	Q9UT63	MALDI-TOF-MS	44%	9	17	25.2	5.94	27.3	6.16
327	57 313	SERC_SCHPO	Putative phosphoserine aminotransferase	Q10349	MALDI-TOF-MS	17%	5	19	42.8	6.02	22.1	6.91
328	5 309	SODC_SCHPO	Superoxide dismutase [Cu-Zn]	P28758	MALDI-TOF-MS nanoLC-MS/MS	90% 62%	8 11	16 22	15.9	5.80	14.1	5.87
329	87 333	SPEE_SCHPO	Spermidine synthase	Q09741	nanoLC-MS/MS	8%	4	88	33.1	5.49	31.9	5.52
330	243 394	STI1_SCHPO	Heat shock protein sti1 homolog	Q9USI5	MALDI-TOF-MS nanoLC-MS/MS	17% 15%	8 9	9 138	65.5	5.42	67.9	5.57
331	106 338	TPIS_SCHPO	Triosephosphate isomerase	P07669	MALDI-TOF-MS	82%	23	17	27.1	6.61	25.5	6.81
332	70 330	TPIS_SCHPO	Triosephosphate isomerase	P07669	MALDI-TOF-MS	50%	8	12	27.1	6.61	25.3	4.51
333	41 324	UCRI_SCHPO	Ubiquinol-cytochrome C reductase iron-sulfur subunit. mitochondrial [Precursor]	Q09154	MALDI-TOF-MS nanoLC-MS/MS	25% 15%	6 2	17 30	24.7	8.32	23.3	5.54
334	144 369	VIP1_SCHPO	Protein vip1	P87216	MALDI-TOF-MS nanoLC-MS/MS	69% 38%	15 9	11 131	27.5	5.54	33.1	5.43
335	87 333	VIP1_SCHPO	Protein vip1	P87216	MALDI-TOF-MS nanoLC-MS/MS	74% 37%	15 8	18 135	27.5	5.54	31.9	5.52
336	71 328	YAAB_SCHPO	Hypothetical protein C22G7.11c in chromosome I	Q09802	MALDI-TOF-MS nanoLC-MS/MS	56% 27%	9 6	22 92	15.4	4.24	27.2	4.16
337	127 372	YBI8_SCHPO	Protein C16A3.08c in chromosome II	O42914	MALDI-TOF-MS nanoLC-MS/MS	48% 30%	19 10	10 120	30.9	10.14	35.7	4.18
338	14 305	YBL5_SCHPO	Hypothetical protein C106.05c in chromosome II	Q9URV6	MALDI-TOF-MS	65%	7	11	11.2	5.77	11.1	5.49
339	236 389	YDGE_SCHPO	Putative flavoprotein C26F1.14C.	Q10499	MALDI-TOF-MS nanoLC-MS/MS	62% 40%	31 15	15 96	62.1	6.20	61.2	6.51
340	160 360	YEPF_SCHPO	Hypothetical protein C23H3.15c in chromosome I	P78890	MALDI-TOF-MS nanoLC-MS/MS	91% 36%	28 11	20 33	34.7	5.86	40.9	5.83
341	42 323	YHZ8_SCHPO	Hypothetical protein SPBC21B10.08c in chromosome II	P78833	MALDI-TOF-MS	78%	13	18	21.8	5.65	22.5	5.62

a) Number in figure 3.7 and 4.1

b) Entry name, protein name and accession number according to Swiss-Prot (http://kr.expasy.org/sprot/)

c) Amino acid sequence coverage for the identified proteins

d) Number of matching peptides according to the MASCOT™ search engine

e) Error in ppm according to the MASCOT™ search engine

f) Theoretical Mr and pI according to protein sequence and Swiss 2-D PAGE database

g) Gel-estimated Mr and pI calculated by analysis of the gel images with PDQuest 7.2.0 software

Acknowledgment

First of all, I would like to thank Prof. Rita Bernhardt! In the last couple of years, she has been my scientific advisor who has strongly influenced my understanding and view of science. I am very thankful that she has introduced me into this very interesting research area and that she has given me the possibility to learn from her!

I thank the Deutsche Forschungsgemeinschaft (DFG) for the financial support of this work in the frame of the project: the International Research Training Group 532 within the project "Physical Methods for the Structural Characterisation of New Materials" as well as Prof. Dr. Michael Veith and Dr. Markus Ehses for the coordination of the project.

Many thanks to my three "proteomics team" Dr. Susanne Zöllner, Dipl. Biol. Britta Wilzewski and Dipl. Biol. Martin Wörner. Without the both of you these last years would have been much more boring! Specially, I would like to thank Dr. Susanne Zöllner for letting me profit from her experience with the 2-DE technique.

Special thanks to Dr. Andy Zöllner for the proof reading of the present manuscript and to our cooperation partners at the Strasbourg University, Dr. Christine Carapito, Dr. Emmanuelle Leize and Prof. Alain Van Dorsselaer.

Also many thanks to all other members of the group for the excellent working classmate! Unfortunately, I cannot mention everybody but be sure I am not going to forget a single one of you! I had an awesome time working together with all of you!

At this point I would like to thank my parents Mrs. Yang Ja Cho and Mr. Woon Young Hwang who where always there for me when I needed help or advise. I am very thankful for having such wonderful and loving parents. Without your financial sacrifice during my study I would not have been able to accomplish all of this! 진심으로 감사합니다**!**

Finally, I dedicate this work to my wife Tae-Hee Kim. I am very happy that I have become a part of your family and you a part of mine! You are the most important person in my life!